

**Characterization of putative virulence-
associated genes of *Burkholderia pseudomallei***

Inauguraldissertation

zur

Erlangung des akademischen Grades

Doctor rerum naturalium (Dr. rer. nat.)

an der Mathematisch-Naturwissenschaftlichen Fakultät

der

Ernst-Moritz-Arndt-Universität Greifswald

2014

vorgelegt von

Duong Tuan Linh

geboren am 27. 02. 1982

in Hanoi, Vietnam

Greifswald, 16.07.2014

Dekan: Prof. Dr. Klaus Fesser

1. Gutachter 1: Prof. Dr. med. Ivo Steinmetz

2. Gutachter 2: Prof. Dr. Jan Buer

Tag der Promotion: 2014-11-21

CONTENTS

Contents	III
Abstract	VII
List of tables	IX
List of figures.....	X
List of abbreviations	XIII
1 Introduction	1
1.1 <i>Burkholderia pseudomallei</i>, the causative agent of melioidosis.....	1
1.1.1 Characteristics of <i>B. pseudomallei</i>	1
1.1.2 Epidemiology and clinical features of melioidosis	1
1.2 Virulence factors of <i>B. pseudomallei</i>.....	3
1.2.1 Overview of <i>B. pseudomallei</i> virulence factors.....	3
1.2.2 Secretion systems of <i>B. pseudomallei</i>	3
1.3 LysR-type transcriptional regulator family	6
1.3.1 Origin and evolution of LTTRs	6
1.3.2 Structure and function of LTTR family proteins	6
1.4 Intracellular life cycle of <i>B. pseudomallei</i>	8
1.5 <i>In vivo B. pseudomallei</i> infection models	8
1.5.1 Murine <i>B. pseudomallei</i> infection models	9
1.5.2 Experimental vaccines against <i>B. pseudomallei</i> infection	9
1.6 Aims of the study	10
2 Materials and methods	11
2.1 Bacteria	11
2.1.1 Bacterial strains	11
2.1.2 Preparation of bacterial glycerol stocks	12
2.1.3 Preparation of competent cells	12
2.1.4 Adjustment of bacterial dosages.....	13
2.1.5 Growth kinetics	13
2.1.6 Motility assays.....	13

2.1.7	Biofilm assay	13
2.1.8	Protease assay	14
2.1.9	Antibiotic susceptibility testing	14
2.2	Plasmids	15
2.3	Oligonucleotides	16
2.4	DNA manipulations	17
2.4.1	Isolation of genomic DNA of <i>B. pseudomallei</i>	17
2.4.2	Polymerase chain reaction.....	17
2.4.3	Agarose gel electrophoresis	18
2.4.4	Purification of DNA fragment and gel extraction	19
2.4.5	Restriction enzymes and dephosphorylation	19
2.4.6	Ligation.....	20
2.4.7	Heat shock transformation	20
2.4.8	Mini-preparation of DNA plasmid	20
2.5	Mutagenesis and complementation of <i>B. pseudomallei</i> genes	20
2.5.1	Construction of knockout mutants	20
2.5.2	Conjugation	21
2.5.3	Isolation of markerless mutants	21
2.5.4	Complementation	22
2.6	Protein manipulations	23
2.6.1	Protein preparation with Trizol	23
2.6.2	Protein preparation by ribolyser method.....	23
2.6.3	Purification of extracellular protein.....	23
2.6.4	Bradford protein quantification	24
2.6.5	SDS polyacrylamide mini gel electrophoresis.....	24
2.6.6	Western blot	25
2.7	Quantitation of cytoplasmic proteins by using stable isotope labelling with amino acids in cell culture	26
2.7.1	Preparation of a heavy-labelled <i>B. pseudomallei</i> protein standard	26
2.7.2	Sample preparation for proteomic analysis	26
2.7.3	Mass spectrometry and data analysis	26

2.8	RNA manipulations	27
2.8.1	RNA preparation	27
2.8.2	DNase I treatment of RNA	27
2.8.3	Reverse transcription	27
2.8.4	Semi quantitative expression analysis	28
2.9	Experiments with mammalian cells	28
2.9.1	Cultivation of mammalian cell lines.....	28
2.9.2	Generation and cultivation of primary murine bone marrow macrophages	28
2.9.3	Counting, seeding and maintaining cell lines.....	29
2.9.4	Infection of mammalian cells	29
2.9.5	Invasion and intracellular replication assays	29
2.9.6	Actin tail formation assay	30
2.10	<i>In vivo</i> infection experiments	30
2.10.1	Bioethics.....	30
2.10.2	Infection procedures	31
2.10.3	Determination of the bacterial load in internal organs	31
2.10.4	Immunization procedures.....	31
2.10.5	Detection of anti- <i>Bp</i> antibodies in the serum	31
2.10.6	Enzyme linked immunosorbent assay (ELISA).....	32
2.11	<i>In silico</i> sequence analysis	32
2.12	Statistics and software	32
3	Results	33
3.1	Charaterization of the putative LysR–type trascriptional regulator BPSL0117 of <i>B. pseudomallei</i>	33
3.1.1	Complementation of the <i>B. pseudomallei</i> transposon mutant Δ BPSL0117	33
3.1.2	<i>In vitro</i> characterization of <i>B. pseudomallei</i> Δ BPSL0117	34
3.1.3	Roles of BPSL0117 in mammalian cell models	38
3.1.4	Influence of BPSL0117 on <i>B. pseudomallei</i> virulence	40
3.1.5	Usage of <i>B. pseudomallei</i> Δ BPSL0117 as a live vaccine.....	42
3.1.6	Global protein expression profile	45

3.1.7	<i>In silico</i> analysis of BPSL0117	52
3.2	Characterization of the T3SS3 gene BPSS1528 (<i>bapA</i>)	55
3.2.1	Expression analyses of <i>bapA</i> , <i>bapB</i> and <i>bapC</i> genes	55
3.2.2	Construction of <i>B. pseudomallei</i> Δ <i>bapA</i> mutants and complementation.....	57
3.2.3	Functional analysis of <i>B. pseudomallei</i> Δ <i>bapA</i> #1	58
3.2.4	Influence of BapA on <i>B. pseudomallei</i> virulence	64
3.2.5	Characterization of <i>B. pseudomallei</i> Δ <i>bapA</i> #2 and <i>B. pseudomallei</i> Δ <i>bapA</i> #3	65
4	Discussion	68
4.1	Characterization of the LTTR BPSL0117	68
4.1.1	Structure and regulatory functions of BPSL0117	68
4.1.2	Regulation of virulence factors	68
4.1.3	Regulation of metabolic pathways	69
4.1.4	Usage of <i>B. pseudomallei</i> Δ BPSL0117 as a live vaccine.....	71
4.2	Characterization of BPSS1528 (BapA).....	71
4.2.1	BapA and its role for the <i>in vivo</i> virulence of <i>B. pseudomallei</i>	71
4.2.2	Role of <i>bap</i> genes for the adaptation of <i>B. pseudomallei</i> in the environment	72
	References	74
	Erklärung.....	82
	Appendices	83
	Curriculum Vitae..... Fehler! Textmarke nicht definiert.	
	Acknowledgements.....	131

ABSTRACT

The Gram-negative rod *Burkholderia pseudomallei* (*Bp*) is the causative agent of the disease melioidosis, an often fatal infection of humans and animals. The bacteria can be isolated from soil and water in tropical and sub-tropical areas around the world. Moreover, *Bp* is a facultative intracellular bacterium that can survive in phagocytic cells. *Bp* possesses a wide array of virulence genes including numerous secretion systems such as three type 3 secretion system clusters (T3SS) and six type VI secretion clusters (T6SS). Furthermore, the genome of *Bp* consists of 88 paralogous LysR-type transcriptional regulator (LTTR) genes including *BPSL0117* gene that may regulate other virulence factors.

In the first part of this study, we characterised a role of the putative LTTR *BPSL0117* of *Bp* for the virulence of this pathogen. For this purpose, a *Bp* Δ *BPSL0117* transposon mutant that was already available was successfully complemented by using pUC18T-mini-Tn7T-FRT-Zeo vector. The *Bp* Δ *BPSL0117* transposon mutant exhibited impaired biofilm formation, motility, exoproteases activity, and intracellular growth. *Bp* Δ *BPSL0117* also showed more sensitivity to beta-lactamase antibiotics. Besides *in vitro* phenotypes, *Bp* Δ *BPSL0117* presented reduced bacterial load in organs and highly attenuated virulence in the BALB/c mouse model of melioidosis. All observed phenotypes were reverted to wild type level in the complemented mutant strain. Next, a protein expression profile analysis should help to examine *BPSL0117* dependent protein expression. Using stable isotope labeling by amino acids in cell culture (SILAC), we were able to detect 1608 cytoplasmic proteins. Beside others, we found that *BPSL0117* regulates the expression of T3SS3 and T6SS1 associated proteins and enzymes involved in metabolic pathways. *In silico* analysis, predicted *BPSL0117* structure showed high similarity with full-length crystal structures of LTTR proteins like CbnR and CrgA. Collectively, *BPSL0117* works as both a positive and a negative regulator.

Finally, due to the high attenuation in mice of the *Bp* Δ *BPSL0117* transposon mutant, we examined whether this strain might serve as a promising live vaccine candidate. BALB/c mice were intranasally immunized with a high dose of *Bp* Δ *BPSL0117* and then challenged with *Bp* E8 wild type via either the intranasal, intraperitoneal or intravenous route. Vaccinated mice showed increased titers of specific IgG anti-*Bp* antibodies and a delayed time to death compared to unvaccinated mice. Thus, *Bp* Δ *BPSL0117* could partially protect mice against melioidosis but was less protective efficiency compared to other experimental vaccine strategies against *Bp*.

In the second part of this study, the focus was to unravel function for the genes *bapA*, *bapB* and *bapC*, which are encoded within the T3SS cluster 3 of *Bp* and have rarely been addressed in other studies so far. In a first set of experiments, it was shown that the expression levels of *bapB* and *bapC* genes increased when *Bp* was cultivated *in vitro* under high salt concentrations. While the expression levels of all *bap* genes increased when *Bp* was cultured *in vitro* under low pH. To further evaluate the role of the *bapA* gene, an *in-frame* deletion mutant was constructed. The *Bp* Δ *bapA*#1 mutant strain derived from *Bp* K96243

wild type exhibited increased biofilm formation compared to wild type bacteria. Interestingly, this mutant was also able to replicate more efficiently inside macrophages and showed increased virulence in BALB/c mice. However, these phenotypes were not observed in the independently derived mutants *Bp* Δ bapA#2 from parental *Bp* K96243 and *Bp* Δ bapA#3 from parental *Bp* 1026b since it was not possible to successfully complement the *Bp* Δ bapA#1 mutant strain. Thus, the *bap* genes seem to play a role for the adaptations to environmental stress, but at least the *bapA* gene is not directly involved in the pathogenic potential of *Bp* in experimental murine infection.

LIST OF TABLES

Table 1. Bacterial strains used in this study	12
Table 2. Plasmids used in this study	15
Table 3. Xtreme™ KOD PCR mixture.....	17
Table 4. Xtreme™ KOD PCR running condition	18
Table 5. Reaction setup using taq DNA polymerase	18
Table 6. Optimized cycling condition for <i>Taq</i> DNA polymerase.....	18
Table 7. Restriction mixtures	19
Table 8. Dephosphorylation mixtures	19
Table 9. Ligation mixture	20
Table 10. Bradford reagents.....	24
Table 11. Composition of one mini polyacrylamide gel used.....	24
Table 12. Procedure of western blot	25
Table 13. Antibodies used for western blot analyses	25
Table 14. Cell lines and their cultivation conditions	28
Table 15. Buffer and substrate for antibody titer	32
Table 16. Immunization of BALB/c mice with the live <i>Bp</i> ΔBPSL0117 and survival after challenge with <i>Bp</i> E8 WT	444
Table 17. Predicted functions of proteins encoded within the probable operon(s) from <i>BPSL0475</i> to <i>BPSL0493</i>	50

LIST OF FIGURES

Figure 1. A distribution map of melioidosis.	2
Figure 2. Schematic model for the T3SS with putative function and positions of proteins.	5
Figure 3. Schematic model for T6SS compared with bacteriophage T4.	6
Figure 4. Plasmid maps used in this study	16
Figure 5. Schematic of allele replacement procedure.	22
Figure 6. Complementation of <i>Bp</i> Δ BPSL0117	33
Figure 7. Growth kinetics of <i>Bp</i> Δ BPSL0117 compared to that of <i>Bp</i> E8 WT and <i>Bp</i> Δ BPSL0117::BPSL0117.	34
Figure 8. Biofilm formation of <i>Bp</i> Δ BPSL0117 compared to <i>Bp</i> E8 WT and <i>Bp</i> Δ BPSL0117::BPSL0117.	35
Figure 9. Motility of <i>Bp</i> Δ BPSL0117 compared to <i>Bp</i> E8 WT and <i>Bp</i> Δ BPSL0117::BPSL0117.	36
Figure 10. Protease activity of <i>Bp</i> Δ BPSL0117 compared to that of <i>Bp</i> E8 WT and <i>Bp</i> Δ BPSL0117::BPSL0117.	36
Figure 11. Expression and secretion of T3SS3 proteins of <i>Bp</i> Δ BPSL0117 compared to that of <i>Bp</i> E8 WT and <i>Bp</i> Δ BPSL0117::BPSL0117	37
Figure 12. Minimal inhibitory concentration of imipenem and cetazidime	38
Figure 13. Comparison of uptake and intracellular replication of <i>Bp</i> E8 WT, <i>Bp</i> Δ BPSL0117 and <i>Bp</i> Δ BPSL0117::BPSL0117	39
Figure 14. Actin tail formation of <i>Bp</i> E8 WT, <i>Bp</i> Δ BPSL0117 and <i>Bp</i> Δ BPSL0117::BPSL0117 in HeLa cells.	40
Figure 15. Mortality curves of BALB/c mice (n = 4) after intranasal infection with <i>Bp</i> E8 WT (dose infection ~ 200 CFU), <i>Bp</i> Δ BPSL0117 (dose infection 200 - 10 ⁶ CFU) and <i>Bp</i> Δ BPSL0117::BPSL0117 (dose infection ~ 200 CFU).	41
Figure 16. Bacterial burden in organs of infected BALB/c mice (n = 4) 48 h after intranasal infection with <i>Bp</i> E8 WT (dose infection ~ 332 CFU per mouse), <i>Bp</i> Δ BPSL0117 (dose infection ~ 312 CFU per mouse) and <i>Bp</i> Δ BPSL0117::BPSL0117 (dose infection ~ 303 CFU per mouse).	42

Figure 17. Humoral immune responses in <i>Bp</i> ΔBPSL0117 immunized BALB/c mice. ...	43
Figure 18. Mortality curves of BALB/c mice after four weeks intranasal immunization with <i>Bp</i> ΔBPSL0117 strain (immunization dose from 5×10^4 to 10^6 CFU per mouse, n = 7), non-immunized mice (n = 3) and challenge with <i>Bp</i> E8 WT (dose infection from 1.7×10^5 to 2.5×10^5 CFU per mouse) via the intraperitoneal route.....	44
Figure 19. Mortality curves of BALB/c mice after four weeks intranasal immunization with <i>Bp</i> ΔBPSL0117 strain (immunization infection from 5×10^4 to 10^6 CFU per mouse, n = 9), non-immunized mice (n = 9) and challenge with <i>Bp</i> E8 WT (dose infection from 290 to 600 CFU per mouse) via the intravenous route	44
Figure 20. Mortality curves of BALB/c mice after four weeks intranasal immunization with <i>Bp</i> ΔBPSL0117 strain (immunization infection from 5×10^4 to 10^6 CFU per mouse, n = 7), non-immunized mice (n = 6) and challenge with <i>Bp</i> E8 WT (dose infection from 370 to 500 CFU per mouse) via the intranasal route. ...	45
Figure 21. Significantly up or down regulated proteins and operons in <i>Bp</i> ΔBPSL0117 compared to <i>Bp</i> E8 WT, clustered by functional category.....	47
Figure 22. Orthologs of <i>Bp</i> K96243 BPSL0474 – BPSL0494 genes compared to <i>Burkholderia</i> spp.	49
Figure 23. Relative alteration of cytoplasmic proteins involved in the TCA and MCC pathways of <i>Bp</i> ΔBPSL0117 compared to the E8 WT during exponential growth phase.....	52
Figure 24. Partial genome map of <i>Burkholderia pseudomallei</i> K96243	53
Figure 25. Predicted BPSL0117 fold and domain architecture.....	54
Figure 26. Genetic organization of the <i>B. pseudomallei</i> T3SS cluster 3	55
Figure 27. mRNA expression levels of <i>bap</i> genes in <i>Bp</i> E8 WT at 6 h after inoculation in YT medium containing various NaCl concentrations.	56
Figure 28. mRNA expression levels of <i>bap</i> genes in <i>Bp</i> E8 WT at 6 h after inoculation in LB medium with various pH.	56
Figure 29. mRNA expression of <i>bapA</i> gene in <i>Bp</i> K96243 WT at 2 h and 5 h post infection of RAW264.7 cells.....	57
Figure 30. Detection of the <i>bapA</i> gene deletion by PCR reaction.....	57

Figure 31. Detection of the complementation of <i>bapA</i> gene by PCR.	58
Figure 32. Growth curve of <i>Bp</i> Δ bapA#1 compared to that of <i>Bp</i> K96243 WT.	59
Figure 33. Motility of <i>Bp</i> Δ bapA#1 compared to that of <i>Bp</i> K96243 WT.....	59
Figure 34. Biofilm formation of <i>Bp</i> Δ bapA#1 compared to that of <i>Bp</i> K96243 WT.....	60
Figure 35. Activity of exo-proteases was determined by using azocasein method.....	60
Figure 36. Comparison of the T3SS3 effector and translocation proteins of <i>Bp</i> K96423 WT and <i>Bp</i> Δ bapA #1 in LB medium inoculation at different time points. ...	61
Figure 37. Comparison of extracellular proteins of <i>Bp</i> K96243 WT and <i>Bp</i> Δ bapA #1 in LB medium inoculation at different time points.	62
Figure 38. Comparison of cytosolic proteins of <i>Bp</i> K96423 WT and <i>Bp</i> Δ bapA #1 in LB medium inoculation at different time points.	62
Figure 39. Comparison of uptake and intracellular replication of <i>Bp</i> K96243 WT and <i>Bp</i> Δ bapA #1.	63
Figure 40. Comparison of actin tail formation in HepG2 infected <i>Bp</i> K96243 WT and <i>Bp</i> Δ bapA#1 at 8 h and 18 h post infection.....	64
Figure 41. Mortality curves of BALB/c mice after infection. A: Intranasal infection of BALB/c mice (n = 9) with <i>Bp</i> K96243 WT, mutant Δ bapA#1 (infection dose from 14 to 25 CFU per animal).....	64
Figure 42. Bacterial burden in organs' BALB/c mice (n = 10) after 48 h intranasal infection with <i>Bp</i> K96243 WT (dose infection from 69 to 139 CFU) and <i>Bp</i> Δ bapA#1 (dose infection from 90 to 95 CFU).	65
Figure 43. Biofilm formation after 48 h static incubation in LB broth containing various NaCl concentrations at 37°C.....	66
Figure 44. Uptake and intracellular replication assays in RAW 264.7 macrophages.....	67
Figure 45. Mortality curves of BALB/c mice (n = 5) after intranasal infection with <i>Bp</i> 1026b WT, <i>Bp</i> Δ bapA#3 (infection dose from 20 to 22 CFU per animal).....	67

LIST OF ABBREVIATIONS

%	Percentage
°C	Celsius degree
#N/A	No value is available
ABC	ATP-binding cassette
ABS	Activation binding site
AHL	N-Acyl-Homoserine lactone
AMP	Adenosine monophosphate
Ampr or Amp ^R	Ampicillin resistance
ANOVA	Analysis of variance
AP	Alkaline phosphatase
Approx.	Approximate
ATP	Adenosin triphosphate
ATCC	American Type Culture Collection
bp	Base pair
Bcc	<i>Burkholderia (ceno)cepacia</i> complex
BDSF	Burkholderia diffusible signal factor
BMM	Bone marrow-derived macrophages
BPSL	<i>Burkholderia pseudomallei</i> large chromosome
BPSS	<i>Burkholderia pseudomallei</i> small chromosome
<i>B. pseudomallei</i> ; <i>Bp</i>	<i>Burkholderia pseudomallei</i>
<i>B. m.</i>	<i>Burkholderia mallei</i>
<i>B. thailandensis</i> ; <i>B. th.</i>	<i>Burkholderia thailandensis</i>
<i>bsa</i>	<i>Burkholderia secretion apparatus</i>
BSA	Bovine serum albumin
<i>bsa</i>	Burkholderia secretion apparatus
BSL3	Biosafety level 3 laboratory
CD	Cluster differentiation
CDC	United States Centers of Disease Control and Prevention
cDNA	Complementary deoxyribonucleic acid
CFU	Colony forming unit
CHAPS	3-[(3-Cholamidopropyl)-dimethylammonio]-1-propanesulfonate

CID	Collision induced dissociation
CoA	Coenzyme A
Compl.	Complementation
CPS	Capsule polysaccharides
Da	Dalton
dATP	Deoxyadenosine triphosphate
DAP	Diaminopimelic acid
DBD	DNA binding domain
dCTP	Deoxycytidine triphosphate
dGTP	Deoxyguanosine triphosphate
DNA	Deoxyribonucleic acid
dNTPs	Deoxynucleotide triphosphates
DSMZ	Deutsche Sammlung von Mikroorganismen und Zellkulturen GmbH (German Collection of Microorganisms and Cell Cultures)
DTT	Dithiothreitol
dTTP	Deoxythymidine triphosphate
<i>E. coli</i>	<i>Escherichia coli</i>
EDTA	Ethylenediaminetetraacetic acid
<i>e.g.</i>	Exempli grātiā (for example)
ELISA	Enzyme-linked immunosorbent assay
EPS	Exopolysaccharide
ESI HPLC MS/MS	Electrospray ionization high performance liquid chromatography tandem mass spectrometry
<i>et al.</i>	And others
Fig.	Figure
FRT	Flippase recognition target sequence
FCS	Fetal calf serum
g	Gravitational force: 9.81 m/s ²
glmS	Glucosamine-6-phosphate synthase
GmbH	Gesellschaft with beschränkter Haftung
GM-CSF	Granulocyte-macrophage colony-stimulating factor
<i>GusA</i>	<i>β-Glucuronidase</i>
h	Hour (s)
HTH	Helix-turn-helix
<i>I-SceI</i>	Homing endonuclease

<i>i.n</i>	Intranasal
<i>i.p</i>	Intraperitoneal
<i>s.c</i>	subcutaneous
<i>i.v</i>	Intravenous
ICL	Isocitrate lyase
IFN	Interferon
Ig	Immunoglobulin
kBp	Kilo base pairs
kDa	Kilo Dalton
KEGG	Kyoto encyclopedia of genes and genomes
Km ^R or Kmr	Kanamycin resistance
LB	Luria Bertani
LC3	Light chain 3
LC-MS/MS	Liquid chromatography-Tandem mass spectrometry
LD50	Median lethal dose
LOOPP	Learning, Observing and Outputting Protein Patterns
LPS	Lipopolysaccharide
LTTR(s)	LysR-type transcriptional regulator(s)
M	Molar
M9	M9 minimal medium
mA	Milli ampere
mAb	Monoclonal antibody
MCC	Methylcitrate cycle
MCL	Methylisocitrate lyase
MIC	Minimal inhibitory concentration
Min	Minute (s)
mM	Milli molar
M-MLV RT	Moloney Murine Leukemia Virus Reverse Transcriptase
MNGC	Multi-nucleated giant cells
MOI	Multiplicity of infection
mRNA	Messenger ribonucleic acid
MS	Mass spectrometry
NC	Negative control
NCTC	National Collection of Type Cultures
ng	Nano gram

LIST OF ABBREVIATIONS

NL	Non-linear
No	Number
OD	Optical density
orf	Open reading frame
<i>p.i</i>	Post infection
PAGE	Polyacrylamide gel electrophoresis
PBS	Phosphate buffered saline
PC	Positive control
PCR	Polymerase chain reaction
PMSF	Phenylmethanesulfonylfluoride
PMT	Photomultiplier tube
QS	Quorum sensing
RBS	Regulatory binding site
RNA	Ribonucleic acid
RT	Room temperature
RT-PCR	Reverse transcriptase polymerase chain reaction Or Real-time polymerase chain reaction
s	Second (s)
<i>SacB</i>	<i>Sucrose suicide cassette</i>
SD	Standard deviation
SDS	Sodium dodecyl sulfate
SILAC	Stable isotope labeling with amino acids in culture
T1SS	Type 1 secretion system
T2SS	Type 2 secretion system
T3SS	Type 3 secretion system
T4SS	Type 4 secretion system
T5SS	Type 5 secretion system
T6SS	Type 6 secretion system
TCA	Trichloroacetic acid
U	Unit
V	Volt
v/v	Volume per volume
VB	Vogel-Bonner medium
W	Watt
w/v	Weight per volume

LIST OF ABBREVIATIONS

wHTH	Winged-helix-turn-helix
WB	Western blot
WT	Wild type
YT	Yeast trypton
Zeo ^R or Zeor	Zeocin resistance
μA	Microampere
μg	Microgram
μl	Microliter

1 INTRODUCTION

1.1 *Burkholderia pseudomallei*, the causative agent of melioidosis

1.1.1 Characteristics of *B. pseudomallei*

Burkholderia pseudomallei (*Bp*) is an aerobic, non-spore forming, Gram-negative bacillus (1 - 5 µm length and 0.5 – 1.0 µm width) and the causative agent of melioidosis, an infectious disease of tropical and subtropical areas around the world. As a saprophytic bacterium, *Bp* can be isolated from soil, pooled surface water and rhizospheres of grass tissues (Currie *et al.*, 2001; Kaestli *et al.*, 2012; Suarez-Moreno *et al.*, 2012; Sprague & Neubauer, 2004; Inglis & Sagripanti, 2006). The genome of *Bp* consists of two large circular chromosomes that are defined as chromosome 1 and 2 of approximately 4.07 and 3.17Mb, respectively. Chromosome 1 predominantly possesses housekeeping genes for growth and metabolism, whereas chromosome 2 mainly encodes for virulence genes and allows the adaptation to environmental conditions (Holden *et al.*, 2004). Thus, *Bp* is able to resist even extreme conditions like low pH or lack of nutrition. The bacterium possesses a wide range of virulence genes including three type 3 secretion systems and six type 6 secretion systems (Attree & Attree, 2001; Rainbow *et al.*, 2002; Burtnick *et al.*, 2011). In addition, *Bp* is naturally resistant against multiple classes of antibiotics such as numerous penicillin, cephalosporin, macrolides and fluochinolones (Schweizer, 2012).

1.1.2 Epidemiology and clinical features of melioidosis

Melioidosis, a term derived from the Greek “*melis*” meaning donkey distemper and “*eidos*” meaning resemblance, is a serious infectious disease of humans and animals. The disease is predominantly endemic in South-East Asia, Northern Australia, but there are also melioidosis case reports from Africa, and South and Central America (Currie *et al.*, 2008; Limmathurotsakul & Peacock, 2011).

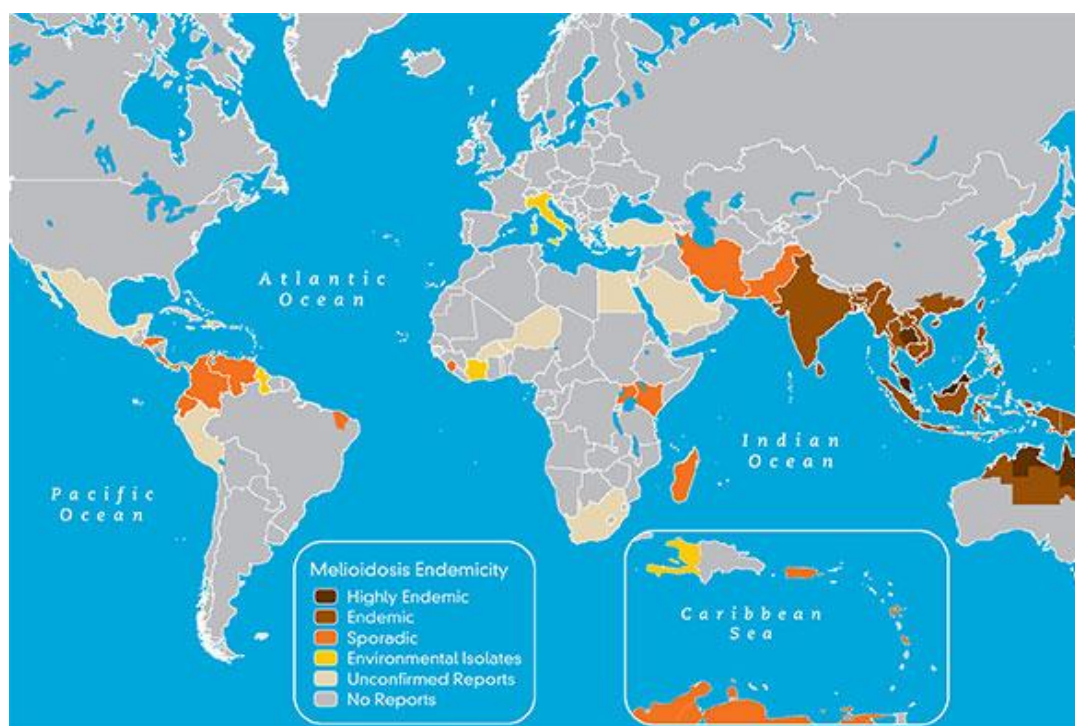


Figure 1. A distribution map of melioidosis (from Cheng & Currie, 2005).

Melioidosis is an often-fatal infection and even after appropriate antibiotic treatment of an acute infection, the mortality rate is up to 40% (Wiersinga *et al.*, 2012). Frequent infection routes include inhalation of bacteria containing aerosols and the ingestion via minor abrasions and wounds (Yabuuchi & Arakawa, 1993; Wiersinga & van der Poll T, 2009). The incubation time is variable and ranges from a few days up to several months (Currie *et al.*, 2000; Wiersinga *et al.*, 2012). One report describes a patient in that manifest melioidosis occurred as late as 62 years after contact with the pathogen (Ngaui *et al.*, 2005). Clinical manifestation of melioidosis is widely different and ranges from asymptomatic seroconversion, acute and chronic courses, and latent infection. Acute melioidosis is mainly associated with pneumonia and sepsis. Without treatment, the infection is fatal in almost all cases. Chronic infections are often less severe and associated with the formation of splenic and hepatic abscesses, infection of the skin, arthritis, osteomyelitis and prostatitis (Rode & Webling, 1981; Thin *et al.*, 1970; Ngaui *et al.*, 2005; Vatcharapreechasakul *et al.*, 1992; Wong *et al.*, 1995). Frequency of recrudescence is from 10% to 30% of all cases with appropriate treatment. Relapse occurs in 75% of these patients and re-infection results in 25% of recrudescence cases (Limmathurotsakul *et al.*, 2006; Patel *et al.*, 2011). Underlying diseases including diabetes mellitus, alcoholism, chronic pulmonary and renal diseases are proven risk factors for developing clinical manifest melioidosis (Limmathurotsakul *et al.*, 2010; Currie *et al.*, 2010; Wiersinga *et al.*, 2012).

Beside humans, *Bp* can also infect a number of animals such as cattle, horses, rodents, sheep, pigs, cats, dogs, goats, camels, dolphins, kangaroos, and water buffalo (Titball *et al.*, 2008).

Bp is listed as a category B selective agent by the Centers for Diseases Control and Prevention, and considered to be a potential bioweapon (Rotz *et al.*, 2002).

1.2 Virulence factors of *B. pseudomallei*

1.2.1 Overview of *B. pseudomallei* virulence factors

Bp harbors numerous virulence factors such as exopolysacchararides and lipopolysaccharides that are frequent components of pathogenic bacteria. *Bp* capsular polysaccharides (CPS), liposaccharides (LPS) and two surface O-polysaccharides are essential for full bacterial virulence and serve as antigens that can be detected with certain diagnostic tools (Warawa *et al.*, 2009; Aucoin *et al.*, 2012; Deshazer *et al.*, 1998; Nelson *et al.*, 2004; Ngugi *et al.*, 2010). Flagella and pili play a role for *Bp* motility and adhesion (Brett *et al.*, 1994, Brett & Woods, 1996; Inglis *et al.*, 2003). The *Bp* gene *BPSL1549* encodes for lethal factor 1 that is homologous with the *Escherichia coli* cytotoxic necrotizing factor, which leads to actin cytoskeleton assembly of the host cell and inhibits helicase activity of translation factor eIF4A that finally leads to cell death (Cruz-Migoni *et al.*, 2011).

Beside this, *Bp* can express various quorum sensing signaling molecules known as N-acyl homoserine lactones (AHL) (Ulrich *et al.*, 2004). Quorum sensing has an important role in modulating antibiotic resistance, biofilm formation, adhesion, motility, secretion of lipases and proteins, and other virulence factors (Valade *et al.*, 2004; Song *et al.*, 2005; Chan *et al.*, 2007; Chan & Chua, 2010; Gamage *et al.*, 2011; Wongtrakoongate *et al.*, 2012).

Remark is the expression of numerous secretion systems including three type 3 secretion system (T3SS) and six type 6 secretion system (T6SS) clusters encoded within the genome of *Bp* (Attree & Attree, 2001; Rainbow *et al.*, 2002; Burtneck *et al.*, 2011).

1.2.2 Secretion systems of *B. pseudomallei*

In Gram-negative bacteria, secreted proteins have to across hydrophobic barriers from the inner membrane (IM), to the periplasmic space and the outer membrane (OM) (Bleves *et al.*, 2010). In the last few decades, six different types of secretion systems have been identified, which are defined as type I secretion system (T1SS) up to the type VI secretion system (T6SS) (Economou *et al.*, 2006). The secretion machineries have been classified into one-step secretion mechanism including T1SS, T3SS, T4SS and T6SS and two-step secretion mechanism such as T2SS and T5SS (Bleves *et al.*, 2010; Filloux, 2011). In 2006, a type VII secretion system has been provisionally referred in *Mycobacterium* species (Abdallah *et al.*, 2006).

Numerous pathogenic Gram-negative bacteria are equipped with a T3SS that mediates the secretion of bacterial effector proteins into the host cells cytoplasm. The T3SS has been developed from the flagella system and is conserved among a wide range of bacterial species (Saier, 2004; Arnold *et al.*, 2010). The T3SS is a complex macromolecular machinery and contains a basal apparatus spanning from the IM, the periplasm, and the OM. Numerous effectors of bacteria are delivered from their cytosol to surrounding environments through

basal apparatus and needle-like proteins with trafficking of translocators (Cornelis, 2006). *Bp* encodes for three T3SSs that are defined as *T3SS1*, *T3SS2* and *T3SS3*. The *T3SS-1* and *T3SS-2* of *Bp* share homologies to the T3SSs of the plant pathogens *Ralstonia solanacearum* and *Xanthomonas* spp (Attree & Attree, 2001; Rainbow *et al.*, 2002) and seem to be associated with the infection of plants (Lee *et al.*, 2010). The *Bp T3SS3* gene cluster shares homology to the *Inv/Mxi-Spa T3SS* of *Salmonella* spp and *Shigella* spp in that the T3SS plays a crucial role for the infection of mammalian cells (Stevens *et al.*, 2002; Stevens *et al.*, 2004; Ulrich & DeShazer, 2004; Sun *et al.*, 2010). This cluster also contains 35 genes in at least 11 operons including several *bpr* genes for transcriptional regulation and three *bap* genes with little known function (Sun *et al.*, 2010; Treerat 2014). Similar to T3SS of other bacterial pathogens, the secretion machinery of *Bp T3SS3* is made of a broad range of proteins that are characterized as *Burkholderia* secretion apparatus (Bsa) proteins, translocator proteins and various effector proteins. Components of the Bsa proteins assemble a bacterial trans-membrane complex that is likely to form a syringe that allows to inject effector proteins from bacterial cytosol into host cell cytoplasm (Kubori *et al.*, 1998; Cornelis & Van Gijsegem, 2000). Bip translocator proteins are likely chaperones of effectors and help them transport through the needle. Even the T3SS machinery in different species shares similarity of structure and function, but pathogenic bacteria consist of various virulence effectors. *Bp* also contains the impressive arsenal of virulence proteins such as Bop proteins, Cif_{Bp} (cycle inhibiting factor) and Beps (*Burkholderia* effector proteins) that are considered to be secreted via the T3SS pathway (Stevens *et al.*, 2002; 2004; Hii *et al.*, 2008; Nougayrede *et al.*, 2005; Galyov *et al.*, 2010). The T3SS3 of *Bp* plays an important role for bacteria escape from autophagy and intracellular replication, and contribute partial virulence in murine and hamster infection models as well (Stevens *et al.*, 2002, 2004; Warawa & Woods, 2005; Gong *et al.*, 2011, Srinon *et al.*, 2013; Muangman *et al.*, 2011).

Bp is unique to express six evolutionary distinct T6SS gene clusters defined from *T6SS1* up to *T6SS6*. The cluster *T6SS1* plays a crucial role for virulence in mammalian hosts (Shalom *et al.*, 2007; Schell *et al.*, 2007; Burtnick *et al.*, 2011). The T6SS machinery is hypothesized to form the T4 bacteriophage tail spike that uses to eject bacterial effector proteins across the cellular envelope into an adjacent target cell (Basler *et al.*, 2012). The T6SS protein components can be categorized into two groups: membrane or membrane-associated proteins that form a needle-like complex and energy generated; and soluble proteins that act like effectors (Bleves *et al.*, 2010; Filloux, 2011). The first well-characterized effectors of the T6SSs are hemolysin-coregulated protein (Hcp) and valine-glycine repeat protein G (VgrG) (Pukatzki *et al.*, 2006). Substrates of the T6SSs lack N-terminal signal peptides and are secreted into the surrounding milieu by multi-component complex proteins. In *Bp*, lack of Hcp1 expression was associated with impaired intracellular survival, impacted formation of MNGCs in infection of RAW 264.7 macrophages and attenuation in experimental infection models of melioidosis (Burtnick *et al.*, 2011; Hopf *et al.*, 2014). Recently, Hopf and colleagues (2014) have revealed that deletion of *tssF* (*BPSS1504*) gene in *Bp* led to reduce intracellular replication in macrophages, impaired formation of MNGCs and attenuation in mice. Lack of

TssF was associated with a lack of Hcp1 secretion whereas expression of the *T6SS* genes was normal (Hopf *et al.*, 2014). The complex regulatory cascades of *T6SS* gene expression and the cross-talk between T3SS and T6SS proteins in *Bp* have been recently unraveling. BprC, encoded within the adjacent *T3SS3* and is an AraC-type regulator, regulates *T6SS1* gene expression (Sun *et al.*, 2010; Chen *et al.*, 2011), and the T3SS3 regulator BsaN is involved in the transcription of the T6SS1 regulator *virA-virG* (*virAG*) (Sun *et al.*, 2010). *VirAG*, located within the *T6SS1* cluster and is a two-component histidine sensory kinase, positively regulates other *T6SS1* genes such as *hcp1* gene after internalization of bacteria in host cells (Chen *et al.*, 2011, Burtnick & Brett, 2013). Recently, *T6SS1* gene expression was shown to be negatively regulated by iron and zinc (Burtnick & Brett, 2013).

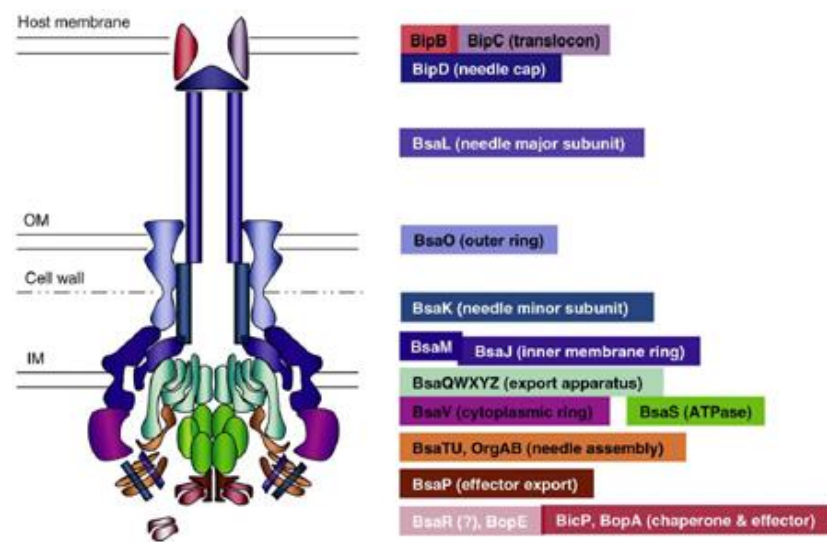
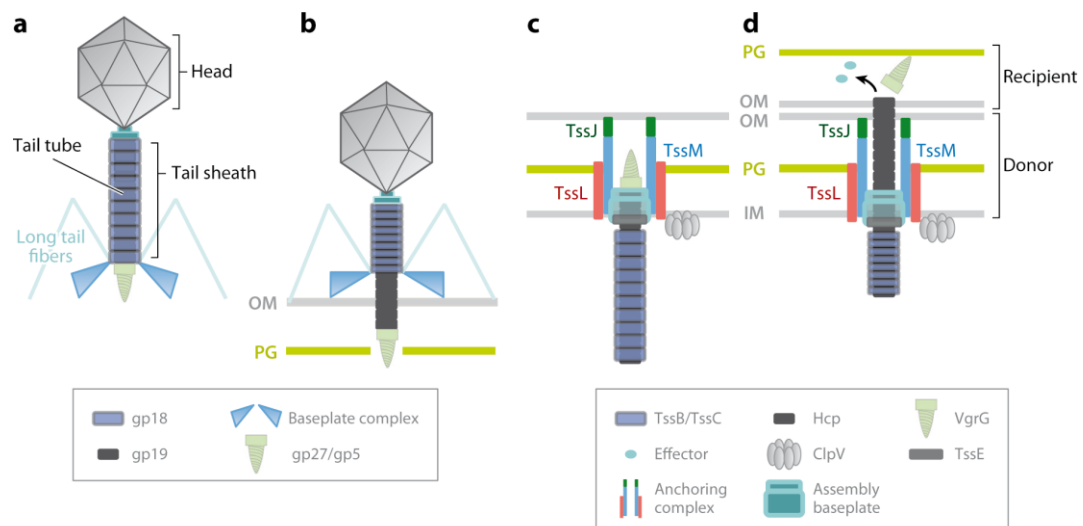


Figure 2. Schematic model for the T3SS with putative function and positions of proteins. Components with different identities/functions are drawn in different shapes and colors (from Sun *et al.*, 2010).




 Silverman JM, et al. 2012.
Annu. Rev. Microbiol. 66:453–72

Figure 3. Schematic model for T6SS compared with bacteriophage T4. Homologous and analogous T6SS and their T4 phage equivalent are colored the same. **A:** The architecture of the bacteriophage T4. **B:** the bacteriophage T4 punctures its tail across outer membrane of the host cell and delivers its DNA. **C:** inactivated and **D:** activated conditions of T6SS derived from protein rearrangement and interactions between T6SS subunits (from Silverman *et al.*, 2012).

1.3 LysR-type transcriptional regulator family

The family of LysR-type transcriptional regulators (LTTRs) was first described by Henikoff and colleagues in 1988 (Henikoff *et al.*, 1988). LTTRs regulate diverse genes and complex regulons among bacteria, archaea and eukaryotic organisms (Perez-Rueda & Collado-Vides, 2001; Sun & Klein, 2004; Stec *et al.*, 2006; Maddocks & Oyston, 2008). The genome of *Burkholderia pseudomallei* encodes for 88 putative genes belonging to the LTTR family (Holden *et al.*, 2004).

1.3.1 Origin and evolution of LTTRs

Comparative analyses of LysR amino acid and DNA sequences suggest that LTTRs have developed from a common ancestor. Numerous bacterial species possess LTTRs that have a conserved structure and function. Many bacterial species encode for multiple paralogous LTTRs within one single genome. It is likely that during evolution LTTRs have been acquired by horizontal transfer. The LTTRs usually consist of approximate 330 amino acids and contain a DNA-binding domain at the amino acid terminal residues and a regulatory domain at the carboxyl terminal residues joined by a linker region (Maddocks & Oyston, 2008).

1.3.2 Structure and function of LTTR family proteins

The DNA binding domain of LTTRs is highly conserved at the N terminus, and comprises three α -helices and two β -strands that create a winged-helix-turn-helix (HTH). The HTH can interact with DNA (Maddocks & Oyston, 2008). On the other hand, the C terminus is less conserved and consists of two distinct regulatory subdomains that are also α and β structures.

The flexible hinge or cleft that lies between the regulatory subdomains seems to accommodate the co-inducer domain (Stec *et al.*, 2006). The differential binding ability of LTTRs is correlated to interactions between LTTRs at tertiary structure and their co-inducer (Maddocks & Oyston, 2008).

Interaction sites of a LTTR and its associated gene/operon were identified by using DNA-foot-printing, DNase I protection footprinting and mutagenesis (Maddocks & Oyston, 2008). LTTR proteins can bind internal or close to or far away from upstream of their associated genes as well. Sequences of a DNA-binding box are characterized as an interrupted palindrome and dyad region upstream of genes (Muraoka *et al.*, 2003). In addition, consensus sequences of the box are generally T-N₁₁-A, called a TA-box, but they can differ from base pair composition and length. The LTTR box contains a regulatory binding site (RBS) and an activation-binding site (ABS) (Maddocks & Oyston, 2008). A co-inducer bound a LTTR and its LTTR box at a functionally active form can interact together at different affinity. The affinity may have an effect on preferential binding at the regulatory binding or activation binding sites and leading to the interaction between RNA polymerase and a regulated gene. The presence or absence of a co-inducer bound to several LTTRs can affect the degree of DNA bending which is usually in the range from 9° to 100°. The relaxation of DNA bending from 9° to 50° is caused by the interaction of a co-inducer bound to an LTTR. Interaction between co-inducer bound to its LTTR and DNA-binding box can lead to transcriptional activation or repression (van Keulen *et al.*, 1998; Maddocks & Oyston, 2008). LTTRs can play a role for local or global transcriptional regulation.

Some divergent LTTRs may have an auto-regulatory function due to LTTR boxes appearing on their regulatory binding sites. DNA foot-printing studies suggest that a TA-box at the RBS is able to create the apo-form itself and has a higher affinity than the co-inducer that can bind the tetrameric form (Maddocks & Oyston, 2008).

A number of LTTRs play a role as transcriptional activation and negative auto-regulation. As an example, the LTTR CidR has been well-characterized in *Staphylococcus* spp and *Bacillus anthracis*. It regulates and activates transcription of the *cidABC* operon. This operon plays a role in the metabolism of glucose. A certain level of glucose concentration is a co-inducer for transcriptional activation, and the release of acetic acid, is generated in this pathway, serves as a negative feedback signal for auto-regulation (Yang *et al.*, 2005; Ahn *et al.*, 2006).

Numerous identified LTTRs have been also characterized as transcriptional repressors. For example, CcpC is a global negative regulator of genes encoding enzymes involved in the tricarboxylic acid cycle such as *citB* (aconitase) and *citZ* (citrate synthase). CcpC binds at -66 to -27 regions of *citB* and *citZ* genes and leading to repress transcription. While citrate concentration serves as co-factor, the expression of these genes can be de-repressed (Jourlin-Castelli *et al.*, 2000; Kim *et al.*, 2002, 2003).

LTTRs also can serve as transcriptional repressors or activators and have been characterized as positive auto-regulation. For example, *LrhA* in *E. coli*, *HexA* and *PecT* in *Erwinia* and *YtxR* in *Yersinia enterocolitica* negatively regulate the expression of other transcriptional regulators. These genes involve to the expression of toxin genes such as motility, chemotaxis and toxin.

There is currently no evidence for a regulatory mechanism under environmental changes or co-factor identified. The regulation is related to a global and complex regulatory network (Gibson & Silhavy, 1999; Axler-Diperte *et al.*, 2006; Maddocks & Oyston, 2008).

1.4 Intracellular life cycle of *B. pseudomallei*

Burkholderia pseudomallei is a facultative intracellular pathogen and able to invade, survive and replicate in both phagocytic and non-phagocytic cells (Jones *et al.*, 1996). *Bp* strains lacking certain components of the T3SS3 such as the Bsa protein BsaZ, the translocator protein BipD, or the effectors BopE and BopA show reduced intracellular replication (Stevens *et al.*, 2002; Gong *et al.*, 2011). Once inside the cytosol, *Bp* is able to recruit cellular F-actin to one of its poles. This process is mediated by BimA, a protein required for the initiation of actin polymerization, leading to the formation of actin tails and the intracellular motility of this pathogen (Stevens *et al.*, 2005). *Bp* utilizes the actin-based motility in host cells to form membrane protrusions that enables the pathogen to invade into neighboring cells via a direct cell-to-cell-spread (Gouin *et al.*, 2005; Stevens *et al.*, 2005).

Moreover, *Bp* has also been shown to induce the fusion of host cells, leading to the formation of multinucleated giant cells (MNGCs) that supports bacterial growth inside their host cells (Kespichayawattana *et al.*, 2000). Several studies reported that the T6SS cluster 1 is involved in the induction of MNGCs (Burnick *et al.*, 2011; Chen *et al.*, 2011; Schwarz *et al.*, 2014; Hopf *et al.*, 2014). In recent study, the deletion of *bimA* in *Bp* also abolished the formation of MNGCs. However, deletion of *bpsI1*, 2 and 3 genes related to AHL production showed an induction of MNGCs formation but not increased intracellular replication (Horton *et al.*, 2013). These results suggest that MNGCs might not involve survival in host cells.

It is likely that the ability of intracellular survival might protect the pathogen from extracellular immune responses such as the contact to components of the complement system and the linking to antibodies.

1.5 *In vivo B. pseudomallei* infection models

There are currently several different *in vivo* infection models that are used to study bacterial virulence factors of *Bp* or immunological functions of the host during infection. The slime mould (*Dictyostelium discoideum*), tomato plants (*Solanum lycopersicum*), greater wax moths (*Galleria mellonella*) and nematodes (*Caenorhabditis elegans*) have been used as *in vivo* models for screening virulence of *Bp* (Hasselbring *et al.*, 2011; Lee *et al.*, 2010; Thomas *et al.*, 2013; O'Quinn *et al.*, 2001). However, these models lack a specific immune system that makes it difficult to examine immune responses of the hosts. In addition, transfer results from invertebrates and plants to mammalian hosts are matters of concern. Thus, rodent models such as various inbred mouse strains and the Syrian golden hamster are commonly used, especially for examining innate and adaptive immune functions that play a role in *Bp* infection (Brett *et al.*, 1997; Fritz *et al.*, 1999; Warawa & Woods, 2005; Patel *et al.*, 2011; Choh *et al.*, 2013).

1.5.1 Murine *B. pseudomallei* infection models

BALB/c and C57BL/6 mice are inbred mouse strains and frequently used for experimental infection with *Bp*. These mouse strains clearly differ in their susceptibility against *Bp*. In this context, BALB/c mice are highly susceptible and show a rather acute course of *Bp* infection (Leakey *et al.*, 1998; Liu *et al.*, 2002). In contrast, C57BL/6 mice are relatively resistant against *Bp* infection and often show rather chronic forms of melioidosis such as the development of abscesses (Leakey *et al.*, 1998; Hoppe *et al.*, 1999; Ulett *et al.*, 2000; Liu *et al.*, 2002). In both BALB/c and C57BL/6 mice models, the intranasal (*i.n*) and inhalation (aerosol) infection routes are the most challenging compared to intraperitoneal (*i.p*) or subcutaneous (*s.c*) infection routes (Titball *et al.*, 2008; Lever *et al.*, 2009; Patel *et al.*, 2011).

1.5.2 Experimental vaccines against *B. pseudomallei* infection

There are vivid activities to identify promising vaccine candidates to initiate a protective immune response in *Bp* infected mice. Experimental vaccines against *Bp* can be categorized into three groups such as subunit, inactivated whole cell and live attenuated vaccines. BALB/c mice are widely used in vaccine studies to test experimental immunization procedures including the usage of attenuated *Bp* mutants as live vaccines (Patel *et al.*, 2011; Choh *et al.*, 2013; Silva & Dow, 2013).

Live attenuated vaccines are able to replicate *in vivo* before being removed by the host. Such kind of vaccines is often the most effective vaccines compared to others (Pirofski & Casadevall, 1998; Liljeqvist & Stahl, 1999; Titball, 2008; Patel *et al.*, 2011). Due to a strong stimulation of both humoral and cell-mediated immunity, live vaccines require lesser dose for vaccination and the protection is often sustained for a very long time, even lifetime. However, there are generally concerns about the safety when using live attenuated vaccines due to the risk of reversion to virulence of initially attenuated pathogens. A number of naturally attenuated and genetically modified *Bp* strains have been evaluated for protective effects when being used as a live vaccine in murine infection models. The T3SS3 BipD mutant of *Bp* was tested for protective efficacy. BALB/c mice immunized with the *Bp* BipD mutant strain revealed partial protection against challenge via *i.p* route with *Bp* WT strain (Stevens *et al.*, 2004). In other live vaccine approaches, *Bp* auxotrophic mutant strains have been investigated. BALB/c mice immunized with a mutant defective in capsule polysaccharides (CPS) were partially protected from *Bp* WT challenge (Atkins *et al.*, 2002). BALB/c mice immunized with *Bp* strains harboring defects in either the *purN*, *purM*, *hisF*, *pabB*, *aroB*, *aroC* or *asd* genes, respectively, did also show some degree of protection against virulence challenge (Cuccui *et al.*, 2007; Breitbach *et al.*, 2008; Srilunchang *et al.*, 2009; Norris *et al.*, 2011; Silva *et al.*, 2013).

Due to cytosolic intracellular pathogen, *Bp* possesses various mechanisms for escape from both innate and adaptive immune responses of hosts. Therefore, there is currently no vaccine conferring full protection against *Bp* challenge.

1.6 Aims of the study

Pathogenesis of *Bp* is far away from being completely understood. *Bp* possesses numerous genes that are involved in virulence of the pathogen, from that several have not been examined yet. This study aimed to investigate and characterize two genes that are likely to play a role in *Bp* mediated virulence.

In the first part of this thesis, the function of the putative LysR regulatory gene *BPSL0117* and its role in *Bp* infection are addressed. In preliminary experiments of our working group, it was shown that a transposon mutant harboring a defect in the *BPSL0117* gene was attenuated in BALB/c mice. The transposon mutant should be complemented for further studies. *In vitro* experiments were undertaken to unravel influences of *BPSL0117* on the intracellular life style of *Bp*, biofilm formation, and the induction of actin tails. A proteome analysis should give insights into proteins whose expression is dependent on *BPSL0117*. Furthermore, the putative structure of the *BPSL0117* protein should be predicted using the *in silico* analysis approach. Finally, the *Bp* Δ *BPSL0117* mutant should be applied in a murine immunization model to evaluate putative protective effects of this mutant when being used as a live vaccine.

In the second part of this study, a role of the hypothetical *T3SS3 bapA* gene of *Bp* should be investigated. The *bapA* gene merely shows homology to *T3SS* genes from other bacteria and is located between the translocator and effector genes in the *T3SS3* cluster. First, the expression of all *bap* genes (*bapA*, *bapB* and *bapC*) were examined under salt and pH stress. *BapA* deletion mutants should be derived from two different *Bp* strains and examined for defects in their pathogenic potential. In this context, the biofilm formation, intracellular replication, polymerization of actin tails, as well as expression and secretion of the *T3SS3* proteins *BipD* and *BopE* should be examined. The murine model of melioidosis should be used to test the contribution of the *bapA* locus on the virulence in mammalian hosts during *Bp* infection.

2 MATERIALS AND METHODS

2.1 Bacteria

2.1.1 Bacterial strains

Bacterial strains used in this study are listed in Table 1. *Bp* strains were grown on Luria Bertani (LB) agar with appropriate antibiotics, Columbia blood agar, Ashdown selective agar (Ashdown, 1979) or in LB broth at 37°C. *E. coli* strains were grown on LB agar or in LB broth containing appropriate antibiotics or respective supplements where necessary. If not stated otherwise, antibiotics were added at the following concentrations: 50 µg ampicillin, 50 µg kanamycin, 3,000 µg zeocin and 50 µg polymyxin B per ml. Km^r containing plasmids used for conjugation of *Bp* strains were selected with 1000 µg Km per ml. All experiments with *Bp* were carried out in biosafety level 3 (BSL-3) laboratories.

Table 1. Bacterial strains used in this study

Strain	Relevant genotype or properties	Source or reference
<i>E. coli</i>		
DH5 α	Host for cloning	Invitrogen
XL1-Blue	Host for cloning	Stratagene
RHO3	SM10 (<i>Apir</i>) Δ asd::FRT Δ aph::FRT, Kms; DAP auxotroph	López <i>et al.</i> , 2009
HB101 pRK2013	Mobilizing helper strain for conjugation	Phadnis & Berg, 1987
DH5 α pTNS3	Helper strain for conjugation	Choi <i>et al.</i> , 2008
<i>B. pseudomallei</i>		
1026b	Clinical isolate	Thailand
E8	Environmental isolate	Thailand
K96243	Clinical isolate	Thailand
K96243 Δ bapA #1	Deletion mutant	This study
K96243 Δ bapA #2	Deletion mutant	This study
1026b Δ bapA #3	Deletion mutant	This study
E8 Δ BPSL0117	E8 derived from Tn5-OT182-transposon mutant	Eske-Pogodda, 2010
K96243 Δ bapA#1::Tn7 :bapA1	Δ bapA with chromosomal integrated minTn7::FRT:Zeo-bapA1 orf	This study
K96243 Δ bapA#1::Tn7:bapA2	Δ bapA with chromosomal integrated minTn7::FRT:Zeo-bapA2 orf	This study
E8 Δ BPSL0117::Tn7:BPSL0117	Δ BPSL0117 with chromosomal integrated minTn7::FRT:Zeo-BPSL0117 orf	This study

2.1.2 Preparation of bacterial glycerol stocks

E. coli and *Bp* strains were grown on LB and blood agars at 37°C overnight, respectively. Single colonies were picked and inoculated in 4 ml LB medium. After growth overnight at 37°C in a shaking incubator (140 rpm), glycerol was added to the bacterial suspensions to a final concentration of 30% (v/v) of glycerol. The bacteria were aliquoted into cryoconservation tubes and stored at – 70°C.

2.1.3 Preparation of competent cells

The stocks of *E. coli* DH5 α , XL-1 blue or RHO3 strains were streaked on agar plates or agar plates containing 400 μ g/ml 2,6-diaminopimelic acid (DAP) for the auxotrophic strain RHO3 and incubated overnight at 37°C. Single colonies of each strain were picked and inoculated in 25 ml of LB broth or LB broth supplemented with 400 μ g/ml DAP and incubated at 37°C in a

shaking incubator (140 rpm) for 4 – 6 hours. When the OD_{650nm} reached approximately 0.5, the cells were placed on ice for 10 minutes and harvested by centrifugation at 4°C, 6,000 x g for 3 minutes. Then the pellets were gently resuspended in 10 ml ice-cold 0.1M CaCl₂ and incubated on ice for 20 minutes, and then centrifuged again at 6,000 x g at 4°C for 3 minutes. Washing steps were performed twice to remove remaining cell debris. Bacteria were gently resuspended in 5 ml ice-cold 0.1 M CaCl₂/15% glycerol, aliquoted in 1.5 ml tubes (100 µl/tube) and subsequently frozen in liquid nitrogen and stored at -70°C. The competent ability of bacteria was tested by heat shock transformation.

2.1.4 Adjustment of bacterial dosages

Bp strains were grown on Columbia blood agar overnight at 37°C or in LB broth in a shaking incubator (140 rpm) at 37°C. Bacteria were resuspended in 10 ml sterile phosphate buffered saline (PBS) and adjusted to an OD_{650nm} of 0.25, containing approximately 1,18x10⁸ colony forming unit (CFU) per ml. The bacterial suspension was diluted to the desired bacterial numbers based on calibration curve for further experiments.

2.1.5 Growth kinetics

For growth curve experiments, *Bp* strains were cultured in minimal Vogel-Bonner (VB), minimal M9 or complex nutrient LB broth. Bacteria were adjusted in the respective broth to an initial OD_{650nm} of 0.01 and incubated at 37°C in a shaking incubator (140 rpm). The samples were measured at indicated time points of OD_{650nm}.

2.1.6 Motility assays

Bacteria were grown overnight in LB broth and adjusted to an OD_{650nm} of 0.25 in sterile PBS. One µl of the adjusted bacteria was spotted into soft agar plates (LB broth with 0.3% (w/v) and 0.6% (w/v) agar), and statically incubated at 37°C for 24 and 48 h. The radius of the circular expansion pattern of bacterial migration from the point of inoculation was measured at the indicated time points.

2.1.7 Biofilm assay

Overnight grown bacteria were inoculated to an initial OD_{650nm} of 0.01 in 0.5 ml of the indicated media in 5 ml polystyrene tubes and grown statically at 37°C for up to 48 h. Media were discarded at the indicated time points, and the tubes were washed with sterile water. To stain adherent biofilms, two ml of 1 % (w/v) crystal violet solution was added to each tube and incubated at room temperature (RT) for 15 min. The solution was then discarded and the tubes were washed three times with sterile water to remove unbound crystal violet. Finally, 2 ml of 100% methanol were added to destain biofilms and coloring of the liquid was measured at 540 nm.

2.1.8 Protease assay

Overnight grown bacteria were adjusted at an OD_{650nm} of 0.25 in sterile PBS, spotted 1 µl of the adjusted bacteria onto LB agar plates containing 2% skim milk, and incubated at 37°C for 24h and 48h. The radius of the circular expansion pattern of catalyzed protein from the point of inoculation was measured at the indicated time points. On the other way, the azocasein method was used. Briefly, bacteria were grown overnight in 2ml LB broth and centrifuged at 7,000 x g for 5 min at 4°C before supernatants were collected. 100 µl of supernatants were diluted by serial10 times, mixed with 200 µl of proteinase K (0.5 mg/ml), 50 µl Azocasein (0.02% w/v) and 20 µl Tris-HCl (250 mM, pH 7.5) and then incubated at 37°C for 2 h. The enzyme activity was inactivated by adding 150 µl TCA (10%) to each sample. After incubation for 5 min at RT, the supernatants were collected by centrifugation at 9,000 x g for 5 min and transferred into 96 well plates (120 µl per well) containing 150 µl NaOH (1N). The absorbance of exo-protease activity at 405 nm was measured using Infinite M200 pro spectrophotometer from Tecan.

2.1.9 Antibiotic susceptibility testing

To examine the antibiotic susceptibility of *Bp* strains, overnight grown bacterial strains were adjusted at an OD_{650nm} of 0.25 in sterile PBS. Bacteria were spread onto Müller-Hinton agar plates using sterile cotton swabs. E-test strips Ceftazidime and Imipenem from BioMérieux Company for the determination of minimal inhibition concentrations (MIC) of antibiotics were placed onto the agar plates and bacteria were grown at 37°C. After 24 h incubation and ellipse will appear that intersects the MIC reading scale (in µg/ml) where the concentration of the antibiotic tested inhibits microorganism growth.

2.2 Plasmids

Plasmids used in this study are listed in table 2.

Table 2. Plasmids used in this study

Plasmids	Character	Source or reference
pEX-Km5	Km ^R marker, GusA color marker, flippase recognition target sequence, homing endonuclease (I-SceI), original replication (ColE1), SacB suicide marker optimized for <i>Burkholderia ssp</i>	López <i>et al.</i> , 2009
pEX-Km5-bapAKO	pEX-Km5 vector with 619 bp upstream and 1005 bp downstream of <i>bapA</i> orf	This study
pUC18T-miniTn7::FRT:Zeo	Amp ^R and Zeo ^R resistance markers, FRT sequences	Choi <i>et al.</i> , 2008
pUC18T-miniTn7::FRT:Zeo-bapA1	pUC18T-miniTn7::FRT:Zeo with <i>bapA</i> orf	This Study
pUC18T-miniTn7::FRT:Zeo-bapA2	pUC18T-miniTn7::FRT:Zeo with around 1,000 bp upstream of <i>bapA</i> orf	This study
pUC18T-miniTn7::FRT:Zeo-BPSL0117	pUC18T-miniTn7::FRT:Zeo with <i>BPSL0117</i> orf include around 500 bp upstream of the gene and the operon of <i>B.th</i>	This study

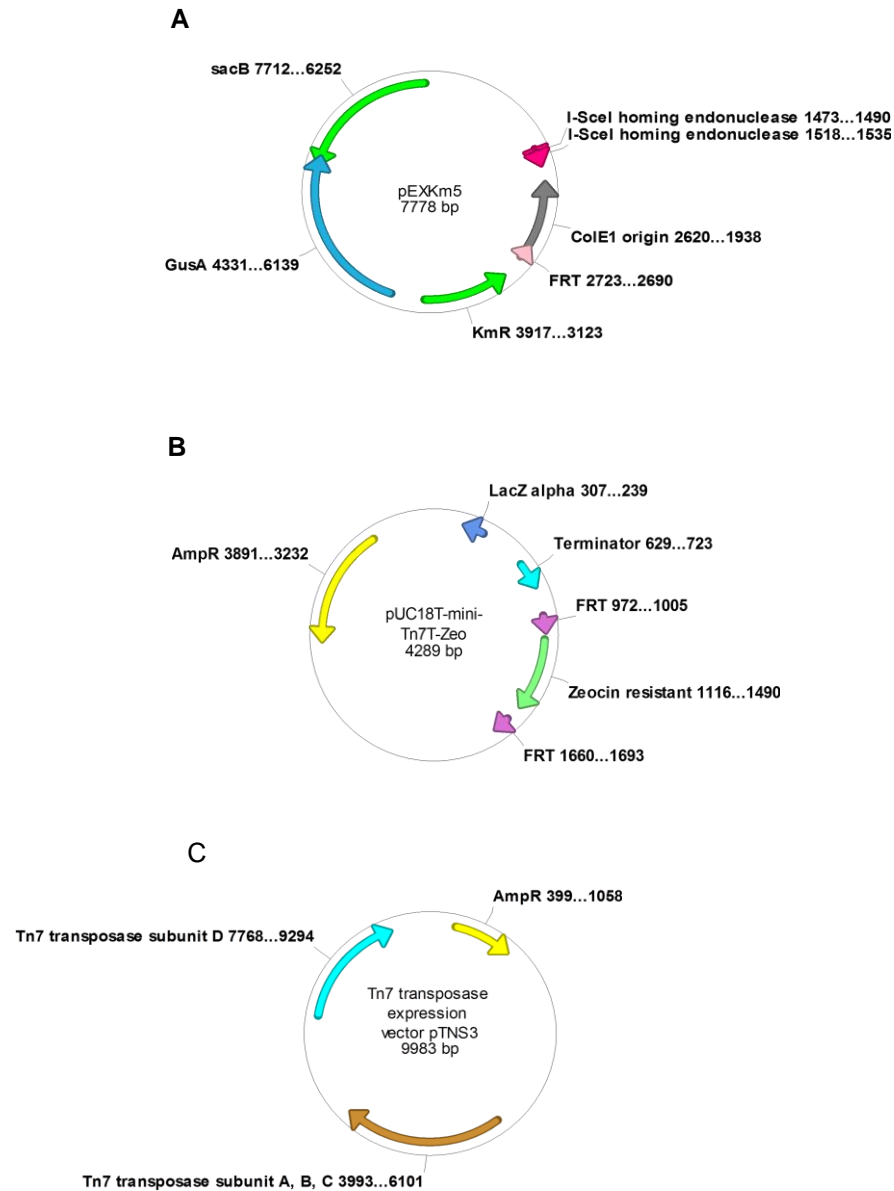


Figure 4. Plasmid maps used in this study. **A:** Dual allelic replacement vector pEXKm5 containing a kanamycin resistance cassette (*Km^R*), beta-D-glucuronidase (*GusA*), levansucrase counter-selection marker (*sacB*), Flp recombinase target site (*FRT*), homing endonuclease (*I-SceI*) and original replication and transcription (*ColE1*) (modified from Lopéz *et al.*, 2009); **B:** pUC18T-mini-Tn7T-Zeo cloning vector for gene complementation including *Flp* recombinase target site (*FRT*), an original replication, dual *Amp^R* and *Zeo^R* resistance cassettes (modified from Choi *et al.*, 2010); **C:** pTNS3 helper conjugation vector containing ampicillin resistance marker and Tn7 transposase subunits (modified from Choi *et al.*, 2008).

2.3 Oligonucleotides

Random Primers for the RT-PCR were from at Promega Company. The other primers were obtained from MWG Eurofins Company (see Appendix V).

2.4 DNA manipulations

2.4.1 Isolation of genomic DNA of *B. pseudomallei*

To isolate total DNA of *Bp*, 2 ml of overnight cultures were harvested in 2 ml safe-seal tubes by centrifugation at 11,000 x g for 1 minute. The bacterial pellets were resuspended in 600 µl of lysis buffer. DNA was separated by adding 600 µl of phenol-chloroform-isoamylalcohol mixture (25:24:1) and centrifuged at 16,000 x g for 5 minutes at 4°C. DNA in the aqueous phase was carefully transferred into new tubes containing 500 µl of chloroform. The tubes were rigorously mixed, and then centrifuged at 16,000 x g for 5 minutes at 4°C. Supernatants were collected into new tubes containing 1 ml of 96% ethanol and 25 µl of sodium acetate 3 M at pH 5.5, and kept at - 20°C for 1 h. DNA was pelleted by a centrifugation step at 16,000 x g for 30 minutes at 4°C. DNA pellets were washed with 500 µl of 70% ethanol, centrifuged at 16,000 x g for 10 minutes at 4°C, air dried and resolved in 50 – 80 µl of nuclease-free H₂O. Genomic DNA was stored at 4°C.

2.4.2 Polymerase chain reaction

Polymerase chain reaction (PCR) was used to amplify targeted genes from purified genomic DNA templates or bacterial colonies. For the cloning of desired genes and orfs, KOD Xtreme™ Hot Start DNA polymerase was used to ease PCR reactions using GC-rich DNA templates. Obtained PCR products contained blunt ends.

Table 3. Xtreme™ KOD PCR mixture

KOD Xtreme™ standard reaction setup		
Component	Volume	Final concentration
2 x Xtreme™ buffer	25 µl	1 x
dNTPs (2 mM each)	10µl	0.4 mM of each
PCR grade water	10 µl	
Forward primer (10 µM)	1.5 µl	0.3 µM
Revert primer (10 µM)	1.5 µl	0.3 µM
KOD Xtreme™ hot start DNA polymerase (1 U/µl)	1 µl	
Template DNA	1 µl	0.02 U/µl
Total reaction volume	50 µl	

Table 4. Xtreme™ KOD PCR running condition

Polymerase activation	98°C for 5 min	
Denature	98°C for 30 s	32 cycles
Annealing	60°C for 30 s	
Extension	68°C for 1 min/kbp	
Final extension	68°C for 5 min	

To check the correct insertion and expression of targeted genes, QIAGEN *taq* PCR kit was mixed with 5x Q-solution due to the high GC-content in the genomic DNA of *Bp* 5x Q-solution helps to change annealing temperature and complex secondary structure of targeted genes. To help amplify rich GC-content fragments, PCRs were also added to final 2 - 4% betaine or DMSO concentration.

Table 5. Reaction setup using *taq* DNA polymerase

Component	Volume	Final concentration
Reaction mix: 10 x PCR buffer Or 10 x CoralLoad PCR buffer	2.5 µl	1 x (contains 15 mM MgCl ₂)
5 x Q-Solution	5 µl	1 x
dNTPs (10 mM each)	0.5 µl	0.2 mM of each
Forward primer (10 µM)	0.75 µl	0.3 µM
Revert primer (10 µM)	0.75 µl	0.3 µM
<i>taq</i> DNA polymerase (1 U/µl)	0.125 µl	2.5 U/reaction
Template DNA	2 µl	
Free-nuclease water	13.375 µl	
Total reaction volume	25 µl	

Table 6. Optimized cycling condition for *Taq* DNA polymerase

Initial denaturation	94°C for 5 min	
Denaturation	94°C for 30 s	35 cycles
Annealing	54-60°C for 30 s	
Extension	72°C for 1 – 1.5 min	
Final extension	72°C for 10 min	

2.4.3 Agarose gel electrophoresis

DNA fragments were separated using agarose gel electrophoresis. 4 – 10 µl of DNA solution were mixed with 6 x DNA loading buffer according to ratio 6:1, and then loaded into each well of a gel. To compare molecular weight of DNA fragments, 5 µl of DNA-ladder were applied as a molecular marker. The electrophoresis was run into 0.5 x electrophoresis buffer under 110 V in 40 minutes. DNA fragments were dyed by using SYBR® safe (1:10,000) and visualized using a UV lamp.

2.4.4 Purification of DNA fragment and gel extraction

Purification of DNA fragments was performed by using the QIAquick PCR purification or QIAquick gel extraction kits (QIAGEN) according to the instructions of the company.

2.4.5 Restriction enzymes and dephosphorylation

DNA and vectors were treated with the same double restriction enzymes of New England Biolabs (NEB) or Fermentas (Thermo Scientific) companies.

Table 7. Restriction mixtures

Option 1	Or	Option 2
4 - 6 µg of purified PCR product or 10 µg of plasmid		0.2 µg of purified PCR product or 1 µg of plasmid
6 µl optimal 10x reaction buffers		2 µl universal 10x reaction buffers
0.6 µl of 100x BSA		1 µl restriction enzyme 1
40 U restriction enzyme 1		1 µl restriction enzyme 2
40 U restriction enzyme 2		1 µl fast AP (only for dephosphorylation of plasmid)
X µl of H ₂ O is up to total 60 µl		X µl of H ₂ O is up to total 20 µl

The mixture was incubated at 37°C for 30 min with fast digestion or at least 1 h for NEB enzymes. The activities of enzymes were inactivated by heat. To remove remaining proteins and element traces, QIAquick PCR purification kit was used to purify PCR products and plasmids. Additionally, cut plasmids in option 1 were dephosphated at 5' end by alkaline phosphatase following below formula.

Table 8. Dephosphorylation mixtures

DNA premix:	Enzyme premix:
5 µl of free DNase water	6 µl of free DNase water
5 µl of 10x AP buffer	1 µl of 10x AP buffer
40 µl of lineared Plasmid	3 µl of AP

The reaction of dephosphorylation was performed at 37°C for 1 hour and then inactivated by heating at 65°C for 15 minutes.

2.4.6 Ligation

The ligation of DNA and plasmids treated were carried out by T4 DNA ligase.

Table 9. Ligation mixture

5x T4 DNA ligase buffer	2 µl
Treated plasmid	50 – 100 ng
Insertion DNA	1:1 to 5:1 molar ratio over vector (depend on blunt or stick ends)
T4 DNA ligase	5 U
Free nuclease water	Up to 10 µl

The mixture was incubated at 22°C for 30 min with fast ligation or 4 - 8°C overnight. The ligase enzyme was inactivated at 65°C for 10 minutes.

2.4.7 Heat shock transformation

Chemical competent bacteria were taken and thawed on ice for 15 min. 5 µl of the ligation mixture were added to 100 µl of competent cells, incubated at 42°C water bath for 45 seconds, and immediately put on ice for 3 minutes. The transformed bacteria were pre-inoculated with 200 µl of pre-warm LB broth, at 37°C for 1 h, then plated on an appropriate selective agar and incubated overnight at 37°C. Single grown colonies were picked and insertion was tested by colony PCR or restriction of plasmids after plasmid purification.

2.4.8 Mini-preparation of DNA plasmid

Single colonies were picked from agar plates, inoculated 3 ml LB containing appropriate antibiotics or/and supplements and then incubated overnight at 37°C and 220 rpm. The bacterial cells were collected by centrifugation at 13,000 x g for 1 minute. The pellets were resuspended in 300 µl of buffer 1. 300 µl of alkaline lysis buffer 2 were added and the mixture was incubated at RT for 5 minutes. 350 µl of buffer 3 were added to neutralize the lysate and precipitate proteins. Following centrifugation at 12,000 x g and 4°C for 5 minutes, supernatants were collected into fresh tubes containing 600 µl Isopropanol. Mixture was vortexed and centrifuged at 13,000 x g, 4°C for 12 minutes. DNA pellets were washed with 500 µl of 70% ethanol, centrifuged at 13,000 x g, 4°C for 5 minutes and dried on air.

Alternatively, PeqGOLD Plasmid miniPrep kit (PeqLab) was used to purify plasmids. DNA pellets were diluted in 50 µl of nuclease-free water and DNA concentration was measured at 260 nm.

2.5 Mutagenesis and complementation of *B. pseudomallei* genes

2.5.1 Construction of knockout mutants

The selective mutagenesis of *bapA* gene (BPSS1528) was successfully performed as previously described (López *et al.*, 2009). Briefly, 600 – 1,000 bp homolog sequences of up and down stream of the *bapA* gene were cloned into an allelic replacement pEXKm5 vector

and verified by PCR and sequence. pEXKm5- Δ bapA plasmid was transformed into *E. coli* RHO3 by heat shock and selected on LB plates containing 50 μ g Km and 400 μ g DAP per ml.

2.5.2 Conjugation

Both donor *E. coli* RHO3 and recipient *Bp* strain were grown overnight at 37°C in a shaking incubator (140 rpm) in 3 ml of LB medium containing 400 μ g of/ml DAP and 50 μ g/ml kanamycin (RHO3) or 3 ml of LB medium (*Bp*), respectively. 100 μ l of each culture were mixed in sterile 1.5 ml tubes and washed twice with 1 ml of 10 mM MgSO₄ followed by centrifugation at 7,000 x g for 2 minutes. The pellets were resuspended in 30 μ l of 10 mM MgSO₄. The bacterial mixture was applied to a cellulose acetate membrane filter (0.45 μ m pore size; Ø 13mm) on a pre-warmed LB agar plate containing only 400 μ g/ml DAP and the plate was incubated at 37°C for 8 – 18 hours. The membrane was transferred to a 2 ml safe-seal tube containing 1.5 ml of LB and then centrifuged at 7,000 x g for 2 minutes to dislodge the bacteria. The supernatant was discarded, the bacterial pellet was washed in 1 ml of LB broth to remove DAP residues. After centrifugation, cells were resuspended in 200 μ l of LB, diluted serial 10-fold, plated on selective LB agars containing 1 mg/ml Kanamycin and 100 μ g/ml X-Gluc and incubated at 37°C for 2 days.

2.5.3 Isolation of markerless mutants

Single blue colonies appeared after conjugation and 2 days incubation at 37°C were picked and streaked on yeast tryptone (YT) agar plates including 15% sucrose and 100 μ g/ml X-Gluc and then incubated at 25°C for 3 days for selection of mutants that lost the plasmid backbone. Single white colonies were then picked up and grown overnight in 3 ml of LB medium at 37°C with shaking at 140 rpm. The allelic exchange (successful mutagenesis) was confirmed by PCR with forward primer upstream and reverse primer downstream of *bapA* gene. Additionally, the elimination of pEXKm5 backbone vector was confirmed by streaking the colonies on agar plates containing 1 mg/ml Km.

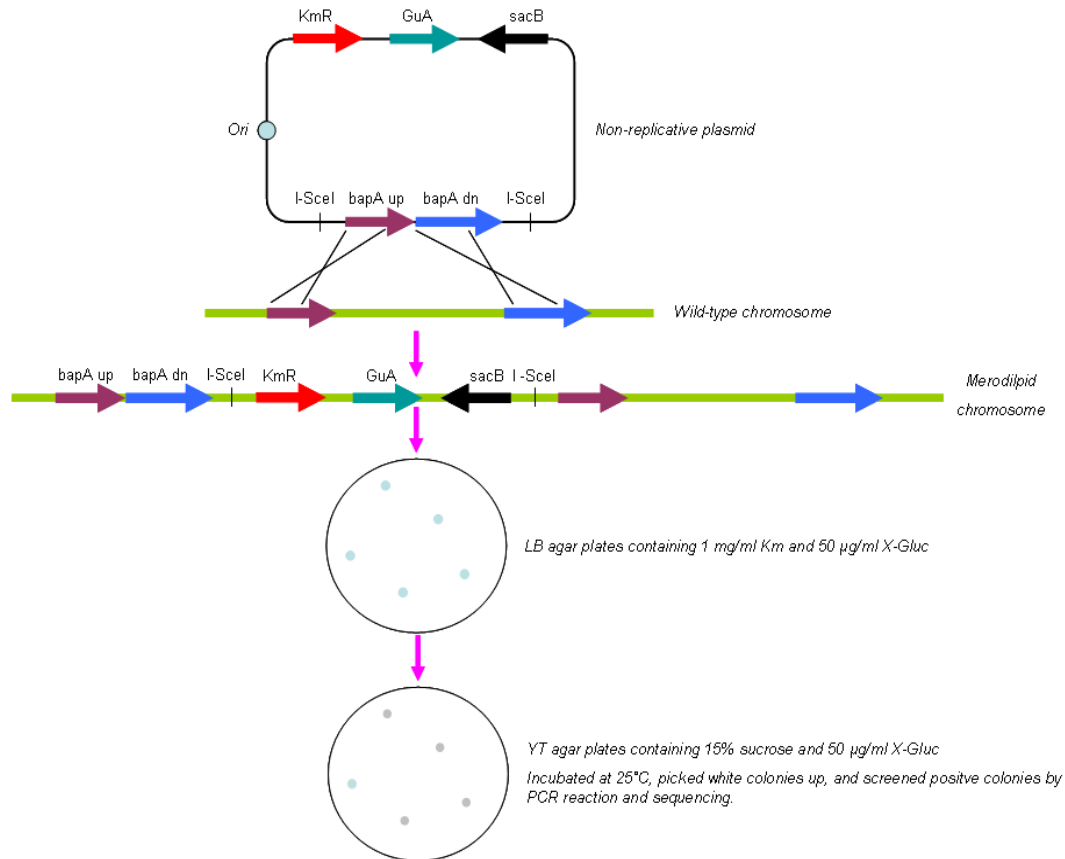


Figure 5. Schematic of allele replacement procedure. For allelic exchange, up and down streams of *bapA* genes were cloned into pEXKm5 plasmid. The plasmid was delivered to the host *Bp* strains by conjugation. The integration of plasmid and host chromosome was a result that mating colonies were able to grow and appear blue on 1 mg/ml Km and 50 µg/ml X-Gluc-containing LB agar plates. For *sacB*-mediated counter-selection, the merodiploid strains were directly streaked onto YT agar containing 15% sucrose and 50 µg/ml X-Gluc. During this suicide step, bacterial genotypes would either revert to wild type or result in deletion of the target gene (modified from López et al., 2009).

2.5.4 Complementation

To complement *Bp* $\Delta bapA$ and *Bp* $\Delta BPSL0117$ the mini-Tn7 system was used as recently described (Choi *et al.*, 2008). The primers were used to amplify the ORFs *BPSS1528* of *Bp* WT K96243 and ORF *BPSL0117* of *Bp* WT E8 by PCR using genomic *Bp* DNA as template (Appendix E). Following amplification and digestion with the appropriate restriction enzymes, the fragments were cloned into the pUC18T mini-Tn7T-Zeo vector, and transformed into *E. coli* DH5 α . Recipient *Bp* $\Delta bapA$ or *Bp* $\Delta BPSL0117$ strains were conjugated with donor *E. coli* DH5 α pUC18T mini-Tn7T-Zeo-BPSS1528 or *E. coli* DH5 α pUC18T mini-Tn7T-Zeo-BPSL0117, respectively, and two *E. coli* helper strains *E. coli* HB101 (pRK2013) and *E. coli* DH5 α (pTNS3). Bacteria were selected on LB agar plates containing 3,000 µg zeocin and 50 µg polymyxin B per ml. Successful insertions of *bapA* and *BPSL0117* genes in the recipient strains *Bp* $\Delta bapA$ and *Bp* $\Delta BPSL0117$ were verified by PCR. The miniTn7-elements were transposed to the *attTn7* site downstream of the glutamine-6-phosphate synthase encoding genes *glmS1* or/and *glmS2* or/and *glmS3* on chromosome as verified by PCR.

2.6 Protein manipulations

2.6.1 Protein preparation with Trizol

To purify total proteins bacterial cells or mammalian host cells infected with bacteria were treated with 0.5 – 1 ml of Trizol reagent and incubated at RT for 10 min. Lysates were transferred to 2 ml tubes and 1-Bromo-3-chloropropane (100%) was added to 10% final concentration. The mixture was vortexed for 15 seconds, incubated at RT for 10 min and centrifuged at 12,000 x g for 15 min at 4°C to separate into a lower red phenol-chloroform phase, an interphase, and a colorless upper aqueous phase.

The red phase containing the protein was collected in 2 ml tubes, 300 µl (per 1 ml Trizol) 100% ethanol were added, mixture was inverted, incubated at RT for 3 min and centrifuged at 2,000 x g for 5 min at 4°C. The supernatant was collected in 1.5 ml new tube containing 600 µl isopropanol (100% v/v), inverted and kept at RT for 10 min. Proteins were precipitated by centrifugation at 12,000 x g for 10 min at 4°C. Protein pellets were washed three times with 0.3 M guanidine hydrochloride in 95% ethanol for 20 min. After this 2 ml 100% ethanol was added, vortexed rigorously, incubated again at RT for 20 min, and centrifuged at 7,500 x g for 5 min at 4°C. The supernatants were removed and the pellets were dried in a speed vacuum machine for 3 - 5 min or on air. The protein pellets were resuspended in appropriate volume of 2D lysis buffer and stored at - 20°C until to use.

2.6.2 Protein preparation by ribolyser method

For preparation of cell extracts, bacteria were grown in M9 medium. At different optical densities ($OD_{650} = 0.5$ and 4), cells of 1000-ml cultures were separated from the supernatant by centrifugation (8,000 x g) for 10 min at 4°C, washed twice with ice-cold TE buffer (10 mM Tris-HCl, 10 mM PMSF, pH 8.0), and resuspended in 1 ml TE buffer. The cells were disrupted by homogenization using glass beads and MagNA Lyser machine for 30 s at 6.5 m/s. Afterwards the lysate was centrifuged for 25 min at 21,000 x g at 4°C in order to remove cell debris, then for 45 min at 21,000 x g at 4°C in order to remove insoluble and aggregated proteins. The supernatants were filtered using 0.22 µm pore size filter and 10 µl of each sample were used to control of sterility by incubation in 4 ml LB broth at 37°C and 140 rpm for three days. In order to remove membrane fragments, the lysate was centrifuged 30 min at 100,000 x g at 4°C. Obtained protein samples were stored at - 20°C until use. To prevent proteases activity, all steps were performed on ice.

2.6.3 Purification of extracellular protein

For analysis of BipD and BopE secretion as well as total extracellular protein, overnight grown *Bp* were adjusted in 50 ml LB to an OD_{650} of 0.01 and incubated at 37°C with shaking at 140 rpm. Supernatants of bacterial cultures were harvested at indicated time points or OD_{650nm} values by centrifugation at 6,500 x g for 10 min at 4°C. Proteases in supernatant were inhibited by using one tablet of Complete™ Mini Protease inhibitor cocktail (Roche).

Extracellular proteins were precipitated by adding Trichloride acetic acid (TCA) to 10% final concentration. After incubation at 4°C overnight, proteins were collected by centrifugation at 8,800 x g for 10 min at 4°C. Precipitated proteins were washed three times with 96% ethanol and once with 70% ethanol followed by centrifugation at 8,800 x g at 4°C for 10 min. Air-dried protein pellets were resuspended in 8M urea/2M thio urea and stored at -20°C.

2.6.4 Bradford protein quantification

Bradford method was used to quantify total proteins concentration. Principle of this method is the reaction of proteins with coomassie brilliant blue G-250 dye leading to colorimetric changes. Mixture of 100 µl diluted protein and 1.9 ml filtered Bradford reagent or mixture of 800 µl of diluted protein in PBS and 200 µl of 5 x Roti®-quant were incubated at RT for 5 min, but no longer 30 min and absorption was measured at 595 nm. Standard curve was built within a rank from 1 to 20 µg of bovine serum albumin (BSA). The protein concentration was determined by comparing to the standard curve.

Table 10. Bradford reagents

Chemicals	Composition
Coomassie Brilliant Blue G-250	100 mg
Ethanol	50 ml 96%
Phosphoric acid	100 ml 85% (w/v)
H ₂ O	Up to 1 liter

The Bradford reagent was stored in dark and filtered before use.

2.6.5 SDS polyacrylamide mini gel electrophoresis

Using discontinuous SDS-PAGE method proteins were separated based on their molecular weight. For this purpose, 40-50 µg of total proteins were diluted in respective buffer and mixed with 4 x loading buffer in 25 µl of final total volume. These mixtures were loaded onto a 12% polyacrylamide gel. Molecular weights were estimated by comparing to 5 µl of pre-stained protein marker line.

Table 11. Composition of one mini polyacrylamide gel used

Composition	Separating gel (12%)	Stacking gel
H ₂ O	1.65 ml	1.4 ml
Buffer	1.25 ml separating buffer	0.25 ml stacking buffer
Acrylamide (30%) and bis-acrylamide (0.8%) mixed	2 ml	0.8 ml
SDS (10%)	50 µl	25 µl
APS (10%)	50 µl	25 µl
TEMED	5 µl	2.5 µl

The gel was run in 1 x SDS-PAGE running buffer following procedures: 120 V for 15 min and then 150 V for 120 min.

2.6.6 Western blot

After equal amounts of total proteins were separated by SDS-PAGE, the proteins were transferred onto nitrocellulose membranes by semidry electro-blotting at 1 mA current per 1 cm² gel area for 1 h. For this purpose, the order of layer for blotting were initially three Whatman papers and SDS gel absorbed cathode buffer, one nitrocellulose membrane and one Whatman paper soaked in anode buffer II, and finally two Whatman papers equilibrated in anode buffer I. Air bubbles between the layers were removed by rolling.

Table 12. Procedure of western blot

(-) Cathode	Soaked in buffer
3 x Whatman filter paper	Cathode buffer
Gel	Cathode buffer
Nitrocellulose membrane	Anode buffer II
1 x Whatman filter paper	Anode buffer II
2 x Whatman filter paper	Anode buffer I
(+) Anode	

After blotting step, the transfer efficiency was controlled by staining membranes with Ponceau S solution. The membranes were then destained by rinsing in water and 1 x TBS buffer, and subsequently blocked in 1 x Roti-block at RT for 1 h. To detect specific proteins, the membranes were incubated overnight at 4°C with proper primary antibodies. Next day, unbound primary antibodies were removed by washing three times with TBST buffer for 5 min. Subsequently horseradish peroxidase conjugated anti-rabbit IgG antibody was used as secondary antibody at RT for 1 h. Again, membranes were washed three times with TBST buffer for 5 min and incubated with 10 ml LumiGlo™/Peroxide mixture at RT for 2 – 3 min. Meanwhile the linked peroxidase enzyme activity cleavages the substrate and chemiluminescence signal was analyzed by using the Fusion FX 7 machine and Fusion 1 software.

Table 13. Antibodies used for western blot analyses

Antibody	Dilution	Incubation
BopE	1:2,000 in TBST buffer plus 1% BSA	4°C overnight
BipD	1:2,000 in TBST buffer plus 1% BSA	4°C overnight
Anti-rabbit- IgG, HRP-conjugated™	1:5,000 in 1 x Roti ®-Block	RT for 1 h
Anti-mouse-IgG, HRP-conjugate™	1:7,000 in 1 x Roti ®-Block	RT for 1 h

2.7 Quantitation of cytoplasmic proteins by using stable isotope labelling with amino acids in cell culture

2.7.1 Preparation of a heavy-labelled *B. pseudomallei* protein standard

Overnight cultures and subsequent main cultures of *Bp* strains E8 and Δ BPSL0117 were grown in minimal M9 broth supplemented with 1 mM stable isotope-labeled lysine and arginine ($^{13}\text{C}_6^{15}\text{N}_2$ -L-lysine/lys-8 and $^{13}\text{C}_6^{15}\text{N}_4$ -L-arginine/arg-10, Silantes). Cells were harvested at $\text{OD}_{650\text{nm}}=0.5$ and $\text{OD}_{650\text{nm}}$ approx. 4 and labeling efficacy was tested by an in-solution tryptic digest and ESI HPLC MS/MS and determined to be greater than 90% for both heavy amino acids under all conditions. A heavy-labeled reference mix was generated by mixing protein extracts from wild type and mutant strains in equal protein amounts and used as 'spike-in' standard for all replicates of bacterial cultures grown in standard media.

2.7.2 Sample preparation for proteomic analysis

Equal protein amounts (10 μg) from cell lysates of all sampling points were mixed with the heavy-labeled protein standard in a ratio of 1:2. Proteins were separated with SDS PAGE and gel lanes were cut into ten slices. In-gel digestion of proteins and extraction of peptides were performed following standard protocols. Samples were cleaned-up using C18 StageTips (Thermo Scientific) following manufactures' instructions.

2.7.3 Mass spectrometry and data analysis

LC-MS/MS analyses were performed using an EASY-nLCII nanoflow HPLC system coupled directly to an LTQ Orbitrap Velos Pro hybrid mass spectrometer (Thermo Fisher Scientific). Peptide samples were dissolved in 20 μl 5 % (v/v) acetonitrile, 0.1 % (v/v) acetic acid and loaded onto a 20 cm-long self-packed C18 (Aeris Peptide 3.6 μm , pore size 100 \AA ; Phenomenex) analytical column. Gradual elution of peptides was achieved by running a binary linear gradient from 1 % (v/v) acetonitrile/0.1 % (v/v) acetic acid to 75 % (v/v) acetonitrile/0.1 % (v/v) acetic acid over a period of 46 with a flow rate of 300 nl/minute. The MS was operated in data-dependent mode, automatically switching between full survey scan (m/z 300-1600) with a resolution of 30,000 followed by fragmentation analyses of the top 10 precursors with a charge state greater than one using collision induced dissociation (CID). Fragmentation by CID was performed in the linear ion trap with an AGC target value of 5×10^3 ions and normalized collision energy of 35%. Precursors were dynamically excluded for repeated fragmentation for 30 s.

Resulting spectra were analyzed with MaxQuant version 1.3.0.5, which includes the Andromeda search engine h. Briefly, the MS spectra of all measurements were searched against a *Bp* protein database extracted/received from Δ BPSL0117 and E8 WT. Key search parameters were set as follows: Variable methionine oxidation, fixed carbamidomethylation; heavy labels arg-10 and lys-8; false discovery rate cut-offs for identifications were set to 1 % at modification site, peptide and protein level. 'Match between runs' and 'Re-quantify' functions

were enabled. Proteins in the output tables were only considered if at least one unique peptide was identified.

Protein quantification was carried out using summed-up peptide intensities provided in the 'protein groups' output table in MaxQuant. Global normalization of intensities was performed based on the spike-in heavy standard. Intensity-based ratios were calculated for *Bp* ΔBPSL0117/E8 WT at OD0.5 and OD approx. 4. Proteins with an at least 2-fold change in at least 2 of 3 biological replicates were considered as significantly altered.

2.8 RNA manipulations

2.8.1 RNA preparation

For analyses of bacterial gene expression in infected macrophages, RAW264.7 cells were infected in 6-well cell culture plate. The day before of infection RAW264.7 were seeded 650,000 cells per well in 2.5 ml of medium and incubated overnight at 37°C and 5% CO₂. The infection procedure was performed as described above with an MOI of 100 at 37°C and 5% CO₂ for 30 min. Cells were then washed twice with sterile PBS, 2.5 ml medium containing 250 µg/ml kanamycin were added to each well before plates were further incubated at 37°C and 5% CO₂. After 2 h and 5 h, the medium was removed; the cells were washed twice with PBS and lysed in 0.5 ml of Trizol reagent per well. Moreover, bacteria were grown in LB broths and harvested at indicative time points or OD_{650nm} value by centrifugation at 6,500 x g for 10 minutes at 4°C. The bacterial pellets were also lysed in 1.5 ml Trizol. After 5 min incubation at RT, the lysates were collected in 2 ml safelock tubes and stored at – 20°C prior to use.

The colorless upper aqueous phase was carefully collected to 1.5 ml tubes containing 1.5 ml of isopropanol and mixed by inversion. Total RNA was precipitated by incubation at RT for 10 min followed by centrifugation at 12,000 x g for 5 min at 4°C. After supernatant has been removed, RNA pellets were washed with 1 ml of 70% ethanol and centrifuged at 12,000 x g for 5 min at 4°C. RNA pellets were dried on air, solved in 22 µl of nuclease-free water and stored at – 20°C.

2.8.2 DNase I treatment of RNA

To remove contingent residues of genomic DNA from RNA samples, 2 µg of total RNA were treated with 2 U DNase I in the appropriate 1x buffer and a total volume of 20 µl at 37°C for 45 min. DNase I activity was inactivated by adding 2 µl of 50 mM EDTA and incubation at 65°C for 10 min.

2.8.3 Reverse transcription

To generate single-stranded complementary DNA (cDNA) from RNA the Moloney murine leukemia virus reverse transcriptase (MLV-RTase) was deployed and random hexamer primers were utilized to provide a starting point with a free 3'- end hydroxyl group. For hybridization, 500 ng of random primers were added to 1.1 µg RNA in a total volume of 12 µl and incubated at 65°C for 5 min. Tubes were then kept on ice for 10 min. The mixture

including 4 µl of 5x M-MLV Reverse transcriptase buffer, 1 mM dNTPs, 20 U RNasin®, 200 U M-MLV Reverse transcriptase and nuclease-free water up to final 20 µl was added into tubes. The reverse transcription was performed at 42°C for 1 h. Subsequently, the enzyme activity was inactivated at 70°C for 10 min. cDNA was stored at – 20°C.

2.8.4 Semi quantitative expression analysis

For the semi quantitative expression analysis, cDNA obtained from 40 – 100 ng RNA served as a template of PCR reaction using *peqGOLD Taq* DNA polymerase. Primers were selected for amplification of DNA sections from 161 to 298 bp. As a control for using equal amounts of cDNA, PCR was performed for target genes and 23S rRNA in parallel.

2.9 Experiments with mammalian cells

2.9.1 Cultivation of mammalian cell lines

Table 14. Cell lines and their cultivation conditions

Name	Cell type	Source	Cultivation
HeLa	Human cervical carcinoma cell line	Friedrich Loeffler Institute for Medical Microbiology, University of Greifswald	DMEM with 10% FCS
RAW264.7	Murine macrophage leukemia cell line	Prof. Walther, Institute for Medical Biochemistry and Molecular Biology, University of Greifswald	RPMI1640 with 4% panexin
HepG2	Human hepatocellular carcinoma cell line	DSMZ	RPMI1640 with 10% FCS

All cell lines were incubated at 37°C in an atmosphere containing 5% CO₂. For harvesting RAW264.7 cells, a cell scraper was used to gently remove the cells from the surface. To harvest HeLa and HepG2 cells, cells were treated with 1.5 ml of 0.05% trypsin-EDTA at 37°C for 5 min and detached cells were resuspended in the respective medium. For passaging, one ml of the harvested cell suspension was transferred into a new flask containing 19 ml medium. All cell lines were passaged maximum 30-times.

2.9.2 Generation and cultivation of primary murine bone marrow macrophages

Murine bone-marrow-derived macrophages (BMMs) were cultivated under serum-free conditions. BALB/c mice were euthanatized and killed by cervical dislocation. Tibias and femurs were aseptically removed, dissected free of adherent tissue, disinfected in 70% ethanol for at least 5 minutes and then transferred into sterile pyrogen-free PBS buffer. The bone ends were

cut and marrow was flushed out with 5 ml sterile PBS. Cells were pelleted by centrifugation conditions by using Panexin BMM[®] as a serum supplement (Eske *et al.*, 2009). To obtain at 450 x g for 15 minutes, cells were resuspended in the serum-free medium and seeded in three 75 mm² flasks with 20 ml of RPMI medium containing 5% Panexin BMM[®], 2 ng/ml recombinant murine granulocyte-macrophage colony-stimulating factor (GM-CSF) and 50 µM mercaptoethanol. Cells were incubated at 37°C and 5% CO₂ and fed on day 5 and 7 by replacing 10 ml with fresh medium. Cells were harvested on day 10 for further experiments. For this purpose, the medium was removed and cells were washed twice with sterile PBS, treated with 1.5 ml of 0.05% Trypsin-EDTA for 10 – 15 minutes at 37°C and detached in 5 ml fresh medium by using a cell scraper. Cell were then centrifuged at 450 x g for 15 minutes and washed with PBS to remove the remaining Trypsin. Following centrifugation, cell pellets were resuspended in 3 ml of BMM medium. Cell numbers were enumerated as described in chapter 2.8.3 and then seeded into well-plates as indicated in the respective experimental procedures.

2.9.3 Counting, seeding and maintaining cell lines

For the enumeration of cells, HeLa, RAW264.7, HepG2, and BMM-BALB/c cells were performed after staining of cells with 0.4 % trypan blue using a Neubauer counter chamber. Unstained blue cells were counted in bright field microscope with 100 x magnified. Numbers of cells were calculated as following:

$$\text{Cell numbers in ml} = \frac{\text{Counted cell numbers} * \text{dilution factor (from 2 to 5)} * 10.000}{\text{Total numbers of areas counted}}$$

Counted cell numbers is defined as numbers of cells in 16 largest squares of counter chamber. For cryo-conservation, cells that were cultivated and covered whole area in 175 cm² flask as monolayer were harvested by centrifugation at 450 x g for 10 min. Cells were resuspended in the respective medium containing 10% DMSO and aliquoted into cryo-tubes with one ml per tube. Cells were frozen at -70°C overnight and stored in liquid nitrogen for the long-term storage.

2.9.4 Infection of mammalian cells

For the infection of cells, *Bp* strains were grown overnight on blood agar plates at 37°C or in 4 ml LB broth at 37°C in a shaking incubator overnight. The bacterial suspensions were adjusted to an OD_{650nm} of 0.25 in sterile PBS and bacteria were adjusted to the desired multiplicity of infection (MOI) in the respective medium.

2.9.5 Invasion and intracellular replication assays

For invasion and intracellular replication assays, cell lines were seeded in 48-well cell culture plates one day prior to infection (90,000 cells/well for HeLa or RAW264.7 cell lines, 150,000 cells/well for BMM-BALB/c). Cells were infected with the adjusted *Bp* strain suspensions. When infecting BMM, the infected cells were centrifuged at 120 x g for 4 min. Infected cells

were incubated for 30 min at 37°C and 5% CO₂. Cells were then rinsed with sterile PBS three times to eliminate extracellular bacteria and 400 µl of medium containing 120 µg/ml kanamycin were added to each well. Time zero (0 h) was defined after 20 min incubation time under kanamycin-containing medium. At indicated time points, the medium was removed, cells were washed twice with PBS and lysed with 150 µl of 1% (v/v) tergitol/0.5% (w/v) BSA in PBS or 150 µl of 1% (w/v) saponin/0.5% BSA (w/v) in PBS at 37°C, 5% CO₂ for 10 min. Cell lysates were diluted by serial 10-time in PBS and 100 µl of diluted samples were plated on agar plates in triplicate. After incubation at 37°C for 2 days, the numbers of single colonies on each plate were counted and the final CFU at each time point was calculated.

2.9.6 Actin tail formation assay

One day prior to infection, HeLa or HepG2 cells were seeded on cover slides (ø 13mm) coated with rat tail collagen type I (4 mg/ml, Sigma-Aldrich, Germany) in 24 well plates (1,2 x 10⁵ cells per well). Cells were infected at an MOI of 100 with the indicated *Bp* strains. After infection, cells were centrifuged at 400 x g for 4 min to allow bacteria to attach to the cells. After incubation at 37°C and 5% CO₂ for 30 min, infected cells were washed three times with sterile PBS and kanamycin containing medium (250 µg/ml) was added. At indicated time points, nuclei of living cells were stained with 1 mg/ml Hoechst 33342 fluorescence dye (Invitrogen, Germany) in H₂O at 37°C and 5% CO₂ for 10 min. Medium was removed and cells were washed three times with sterile PBS and fixed with 1 ml cold methanol at – 20°C for 10 min or overnight. Cells were then washed three times with IF buffer (0.5% (w/v) BSA, 0.1% sodium azide in PBS buffer) to remove methanol and trace elements. Subsequently, cells were incubated with the monoclonal mouse anti-*Bp* EPS 3015 γ2b (1:2000; Steinmetz *et al.*, 1995) and polyclonal rabbit anti-β-actin antibodies (1:100; Cell Signaling, Frankfurt am Main, Germany) overnight at 4°C. Cells were then washed three times with IF buffer and stained with Alexa Fluor® 488 goat anti-mouse IgG2b (1:800, Invitrogen, Darmstadt, Germany) and Alexa Fluor® Cy3-conjugated goat anti-rabbit IgG (1:400; Dianova, Hamburg, Germany) at RT for 1 h. Stained cells were washed three times with IF buffer and mounted to slides by using Fluoprep. Intracellular bacteria and their association with cellular actin filaments were visualized by using the fluorescence microscope BZ-9000 with BZ-image viewer and BZ-analyzer software version 1.4.

2.10 *In vivo* infection experiments

2.10.1 Bioethics

Specific pathogen-free 6 – 8 week old female BALB/c mice were obtained from Charles River Laboratories (Sulzfeld, Germany). A maximum of five animals were housed in micro-isolator cages and were fed with food pellets (sniff) and water *ad libitum*. All the animal experiments described in the study were conducted in strict accordance with the recommendations in the Guide for the Care and Use of Laboratory Animals of the National Institutes of Health. All animal studies were conducted under a protocol approved by the Landesamt für

Landwirtschaft, Lebensmittelsicherheit und Fischerei Mecklenburg-Vorpommern (LALLF M-V; 7221.3-1.1-020/11). All efforts were made to minimize suffering and ensure the highest ethical and human standards. The *in vivo* infection procedures were conducted by Dr. med. Katrin Breitbach.

2.10.2 Infection procedures

Prior to intranasal infection, procedures mice were anesthetized with 100 mg/kg ketamine and 10 mg/kg xylazine by intraperitoneal injection. Bacteria were cultured overnight in LB broth, adjusted to an OD_{650nm} of 0.25 (containing approximately 1×10^8 CFU per ml) in PBS and diluted to the desired concentration. Mice received either 30 µl of the bacterial suspension via the intranasal route, or were infected with 100 µl via the intraperitoneal route or received 200 µl when infected intravenously. Mice were monitored daily after infection.

2.10.3 Determination of the bacterial load in internal organs

Lungs, livers and spleens of infected BALB/c mice were aseptically removed at the indicated time points. Organs were placed in 5 ml tubes containing 1% tergitol/0.5% BSA in PBS. Organs were homogenized, serially diluted in PBS and plated on Ashdown agar plates. After incubation at 37°C for 2 - 3 days, grown colonies were count and the number of bacteria in one organ was calculated. Remaining undiluted homogenates were added to 3 ml of LB broth, incubated at 37°C in a shaking incubator (140 rpm) for 3 days, and plated on Ashdown or LB agar to check sterility in case there was no growth from the diluted organ suspensions. Data are presented as the total bacterial count per organ.

2.10.4 Immunization procedures

To examine whether application of the attenuated *Bp* strain lacking the *BPSL0117* gene might confer protection against challenge with the *Bp* WT strain, mice were intranasally immunized (see chapter 2.9.2) with *Bp* Δ*BPSL0117* using the indicated doses. Control mice received sterile PBS. Four weeks later, vaccinated and control-vaccinated mice were challenged with *Bp* WT E8 via the intranasal route, intravenous route, or intraperitoneal route with different doses as described in each experiment.

2.10.5 Detection of anti-*Bp* antibodies in the serum

To examine the presence of specific anti-*Bp* antibodies in immunized and control animals, blood was collected from the retro orbital sinus (retro bulbar) three weeks after immunization procedures. Blood was allowed to clot for 30 min at 4°C, and then centrifuged at 5000 x g for 2 min and serum samples were collected and stored at -20°C prior to use. Anti-*Burkholderia* IgG titers were quantified by using ELISA.

2.10.6 Enzyme linked immunosorbent assay (ELISA)

Overnight grown bacteria in LB broth were adjusted to an OD_{650nm} of 0.25 in sterile PBS and heat-inactivated at 80°C for 30 minutes. 96-well plates were then coated with 150 μ l of the suspension at 4°C overnight and washed three times with sterile PBS. The plates were blocked with 200 μ l of 1% BSA in PBS at RT for 1 h. After the buffer has been removed, plates were stored at – 20°C.

Prior to use the plates were washed with PBS once. Sera were serially diluted (start at 1:20 and then 2-fold dilutions) in PBS. 20 μ l of the diluted sera were incubated on bacteria coated plates at RT for 1 h. Plates were then washed three times with PBS, and incubated with 20 μ l of a 1:1000 dilution of the goat anti-mouse secondary antibody linked with horseradish peroxidase at RT for 30 minutes. The plates were then washed three times with PBS and incubated with 200 μ l of the ELISA substrate at RT for 20 minutes in the dark. The absorbance at 450 nm was measured using the using Infinite M200 pro spectrophotometer from Tecan.

Table 15. Buffer and substrate for antibody titer

ELISA buffer	1% BSA in PBS
Substrate	50 mM di-sodium hydrogen Phosphate
	25 mM citric acid
	0.9 mM o-phenylenediamine di-hydrochloride
	1.2×10^{-4} (v/v) H_2O_2
	In 20 ml H_2O

2.11 *In silico* sequence analysis

DNA and protein sequences were downloaded and analyzed at www.ncbi.nlm.nih.gov, <http://www.genome.jp>, and <http://clsb.ices.utexas.edu/loopp/web/> websites. The data from predicted protein structures were animated by using PyMOL software (Version 1.6; DeLano Scientific LLC). Multiple DNA and protein sequences were aligned via using ClustalX 2.1 program or using the BLAST tool on www.ncbi.nlm.nih.gov.

2.12 Statistics and software

To determine significant differences among groups, either a Student's t-Test or One-way-ANOVA-Test with Bonferroni multiple comparison posttest were used as indicated for each experiment. Mortality curves were compared using the log rank Kaplan-Meier Test. All statistical results were performed using GraphPad Prism Version 5.0. Significantly different values were indicated as astericks: * $p < 0.05$; ** $p < 0.005$; *** $p < 0.001$.

PyMOL program was applied to animate 3D structure of protein following the **LOOPP** (Learning, Observing and Outputting Protein Patterns) model by using server of The University of Texas at Austin.

3 RESULTS

3.1 Characterization of the putative LysR-type transcriptional regulator BPSL0117 of *B. pseudomallei*

In preliminary experiments of our group, a *Bp* transposon mutant defective in the putative LysR regulator *BPSL0117* (*Bp* Δ BPSL0117) showed reduced plaque formation in a cellular based plaque assay. Pilot experiments revealed that the mutant was attenuated in BALB/c mice (Eske-Pogodda, 2010). In the present study, the *BPSL0117* locus and its influence on *Bp* virulence was further investigated.

3.1.1 Complementation of the *B. pseudomallei* transposon mutant Δ BPSL0117

In a first step, the transposon mutant *Bp* Δ BPSL0117 was successfully complemented. The stable re-integration of the *BPSL0117* gene into the genome of *Bp* Δ BPSL0117 was carried out by using the pUC18-mini-Tn7::FRT:Zeo vector (Choi *et al.*, 2008). To verify that the *BPSL0117* gene was successfully integrated downstream of one of the three *glutamine-6-phosphate synthase*-encoding loci within the genome of *Bp*, PCR was performed. As shown in Fig. 6, the *BPSL0117* gene was inserted downstream of the *glmS2* (Fig. 6A) or the *glmS3* genes (Fig. 6B). The successfully complemented mutant strain *Bp* Δ BPSL0117::BPSL0117 was included in the following experiments to exclude that phenotypes obtained in the Δ BPSL0117 mutant strain were not caused by polar side effects.

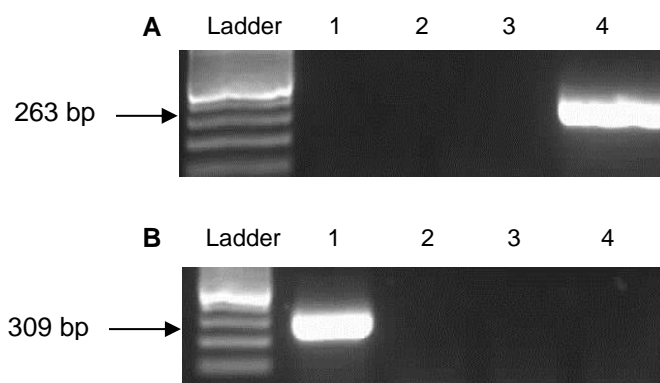


Figure 6. Complementation of *Bp* Δ BPSL0117. Insertion site of the *BPSL0117* gene was verified by PCR. PCR fragments were electrophoresed on 1.5% agarose gel and stained by SYBR[®] safe nucleic acid stain. **A:** PCR were verified mini-Tn7 insertion in *Bp* Δ BPSL0117 at *glmS2* by use of the primer pairs Tn7 and *glmS2*. **B:** PCR were verified of mini-Tn7 insertion in *Bp* Δ BPSL0117 at *glmS3* by use of the primer pairs Tn7 and *glmS3*. In this experiment, lane no. 1 and no. 4 are detected an insertion at *glmS2* and *glmS3*, respectively. However, lane no. 3 and no. 4 are not detected any specific insertion.

3.1.2 *In vitro* characterization of *B. pseudomallei* Δ BPSL0117

3.1.2.1 Growth kinetics

In a first set of experiments, the influence of the BPSL0117 gene on the *in vitro* growth of *Bp* was examined. For this purpose, the bacterial strains were cultivated in either LB broth or the minimal M9 medium under aerobic or anaerobic conditions, respectively. As shown in Fig. 7, growth of *Bp* Δ BPSL0117 did not severely differ compared to the WT strain in LB medium under aerobic condition (Fig. 7A). The growth rate of the mutant in M9 medium under aerobic conditions was impaired compared to WT bacteria in the logarithmic growth phase. Interestingly, in the stationary growth phase the Δ BPSL0117 mutant showed increased growth rates compared to the WT and the complemented mutant strain Δ BPSL0117::BPSL0117 (Fig. 7B). The growth of *Bp* Δ BPSL0117 in LB broth under anaerobic condition was slightly impaired compared to the WT and the complemented mutant strain (Fig. 7C). In M9 medium, the growth kinetics of *Bp* Δ BPSL0117 was also reduced compared to the WT strain. However, the phenotype was not recovered in the complemented mutant strain (Fig. 7D). However, we cannot exclude that minor polar effects on anaerobic metabolism pathways might have caused the observed impact on the complemented mutant strain.

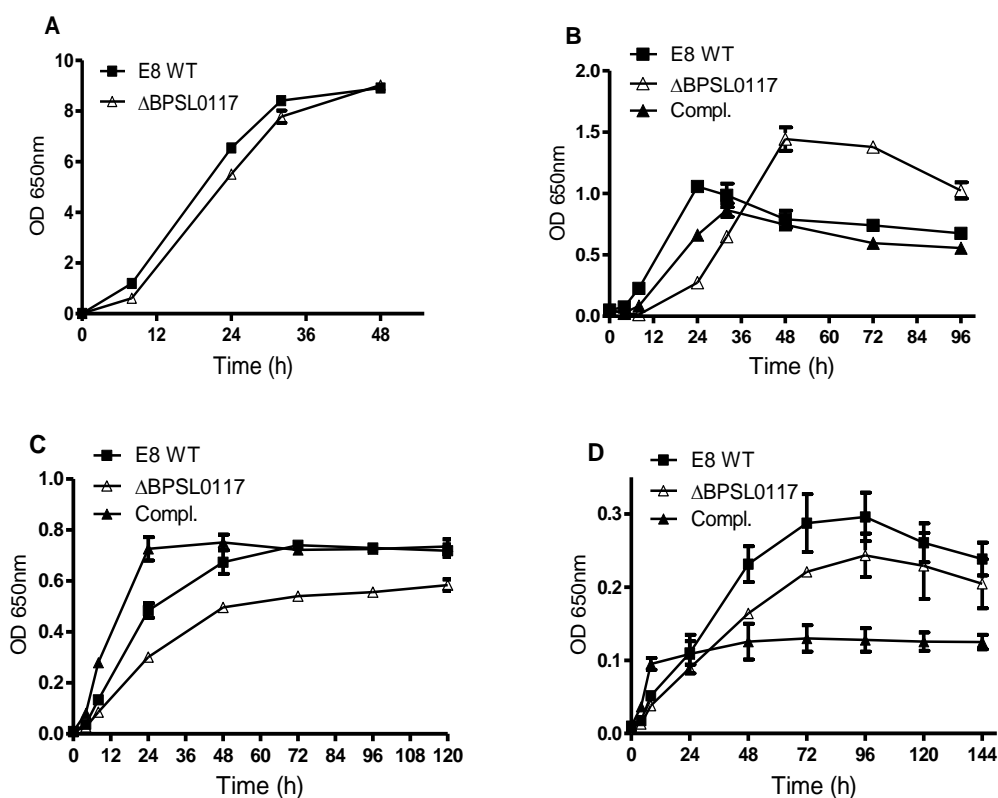


Figure 7. Growth kinetics of *Bp* Δ BPSL0117 compared to that of *Bp* E8 WT and *Bp* Δ BPSL0117::BPSL0117. A: Normal LB (aerobic), **B:** M9 (aerobic), **C:** Normal LB containing 50 mM KNO₃ (anaerobic), **D:** M9 containing 50 mM KNO₃ (anaerobic). One out of three experiments with similar results is shown.

3.1.2.2 Biofilm formation

To assess a role of BPSL0117 in biofilm formation, the extent of biofilm production was tested by static incubating of the bacterial strains in LB broth in plastic tubes. Biofilm production was measured at the indicated time points. As shown in Fig. 8, *Bp* Δ BPSL0117 showed significantly reduced biofilm formation compared to the *Bp* WT strain. In the complemented mutant strain Δ BPSL0117::BPSL0117 the biofilm formation was partially restored. These data show that BPSL0117 is clearly involved in the biofilm formation of *Bp*.

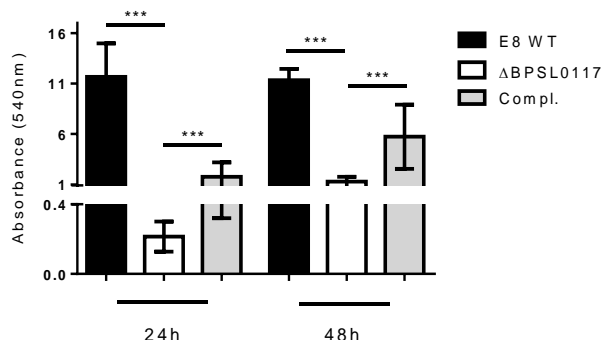


Figure 8. Biofilm formation of *Bp* Δ BPSL0117 compared to *Bp* E8 WT and *Bp* Δ BPSL0117::BPSL0117. Biofilm formation was assayed after 24 h and 48 h static incubation at 37°C in normal LB. Crystal violet retention of adherent bacteria was measured at 540 nm. Pooled values from three independent experiments are shown and analyzed using one-way ANOVA with Bonferroni multiple comparisons posttest. Values are the mean \pm standard deviations (SD) from experiments. *** denotes a P value <0.001.

3.1.2.3 Motility

To check whether the BPSL0117 gene might be involved in the *in vitro* motility of *Bp*, bacterial strains were spotted into soft agar and incubated for 24 h and 48 h at 37°C. As shown in Fig. 9, the *Bp* Δ BPSL0117 strain was impaired in both swimming (Fig. 9A) and swarming (Fig. 9B) motility compared to the WT strain, whereas the phenotypes were fully restored in the complemented mutant strain. These results show that BPSL0117 plays a role for the bacterial motility.

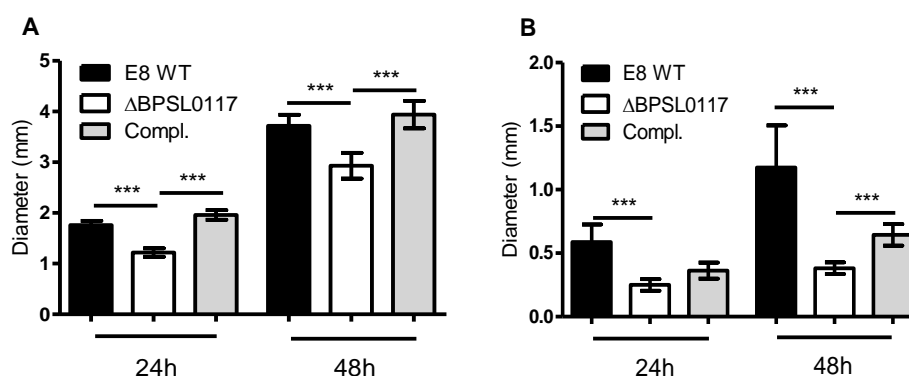


Figure 9. Motility of *Bp* ΔBPSL0117 compared to *Bp* E8 WT and *Bp* ΔBPSL0117::BPSL0117. Motility was assayed after 24 h and 48 h incubation at 37°C by measuring the diameters of the circular bacterial migration from the point of inoculation. **A:** Swimming into 0.3% agar plates, **B:** Swarming into 0.6% agar plates. Pooled results from three independent experiments are shown and analyzed using one-way ANOVA with Bonferroni multiple comparisons posttest. Values are the mean ± SD from experiments. *** denotes a P value <0.001.

3.1.2.4 Secretion of proteases

To determine whether BPSL0117 might influence secretion of extra-cellular proteases, we spotted overnight grown bacteria into soft LB agar containing 2% (w/v) casein and measured diameters of the catalyzed substrate zones after 24 h and 48 h incubation at 37°C. As shown in Fig. 10, *Bp* ΔBPSL0117 showed significantly decreased protease activity compared to the WT strain E8. The phenotype was fully restored in the complemented mutant strain. Thus, BPSL0117 seems to influence the expression and secretion of extra-cellular proteases of *Bp*.

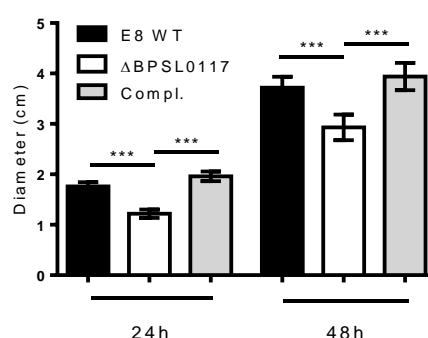


Figure 10. Protease activity of *Bp* ΔBPSL0117 compared to that of *Bp* E8 WT and *Bp* ΔBPSL0117::BPSL0117. The results were analyzed at 24 h and 48 h of incubation at 37°C by measuring diameters of catalyzed casein zone from the inoculation points. Pooled data are shown and analyzed using one-way ANOVA with Bonferroni multiple comparisons posttest. Values are the mean ± SD from experiments. *** denotes a P value <0.001.

3.1.2.5 Expression and secretion of the T3SS proteins BopE and BipD

To assess whether BPSL0117 affects the expression or secretion of proteins belonging to the T3SS cluster 3, we analyzed the T3SS3 effector protein BopE and its chaperone and translocator protein BipD. Bacteria were grown in LB broth at 37°C and harvested after 3 h and 6 h. As shown in Fig. 11, the *Bp* ΔBPSL0117 strain exhibited lower expression levels of BopE and BipD at 3 h after incubation compared to the WT strain E8 and *Bp*

Δ BPSL0117::BPSL0117. However, after 6 h of incubation, the mutant showed increased expression and secretion of these T3SS3 proteins compared to the WT and Δ BPSL0117::BPSL0117. Thus, it seems that the T3SS3 proteins were degraded in the WT and the complemented mutant strain at that time point. It is more precise when the comparison of T3SS3 expression was evaluated by following defined optical density (see part 3.1.6). One could therefore suggest that lack of BPSL0117 leads to a delayed expression and secretion of T3SS3 proteins.

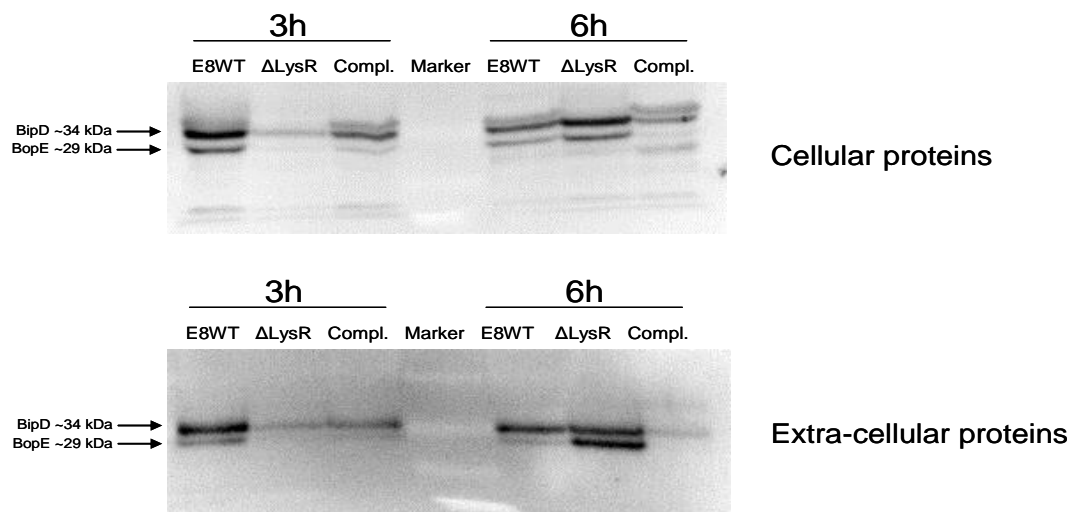


Figure 11. Expression and secretion of T3SS3 proteins of *Bp* Δ BPSL0117 compared to that of *Bp* E8 WT and *Bp* Δ BPSL0117::BPSL0117. Proteins were separated by 12.5% SDS-PAGE, transferred onto a membrane and detected by primary anti-BipD and anti-BopE and secondary goat anti-mouse IgG linked horseradish peroxidase antibodies. Strains were inoculated in LB medium and cultivated for 3 h and 6 h. One representative result out of three experiments with similar results is shown.

3.1.2.6 Susceptibility to antibiotics

Next, we examined whether BPSL0117 might affect the sensitivity against β -lactam antibiotics of *Bp*. Overnight grown bacterial strains were plated onto Mueller-Hinton agar and E-test strips of imipenem and ceftazidime were subsequently put onto the plates. As shown in Fig. 12, the minimal inhibitory concentrations of both antibiotics were significantly decreased in the *Bp* Δ BPSL0117 strain compared to the WT strain E8. The phenotype was fully restored to WT level in *Bp* Δ BPSL0117::BPSL0117. Thus, the putative LTTR locus BPSL0117 is clearly involved in mechanisms that determine resistance against β -lactam antibiotics in *Bp*.

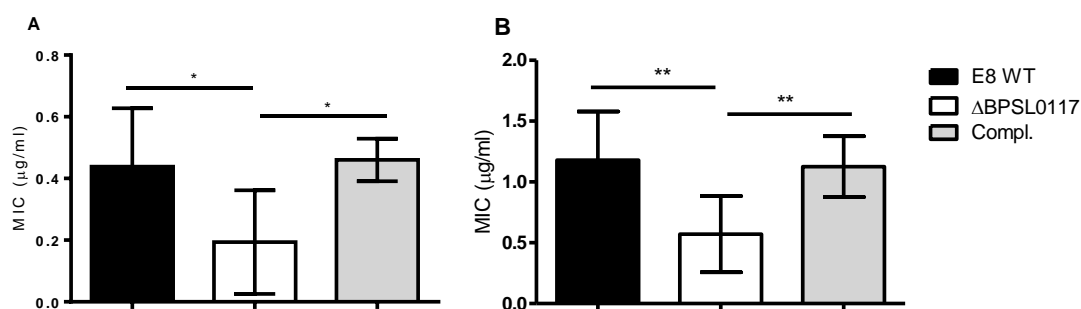


Figure 12. Minimal inhibitory concentration of imipenem and ceftazidime. **A:** Imipenem E-test, **B:** Ceftazidime E-test. Sterile zones were determined according to the manufacturer's instructions. Pooled data from three independent experiments are shown and analyzed using Student t-test. Values are the mean \pm SD from experiments. * and ** indicate P values of <0.05 and <0.01, respectively.

3.1.3 Roles of BPSL0117 in mammalian cell models

3.1.3.1 Uptake and intracellular replication

To determine whether BPSL0117 influences invasion, uptake and/or intracellular replication, human cervical carcinoma epithelia cells (non-phagocytic HeLa cells), murine macrophage leukemia cells (RAW264.7) and bone marrow-derived macrophages of BALB/c mice (BALB/c-BMM) were infected. As shown in Fig. 13, there was no difference in the invasion in HeLa cells (Fig. 13C) or the uptake of bacteria in the macrophage cell line RAW264.7 cells (Fig. 14A) and BALB/c-BMM (Fig. 13B). The small differences seen in BALB/c BMM at after 0 h are likely to be caused by the rapid elimination of the *Bp* Δ BPSL0117 in these cells. *Bp* Δ BPSL0117 was significantly impaired in its intracellular survival in all three cell types. However, in the absence of BPSL0117, *Bp* was still able to replicate inside the immortalized cell lines. However, *Bp* Δ BPSL0117 was not able to replicate in the primary macrophages and exhibited a linear decline inside these cells. In the *Bp* Δ BPSL0117::BPSL0117 strain the ability to replicate inside the cells was fully restored in the macrophages to WT level. These data clearly implicate that BPSL0117 has an essential role for the intracellular survival of *Bp* in mammalian cells.

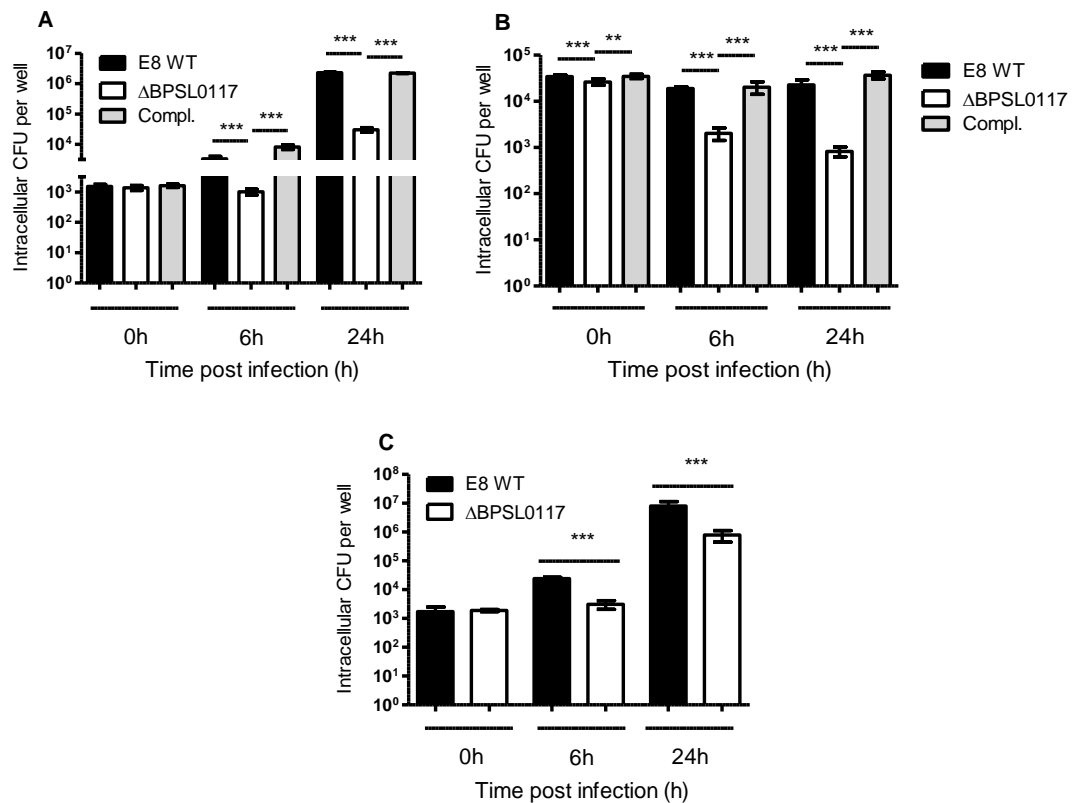


Figure 13. Comparison of uptake and intracellular replication of *Bp* E8 WT, *Bp* Δ BPSL0117 and *Bp* Δ BPSL0117::BPSL0117. **A:** Infection in RAW 264.7 macrophages with MOI = 1, **B:** Infection in BALB/c-BMM macrophages with MOI = 2, **C:** Infection in HeLa cells with MOI = 2. Values are the means \pm SD of triplicate determinations in single representative experiments. Similar results were obtained in at least three independent experiments with each bacterial strain. The data are analyzed using one-way ANOVA with Bonferroni multiple comparisons posttest (A, B) and Student t-test (C). *** denotes a P value <0.001.

3.1.3.2 Actin polymerization assay

Next, we assessed the influence of BPSL0117 on the formation of actin tails inside host-cells. For this purpose, HeLa cells were infected with the WT, *Bp* Δ BPSL0117 and *Bp* Δ BPSL0117::BPSL0117. The formation of actin tails was investigated at 3 h and 8 h after infection by immunofluorescence microscopy. As shown in Fig. 14, the *Bp* Δ BPSL0117 mutant was able to form normal actin tails as observed with the WT and the complemented strain. Thus, BPSL0117 seems to have no influence on the recruitment of cellular actin within host cells.

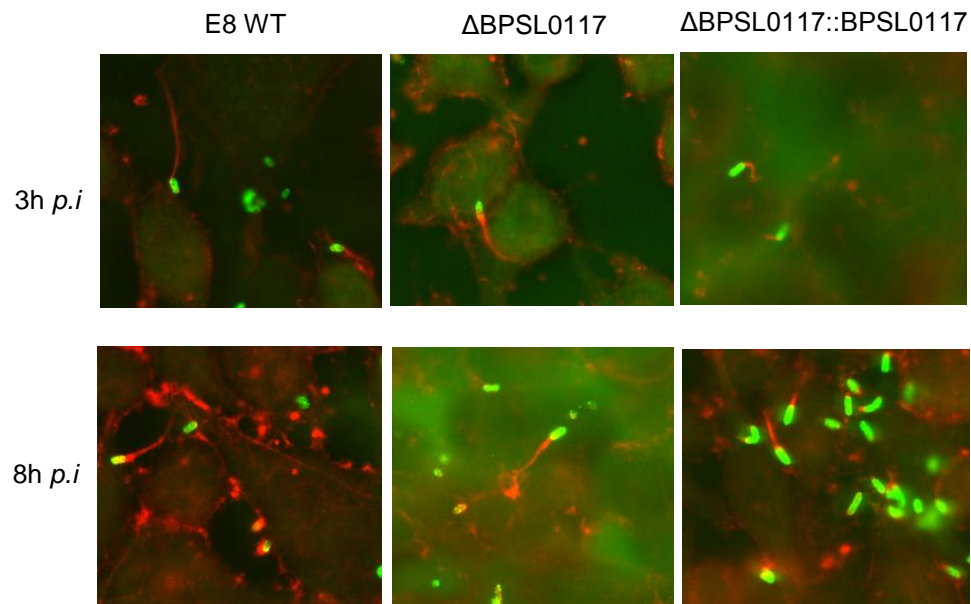


Figure 14. Actin tail formation of *Bp* E8 WT, *Bp* Δ BPSL0117 and *Bp* Δ BPSL0117::BPSL0117 in HeLa cells. Bacteria were stained green with mouse anti-*Bp* EPS and anti-mouse IgG-Alexa488. Filamentous actin was stained red with anti-rabbit Ig-Alexa568 phalloidin.

3.1.4 Influence of BPSL0117 on *B. pseudomallei* virulence

3.1.4.1 Mortality

To elucidate the *in vivo* role of BPSL0117, BALB/c mice were intranasally infected with *Bp* Δ BPSL0117, WT E8 and *Bp* Δ BPSL0117::BPSL0117. As shown in Fig. 15, mice infected with WT and *Bp* Δ BPSL0117::BPSL0117 succumbed within first month after infection, whereas mice inoculated with various doses of *Bp* Δ BPSL0117 survived up to 90 days post infection. No remaining bacteria could be detected inside lung, liver and spleen of the euthanized survivor-animals (data not shown). These data show that BPSL0117 has a crucial role for *in vivo* virulence in the mouse model of melioidosis and that the lack of BPSL0117 leads to a strong attenuation, since no animal died even after challenge with very high infection doses (Fig. 15).

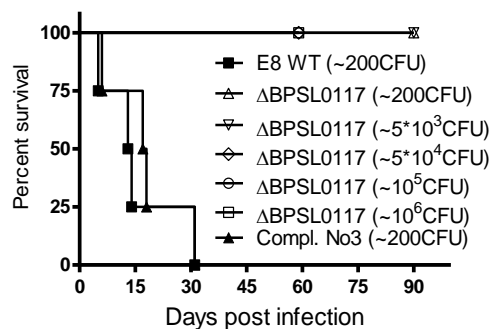


Figure 15. Mortality curves of BALB/c mice (n = 4) after intranasal infection with *Bp* E8 WT (dose infection ~ 200 CFU), *Bp* ΔBPSL0117 (dose infection 200 - 10⁶ CFU) and *Bp* ΔBPSL0117::BPSL0117 (dose infection ~ 200 CFU). Pooled results from two independent experiments are shown. Curves were compared by using the log rank Kaplan-Meier test.

3.1.4.2 Determination of bacterial load in organs

Next, the bacterial burdens in organs of infected animals were investigated at 48 h after infection. BALB/c mice were intranasally infected with *Bp* WT E8, *Bp* ΔBPSL0117 and *Bp* ΔBPSL0117::BPSL0117, and lungs, livers and spleens were examined for viable bacteria. As shown in Fig. 16, the bacterial burdens in these organs were significantly higher in mice received either the WT or *Bp* ΔBPSL0117::BPSL0117 compared with mice infected with *Bp* ΔBPSL0117. Among these, remaining bacteria were found in only one animal lung (Fig. 16A) and spleen (Fig. 16B). No mutant was isolated in livers (Fig. 16C). The results confirm the strong attenuation of *Bp* in the absence of BPSL0117 and underline the importance of this gene for bacterial virulence.

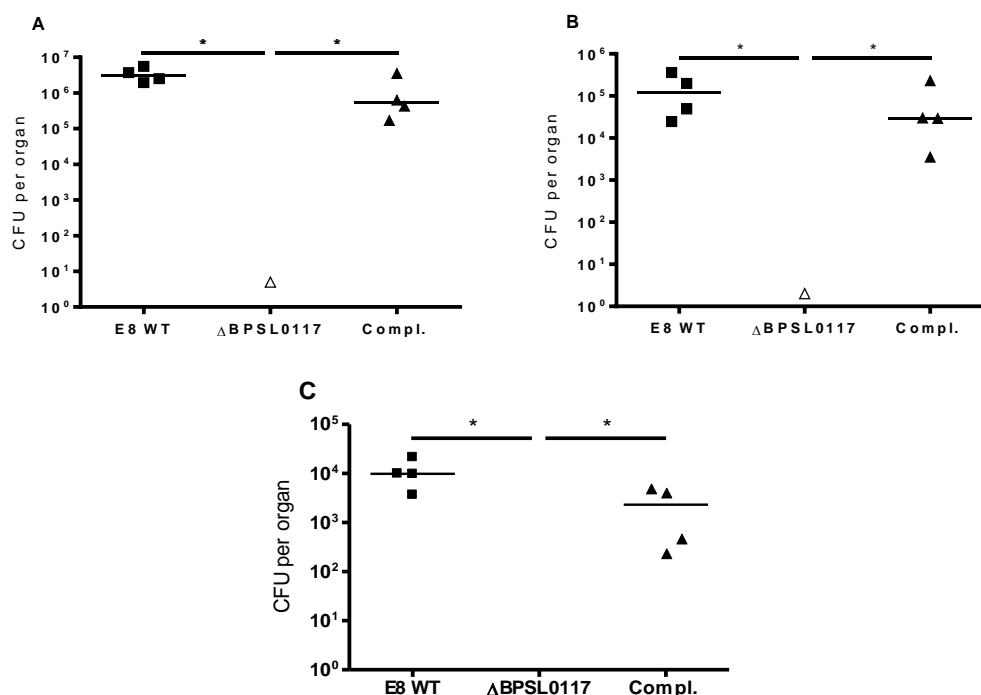


Figure 16. Bacterial burden in organs of infected BALB/c mice (n = 4) 48 h after intranasal infection with *Bp* E8 WT (dose infection ~ 332 CFU per mouse), *Bp* ΔBPSL0117 strain (dose infection ~ 312 CFU per mouse) and *Bp* ΔBPSL0117::BPSL0117 strain (dose infection ~ 303 CFU per mouse). A: Bacterial burdens in lungs, B: Bacterial burdens in spleens, C: Bacterial burdens in livers. Data from one single experiment are shown. Single dots represent the CFU in one organ from a single animal. The horizontal lines represent the geometric means. To select variables for inclusion in regression analysis, preliminary unadjusted univariate tests (the Mann-Whitney U test for skewed data, unpaired Student's t test for approximately normally distributed data, and the one-way ANOVA with Bonferroni posttest for categorical data) were performed. * denotes a P value <0.05.

3.1.5 Usage of *B. pseudomallei* ΔBPSL0117 as a live vaccine

The previous results clearly show that *Bp* ΔBPSL0117 was strongly attenuated in the mouse model of melioidosis and could practically consider being avirulent. Several studies have described the usage of attenuated *Bp* strains or mutants to initiate a protective immunity in experimental animal models (Atkins *et al.*, 2002; Stevens *et al.*, 2004; Cuccui *et al.*, 2007; Breitbach *et al.*, 2008; Srilunchang *et al.*, 2009; Norris *et al.*, 2011; Silva *et al.*, 2013). It was therefore decided to use the *Bp* ΔBPSL0117 mutant as a live vaccine.

3.1.5.1 Induction of specific anti-*Bp* antibodies after immunization

BALB/c mice were intranasally immunized with *Bp* ΔBPSL0117 with doses ranging from 5 x 10⁴ to 10⁶ CFU per mouse. Non-immunized mice were received sterile PBS. Twenty one to twenty three days after immunization, blood was taken from the retro orbital plexus to check whether the immunization procedure could induce the production of antibodies. After taking blood, animals were randomly checked for presence of remaining bacteria after immunization in livers and spleens, but none were detected. As shown in Fig. 17, the production of IgG antibodies against *Bp* was significantly higher in immunized mice compared to the control

group. Thus, mice immunized with the attenuated mutant led to humoral adaptive immune response and the production of specific antibodies.

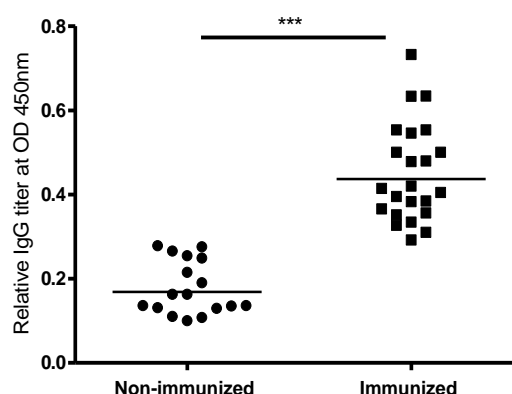


Figure 17. Humoral immune responses in *Bp* ΔBPSL0117 immunized BALB/c mice. Sera were prepared from BALB/c mice intranasally immunized with *Bp* ΔBPSL0117 (dose range 5×10^4 to 10^6 CFU, $n = 23$, diluted 1:20) and sham-immunized BALB/c mice ($n = 17$). Specific antibodies against *Bp* E8 WT were determined by ELISA. The horizontal lines represent the geometric means. Results are pooled from two independent experiments and analyzed using Student t-test. *** denotes a P value <0.001.

3.1.5.2 *B. pseudomallei* ΔBPSL0117 strain as live attenuated vaccine

It was next tested whether the immunization strategy could protect mice *in vivo* from challenge with *Bp* WT E8 bacteria. Mice were intranasally immunized with doses ranging from 5×10^4 to 10^6 CFU per mouse with *Bp* ΔBPSL0117 and showed no signs of clinical illness prior to the challenge. Four weeks after immunization, mice were challenged via either *i.n.*, *i.v.* or *i.p.* route with lethal *Bp* WT E8 doses (370 to 550 CFU/mouse for *i.n.* infection, 290 to 600 CFU/mouse for *i.v.* infection, and 1.7×10^5 to 2.5×10^5 CFU/mouse for *i.p.* infection). As shown in Fig. 18 and 20, a slight delay in median time to death was observed in the groups of mice challenged via the *i.p.* and *i.n.* routes compared to the respective control groups (*i.p.* challenge: vaccinated 32.71 days, PBS 15.67 days and $p=0.1663$; *i.n.* challenge: vaccinated 11.43 days, PBS 7.83 days and $p=0.0675$). However, these observed differences in mortality were not statistically significant differences. Except one animal that survived 90 days after challenge and proved to have no remaining bacteria, all immunized mice finally showed signs of chronic illness and died.

Table 16. Immunization of BALB/c mice with the live *Bp* ΔBPSL0117 and survival after challenge with *Bp* E8 WT

Immunization dose and application (CFU)	Challenge dose (CFU) and route	Number of mice	Median time to death (days)
From 5×10^4 to 10^6 <i>i.n</i>	From 370 to 550 <i>i.n</i>	7	11.43
	From 290 to 600 <i>i.v</i>	9	23.11
	From 1.7×10^5 to 2.5×10^5 <i>i.p</i>	8	32.71
Non-immunized	From 370 to 550 <i>i.n</i>	6	7.83
	From 290 to 600 <i>i.v</i>	9	15.67
	From 1.7×10^5 to 2.5×10^5 <i>i.p</i>	3	15.67

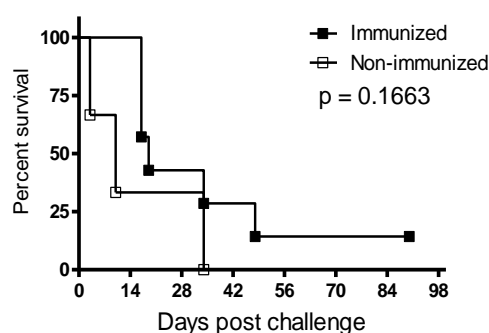


Figure 18. Mortality curves of BALB/c mice after four weeks intranasal immunization with *Bp* ΔBPSL0117 strain (immunization dose from 5×10^4 to 10^6 CFU per mouse, $n = 7$), non-immunized mice ($n = 3$) and challenge with *Bp* E8 WT (dose infection from 1.7×10^5 to 2.5×10^5 CFU per mouse) via the intraperitoneal route. Data are pooled from two independent experiments and analyzed using the log rank Kaplan-Meier test.

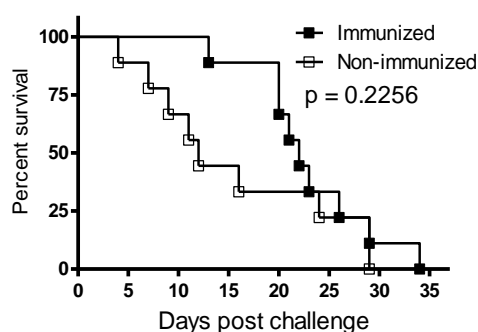


Figure 19. Mortality curves of BALB/c mice after four weeks intranasal immunization with *Bp* ΔBPSL0117 strain (immunization infection from 5×10^4 to 10^6 CFU per mouse, $n = 9$), non-immunized mice ($n = 9$) and challenge with *Bp* E8 WT (dose infection from 290 to 600 CFU per mouse) via the intravenous route. Data are pooled from two independent experiments and analyzed using the log rank Kaplan-Meier test.

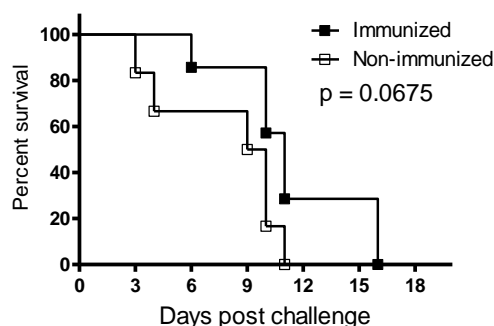


Figure 20. Mortality curves of BALB/c mice after four weeks intranasal immunization with *Bp* Δ BPSL0117 strain (immunization infection from 5×10^4 to 10^6 CFU per mouse, $n = 7$), non-immunized mice ($n = 6$) and challenge with *Bp* E8 WT (dose infection from 370 to 500 CFU per mouse) via the intranasal route. Data are pooled from two independent experiments and analyzed using the log rank Kaplan-Meier test.

3.1.6 Global protein expression profile

Since BPSL0117 is considered to belong to the LTTR family members and its absence led to a strong attenuation in BALB/c mice, it was assumed that this gene might affect on abundance of protein expression that are involved in the pathogenesis of *Bp*. Therefore, the global protein expression profile during growth in the early logarithmic and stationary phases in M9 broth was carried out with *Bp* WT E8 and the *Bp* Δ BPSL0117 mutant using stable isotope labeling with amino acids in cell culture (SILAC). For convenience, the protein fractions obtained were referred as cytoplasmic protein fractions.

SILAC was used to identify candidate proteins that may relatively alter between *Bp* E8 WT and *Bp* Δ BPSL0117. We confirmed the expression of 1608 cytoplasmic proteins with at least one unique peptide identified. The total numbers of detectible proteins represented to 5,935 genes that are computationally predicted compared to 5,467 expressed genes based on mRNA micro array under 82 cultivated conditions (Oong *et al.*, 2013). Among the 1608 identified proteins, the detectible proteins at logarithmic and stationary phases were categorized into the following functional groups: amino acid synthesis; cell envelop; central intermediary metabolism; energy metabolism; fatty acid and phospholipid metabolism; mobile and extrachromosome element functions; protein fate; protein synthesis; purines, pyrimidines, nucleosides and nucleotides; regulatory functions; and protein with unknown functions.

3.1.6.1 General description

Using a 2-fold difference in the expression as a cut-off, proteins were harvested during the logarithmic growth phase, the observation that BPSL0117 positively influenced the expression of 202 proteins and negatively regulated the expression of 142 proteins. In accordance, 18 operons were upregulated and 7 operons were downregulated in *Bp* Δ BPSL0117 compared to the WT E8 (Fig. 21A and 21C). In addition, at the early stationary growth phase we found 362 proteins that showed increased abundance and 211 proteins that exhibited decreased expression in the absence of the BPSL0117. In agreement, 38 operons were up-regulated and

17 operons were downregulated in *Bp* Δ BPSL0117 compared to the WT E8 (Fig. 21B and 21C).

Holden and colleagues (2004) revealed that *Bp* chromosome 1 consists of genes that are mainly associated with core functions, while *Bp* chromosome 2 contains many genes that are associated with accessory and secondary functions, including virulence genes. The present results showed that 240 (6.8%) proteins in the exponential phase and 372 (10.54%) proteins in the stationary phase were differentially expressed that belong to genes encoded within *Bp* chromosome 1. While 104 (4.31%) and 201 (8.33%) proteins at the logarithmic and stationary phase from genes encoded within *Bp* chromosome 2 were found to exhibit different expression, respectively (Fig. 21D). Thus, the proteome data indicated that BPSL0117 affects on many proteins encoded within both chromosomes and can therefore be considered to serve as a global gene regulator.

Additionally, we found a differential protein expression at both exponential and stationary phases of other regulator families like AraC, AsnC, MarR, GntR, NrdR, BadM/Rrf2, XRE family, RpiR, LacI, TetR LuxR family and other members of LysR family like BPSL2733, BPSS0755 and BPSS0365 (Appendix IX). The plenty of all these regulators imply that BPSL0117 may directly and indirectly regulate other genes.

3.1.6.2 Expression of secretion system proteins

Based on our proteome analysis, the altered expression includes specific proteins residing in T3SS3 and six T6SS secretion clusters. Especially, the T3SS3 proteins BicP, BsaR, BopE and BipD, and T6SS1 proteins VirG, TssA, TssB and HcpI showed decreased expression. However, the lack of expression of T3SS1 and T3SS2 proteins may either indicate the absence of an appropriate condition required for triggering protein expression or limitation of the method using to quantify proteins or membrane proteins. In contrast to T6SS1, proteins of other T6SSs exhibited upregulated. In addition, *Bp* Δ BPSL0117 also showed reduced expression of T2SS effector zinc metalloprotease (BPSS0564) compared to the WT. The data could explain to decreased exoproteases activity and *in vivo* virulence (O'Grady *et al.*, 2009; Somvanshi *et al.*, 2010).

3.1.6.3 Proteins involved in EPS and CPS synthesis

Our analysis identified the *Bp* Δ BPSL0117 showed reduced proteins associated with capsule polysaccharides (CPS) II like BPSS0421; CPS III known as BPSS1833; cluster C34 defined as BPSL0481, BPSL0482, BPSL0483, BPSL0485, and BPSL0486; and cluster C121 like BPSS1955 and BPSS1956 (Ooi *et al.*, 2013). Besides, CPS is perhaps one of the most important molecules that make up the maxtrix of biofilms (Antunes & Ferreira, 2011). The results may be a reason that the *Bp* Δ BPSL0117 produced lesser biofilm compared to the WT E8.

3.1.6.4 Proteins involved in antibiotic susceptibility

Following the susceptibility to beta-lactam antibiotics group of *Bp* ΔBPSL0117, the proteome analysis showed that *Bp* ΔBPSL0117 was upregulated to express two negative regulator of beta-lactam proteins BPSS1490 and BPSS1840, and especially down-regulated expression of the beta-lactamase class C and other penicillin binding protein BPSS1311.

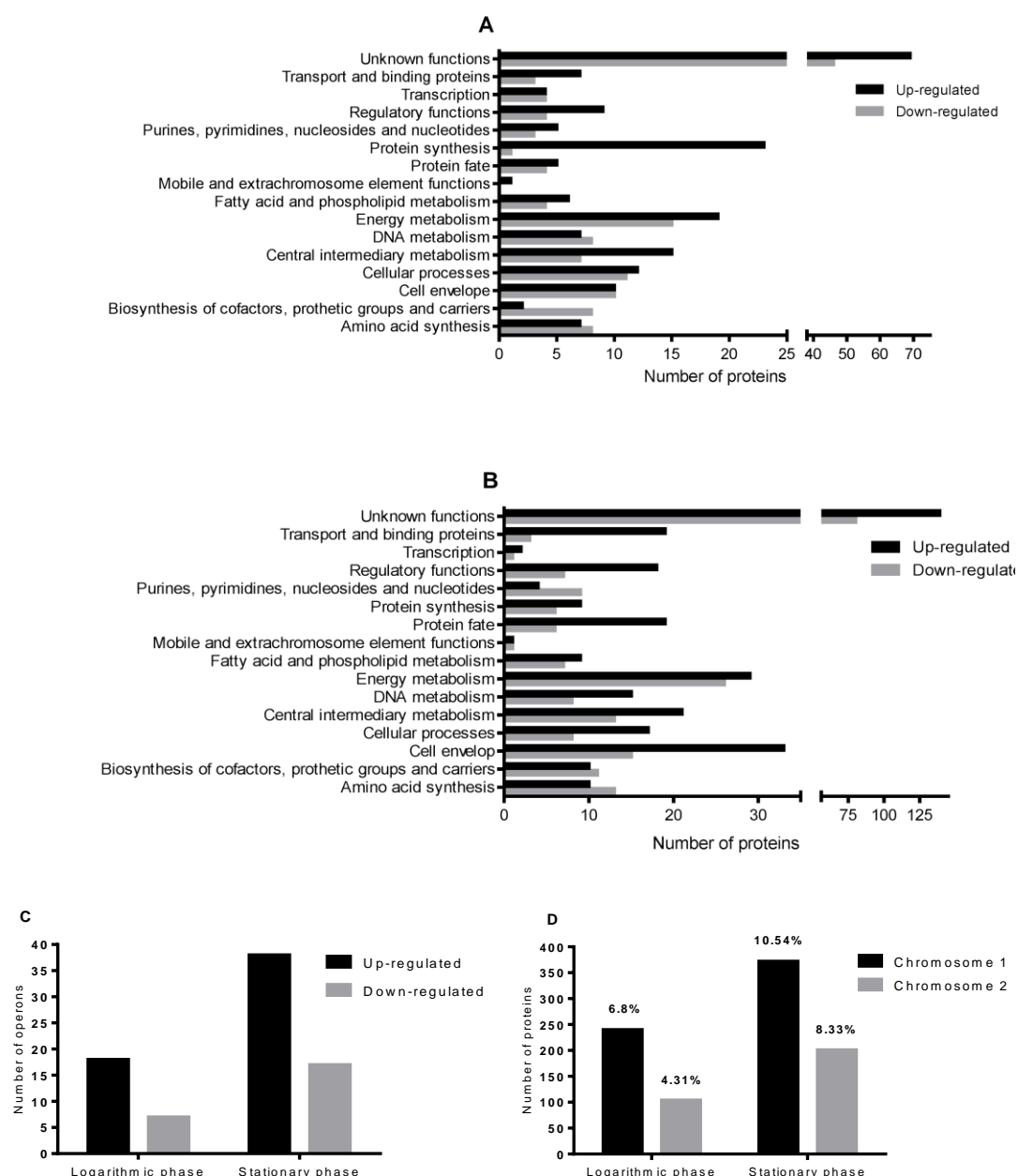


Figure 21. Significantly up or down regulated proteins and operons in *Bp* ΔBPSL0117 compared to *Bp* E8 WT, clustered by functional category. **A:** Altered proteins at logarithmic phase, **B:** Altered proteins at early stationary phase, **C:** Altered Operons at exponential and stationary phases, **D:** Number and percentage of altered proteins based on chromosomes. Fold change (*Bp* ΔBPSL0117/*Bp* E8 WT) of SILAC-Intensity normalized. The data were obtained from the cooperation with Prof. Riedel and Dr. Hochgräfe group. The results were considered significantly different if at least two of three reproducible samples are changed and a threshold of at least a 2.0-fold increase or 0.5-fold decrease. One sample of out of ranking value must be ≤ 0.9 or ≥ 1.1 if samples are decreased or increased, respectively.

3.1.6.5 Changes in metabolic pathways

Besides the impressive changes of protein expression to be important for virulence, we found many strongly altered proteins that were involved in different central carbon metabolism pathways such as the tricarboxylic acid cycle (TCA), the amino acid degradation/biosynthesis, fatty acid degradation/biosynthesis, the glyoxylate shunt and a possible methylcitrate cycle (MCC). The TCA cycle is the central carbon metabolism pathway that generates ATP and delivers biosynthetic intermediates. We found a strong down regulation of the Isocitrate dehydrogenase kinase/phosphatase (BPSL0373) in the mutant, an enzyme regulating the activity of the isocitrate dehydrogenase by phosphorylation (inhibition) and dephosphorylation (activation) as shown for *Escherichia coli*. Theoretically, a repression of this enzyme leads to deregulate the isocitrate dehydrogenase (Icd), one of the key enzymes of the TCA cycle. However, it could only speculate if it comes to a strong activation (missing phosphorylation) or a strong repression (missing dephosphorylation) of the isocitrate synthase. But further the influence on the activity of the TCA cycle is unclear. Additionally, a strong down regulation of the isocitrate lyase (BPSL2188), the key enzyme of the glyoxylate shunt for replenishment reactions during growth on acetate or even-fatty acids, was also determined. In sum, the TCA cycle and the glyoxylate shunt seem to be deregulated that have certainly deep influences on further metabolic pathways. The probably deregulated TCA cycle leads to be manifold reduction of some proteins involved in amino acid metabolism; proteins related to secondary metabolites biosynthesis/transport/catabolism, purine and pyrimidine metabolism; and some proteins associated with fatty acid metabolism.

Interestingly, six proteins (BPSL0486 - Diaminopimelate decarboxylase; BPSL0485 - acyl-CoA ligase (AMP-forming); BPSL0483 - Acyl-CoA dehydrogenases; BPSL0482 - Citrate synthase/2-methylcitrate synthase; BPSL0481 - Methylase involved in ubiquinone/menaquinone biosynthesis and BPSL0476 - diaminobutyrate-2-oxoglutarate aminotransferase) encoded within probable operon(s) (BPSL0475-BPSL0493) were strongly repressed. The operon(s) only exists on genomes of closely related species of *Bp* like *B. mallei*, *B. gladioli*, *B. ambifaria* and *B. cenocepacia*. However, the operon(s) of the other species contains only 12 to 17 genes (Fig. 22). Amazingly, the genome of the non-pathogenic *B. thailandensis* does not contain the loci. Moreover, BPSL0488 and BPSL0491 do not have any paralogous protein. Functions of the operon(s) have not been completely proven, but many proteins seem to be involved in fatty acid metabolism, transport of unknown substrates, carbohydrate metabolism and amino acid metabolism (table 17).

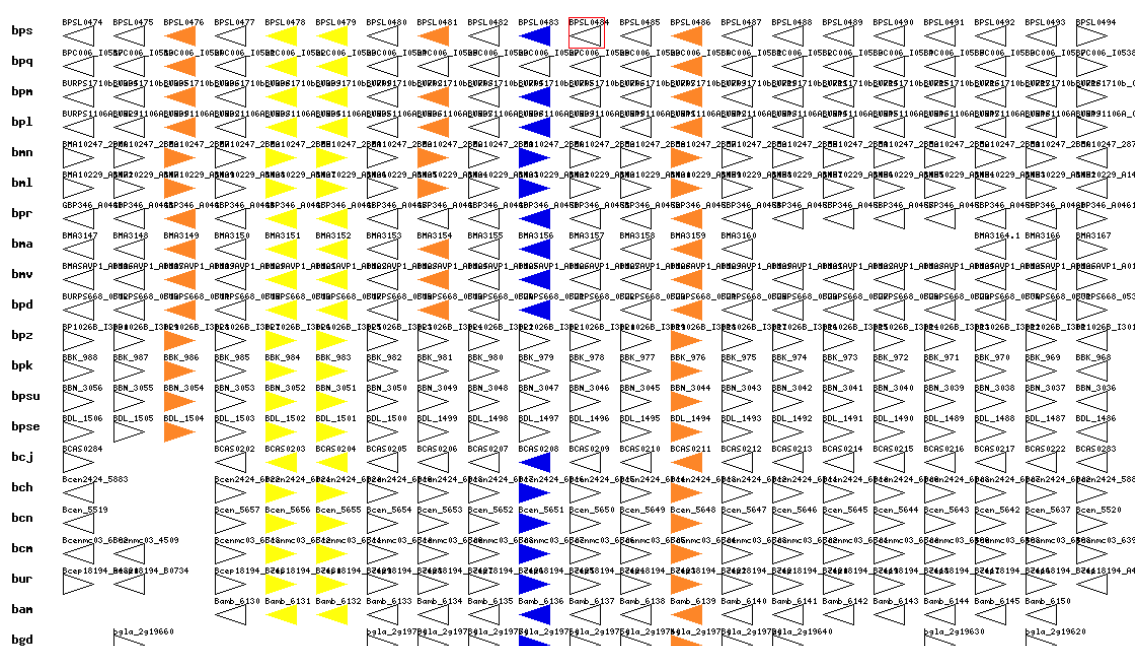


Figure 22. Orthologs of *Bp* K96243 *BPSL0474* – *BPSL0494* genes compared to *Burkholderia* spp. (from Kyoto encyclopedia of genes). Color-coded represents function of genes: Blue is carbohydrate metabolism; Orange is amino acid metabolism; Yellow are cellular processes, organismal systems, genetic information processing, environmental information processing; and white is unassigned. Relevance of bacterial species/strains and their name-coded: bps: *B. pseudomallei* K96243; bpq: *B. pseudomallei* PPC006; bpm: *B. pseudomallei* 1710b; bpl: *B. glumae* BGR1; bmn: *B. mallei* NCTC 10247; bml: *B. mallei* NCTC 10229; bpr: *B. pseudomallei* MSHR346; bma: *B. mallei* ATCC23344; bmv: *B. mallei* SAVP1; bpd: *B. pseudomallei* 668; bpz: *B. pseudomallei* 1026b; bpk: *B. pseudomallei* NCTC 13179; bpsu: *B. pseudomallei* MSHR146; bcj: *B. cenocepacia* J2315; bch: *B. cenocepacia* HI2424; bcn: *B. cenocepacia* AU1054; bcn: *B. cenocepacia* MC0-3; bur: *Burkholderia* sp. 383; bam: *B. ambifaria* AMMD; bgd: *B. gladioli* BSR3.

Table 17. Predicted functions of proteins encoded within the probable operon(s) from BPSL0475 to BPSL0493

<i>Bp</i> K96243 Loci	Protein name	Main role	Sub-role
BPSL0475	Putative fatty acid desaturase	Fatty acid and phospholipid metabolism	Biosynthesis
BPSL0476	Diaminobutyrate-2-oxoglutarate transaminase [EC:2.6.1.76]	No value is available (#N/A)	#N/A
BPSL0477	Hypothetical protein	#N/A	#N/A
BPSL0478	ABC-type multidrug transport system, permease component	Transport and binding proteins	Amino acids, peptides and amines
BPSL0479	ABC transport system ATP-binding protein	Transport and binding proteins	Unknown substrate
BPSL0480	Hypothetical protein	#N/A	#N/A
BPSL0481	Methylase involved in ubiquinone/menaquinone biosynthesis	Amino acid biosynthesis	#N/A
BPSL0482	Citrate synthase	Energy metabolism	Detoxification
BPSL0483	Acyl-CoA dehydrogenases	Unknown function	Heme, porphyrin, and cobalamin
BPSL0484	Hypothetical protein	#N/A	#N/A
BPSL0485	Acyl-CoA ligase (AMP-forming), exosortase A-associated	Protein synthesis	Transposon functions
BPSL0486	Diaminopimelate decarboxylase	Amino acid biosynthesis	#N/A
BPSL0487	Hypothetical protein	#N/A	#N/A
BPSL0488	Hypothetical protein	Hypothetical proteins	Conserved
BPSL0489	Hypothetical protein	#N/A	#N/A
BPSL0490	Hypothetical protein	#N/A	#N/A
BPSL0491	Putative acyl carrier protein	#N/A	#N/A
BPSL0492	Hypothetical protein	#N/A	#N/A
BPSL0493	Putative AMP-binding enzyme	Protein synthesis	tRNA aminoacylation

On the other hand, many strongly upregulated proteins play key roles in the branched-chain amino acids degradation, the fatty acid degradation and the propionate metabolism. The strong induction of almost all downstream parts in these pathways obviously leads to effect on the synthesis of acetyl-CoA, propionyl-CoA, succinate and fumarate (Fig. 23). Acetyl-CoA is

mainly produced during the degradation of even-fatty acids, phenylalanine, leucine and isoleucine. Theoretically, acetyl-CoA is further metabolized via the TCA cycle or can be used for biosynthetic syntheses, the end-product of degradation of valine, isoleucine and odd-fatty acids is propionyl-CoA. The propionyl-CoA is toxic for organisms and should be degraded. We found a strong induction of the 2-methylisocitrate lyase (PrpB = BPSS0206), which catalyzes the last step of the methylisocitrate cycle (MCC), a pathway in which propionyl-CoA is degraded to succinate and pyruvate (Fig. 23). PrpC, the methylcitrate synthase catalyzing the first step of the MCC, should be also strongly induced, because two of three intensity values of *Bp* ΔBPSSL0117 compared to the WT were significantly increased, but the other was lower than 1.1. However, pyruvate can be used by the pyruvate dehydrogenases complex and succinate can be metabolized again in the TCA cycle. Interestingly, two proteins (SdhB and SdhE) of the succinate dehydrogenase complex (SdhABCDE) were strongly induced and therefore suggested that this additional succinate was used by this enzyme complex. Finally, we determined strong accumulation of proteins involved in the degradation of alternative carbon sources like benzoate/cathechol and strong induction of the last enzymatic steps in these pathways (Fig. 23). The last steps produce acetyl-CoA and succinyl-CoA that can reuse in the glycolysis/gluconeogenesis and the TCA cycle.

Beside proteins involved in known pathways, we sought an induction of a protein (BPSSL2846) that may be involved in regulating an amino acid metabolism pathway. The protein is a homolog to the pyridoxal 5'-phosphate binding YggS protein and induced in *E. coli* defect the LysR. YggS was modulated the isoleucine and valine metabolism (Ito *et al.*, 2013). It might speculate that the protein has similar or identical functions in *Bp*.

All together, we found many proteins involved in other pathways, but their repression or induction is a probable consequence of the strong changes in the central metabolic pathways.

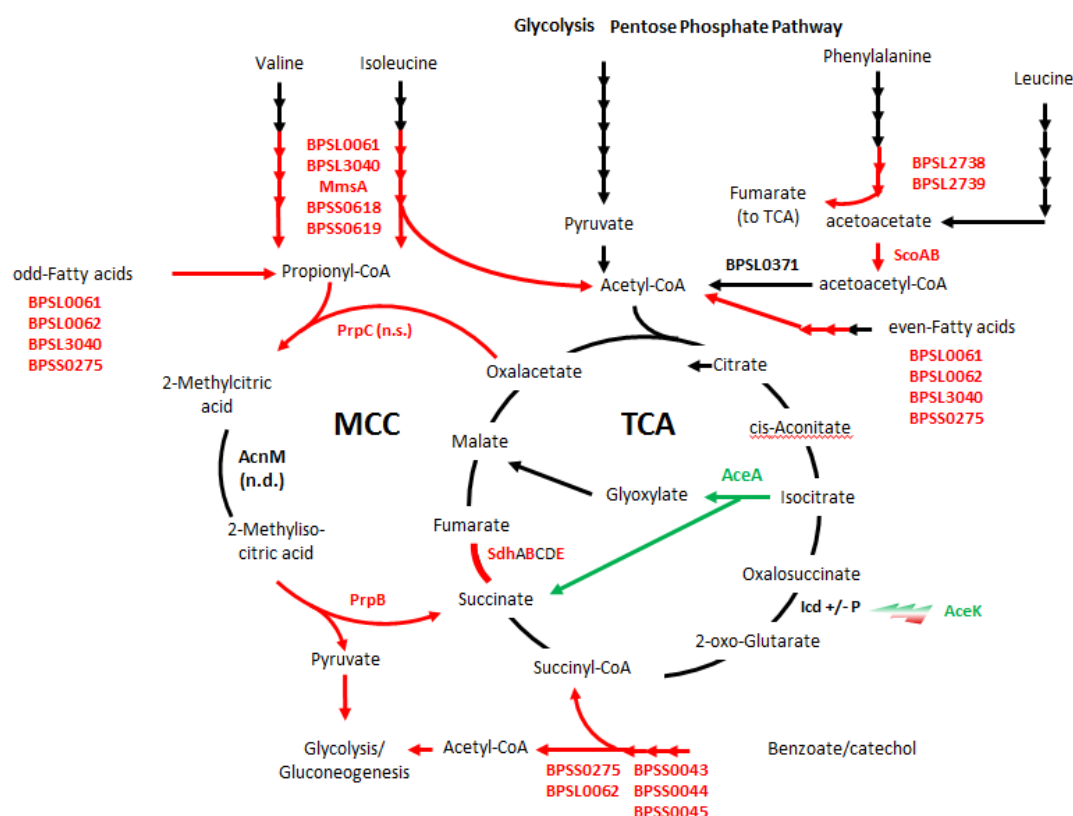


Figure 23. Relative alteration of cytoplasmic proteins involved in the TCA and MCC pathways of *Bp* ΔBPSL0117 compared to the E8 WT during exponential growth phase. Color-coded arrows and texts represent the relatively differential changes. Red, green and black colors imply induction, repression and not change, respectively. Relevance of protein name and locus: BPSL0061: Acyl-CoA dehydrogenases; BPSL0062: acetyl-CoA acetyltransferases; BPSL3034: mraZ protein; BPSS0618: Acyl-coenzyme A synthetases/AMP-(fatty) acid ligases; BPSS0619 (MmsA): methylmalonic acid semialdehyde dehydrogenase; BPSS0275: 3-oxoadipyl-CoA thiolase (EC 2.3.1.174); BPSS0043: 3-oxoadipate CoA-transferase alpha subunit; BPSS0044: 3-oxoadipate CoA-transferase beta subunit; BPSS0045: 3-carboxy-cis,cis-muconate cycloisomerase (EC 5.5.1.2); BPSL2738: fumarylacetoacetate hydrolase (EC 3.7.1.2); BPSL2739: fumarylacetoacetate hydrolase (EC 3.7.1.2); BPSL2739: homogentisate 1,2-dioxygenase (EC 1.13.11.5); BPSS0207 (PrpC): methylcitrate synthase (EC:2.3.3.5); BPSS0206 (PrpB): 2-methylisocitrate lyase (EC:4.1.3.30); BPSL1955 (ScoA): succinyl-CoA:3-ketoacid-coenzyme A transferase subunit A (EC:2.8.3.5); BPSL1954 (ScoB): succinyl-CoA:3-ketoacid-coenzyme A transferase subunit B (EC:2.8.3.5); BPSL2188 (AceA): isocitrate lyase (EC:4.1.3.1); BPSL0373 (AceK) bifunctional isocitrate dehydrogenase kinase/phosphatase (EC:2.7.11.5); BPSS1717 (SdhB): succinate dehydrogenase iron-sulfur subunit (EC:1.3.99.1); BPSS1716 (SdhE): Uncharacterized conserved protein.

3.1.7 *In silico* analysis of BPSL0117

LysR-type transcriptional regulators are the largest family of regulators in bacteria and act as both auto-repressors and activators of target promoters. LTTRs regulate the expression of a broad variety of cellular processes such as operons involved in amino acid metabolism, oxidative stress systems and the degradation of aromatic compounds (Shell, 1993). There are at least 88 loci that encode for hypothetical LTTR genes in the *Bp* genome (Holden *et al.*, 2004). As shown in Fig. 24, the putative LysR-type transcriptional regulator *BPSL0117* gene of *Bp* is located within chromosome 1 and flanked by BPSL0116 and BPSL0118 loci that are

probably involved in energy metabolism and cellular processes, respectively (Holden *et al.*, 2004).

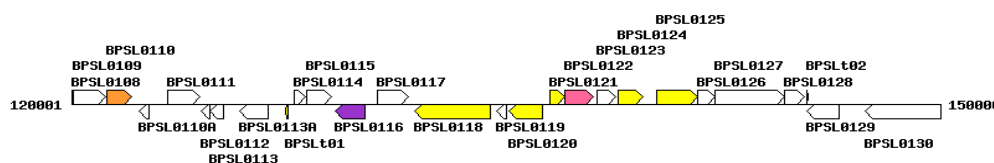


Figure 24. Partial genome map of *Burkholderia pseudomallei* K96243 (nucleotide position from 120,001 bp to 150,000 bp) (Modified from Kyoto encyclopedia of genes and genomes website). Color-coded represents function of genes: Violet is energy metabolism; Pink is metabolism of cofactors and vitamins; Orange is amino acid metabolism; Yellow is cellular processes, organismal systems, genetic information processing, and environmental information processing; and white is unassigned.

LTTs consist of an amino acid terminal DNA-binding domain (DBD) including a winged helix-turn-helix motif and a carboxyl terminal regulator domain joined by a long linker helix (Schell, 1993; Muraoka *et al.*, 2003). As shown in Fig. 25, BPSL0117 structure consists of a DBD, two regulatory domains, a putative effector-binding pocket and a long linker helix. As expected, the DBD comprises a wHTH motif including three α helices. Furthermore, the regulator domain I contains a core of three parallel and one anti-parallel β strands sandwiched among three α helices. The RD I is connected to wHTH through a long linker helix and two hinges. The regulatory domain II consists of one parallel and one anti-parallel β strands, four α helices. The putative effector binding pocket is located at the interface of RD I and RD II. The predicted structure of BPSL0117 protein shows similarity to the structure of the CrgA from *Neisseria meningitidis* and the CbnR from *Ralsonia eutropha* (Sainsbury *et al.*, 2009; Muraoka *et al.*, 2003).

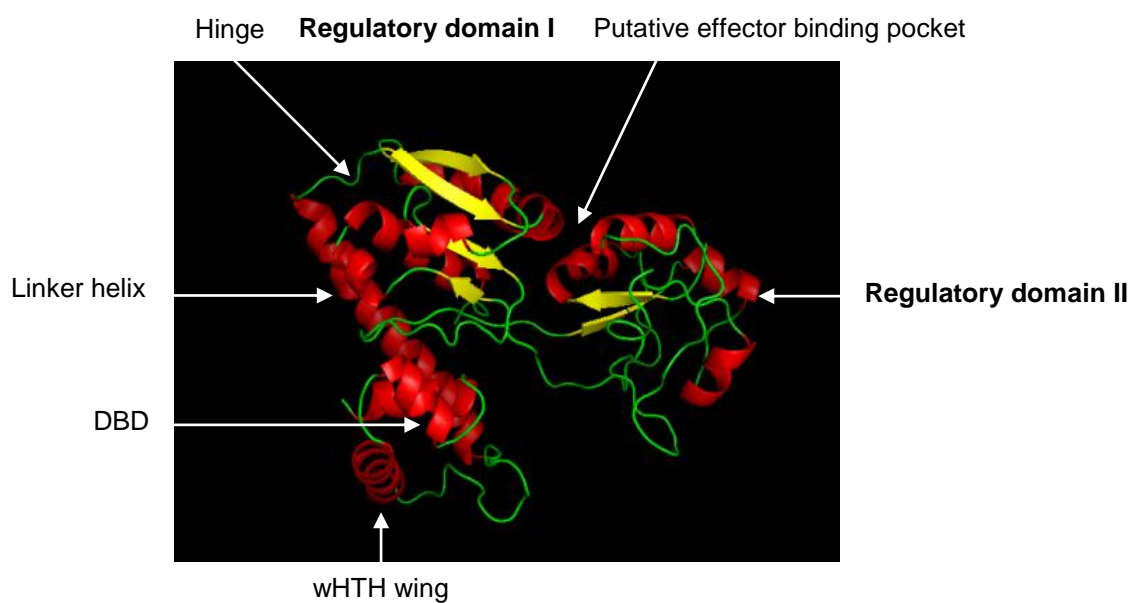


Figure 25. Predicted BPSL0117 fold and domain architecture. BPSL0117 domain architecture was predicted using Learning, Observing and Outputting Protein Patterns (LOOPP) algorithm of Elber group at University of Texas at Austin and animated using PyMOL program (version 1.6).

3.2 Characterization of the T3SS3 gene *BPSS1528* (*bapA*)

In the second part of this thesis, the focus was to characterize the hypothetical T3SS gene *BPSS1528* (*bapA*) of *Burkholderia pseudomallei* that is located within the T3SS3 cluster. *BapA* locus merely shows homology to T3SS genes from other Gram-negative bacteria. It was therefore of interest to evaluate the role of this yet unknown T3SS gene in the context of *Bp* associated virulence.

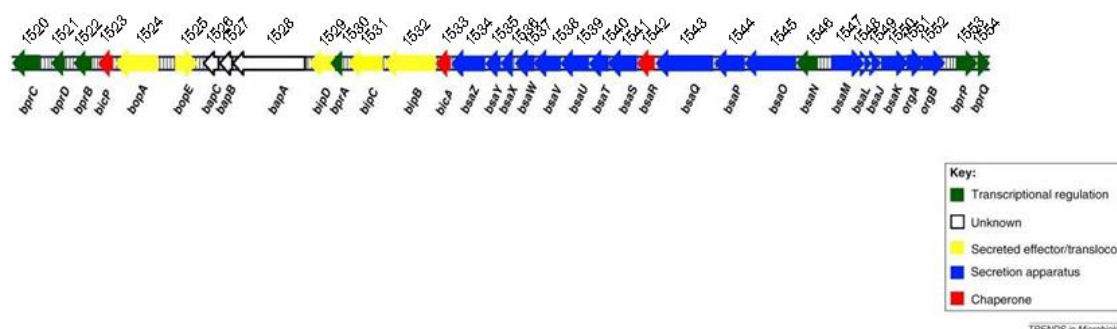


Figure 26. Genetic organization of the *B. pseudomallei* T3SS cluster 3. Genes within this 36-kb locus are annotated according to their putative functions. Color-coded arrows represent putative open reading frames with the respective BPSS number and respective gene names (Modified from Sun & Gan, 2010). The *bapA*, *bapB* and *bapC* genes, referred *BPSS1528*, *BPSS1527* and *BPSS1526* loci, respectively, are located between the effector *bopE* (*BPSS1525*) and the translocator *bipD* (*BPSS1529*).

3.2.1 Expression analyses of *bapA*, *bapB* and *bapC* genes

It is known that several genes of the T3SS3 cluster are expressed under certain environmental stress conditions (Pumirat *et al.*, 2009; 2010; Jitprasutwit *et al.*, 2010). We therefore checked whether expression of the *bap* genes was changed in the presence of various salt concentrations and different acidic gradients. To detect the *bap* transcripts via RT-PCR, specific primer sets for internal *bapA*, *bapB*, *bapC* and 23S genes with 177 bp, 161 bp, 298 bp and 334 bp, respectively, were designed.

3.2.1.1 Expression of *bap* genes under salt stress

Recent studies have been shown that *Bp* grown under salt stress led to increased expression of T3SS-3 genes and respective proteins (Pumirat *et al.*, 2009 & 2010). *Bp* WT E8 was grown in LB broth with various NaCl concentrations ranging from 85 mM to 470 mM at 37°C for 6 h. The transcription of *bap* genes was analysed by semi quantitative RT-PCR. As shown in Fig. 27, expression of *bapA* was clearly increased in NaCl containing medium compared to medium that did not contain any NaCl. The expression level of *bapA* did merely differ within the range of the NaCl concentrations tested. In contrast, the expression levels of *bapB* and *bapC* were proportionally increased at higher salt concentration levels.

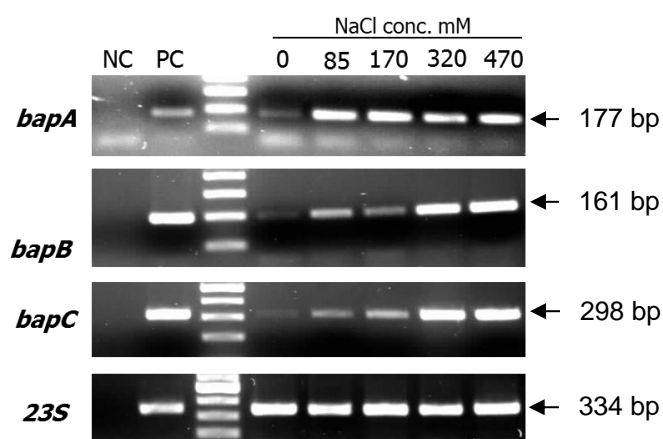


Figure 27. mRNA expression levels of *bap* genes in *Bp* E8 WT at 6 h after inoculation in YT medium containing various NaCl concentrations. The data were obtained using semi quantitative RT-PCR. The 23S *rRNA* gene served as the reference gene. PCR fragments were electrophoresed on 1.5% agarose gel and stained by SYBR® safe nucleic acid stain. NC: negative control, PC: positive control. One representative result out of three experiments with similar results is shown.

3.2.1.2 Expression of *bap* genes under pH stress

A previous study from Jitprasutwit *et al.*, (2010) could show that secretion of the T3SS effector proteins BopE and BipD in both *Bth.* and *Bp* was increased under acidic conditions. It was therefore checked whether expression of the *bap* genes was increased under acidic pH growth condition. As shown in Fig. 28, the expression of all *bap* genes was increased at a lower pH, most prominently at pH 4.

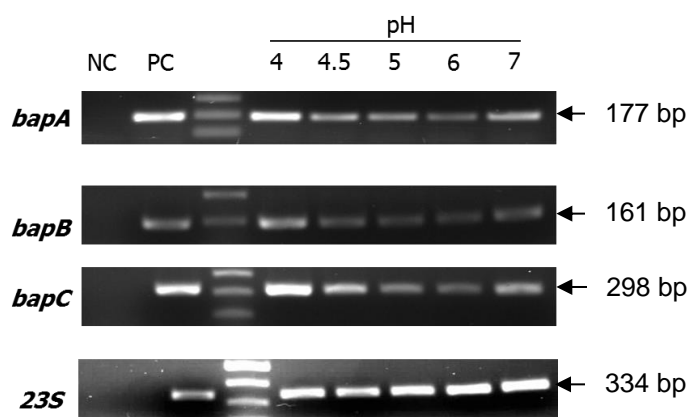


Figure 28. mRNA expression levels of *bap* genes in *Bp* E8 WT at 6 h after inoculation in LB medium with various pH. The data were obtained using semi quantitative RT-PCR. The 23S *rRNA* gene served as the reference gene. PCR fragments were electrophoresed on 1.5% agarose gel and stained by SYBR® safe nucleic acid stain. One representative result out of three experiments with similar results is shown.

3.2.1.3 Expression of *bapA* gene after infection RAW 264.7 macrophages

It was next evaluated whether expression of the *bapA* gene was induced during intracellular infection. Therefore, macrophages were infected at an MOI of 100 with *Bp* K96243 and the expression of *bapA* gene was investigated after 2 h and 5 h post infection. As shown in Fig. 29, expression of *bapA* gene was clearly induced during intracellular infection and detectable by semi quantitative RT-PCR at 5 h post infection.

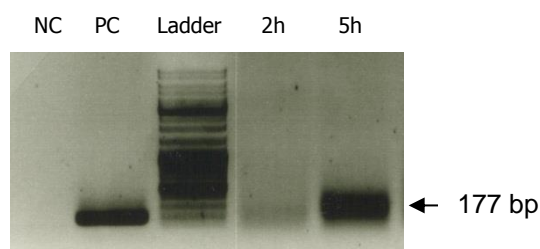


Figure 29. mRNA expression of *bapA* gene in *Bp* K96243 WT at 2 h and 5 h post infection of RAW264.7 cells. The data were obtained using semi quantitative RT-PCR. PCR fragments were electrophoresed on 1.5% agarose gel and stained by SYBR[®] safe nucleic acid stain. NC: negative control, PC: positive control. One representative result out of three experiments with similar results is shown.

3.2.2 Construction of *B. pseudomallei* Δ *bapA* mutants and complementation

3.2.2.1 Targeted mutagenesis

The construction of a *bapA* (*BPSS1528*) deletion mutant was performed by using the dual markerless allelic replacement vector pEXKm5 as previously described by Lopez and colleagues (2009). Successful deletion was verified by PCR. Figure 30 shows two Δ *bapA* mutants in that the respective gene was deleted in comparison to the *Bp* WT K96243.

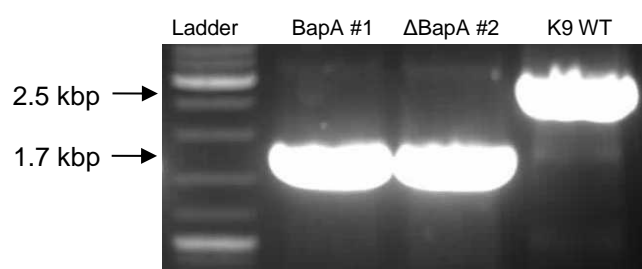


Figure 30. Detection of the *bapA* gene deletion by PCR reaction. PCR was confirmed by using the primer pair BapASmal-Fw1 and BapASmal-Rev3 and the genomic DNA of *Bp* K96243 WT as a control and the potential *bapA* gene deletion mutants. PCR fragments were electrophoresed on 1% agarose gel and stained by SYBR[®] safe nucleic acid stain.

3.2.2.2 Complementation

The stable re-integration of the *bapA* gene in the genome of *Bp* Δ *bapA* was carried out by using the pUC18-mini-Tn7::FRT:Zeo vector (Choi *et al.*, 2008). As shown in Fig. 31, to verify successful *in-trans* complementation of the *Bp* Δ *bapA*, PCR using a forward primer that binds within the Tn7 vector and one of three reverse primers that can either bind in the *glmS1*, *glmS2* or *glmS3* gene loci, respectively, was carried out (Choi *et al.*, 2008). Furthermore, PCR was also done using internal *bapA-orf* forward and reverse primers to check the full insertion of *bapA* gene (Fig. 31B). To confirm the deletion mutation without any polar effect on downstream genes, phenotypes of *bapA* complementation strain was further checked with various experiments.

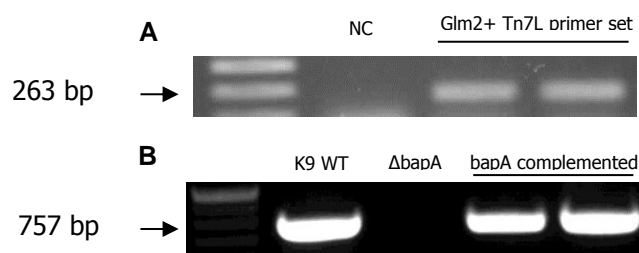


Figure 31. Detection of the complementation of *bapA* gene by PCR. PCR fragments were electrophoresed on 1.5% agarose gel and stained by SYBR[®] safe nucleic acid stain. NC: negative control, PC: positive control. **A:** Determination of the insertion sites of the *bapA* gene for complementation, **B:** PCR with the internal primer BapAComp-Fw1 and BapAComp-Rev1 of genomic DNA obtained from *Bp* K96243 WT, *Bp* Δ*bapA*#1 and *Bp* Δ*bapA*#1 complemented strains.

3.2.3 Functional analysis of *B. pseudomallei* Δ*bapA*#1

3.2.3.1 Growth kinetics

To check whether BapA influences the *in vitro* growth of *Bp*, bacterial strains were grown in either a complex nutrient LB medium or the minimal medium Vogel-Bonner (VB) under aerobic as well as anaerobic conditions. As shown in Fig. 32, growth of the *Bp* Δ*bapA*#1 strain was not different at all in LB medium at aerobic condition compared to the WT strain. Under anaerobic growth condition and in the minimal VB medium one could only observe slightly impaired growth in the absence of BapA.

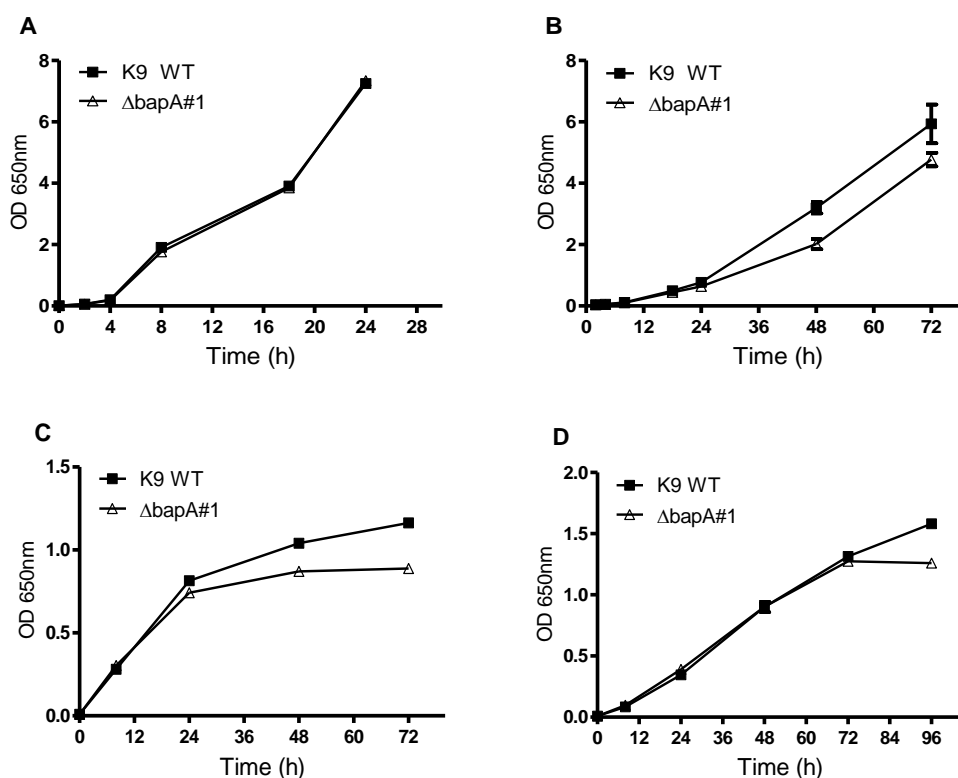


Figure 32. Growth curve of *Bp* ΔbapA#1 compared to that of *Bp* K96243 WT. **A:** Normal LB (aerobic), **B:** VB (aerobic), **C:** Normal LB containing 50 mM KNO₃ (anaerobic), **D:** VB containing 50 mM KNO₃ (anaerobic). Growth kinetics for one of three experiments with similar results is shown.

3.2.3.2 Motility

To check whether BapA influences the *in vitro* motility of *Bp*, bacterial strains were spotted into soft agar and incubated for 24 h and 48 h at 37°C. As shown in Fig. 33, the *Bp* ΔbapA#1 strain was neither impaired in swimming (Fig. 33A) nor swarming motility (Fig. 33B) compared to the WT strain.

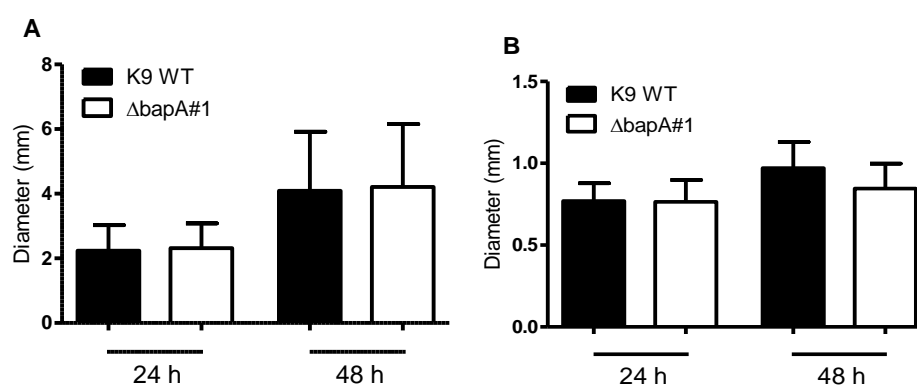


Figure 33. Motility of *Bp* ΔbapA#1 compared to that of *Bp* K96243 WT. Motility was assayed after 24 h and 48 h of incubation at 37°C by measuring diameters of circular bacterial migration from the point of inoculation point. **A:** Swimming in 0.3% agar plates, **B:** Swarming in 0.6% agar plates. Data are pooled from three independent experiments and analyzed using Student t-test.

3.2.3.3 Biofilm formation

To assess whether BapA might be involved in the biofilm formation of *Bp*, this phenotype was tested under various NaCl concentrations and compared to that of the *Bp* WT strain K96243. As shown in Fig. 34, the Δ bapA#1 mutant strain showed significantly more biofilm formation in all YT broth containing various salt concentrations than the WT strain K96243.

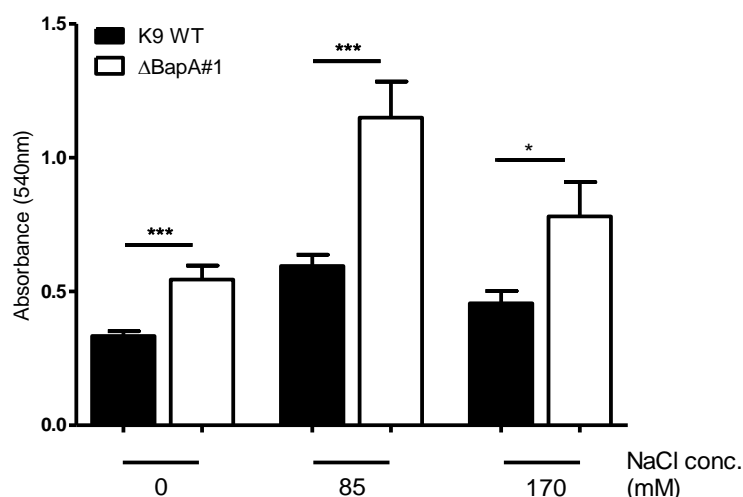


Figure 34. Biofilm formation of *Bp* Δ bapA#1 compared to that of *Bp* K96243 WT. Biofilm formation was assayed after 48 h static incubation at various NaCl concentrations at 37°C. Crystal violet retention of adherent bacteria is shown at 540 nm. Values are the means \pm SD of triplicate determinations. Pooled data from three independent experiments are shown and analyzed using Student t-test. * and *** denote P values <0.05 and 0.001, respectively.

3.2.3.4 Secretion of proteases

To examine whether BapA might be associated with the secretion of proteases, we cultivated bacterial strains in 3 ml LB broth overnight at 37°C with shaking 140 rpm and determined activity of exo-proteases secreted into supernatants with 0.1 mg protease K as an internal control. As shown in Fig. 35, *Bp* Δ bapA#1 showed slightly more protease activity compared to the WT strain K96243, but was not statistically significant.

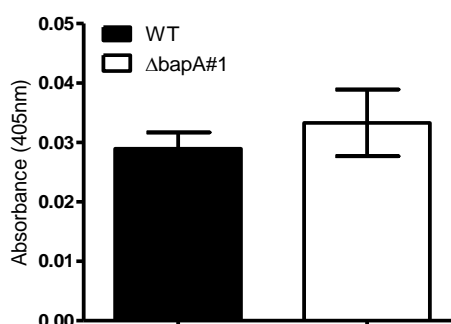


Figure 35. Activity of exo-proteases was determined by the azocasein method. Supernatants of overnight cultures in LB broth of *Bp* K96243 WT and *Bp* Δ bapA#1 were collected and exo-proteases activity was determined by azocasein cleavage with 0.1 mg protease K as internal control.

3.2.3.5 Influence of BapA on the functionality of the *B. pseudomallei* T3SS3

To assess whether BapA might influence the secretion of proteins of the T3SS3, secretion of the T3SS effector proteins BipD and BopE were analyzed. Bacteria were grown in LB medium at 37°C and harvested at indicated time points. *Bp* Δ bapA#1 strain exhibited no difference in the secretion of the T3SS3 BopE and BipD proteins compared to WT bacteria at 4 h inoculation. However, these proteins seemed to be partially cleaved at 8 h and completely degraded at later time points (see Fig. 36). The result shows BapA is not likely to be involved in the secretion of other T3SS3 proteins.

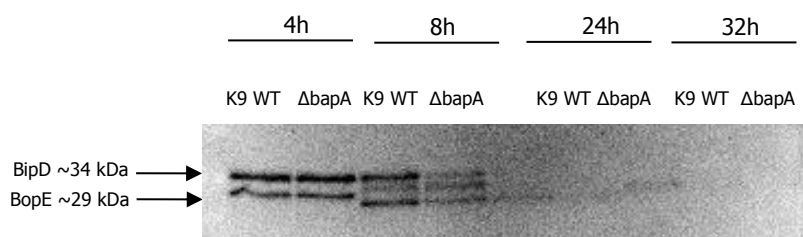


Figure 36. Comparison of the T3SS3 effector and translocation proteins of *Bp* K96423 WT and *Bp* Δ bapA #1 in LB medium inoculation at different time points. Proteins were separated by 12.5% SDS-PAGE, transferred onto a membrane and detected by primary anti-BipD and anti-BopE and secondary goat anti-mouse IgG linked horseradish peroxidase antibodies. One representative result out of three experiments with similar results is shown.

3.2.3.6 Global protein expression

To assess whether BapA affects a global protein expression profile of *Bp*, bacteria were grown in LB broth and collected both cellular and extracellular proteins at indicated time points. As shown in Fig. 37 and 38, deletion of *bapA* gene was resulted in an altered expression profile of extracellular proteins. The *Bp* Δ bapA#1 showed increased expression of a higher molecular weight band compared to the WT after 8 h and 24 h inoculations. The mutant exhibited lack the middle band compared with the WT, whereas the mutant secreted more one small molecular weight band that was absent in the WT. Further experiment was identified that the mutant increased secretion of three extracellular proteases defined as chitoiase, peptidase and x-prolyl-dipeptidyl aminopeptidase (data not shown). In contrast to exoproteins, cellular protein patterns did not show clearly different in *Bp* Δ bapA#1 compared to the WT strains. Thus, the data showed that BapA seems to be involved in global regulation of protein secretion. It seemly does not convince that why we decided to create further independent *bapA* mutants.

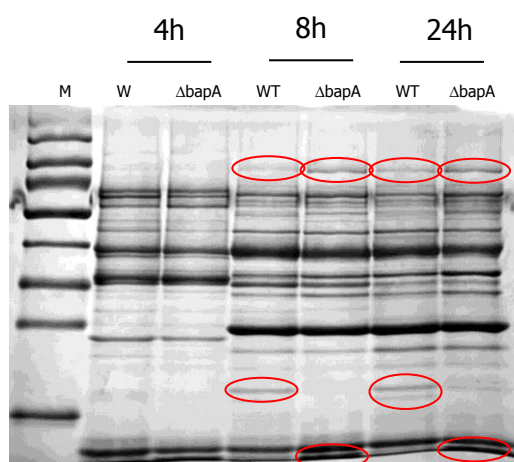


Figure 37. Comparison of extracellular proteins of *Bp* K96243 WT and *Bp* ΔbapA #1 in LB medium inoculation at different time points. Proteins were separated by 12.5% SDS-PAGE and stained by using Coomassie R250. Red ellipses were indicated for altered protein patterns. One representative result out of three experiments with similar results is shown.

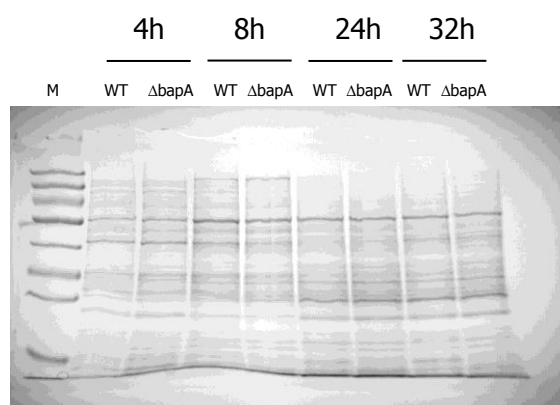


Figure 38. Comparison of cytosolic proteins of *Bp* K96423 WT and *Bp* ΔbapA #1 in LB medium inoculation at different time points. Proteins were separated by 12.5% SDS-PAGE and stained by using Coomassie R250. One representative result out of three experiments with similar results is shown.

3.2.3.7 Uptake and intracellular replication

To examine whether BapA influences uptake and intracellular replication of *Bp* within host cells, RAW264.7 and BALB/c-BMM were infected. As shown in Fig. 39, there was no difference in the uptake of bacteria in either the macrophage cell line (Fig. 39A) or primary macrophages (Fig. 39B). However, *Bp* ΔbapA#1 showed significantly increased intracellular replication in both type of macrophages 24 h after infection.

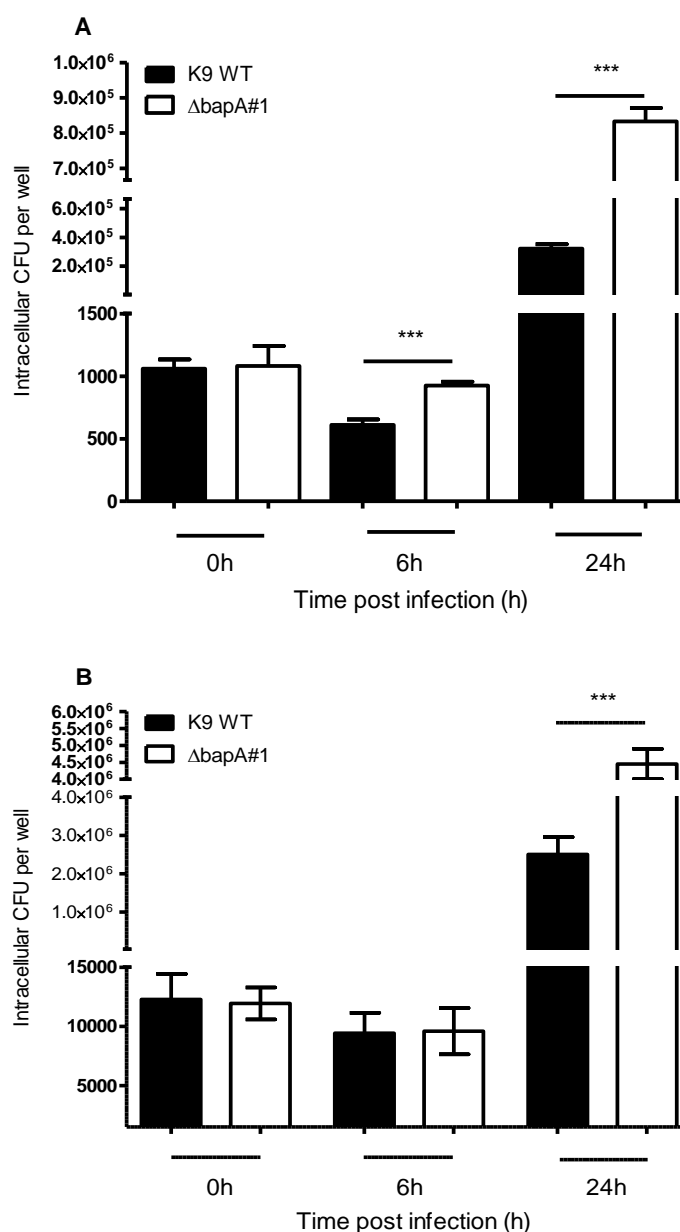


Figure 39. Comparison of uptake and intracellular replication of *Bp* K96243 WT and *Bp* $\Delta bapA$ #1. **A:** Invasion and intracellular replication in RAW 264.7 with MOI = 1; **B:** Invasion and intracellular replication in BALB/c-BMM with MOI = 2. Values are the means \pm SD of triplicate determinations in single representative experiments. Similar results were obtained in at least three independent experiments with each bacterial strain. The data are analyzed using Student t-test. *** denotes a P value <0.001.

3.2.3.8 Actin polymerization assay

It was next investigated whether BapA affects the formation of actin tails of *Bp*. For this purpose, the human hepatocytic cell line HepG2 was infected with the WT and *Bp* $\Delta bapA\#1$ and the formation of actin tails was investigated at 8 h and 18 h after infection by immunofluorescence microscopy. As shown in Fig. 40, the *Bp* $\Delta bapA\#1$ mutant was able to form normal actin tails like WT bacteria. Thus, BapA seems to have no influence on the recruitment of actin within host cells.

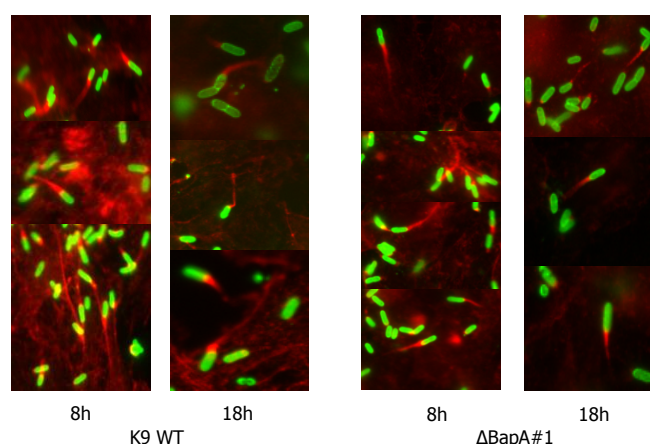


Figure 40. Comparison of actin tail formation in HepG2 infected *Bp* K96243 WT and *Bp* Δ bapA#1 at 8 h and 18 h post infection. Bacteria were stained green with mouse anti-*Bp* EPS and anti-mouse IgG-alexa488. Filamentous actin was stained red with anti-rabbit Ig-Alexa568 phalloidin.

3.2.4 Influence of BapA on *B. pseudomallei* virulence

3.2.4.1 Mortality

To assess whether BapA might contribute for the *in vivo* virulence of *Bp*, BALB/c mice were infected with *Bp* Δ bapA#1 and respective WT bacteria. As shown in Fig. 41A, intranasally infected mice succumbed significantly earlier after infection with the *Bp* Δ bapA#1 mutant strain compared to WT bacteria. The same tendency was seen when mice were infected via the intravenous route (Fig. 41B).

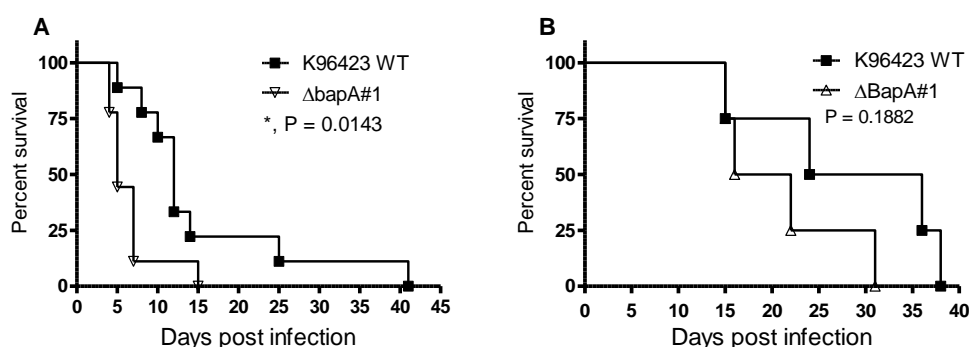


Figure 41. Mortality curves of BALB/c mice after infection. **A:** Intranasal infection of BALB/c mice ($n = 9$) with *Bp* K96243 WT, mutant Δ bapA#1 (infection dose from 14 to 25 CFU per animal). Pooled data from two independent experiments are shown. **B:** Intravenous infection of BALB/c mice ($n = 4$) with *Bp* WT K96243 and mutant Δ bapA#1 (infection dose from 202 to 220 CFU per animal). The data were analyzed using the log rank Kaplan-Meier test.

3.2.4.2 Determination of bacterial load in organs

BALB/c mice were inoculated via the intranasal route with *Bp* WT strain K96243 and *Bp* Δ bapA#1 to examine whether the increased mortality demonstrated in Fig. 41 was associated with increased bacterial burden in lungs, livers and spleens. Organs were collected aseptically 48 h after infection, and the numbers of viable bacteria per organ were evaluated. As shown in Fig. 42, the bacterial burdens in lungs, livers and spleens were

significantly higher in mice that received the *Bp* Δ bapA#1 mutant strain compared to mice infected with *Bp* K96243 WT.

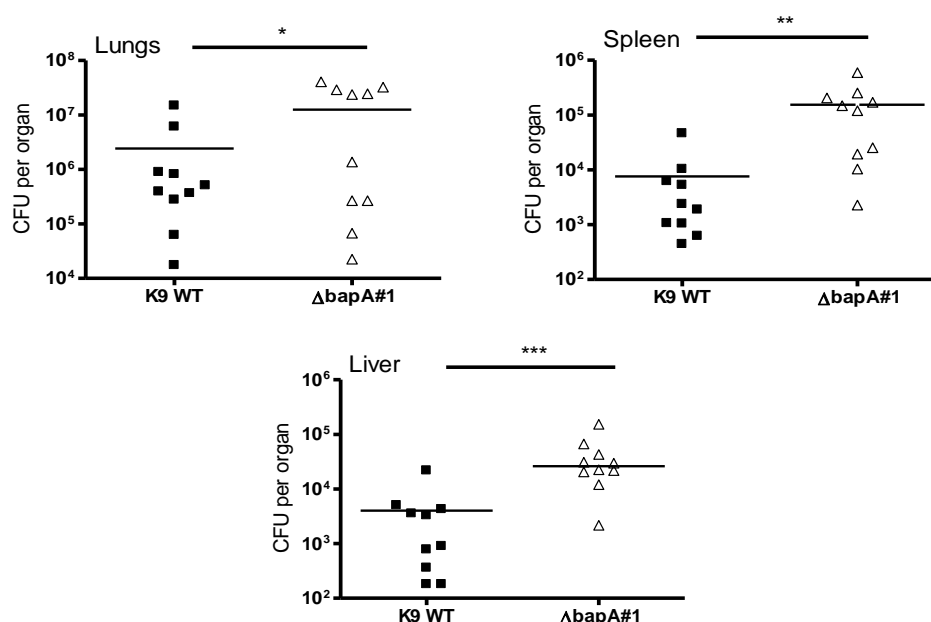


Figure 42. Bacterial burden in organs' BALB/c mice (n = 10) after 48 h intranasal infection with *Bp* K96243 WT (dose infection from 69 to 139 CFU) and *Bp* Δ bapA#1 (dose infection from 90 to 95 CFU). Single dots represent CFU in the respective organs from single animals. The horizontal lines represent the geometric means. Data are pooled from two independent experiments and analyzed using Student t-test. *, **, and *** denote P values <0.05, <0.01, and <0.001, respectively.

3.2.5 Characterization of *B. pseudomallei* Δ bapA#2 and *B. pseudomallei* Δ bapA#3

Bp Δ bapA#1 derived from K96243 showed increased biofilm formation and increased intracellular replication in host cells. Notably, the *in vivo* virulence seems to be increased in the absence of BapA and the overall global protein expression pattern was also changed. However, even successful *in-trans* complementation strains did not reverse the observed phenotypes to any extent. It was therefore decided to create other two independent *Bp* Δ bapA mutant strains. One mutant was again derived from the WT K96243, as before *Bp* Δ bapA#1 mutant (now designed as *Bp* Δ bapA#2) and another mutant was derived from the WT 1026b strain (*Bp* Δ bapA#3). Some of the key experiments were repeated to address whether these independently created mutants exhibit the same phenotype as *Bp* Δ bapA#1.

3.2.5.1 Biofilm formation

To validate whether BapA influences the biofilm formation of *Bp*, the phenotype of *Bp* Δ bapA#2 was compared to that of *Bp* WT strain K96243 and *Bp* Δ bapA#1 in normal LB broth. Additionally, biofilm formation of *Bp* Δ bapA#3 was also compared to that of *Bp* WT 1026b under various NaCl concentrations. As shown in Fig. 43, biofilm formation of *Bp* Δ bapA#2 did not differ compared to the WT strain K96243, and the phenotype observed in *Bp* Δ bapA#1 could not be confirmed (Fig. 43A). In addition, biofilm formation of *Bp* Δ bapA#3 did also not differ compared to the WT strain 1026b, even when different NaCl

concentrations were used (Fig. 43B). Thus, using two other *Bp* Δ bapA mutants derived from different *Bp* strains revealed that BapA is not likely to be directly involved in the process of biofilm formation

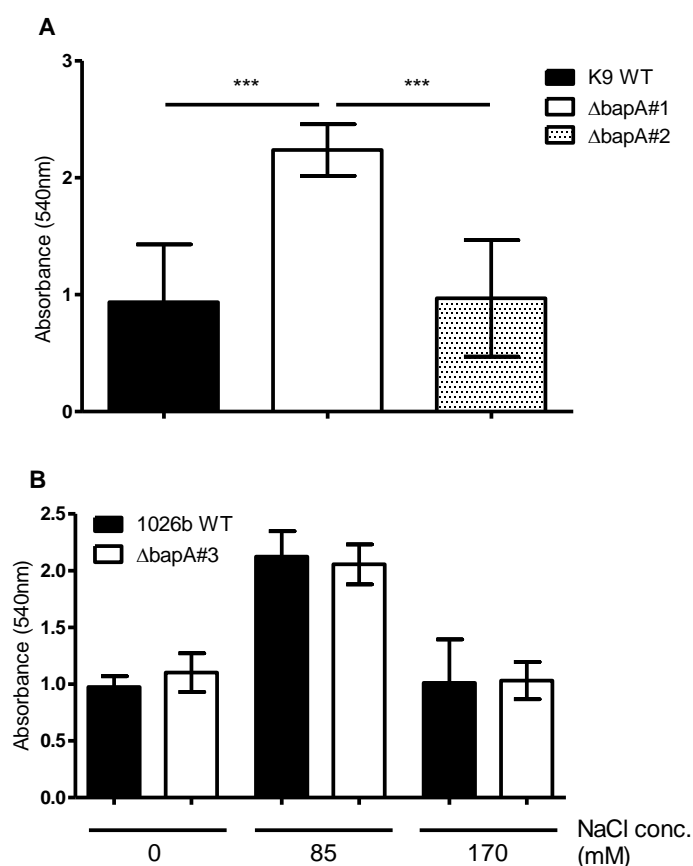


Figure 43. Biofilm formation after 48 h static incubation in LB broth containing various NaCl concentrations at 37°C. **A:** At 48 h static incubation in normal LB broth, **B:** at 48 h static incubation under various NaCl concentrations. Crystal violet retention of adherent bacteria is shown at 540 nm. Values are the means \pm SD of triplicate determinations. Pooled data from three independent experiments are shown and analyzed using one-way ANOVA with Bonferroni multiple comparisons posttest. *** denotes a P value <0.001 .

3.2.5.2 Intracellular survival

To verify whether BapA influences uptake and intracellular replication of *Bp* within host cells, RAW264.7 cells were infected with all three *Bp* Δ bapA mutant strains. As shown in Fig. 44A, there were no differences in the uptake of *Bp* Δ bapA#1 and *Bp* Δ bapA#2 compared to *Bp* WT K96243. Moreover, the ability to replicate inside macrophages was unchanged in *Bp* Δ bapA#2 after 24 h infection compared to *Bp* WT K96243. This was in contrast to *Bp* Δ bapA#1, which showed significant increased bacteria load at 24 h post infection. In addition, *Bp* Δ bapA#3 did not show differences in the uptake and intracellular replication up to 24 h after infection (Fig. 44B). These results clearly suggest that BapA does not seem to have a role for intracellular replication of *Bp*.

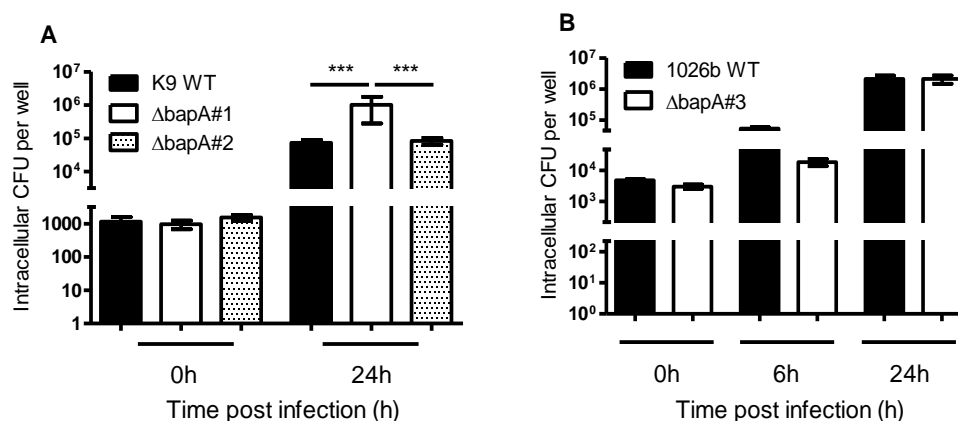


Figure 44. Uptake and intracellular replication assays in RAW 264.7 macrophages. **A:** Infection with *Bp* K96243 WT, *Bp* $\Delta bapA\#1$ and *Bp* $\Delta bapA\#2$, MOI ~ 1; **B:** Infection with *Bp* 1026b WT and *Bp* $\Delta bapA\#3$, MOI ~ 1. Values are the means \pm SD of triplicate determinations in single representative experiments. Similar results were obtained in at least three independent experiments with each bacterial strain. The data are analyzed using one-way ANOVA with Bonferroni multiple comparisons posttest and Student t-test. *** denotes a P value <0.001.

3.2.5.3 *In vivo* virulence

It was next addressed whether the virulence potential of the $\Delta bapA\#3$ mutant strain derived from *Bp* 1026b has changed. Therefore, BALB/c mice were intranasally infected with *Bp* $\Delta bapA\#3$ and 1026b WT bacteria. As shown in Fig. 45, mice infected with *Bp* $\Delta bapA\#3$ mutant strain did not show any differences in the survival compared to the WT bacteria. Thus, BapA does not seem to have a role for *Bp*-associated virulence.

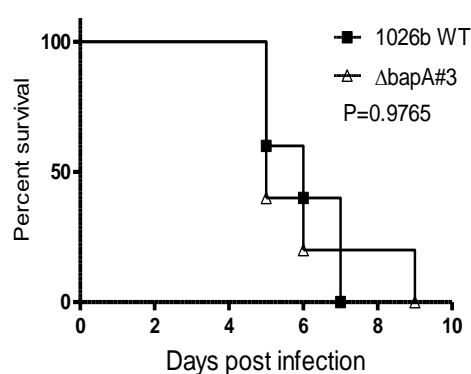


Figure 45. Mortality curves of BALB/c mice (n = 5) after intranasal infection with *Bp* 1026b WT, *Bp* $\Delta bapA\#3$ (infection dose from 20 to 22 CFU per animal). The data were analyzed using the log rank Kaplan-Meier test.

4 DISCUSSION

4.1 Characterization of the LTTR BPSL0117

The LysR-type transcriptional regulators are one of the largest families of prokaryotic transcriptional regulators. One of the aims of this thesis was to analyze and characterize the structure and functions of the putative LTTR BPSL0117 of *Bp* with a focus on its role for the pathogenesis of the pathogen. Recently, BPSL0117 was elucidated upregulation at all-time points during *Bp* lung infection in Sprague-Dawley rat model (Schaik *et al.*, 2008). BPSL0117 could therefore play an important role for the pathogenesis.

4.1.1 Structure and regulatory functions of BPSL0117

Gene expression in response to different environmental signals in bacteria is controlled by a large variety of both global and specific transcription factors. LTTRs function as both induce and repress transcription. Combining computational prediction and characterization, we have elucidated a structure and functions of the LTTR, BPSL0117 protein from *Bp*. To our knowledge, at present there are only two full-length crystal structures of LTTR known: CbnR from *Ralstonia eutropha* NH9 and CrgA from *Neisseria meningitidis* (Muraoka *et al.*, 2003; Sainsbury *et al.*, 2009). It is likely that the predicted structure of BPSL0117 exhibits a common structure of LTTRs as well since we found that the amino acid sequence shares homologies and similarities with other LTTR family proteins. According to the predicted structure of BPSL0117, a co-factor might work as an inducer or/and a repressor in the interaction to BPSL0117 and the regulator may lead to a conformation change and bind to a promoter DNA. The proteome analysis results show that BPSL0117 influenced the abundances of numerous proteins including other transcriptional regulator families. Thus, BPSL0117 can be considered to have a global regulatory function within the *Bp* genome and seems to work as both a primary and a secondary regulator through regulating other transcriptional regulator families.

4.1.2 Regulation of virulence factors

The proteome data revealed that BPSL0117 influences the abundances of numerous proteins that are involved in the pathogenesis of *Bp*. Remarkably, the expression of T3SS3 and T6SS1 proteins was downregulated in the absence of BPSL0117 compared to the WT E8 at the exponential growth phase. Within the T3SS3 gene cluster, the protein BsaR, the chaperon BicP, the effector protein BopE, and translocator protein BipD showed lesser expression in *Bp* Δ BPSL0117 compared to the WT E8 in both western blot (BopE and BipD) and proteome analysis. The T3SS3 plays an essential role for *Bp* to escape from the phagolysosome and contributes to *in vivo* virulence in animal models (Stevens *et al.*, 2002; 2004; Warawa & Woods, 2005, Pilatz *et al.*, 2006; Gong *et al.*, 2011). The data analysis could further show that T6SS1 associated with proteins such as the T6SS regulator VirG

(BPSS1494), the T6SS effector protein Hcp1 (BPSS1498) as well as the T6SS1 proteins TssA (BPSS1496) and TssB (BPSS1497) did also decreased abundances in *Bp* Δ BPSL0117 in the exponential growth phase. Previous studies have revealed that the T6SS1 regulator VirAG and the effector protein Hcp1 play a role for the intact intracellular life cycle and are crucial for the intracellular replication and the formation of multi-nucleated giant cells in macrophages (Burtneck *et al.*, 2011; Chen *et al.*, 2011; Burtneck *et al.*, 2013; Hopf *et al.*, 2014). Moreover, a Δ hcp1 mutant was strongly attenuated in a murine model of melioidosis (Hopf *et al.*, 2014). The impaired expression of T3SS3 and T6SS1 proteins in *Bp* Δ BPSL0117 is likely to contribute to the observed *in vitro* phenotypes in mammalian cells such as the impaired intracellular replication. It also explains the attenuated phenotype of *Bp* Δ BPSL0117 in the BALB/c mouse model.

Virulence in many bacteria is dependent on biofilm formation, *e.g.* in *Pseudomonas*, *Staphylococcus*, *Burkholderia cenocepacia* complex and other pathogenic bacteria (Fux *et al.*, 2005). Biofilms play also a role for the protection against antibiotics and the host immune system (Fux *et al.*, 2005; Hall-Stoodley & Stoodley, 2009; Antunes & Ferreira, 2011). *Bp* Δ BPSL0117 exhibited an impaired biofilm formation in LB medium compared with WT bacteria. This could explain why the Δ BPSL0117 mutant strain was more susceptible to the beta-lactam antibiotics ceftazidime and imipenem compared to WT bacteria. In addition, the proteome data revealed that the beta-lactam class C protein was lower expressed in the absence of BPSL0117 that might additionally contribute to the loss of resistance against beta-lactam antibiotics.

The present data show that an impairment of the putative LTTR BPSL0117 led to an impaired expression of numerous virulence proteins that were in accordance with the strong loss of virulence in *Bp* in the BALB/c mouse model of melioidosis.

4.1.3 Regulation of metabolic pathways

Bp is an intracellular pathogen and must have proper metabolic systems to survive inside the host cells. The major carbon source for many pathogenic bacteria *in vivo* metabolism within host cells are fatty acids through the glyoxylate shunt and the β -oxidation cycles (McKinney *et al.*, 2000; Munoz-Elias & McKinney, 2005; 2006). Besides, the TCA cycle plays the important central in both assimilatory and dissimilatory roles. In this study, the TCA cycle in the BPSL0117 mutant was probably total deregulated. One of the key enzymes, the isocitrate dehydrogenase (Icd) should be significantly less phosphorylate or dephosphorylate, since the regulating enzyme AceK (bifunctional isocitrate dehydrogenase kinase/phosphatase) was strongly downregulated. In *E. coli*, this enzyme is coregulated with the Isocitrate lyase AceA and the malate synthase (AceB) in one operon, but all three genes in *Bp* locate on different loci. The expression of AceB was not changed, but AceA and AceK expression were also strongly repressed. Thus, it was assumption that their expression was influenced by the same regulator.

In contrast to the strongly downregulated AceA protein, the methylisocitrate lyase PrpB involved in the MCC was significantly upregulated. Bifunctional catalysis Isocitrate lyase

(AceA = ICL) and paralogous methylisocitrate lyase (PrpB = MCL) are key metabolic enzymes to sustain growth on even-chain fatty acids and odd-chain fatty acids through the glyoxylate shunt, the MCC and the β -oxidation cycles, respectively (Eoh & Rhee, 2014). Lacking ICL and MCL in *Mycobacterium tuberculosis* shows highly attenuated virulence in mouse model of pulmonary tuberculosis (Munoz-Elias & McKinney 2005; Gould *et al.*, 2006). In contrast to *M. tuberculosis*, single mutant *icl* (BPSL2188) and double mutant *icl/mcl* (BPSL2188/BPSS0206) in *Bp* exhibit increased cytotoxicity of RAW264.7 and virulence in the Sprague-Dawley rat model of acute melioidosis (Schaik *et al.*, 2009). Moreover, chronic *Bp* infection in the rat model was forced into an acute phase by treatment with inhibition of ICL, itaconic acid. The results suggest that ICL and MCL play an important role for dormancy within hosts (Schaik *et al.*, 2009). In the BPSL0117 mutant, ICL (AceA) was repressed, but the MCL (PrpB) was induced. Both enzymes can substitute for the same function in *M. tuberculosis* and *Bp* (Munoz-Elíaz, 2005; Munoz-Elias, 2006; van Schaik, 2009). Thus, no differences of growth could theoretically be expected. However, we observed a severe defect in growth rate of *Bp* Δ BPSL0117 in M9 minimal medium containing glucose as the carbon source. As mentioned above, we found a strong upregulation of proteins involved in the degradation of isoleucine, valine, phenylalanine and fatty acids to pyruvate, acetyl-CoA and propionyl-CoA. For their degradation, a permanent exhaustion of the TCA intermediates oxaloacetate by the MCC and the first reaction of the TCA cycle (Fig. 23) were most probable. We assumed that these heavy disturbances in the TCA cycle provoked the growth behavior of *Bp* Δ BPSL0117. Additionally, leucine/isoleucine/valine/phenylalanine and fatty acids must be synthesized from glucose and their continuous degradation to propionyl-CoA/acetyl-CoA may lead to a reduced growth rate. Further analysis of the intra and extra cellular metabolites should give a hint to elucidate our assumption. Because we found only little differences of growth between the BPSL0117 mutant strain and the wild type if they cultivated in a nutritionally rich LB medium. We could not predict if these disturbances in the central carbon pathways play an essential role in *in vitro* or *in vivo* conditions that leads to strongly attenuated virulence of *Bp* Δ BPSL0117. Further experiments should therefore be necessary to clarify impacts of these changed metabolic pathways for virulence of *Bp*.

The occurrence of the operon(s) BPSL0475 - BPSL0493 that shares homology with only pathogenic *Burkholderia* species, but not *B. thailandensis* and repressed expression in *Bp* Δ BPSL0117 compared to the WT might play an important role in intracellular survival strategies of *Bp*. Unfortunately, functions of the operon(s) have been not completely understood, but many proteins could be involved in transport of unknown substrate(s), fatty acid synthesis/modification, citrate metabolism and amino acid metabolism. Although we could not rule out that the down regulation of the operon(s) contributes to decreased virulence of the mutant strain, but the unique loci should be hot candidates for further analyses using different mutants. Afterwards, global RNA and/or protein expression techniques and detection of intra and extra cellular metabolites should be necessary to elicit the function of these loci.

The number of alteredly regulated proteins showed that LysR (BPSL0117) acts as global regulation in both a repressor and an activator. Moreover, we also found strongly differential expression of other regulatory proteins that may be involved in a regulatory network. To unravel further functions of LTTR BPSL0117, full-length crystal BPSL0117 protein, co-factor and directly regulated genes should be examined. Besides, altered membrane proteins and membrane-associated proteins should be evaluated and interaction of *Bp* Δ BPSL0117 within the host should be also investigated.

4.1.4 Usage of *B. pseudomallei* Δ BPSL0117 as a live vaccine

Currently, there is vivid activity in evaluating different live attenuated vaccines to generate protective immunity against *Bp* (Atkins *et al.*, 2002; Cuccui *et al.*, 2007; Breitbach *et al.*, 2008; Stevens *et al.*, 2004 ; Srilungchang *et al.*, 2009 ; Nelson *et al.*, 2004 ; Harland *et al.*, 2007 ; Silva *et al.*, 2013). Generally, live vaccines are considered to provide a good protection since the immune system is stimulated by living microorganisms. However, there is still no licensed vaccine against melioidosis available. In the present study, the highly attenuated *Bp* Δ BPSL0117 strain was used as a live vaccine and evaluated for its potential to protect against *Bp* WT challenge. First, we could show that mice immunized with *Bp* Δ BPSL0117 via the intranasal route generated specific IgG antibodies against *Bp*. The median survival time of vaccinated mice was longer compared to non-vaccinated animals. However, except one animal, all mice finally died after challenge with the *Bp* WT strain. The differences in the mortality among the groups were not statistically significant difference. Thus, the degree of protection was very low by using *Bp* Δ BPSL0117. The development of a vaccine exhibiting protects against melioidosis remains to be a challenging task.

4.2 Characterization of BPSS1528 (BapA)

Secretion systems, notably T3SS and T6SS, play an important role for the interaction between bacteria and their surrounding environment (Filloux, 2011). The genome of *Bp* contains three T3SS cluster from that the T3SS cluster 3 shares similarities with the Mxi/Spa T3SS from *Salmonella*. This T3SS3 from *Bp* contributes for the virulence in mammalian hosts (Stevens *et al.*, 2002; Lee *et al.*, 2010). The expression of T3SS3 is induced after entry into the host cells and its functionality plays an essential role for the intact intracellular life cycle of *Bp* (Stevens *et al.*, 2002; 2004, Pilatz *et al.*, 2006). However, the function of the three *bap* genes encoded between known translocator and secreted effector proteins within the T3SS3 cluster have rarely been addressed so far.

4.2.1 BapA and its role for the *in vivo* virulence of *B. pseudomallei*

There are conflicting results in the literature about the role of BapA in *Bp* associated virulence. Results from a PhD thesis (Treerat, 2014) showed that two *Bp* Δ bapA mutants that were independently derived from the WT strain K96243 were less virulent compared to the WT bacteria in the BALB/c mouse model. In contrast to this study, Warawa and Woods (2005) found that a *Bp* Δ bapA mutant did not differ in its virulence in the Syrian hamster

model compared to WT bacteria. The data obtained in the present study showed that the *Bp* Δ bapA#1 mutant strain derived from the WT K96243 strain exhibited even increased virulence in the BALB/c mouse model following both intranasal and intravenous infection. However, when mice were infected with another *Bp* Δ bapA mutant strain derived from the *Bp* WT 1026b, we could not observe any differences in the virulence in the absence of BapA in BALB/c mice.

Treerat (2014) could show that the two *bapA* mutants created in her study were not impaired in their abilities to replicate intracellularly in RAW264.7 macrophages. In the present study, the *Bp* Δ bapA#1 mutant strain exhibited even slight but significantly increased intracellular replication in both RAW264.7 and BMM-BALB/c macrophages compared to the WT. In contrast, the other *bapA* mutants *Bp* Δ bapA#2 and *Bp* Δ bapA#3 did not differ in their intracellular survival properties in RAW264.7 macrophages compared to the WT strains K96243 and 1026b, respectively.

Gong and coworkers (2011) could show that a *Bp* strain lacking the T3SS effector protein BopA exhibited increased co-localization with the autophagy marker protein LC3. It was therefore suggested that BopA might modulate autophagy-mediated processes that ease the ability of *Bp* to escape from the lysosome-containing vacuole after phagocytosis (Gong *et al.*, 2011). The authors included also a *Bp* Δ bapA mutant in their experiments and found that the Δ bapA mutant did not show any differences in the co-localization within the autophagy marker protein LC3 compared to WT bacteria. In the present study, *Bp* Δ bapA#1 did not show any difference in the recruitment of actin tails during non-phagocytic HepG-2 infection and in the secretion of the T3SS chaperon BipD and effector BopE. These data implicate that BapA seems to neither be involved in the escape from autolysosome processes nor play a role for the intracellular motility of *Bp*.

The fact that the observed phenotypes of the *Bp* Δ bapA#1 mutant were not present in the independently derived *bapA* mutants #2 and #3 suggests that beside the mutation of the *bapA* gene another modification in the genome might have accidentally happened in the *Bp* Δ bapA#1 strain. This is likely to have caused unspecific effects. Since there were no differences in the virulence potential between two *bapA* mutants derived from two different WT strains suggest that BapA does not play a direct role for the virulence of *Bp*.

4.2.2 Role of *bap* genes for the adaptation of *B. pseudomallei* in the environment

The T3SSs of *Bp* are thought to be acquired by horizontal transfer (Hueck, 1998; Sun *et al.*, 2010). The *bapB* and *bapC* loci within the T3SS3 cluster of *Bp* share homologies to *iapP* and *iagB* genes of *Salmonella enterica* serovar Typhimurium, respectively (Stevens *et al.*, 2002), whereas the *bapA* gene shows only homology with genes encoded by closely related species like *B. mallei* and *B. thailandensis*. Recent reports have been shown that *iapP* plays an important role for invasion ability in INT-407 epithelial cells (Kim *et al.*, 2011). *S. enterica* *iapP* mutant showed impaired expression of flagella proteins FliC and FliB and delayed recruitment of actin tails. Furthermore, deletion of *iapP* gene led to decreased

secretion of the effector proteins SopA, SopA and SopD, but did not influence their translocators and leading to be attenuated in *in vivo* experiments (Kim *et al.*, 2011; Eom *et al.*, 2012). However, lagB is still predicted to involve in invasion of HeLa cells (Miras *et al.*, 1995).

Bp can be isolated from high saline soils in the northeast region of Thailand (Wongpokhom *et al.*, 2008). During lung infection with *Burkholderia cenocapacia* complex (Bcc), that are a closely related species of *Bp*, NaCl concentration in the lung airway surface liquid of patients were found to be increased 2 times compared with healthy people (Joris *et al.*, 1993). It is also known that the expression of T3SS genes from *Pseudomonas aeruginosa* and *Yersinia enterocolitica* are increased under hyperosmotic stress conditions (Aspedon *et al.*, 2006; Mildiner-Earley *et al.*, 2007). Pumirat and coworkers (2009 & 2010) showed that secretion of the T3SS3 proteins BipD and BopE from *Bp* were also increased in the presence of high salt concentrations. A recent study has shown that the expression of the T3SS3 gene *bsaU* is also increased when the bacteria were grown in high NaCl containing medium and achieves the highest level at 470 mM NaCl after 4 h inoculation (Hopf, 2012). Similarly, *bapB* and *bapC* genes also showed increased expression under higher NaCl concentrations after 6 h growth, whereas the expression level of the *bapA* gene was not increased. Thus, BapA may not play an important role in the response to salt stress.

Beside the response to high salt concentrations in the environment, *Bp* can also survive under low pH condition, which enables the bacterium to survive intracellularly *e.g.* in phagolysosomes. *Burkholderia thailandensis* is a closely related organism and shares a homologous T3SS with *Bp*, although it is much less virulent compared to *Bp* and rarely infects humans (Brett *et al.*, 1997; Dharakul *et al.*, 1999; Lertpatanasuwan *et al.*, 1999). In a study from Jitprasutwit and colleagues (2010), the T3SS proteins BipD and BopE of *B. th.* exhibited increased expression 6 h after inoculation in a medium at pH 4.5 compared to bacteria that were grown at pH7. Markham and colleagues (2008) have reported that the BipD protein of *Bp* shows a conformational stability at acidic conditions that indicates that these proteins might be necessary when the surrounding environment exhibit a low pH which can be found in cellular components such as lysosomes and the phagosome of host cells. In this context, it is noteworthy that BipD was found to play an important role for the escape from the lysosome of *Bp* and contributes to the virulence in a murine infection model (Stevens *et al.*, 2002 & 2004). The present study could show that expressions of the *bap* genes were increased at pH 4.5 after 6 h inoculation. It was also demonstrated that the expression of the *bapA* gene was increased in *Bp* during infection of RAW264.7 macrophages. Thus, it is likely that the *bap* genes are involved in the bacterial response to low pH conditions in the environment and play a role during intracellular infection, although the single knockout of *bapA* did not impair the ability of *Bp* to survive inside host cells.

REFERENCES

1. Abdallah AM, Verboom T, Hannes F, *et al.* (2006) A specific secretion system mediates PPE41 transport in pathogenic mycobacteria. *Mol Microbiol* **62**: 667-679.
2. Ahn JS, Chandramohan L, Liou LE & Bayles KW (2006) Characterization of CidR-mediated regulation in *Bacillus anthracis* reveals a previously undetected role of S-layer proteins as murein hydrolases. *Mol Microbiol* **62**: 1158-1169.
3. Antunes LCM & Ferreira RB (2011) Biofilms and bacterial virulence. *Reviews in Medical Microbiology* **22**: 12-16.
4. Arnold T, Zeth K & Linke D (2010) Omp85 from the thermophilic cyanobacterium *Thermosynechococcus elongatus* differs from proteobacterial Omp85 in structure and domain composition. *J Biol Chem* **285**: 18003-18015.
5. Aspedon A, Palmer K & Whiteley M (2006) Microarray analysis of the osmotic stress response in *Pseudomonas aeruginosa*. *J Bacteriol* **188**: 2721-2725.
6. Atkins T, Prior RG, Mack K, *et al.* (2002) A Mutant of *Burkholderia pseudomallei*, Auxotrophic in the Branched Chain Amino Acid Biosynthetic Pathway, Is Attenuated and Protective in a Murine Model of Melioidosis. *Infection and Immunity* **70**: 5290-5294.
7. Attree O & Attree I (2001) A second type III secretion system in *Burkholderia pseudomallei*: who is the real culprit? *Microbiology* **147**: 3197-3199.
8. AuCoin DP, Reed DE, Marlenee NL, *et al.* (2012) Polysaccharide specific monoclonal antibodies provide passive protection against intranasal challenge with *Burkholderia pseudomallei*. *PLoS One* **7**: e35386.
9. Axler-Diperte GL, Miller VL & Darwin AJ (2006) YtxR, a conserved LysR-like regulator that induces expression of genes encoding a putative ADP-ribosyltransferase toxin homologue in *Yersinia enterocolitica*. *J Bacteriol* **188**: 8033-8043.
10. Barken KB, Pamp SJ, Yang L, *et al.* (2008) Roles of type IV pili, flagellum-mediated motility and extracellular DNA in the formation of mature multicellular structures in *Pseudomonas aeruginosa* biofilms. *Environ Microbiol* **10**: 2331-2343.
11. Basler M, Pilhofer M, Henderson GP, Jensen GJ & Mekalanos JJ (2012) Type VI secretion requires a dynamic contractile phage tail-like structure. *Nature* **483**: 182-186.
12. Bleves S, Viarre V, Salacha R, Michel GP, Filloux A & Voulhoux R (2010) Protein secretion systems in *Pseudomonas aeruginosa*: A wealth of pathogenic weapons. *Int J Med Microbiol* **300**: 534-543.
13. Breitbach K, Kohler J & Steinmetz I (2008) Induction of protective immunity against *Burkholderia pseudomallei* using attenuated mutants with defects in the intracellular life cycle. *Trans R Soc Trop Med Hyg* **102 Suppl 1**: S89-94.
14. Brett PJ, Mah DC & Woods DE (1994) Isolation and characterization of *Pseudomonas pseudomallei* flagellin proteins. *Infect Immun* **62**: 1914-1919.
15. Brett PJ & Woods DE (1996) Structural and immunological characterization of *Burkholderia pseudomallei* O-polysaccharide-flagellin protein conjugates. *Infect Immun* **64**: 2824-2828.
16. Brett PJ, Deshazer D & Woods DE (1997) Characterization of *Burkholderia pseudomallei* and *Burkholderia pseudomallei*-like strains. *Epidemiol Infect* **118**: 137-148.
17. Burntnick MN, Brett PJ, Harding SV, *et al.* (2011) The cluster 1 type VI secretion system is a major virulence determinant in *Burkholderia pseudomallei*. *Infect Immun* **79**: 1512-1525.
18. Burntnick MN & Brett PJ (2013) *Burkholderia mallei* and *Burkholderia pseudomallei* cluster 1 type VI secretion system gene expression is negatively regulated by iron and zinc. *PLoS One* **8**: e76767.
19. Chan YY, Bian HS, Tan TM, *et al.* (2007) Control of quorum sensing by a *Burkholderia pseudomallei* multidrug efflux pump. *J Bacteriol* **189**: 4320-4324.
20. Chan YY & Chua KL (2010) Growth-related changes in intracellular spermidine and its effect on efflux pump expression and quorum sensing in *Burkholderia pseudomallei*. *Microbiology* **156**: 1144-1154.
21. Chen Y, Wong J, Sun GW, Liu Y, Tan GY & Gan YH (2011) Regulation of type VI secretion system during *Burkholderia pseudomallei* infection. *Infect Immun* **79**: 3064-3073.
22. Cheng AC, Dance DA & Currie BJ (2005) Bioterrorism, Glanders and melioidosis. *Euro*

- Surveill* **10**: E1-2; author reply E1-2.
23. Cheng AC & Currie BJ (2005) Melioidosis: epidemiology, pathophysiology, and management. *Clin Microbiol Rev* **18**: 383-416.
 24. Choh LC, Ong GH, Vellasamy KM, *et al.* (2013) *Burkholderia* vaccines: are we moving forward? *Front Cell Infect Microbiol* **3**: 5.
 25. Choi KH, Mima T, Casart Y, Rholl D, Kumar A, Beacham IR & Schweizer HP (2008) Genetic tools for select-agent-compliant manipulation of *Burkholderia pseudomallei*. *Appl Environ Microbiol* **74**: 1064-1075.
 26. Cornelis GR & Van Gijsegem F (2000) Assembly and function of type III secretory systems. *Annu Rev Microbiol* **54**: 735-774.
 27. Cornelis GR (2006) The type III secretion injectisome. *Nat Rev Microbiol* **4**: 811-825.
 28. Cruz-Migoni A, Hautbergue GM, Artymiuk PJ, *et al.* (2011) A *Burkholderia pseudomallei* toxin inhibits helicase activity of translation factor eIF4A. *Science* **334**: 821-824.
 29. Cuccui J, Easton A, Chu KK, Bancroft GJ, Oyston PC, Titball RW & Wren BW (2007) Development of signature-tagged mutagenesis in *Burkholderia pseudomallei* to identify genes important in survival and pathogenesis. *Infect Immun* **75**: 1186-1195.
 30. Currie BJ, Fisher DA, Anstey NM & Jacups SP (2000) Melioidosis: acute and chronic disease, relapse and re-activation. *Trans R Soc Trop Med Hyg* **94**: 301-304.
 31. Currie BJ, Mayo M, Anstey NM, Donohoe P, Haase A & Kemp DJ (2001) A cluster of melioidosis cases from an endemic region is clonal and is linked to the water supply using molecular typing of *Burkholderia pseudomallei* isolates. *Am J Trop Med Hyg* **65**: 177-179.
 32. Currie BJ, Dance DA & Cheng AC (2008) The global distribution of *Burkholderia pseudomallei* and melioidosis: an update. *Trans R Soc Trop Med Hyg* **102 Suppl 1**: S1-4.
 33. Currie BJ, Ward L & Cheng AC (2010) The epidemiology and clinical spectrum of melioidosis: 540 cases from the 20 year Darwin prospective study. *PLoS Negl Trop Dis* **4**: e900.
 34. DeShazer D, Brett PJ & Woods DE (1998) The type II O-antigenic polysaccharide moiety of *Burkholderia pseudomallei* lipopolysaccharide is required for serum resistance and virulence. *Mol Microbiol* **30**: 1081-1100.
 35. Dharakul T, Tassaneetrithep B, Trakulsomboon S & Songsivilai S (1999) Phylogenetic analysis of Ara+ and Ara- *Burkholderia pseudomallei* isolates and development of a multiplex PCR procedure for rapid discrimination between the two biotypes. *J Clin Microbiol* **37**: 1906-1912.
 36. Economou A, Christie PJ, Fernandez RC, Palmer T, Plano GV & Pugsley AP (2006) Secretion by numbers: Protein traffic in prokaryotes. *Mol Microbiol* **62**: 308-319.
 37. Eoh H & Rhee KY (2014) Methylcitrate cycle defines the bactericidal essentiality of isocitrate lyase for survival of *Mycobacterium tuberculosis* on fatty acids. *Proc Natl Acad Sci U S A* **111**: 4976-4981.
 38. Eom JS, Kim JS, Jang JI, Kim HG, Bang IS & Park YK (2012) Effect of *iacP* mutation on flagellar phase variation in *Salmonella enterica* serovar typhimurium strain UK-1. *J Bacteriol* **194**: 4332-4341.
 39. Eske K, Breitbach K, Kohler J, Wongprompitak P & Steinmetz I (2009) Generation of murine bone marrow derived macrophages in a standardised serum-free cell culture system. *J Immunol Methods* **342**: 13-19.
 40. Eske-Pogodda K (2010) Identifikation neuer Virulenzfaktoren bei *Burkholderia pseudomallei*. Thesis, Universitätsbibliothek.
 41. Filloux A (2011) Protein Secretion Systems in *Pseudomonas aeruginosa*: An Essay on Diversity, Evolution, and Function. *Front Microbiol* **2**: 155.
 42. Fritz DL (1999) The hamster model of intraperitoneal *Burkholderia mallei* (glanders). *Veterinary Pathology* **36**: 276-291.
 43. Fux CA, Costerton JW, Stewart PS & Stoodley P (2005) Survival strategies of infectious biofilms. *Trends Microbiol* **13**: 34-40.
 44. Galyov EE, Brett PJ & DeShazer D (2010) Molecular insights into *Burkholderia pseudomallei* and *Burkholderia mallei* pathogenesis. *Annu Rev Microbiol* **64**: 495-517.
 45. Gamage AM, Shui G, Wenk MR & Chua KL (2011) N-Octanoylhomoserine lactone signalling mediated by the *BpsI-BpsR* quorum sensing system plays a major role in biofilm formation of *Burkholderia pseudomallei*. *Microbiology* **157**: 1176-1186.
 46. Gibson KE & Silhavy TJ (1999) The LysR homolog LrhA promotes RpoS degradation by modulating activity of the response regulator *sprE*. *J Bacteriol* **181**: 563-571.

47. Gong L, Cullinane M, Treerat P, *et al.* (2011) The *Burkholderia pseudomallei* type III secretion system and BopA are required for evasion of LC3-associated phagocytosis. *PLoS One* **6**: e17852.
48. Gouin E, Welch MD & Cossart P (2005) Actin-based motility of intracellular pathogens. *Curr Opin Microbiol* **8**: 35-45.
49. Gould TA, van de Langemheen H, Munoz-Elias EJ, McKinney JD & Sacchettini JC (2006) Dual role of isocitrate lyase 1 in the glyoxylate and methylcitrate cycles in *Mycobacterium tuberculosis*. *Mol Microbiol* **61**: 940-947.
50. Hall-Stoodley L & Stoodley P (2009) Evolving concepts in biofilm infections. *Cell Microbiol* **11**: 1034-1043.
51. Harland DN, Chu K, Haque A, *et al.* (2007) Identification of a LolC homologue in *Burkholderia pseudomallei*, a novel protective antigen for melioidosis. *Infect Immun* **75**: 4173-4180.
52. Hasselbring BM, Patel MK & Schell MA (2011) Dictyostelium discoideum as a model system for identification of *Burkholderia pseudomallei* virulence factors. *Infect Immun* **79**: 2079-2088.
53. Henikoff S, Haughn GW, Calvo JM & Wallace JC (1988) A large family of bacterial activator proteins. *Proc Natl Acad Sci U S A* **85**: 6602-6606.
54. Hii CS, Sun GW, Goh JW, Lu J, Stevens MP & Gan YH (2008) Interleukin-8 induction by *Burkholderia pseudomallei* can occur without Toll-like receptor signaling but requires a functional type III secretion system. *J Infect Dis* **197**: 1537-1547.
55. Holden MT, Titball RW, Peacock SJ, *et al.* (2004) Genomic plasticity of the causative agent of melioidosis, *Burkholderia pseudomallei*. *Proc Natl Acad Sci U S A* **101**: 14240-14245.
56. Hopf V (2012) Funktionelle Analyse der Sekretionssystem-assoziierten Gene BPSS1504 und bsaU bei *Burkholderia pseudomallei*. Thesis, Universitätsbibliothek.
57. Hopf V, Gohler A, Eske-Pogodda K, Bast A, Steinmetz I & Breitbach K (2014) BPSS1504, a Cluster 1 Type VI Secretion Gene, Is Involved in Intracellular Survival and Virulence of *Burkholderia pseudomallei*. *Infect Immun* **82**: 2006-2015.
58. Hoppe I, Brenneke B, Rohde M, Kreft A, Haussler S, Reganzerowski A & Steinmetz I (1999) Characterization of a murine model of melioidosis: comparison of different strains of mice. *Infect Immun* **67**: 2891-2900.
59. Horton RE, Grant GD, Matthews B, *et al.* (2013) Quorum sensing negatively regulates multinucleate cell formation during intracellular growth of *Burkholderia pseudomallei* in macrophage-like cells. *PLoS One* **8**: e63394.
60. Hueck CJ (1998) Type III protein secretion systems in bacterial pathogens of animals and plants. *Microbiol Mol Biol Rev* **62**: 379-433.
61. Inglis TJ, Robertson T, Woods DE, Dutton N & Chang BJ (2003) Flagellum-mediated adhesion by *Burkholderia pseudomallei* precedes invasion of *Acanthamoeba astronyxis*. *Infect Immun* **71**: 2280-2282.
62. Inglis TJ & Sagripanti JL (2006) Environmental factors that affect the survival and persistence of *Burkholderia pseudomallei*. *Appl Environ Microbiol* **72**: 6865-6875.
63. Ito T, Iimori J, Takayama S, Moriyama A, Yamauchi A, Hemmi H & Yoshimura T Conserved Pyridoxal Protein That Regulates Ile and Val Metabolism. *Journal of bacteriology* **195**: 5439-5449.
64. Jitprasutwit S, Thaewpia W, Muangsombut V, Lulitanond A, Leelayuwat C, Lertmemongkolchai G & Korbsrisate S (2010) Effect of acidic pH on the invasion efficiency and the type III secretion system of *Burkholderia thailandensis*. *J Microbiol* **48**: 526-532.
65. Jones AL, Beveridge TJ & Woods DE (1996) Intracellular survival of *Burkholderia pseudomallei*. *Infect Immun* **64**: 782-790.
66. Joris L, Dab I & Quinton PM (1993) Elemental composition of human airway surface fluid in healthy and diseased airways. *Am Rev Respir Dis* **148**: 1633-1637.
67. Jourlin-Castelli C, Mani N, Nakano MM & Sonenshein AL (2000) CcpC, a novel regulator of the LysR family required for glucose repression of the *citB* gene in *Bacillus subtilis*. *J Mol Biol* **295**: 865-878.
68. Kaestli M, Schmid M, Mayo M, *et al.* (2012) Out of the ground: aerial and exotic habitats of the melioidosis bacterium *Burkholderia pseudomallei* in grasses in Australia. *Environ Microbiol* **14**: 2058-2070.
69. Kespichayawattana W, Rattanachetkul S, Wanun T, Utaisinchaoen P & Sirisinha S (2000) *Burkholderia pseudomallei* Induces Cell Fusion and Actin-Associated Membrane

- Protrusion: a Possible Mechanism for Cell-to-Cell Spreading. *Infection and Immunity* **68**: 5377-5384.
70. Kim HJ, Jourlin-Castelli C, Kim SI & Sonenshein AL (2002) Regulation of the *Bacillus subtilis* *ccpC* gene by *ccpA* and *ccpC*. *Mol Microbiol* **43**: 399-410.
 71. Kim S-I, Jourlin-Castelli C, Wellington SR & Sonenshein AL (2003) Mechanism of Repression by *Bacillus subtilis* CcpC, a LysR Family Regulator. *Journal of Molecular Biology* **334**: 609-624.
 72. Kim JS, Eom JS, Jang JI, *et al.* (2011) Role of *Salmonella* Pathogenicity Island 1 protein IacP in *Salmonella enterica* serovar typhimurium pathogenesis. *Infect Immun* **79**: 1440-1450.
 73. Kubori T, Matsushima Y, Nakamura D, *et al.* (1998) Supramolecular structure of the *Salmonella typhimurium* type III protein secretion system. *Science* **280**: 602-605.
 74. Leakey AK, Ulett GC & Hirst RG (1998) BALB/c and C57Bl/6 mice infected with virulent *Burkholderia pseudomallei* provide contrasting animal models for the acute and chronic forms of human melioidosis. *Microb Pathog* **24**: 269-275.
 75. Lee YH, Chen Y, Ouyang X & Gan YH (2010) Identification of tomato plant as a novel host model for *Burkholderia pseudomallei*. *BMC Microbiol* **10**: 28.
 76. Lertpatanasuwan N, Sermsri K, Petkaseam A, Trakulsomboon S, Thamlikitkul V & Suputtamongkol Y (1999) Arabinose-positive *Burkholderia pseudomallei* infection in humans: case report. *Clin Infect Dis* **28**: 927-928.
 77. Lever MS, Nelson M, Stagg AJ, Beedham RJ & Simpson AJ (2009) Experimental acute respiratory *Burkholderia pseudomallei* infection in BALB/c mice. *Int J Exp Pathol* **90**: 16-25.
 78. Liljeqvist S & Stahl S (1999) Production of recombinant subunit vaccines: protein immunogens, live delivery systems and nucleic acid vaccines. *J Biotechnol* **73**: 1-33.
 79. Limmathurotsakul D, Chaowagul W, Chierakul W, *et al.* (2006) Risk factors for recurrent melioidosis in northeast Thailand. *Clin Infect Dis* **43**: 979-986.
 80. Limmathurotsakul D, Wongratanaheewin S, Teerawattanasook N, *et al.* (2010) Increasing incidence of human melioidosis in Northeast Thailand. *Am J Trop Med Hyg* **82**: 1113-1117.
 81. Limmathurotsakul D & Peacock SJ (2011) Melioidosis: a clinical overview. *Br Med Bull* **99**: 125-139.
 82. Liu B (2002) Model of Differential Susceptibility to Mucosal *Burkholderia pseudomallei* Infection. *Infection and Immunity* **70**: 504-511.
 83. Lopez CM, Rholl DA, Trunck LA & Schweizer HP (2009) Versatile dual-technology system for markerless allele replacement in *Burkholderia pseudomallei*. *Appl Environ Microbiol* **75**: 6496-6503.
 84. Maddocks SE & Oyston PC (2008) Structure and function of the LysR-type transcriptional regulator (LTTR) family proteins. *Microbiology* **154**: 3609-3623.
 85. Majerczyk C, Brittnacher M, Jacobs M, *et al.* (2014) Global analysis of the *Burkholderia thailandensis* quorum sensing-controlled regulon. *J Bacteriol* **196**: 1412-1424.
 86. Markham AP, Birket SE, Picking WD, Picking WL & Middaugh CR (2008) pH sensitivity of type III secretion system tip proteins. *Proteins* **71**: 1830-1842.
 87. Matsukawa M & Greenberg EP (2004) Putative exopolysaccharide synthesis genes influence *Pseudomonas aeruginosa* biofilm development. *J Bacteriol* **186**: 4449-4456.
 88. McKinney JD, Honer zu Bentrop K, Munoz-Elias EJ, *et al.* (2000) Persistence of *Mycobacterium tuberculosis* in macrophages and mice requires the glyoxylate shunt enzyme isocitrate lyase. *Nature* **406**: 735-738.
 89. Mildiner-Earley S, Walker KA & Miller VL (2007) Environmental stimuli affecting expression of the Ysa type three secretion locus. *Adv Exp Med Biol* **603**: 211-216.
 90. Miras I, Hermant D, Arricau N & Popoff MY (1995) Nucleotide sequence of *iagA* and *iagB* genes involved in invasion of HeLa cells by *Salmonella enterica* subsp. *enterica* ser. Typhi. *Res Microbiol* **146**: 17-20.
 91. Muangman S, Korbsrisate S, Muangsombut V, *et al.* (2011) BopC is a type III secreted effector protein of *Burkholderia pseudomallei*. *FEMS Microbiol Lett* **323**: 75-82.
 92. Munoz-Elias EJ & McKinney JD (2005) *Mycobacterium tuberculosis* isocitrate lyases 1 and 2 are jointly required for in vivo growth and virulence. *Nat Med* **11**: 638-644.
 93. Munoz-Elias EJ, Upton AM, Cherian J & McKinney JD (2006) Role of the methylcitrate cycle in *Mycobacterium tuberculosis* metabolism, intracellular growth, and virulence. *Mol Microbiol* **60**: 1109-1122.
 94. Muraoka S, Okumura R, Ogawa N, Nonaka T, Miyashita K & Senda T (2003) Crystal

- Structure of a Full-length LysR-type Transcriptional Regulator, CbnR: Unusual Combination of Two Subunit Forms and Molecular Bases for Causing and Changing DNA Bend. *Journal of Molecular Biology* **328**: 555-566.
95. Nelson M, Prior JL, Lever MS, Jones HE, Atkins TP & Titball RW (2004) Evaluation of lipopolysaccharide and capsular polysaccharide as subunit vaccines against experimental melioidosis. *J Med Microbiol* **53**: 1177-1182.
 96. Ngaui V, Lemeshev Y, Sadkowski L & Crawford G (2005) Cutaneous melioidosis in a man who was taken as a prisoner of war by the Japanese during World War II. *J Clin Microbiol* **43**: 970-972.
 97. Ngugi SA, Ventura VV, Qazi O, *et al.* (2010) Lipopolysaccharide from *Burkholderia thailandensis* E264 provides protection in a murine model of melioidosis. *Vaccine* **28**: 7551-7555.
 98. Norris MH, Propst KL, Kang Y, Dow SW, Schweizer HP & Hoang TT (2011) The *Burkholderia pseudomallei* Deltaasd mutant exhibits attenuated intracellular infectivity and imparts protection against acute inhalation melioidosis in mice. *Infect Immun* **79**: 4010-4018.
 99. Nougayrede JP, Taieb F, De Rycke J & Oswald E (2005) Cyclomodulins: bacterial effectors that modulate the eukaryotic cell cycle. *Trends Microbiol* **13**: 103-110.
 100. O'Grady EP, Viteri DF, Malott RJ & Sokol PA (2009) Reciprocal regulation by the CeiIR and CcilR quorum sensing systems in *Burkholderia cenocepacia*. *BMC Genomics* **10**: 441.
 101. Ooi WF, Ong C, Nandi T, *et al.* (2013) The condition-dependent transcriptional landscape of *Burkholderia pseudomallei*. *PLoS Genet* **9**: e1003795.
 102. O'Quinn AL, Wiegand EM & Jeddelloh JA (2001) *Burkholderia pseudomallei* kills the nematode *Caenorhabditis elegans* using an endotoxin-mediated paralysis. *Cell Microbiol* **3**: 381-393.
 103. Patel N, Conejero L, De Reynal M, Easton A, Bancroft GJ & Titball RW (2011) Development of vaccines against *Burkholderia pseudomallei*. *Front Microbiol* **2**: 198.
 104. Perez-Rueda E & Collado-Vides J (2001) Common history at the origin of the position-function correlation in transcriptional regulators in archaea and bacteria. *J Mol Evol* **53**: 172-179.
 105. Phadnis SH & Das HK (1987) Use of the plasmid pRK 2013 as a vehicle for transposition in *Azobacter vinelandii*. *J. Biosci.* **12**: 131-135.
 106. Pilatz S, Breitbart K, Hein N, *et al.* (2006) Identification of *Burkholderia pseudomallei* genes required for the intracellular life cycle and *in vivo* virulence. *Infect Immun* **74**: 3576-3586.
 107. Pirofski LA & Casadevall A (1998) Use of licensed vaccines for active immunization of the immunocompromised host. *Clin Microbiol Rev* **11**: 1-26.
 108. Pukatzki S, Ma AT, Sturtevant D, *et al.* (2006) Identification of a conserved bacterial protein secretion system in *Vibrio cholerae* using the *Dictyostelium* host model system. *Proc Natl Acad Sci U S A* **103**: 1528-1533.
 109. Pumirat P, Saetun P, Sinchaikul S, Chen ST, Korbsrisate S & Thongboonkerd V (2009) Altered secretome of *Burkholderia pseudomallei* induced by salt stress. *Biochim Biophys Acta* **1794**: 898-904.
 110. Pumirat P, Cuccui J, Stabler RA, *et al.* (2010) Global transcriptional profiling of *Burkholderia pseudomallei* under salt stress reveals differential effects on the Bsa type III secretion system. *BMC Microbiol* **10**: 171.
 111. Rainbow L, Hart CA & Winstanley C (2002) Distribution of type III secretion gene clusters in *Burkholderia pseudomallei*, *B. thailandensis* and *B. mallei*. *J Med Microbiol* **51**: 374-384.
 112. Rode JW & Webling DD (1981) Melioidosis in the Northern Territory of Australia. *Med J Aust* **1**: 181-184.
 113. Rosales-Reyes R, Saldias MS, Aubert DF, El-Halfawy OM & Valvano MA (2012) The *suhB* gene of *Burkholderia cenocepacia* is required for protein secretion, biofilm formation, motility and polymyxin B resistance. *Microbiology* **158**: 2315-2324.
 114. Rotz LD, Khan AS, Lillibridge SR, Ostroff SM & Hughes JM (2002) Public health assessment of potential biological terrorism agents. *Emerg Infect Dis* **8**: 225-230.
 115. Saier MH, Jr. (2004) Evolution of bacterial type III protein secretion systems. *Trends Microbiol* **12**: 113-115.
 116. Sainsbury S, Lane LA, Ren J, *et al.* (2009) The structure of CrgA from *Neisseria meningitidis* reveals a new octameric assembly state for LysR transcriptional regulators.

- Nucleic Acids Res* **37**: 4545-4558.
117. Schell MA (1993) Molecular biology of the LysR family of transcriptional regulators. *Annu Rev Microbiol* **47**: 597-626.
 118. Schell MA, Ulrich RL, Ribot WJ, *et al.* (2007) Type VI secretion is a major virulence determinant in *Burkholderia mallei*. *Mol Microbiol* **64**: 1466-1485.
 119. Schwarz S, Singh P, Robertson JD, *et al.* (2014) VgrG-5 is a *Burkholderia* type VI secretion system-exported protein required for multinucleated giant cell formation and virulence. *Infect Immun* **82**: 1445-1452.
 120. Schweizer HP (2012) Mechanisms of antibiotic resistance in *Burkholderia pseudomallei*: implications for treatment of melioidosis. *Future Microbiol* **7**: 1389-1399.
 121. Shalom G, Shaw JG & Thomas MS (2007) *In vivo* expression technology identifies a type VI secretion system locus in *Burkholderia pseudomallei* that is induced upon invasion of macrophages. *Microbiology* **153**: 2689-2699.
 122. Silva EB, Goodyear A, Sutherland MD, Podnecky NL, Gonzalez-Juarrero M, Schweizer HP & Dow SW (2013) Correlates of immune protection following cutaneous immunization with an attenuated *Burkholderia pseudomallei* vaccine. *Infect Immun* **81**: 4626-4634.
 123. Silva EB & Dow SW (2013) Development of *Burkholderia mallei* and *Burkholderia pseudomallei* vaccines. *Front Cell Infect Microbiol* **3**: 10.
 124. Silverman JM, Brunet YR, Cascales E & Mougous JD (2012) Structure and Regulation of the Type VI Secretion System. *Annu Rev Microbiol* **66**: 453-472.
 125. Somvanshi VS, Viswanathan P, Jacobs JL, Mulks MH, Sundin GW & Ciche TA (2010) The type 2 secretion Pseudopilin, *gspJ*, is required for multihost pathogenicity of *Burkholderia cenocepacia* AU1054. *Infect Immun* **78**: 4110-4121.
 126. Song Y, Xie C, Ong YM, Gan YH & Chua KL (2005) The BpsIR quorum-sensing system of *Burkholderia pseudomallei*. *J Bacteriol* **187**: 785-790.
 127. Sprague LD & Neubauer H (2004) Melioidosis in animals: a review on epizootiology, diagnosis and clinical presentation. *J Vet Med B Infect Dis Vet Public Health* **51**: 305-320.
 128. Srilunchang T, Proungvitaya T, Wongratanacheewin S, Strugnell R & Homchampa P (2009) Construction and characterization of an unmarked *aroC* deletion mutant of *Burkholderia pseudomallei* strain A2. *Southeast Asian J Trop Med Public Health* **40**: 123-130.
 129. Srinon V, Muangman S, Imyaem N, Muangsombut V, Lazar Adler NR, Galyov EE & Korbsrisate S (2013) Comparative assessment of the intracellular survival of the *Burkholderia pseudomallei* *bopC* mutant. *J Microbiol* **51**: 522-526.
 130. Stec E, Witkowska-Zimny M, Hryniewicz MM, *et al.* (2006) Structural basis of the sulphate starvation response in *E. coli*: crystal structure and mutational analysis of the cofactor-binding domain of the Cbl transcriptional regulator. *J Mol Biol* **364**: 309-322.
 131. Steinmetz I, Rohde M & Brenneke B (1995) Purification and characterization of an exopolysaccharide of *Burkholderia* (*Pseudomonas*) *pseudomallei*. *Infection and immunity* **63**: 3959-3965.
 132. Stevens MP, Wood MW, Taylor LA, *et al.* (2002) An Inv/Mxi-Spa-like type III protein secretion system in *Burkholderia pseudomallei* modulates intracellular behaviour of the pathogen. *Mol Microbiol* **46**: 649-659.
 133. Stevens MP, Haque A, Atkins T, *et al.* (2004) Attenuated virulence and protective efficacy of a *Burkholderia pseudomallei* *bsa* type III secretion mutant in murine models of melioidosis. *Microbiology* **150**: 2669-2676.
 134. Stevens MP, Stevens JM, Jeng RL, *et al.* (2005) Identification of a bacterial factor required for actin-based motility of *Burkholderia pseudomallei*. *Mol Microbiol* **56**: 40-53.
 135. Stevens JM, Ulrich RL, Taylor LA, Wood MW, Deshazer D, Stevens MP & Galyov EE (2005) Actin-binding proteins from *Burkholderia mallei* and *Burkholderia thailandensis* can functionally compensate for the actin-based motility defect of a *Burkholderia pseudomallei* *bimA* mutant. *J Bacteriol* **187**: 7857-7862.
 136. Suarez-Moreno ZR, Caballero-Mellado J, Coutinho BG, Mendonca-Previato L, James EK & Venturi V (2012) Common features of environmental and potentially beneficial plant-associated *Burkholderia*. *Microb Ecol* **63**: 249-266.
 137. Subramoni S, Nguyen DT & Sokol PA (2011) *Burkholderia cenocepacia* ShvR-regulated genes that influence colony morphology, biofilm formation, and virulence. *Infect Immun* **79**: 2984-2997.
 138. Sun J & Klein A (2004) A LysR-type regulator is involved in the negative regulation of

- genes encoding selenium-free hydrogenases in the archaeon *Methanococcus voltae*. *Mol Microbiol* **52**: 563-571.
139. Sun GW & Gan YH (2010) Unraveling type III secretion systems in the highly versatile *Burkholderia pseudomallei*. *Trends Microbiol* **18**: 561-568.
 140. Sun GW, Chen Y, Liu Y, Tan GY, Ong C, Tan P & Gan YH (2010) Identification of a regulatory cascade controlling Type III Secretion System 3 gene expression in *Burkholderia pseudomallei*. *Mol Microbiol* **76**: 677-689.
 141. Thin RN, Brown M, Stewart JB & Garrett CJ (1970) Melioidosis: a report of ten cases. *Q J Med* **39**: 115-127.
 142. Thomas RJ, Hamblin KA, Armstrong SJ, *et al.* (2013) *Galleria mellonella* as a model system to test the pharmacokinetics and efficacy of antibiotics against *Burkholderia pseudomallei*. *Int J Antimicrob Agents* **41**: 330-336.
 143. Titball RW, Russell P, Cuccui J, *et al.* (2008) *Burkholderia pseudomallei*: animal models of infection. *Trans R Soc Trop Med Hyg* **102 Suppl 1**: S111-116.
 144. Treerat P (2014) Characterisation of *Burkholderia pseudomallei* type III secretion system III components. Thesis, Monash University.
 145. Ulett GC, Ketheesan N & Hirst RG (2000) Cytokine gene expression in innately susceptible BALB/c mice and relatively resistant C57BL/6 mice during infection with virulent *Burkholderia pseudomallei*. *Infect Immun* **68**: 2034-2042.
 146. Ulrich RL (2004) Role of quorum sensing in the pathogenicity of *Burkholderia pseudomallei*. *Journal of Medical Microbiology* **53**: 1053-1064.
 147. Ulrich RL & DeShazer D (2004) Type III Secretion: a Virulence Factor Delivery System Essential for the Pathogenicity of *Burkholderia mallei*. *Infection and Immunity* **72**: 1150-1154.
 148. Valade E, Thibault FM, Gauthier YP, Palencia M, Popoff MY & Vidal DR (2004) The PmlI-PmlR quorum-sensing system in *Burkholderia pseudomallei* plays a key role in virulence and modulates production of the MprA protease. *J Bacteriol* **186**: 2288-2294.
 149. van Keulen G, Girbal L, van den Bergh ER, Dijkhuizen L & Meijer WG (1998) The LysR-type transcriptional regulator CbbR controlling autotrophic CO₂ fixation by *Xanthobacter flavus* is an NADPH sensor. *J Bacteriol* **180**: 1411-1417.
 150. van Schaik E, Tom M, DeVinney R & Woods DE (2008) Development of novel animal infection models for the study of acute and chronic *Burkholderia pseudomallei* pulmonary infections. *Microbes Infect* **10**: 1291-1299.
 151. van Schaik EJ, Tom M & Woods DE (2009) *Burkholderia pseudomallei* isocitrate lyase is a persistence factor in pulmonary melioidosis: implications for the development of isocitrate lyase inhibitors as novel antimicrobials. *Infect Immun* **77**: 4275-4283.
 152. Vatcharapreechasakul T, Suputtamongkol Y, Dance DA, Chaowagul W & White NJ (1992) *Pseudomonas pseudomallei* liver abscesses: a clinical, laboratory, and ultrasonographic study. *Clin Infect Dis* **14**: 412-417.
 153. Warawa J & Woods DE (2005) Type III secretion system cluster 3 is required for maximal virulence of *Burkholderia pseudomallei* in a hamster infection model. *FEMS Microbiol Lett* **242**: 101-108.
 154. Warawa JM, Long D, Rosenke R, Gardner D & Gherardini FC (2009) Role for the *Burkholderia pseudomallei* capsular polysaccharide encoded by the wcb operon in acute disseminated melioidosis. *Infect Immun* **77**: 5252-5261.
 155. Wiersinga WJ & van der Poll T (2009) *Burkholderia pseudomallei* tropism and the melioidosis road map. *J Infect Dis* **199**: 1720-1722.
 156. Wiersinga WJ, Currie BJ & Peacock SJ (2012) Melioidosis. *N Engl J Med* **367**: 1035-1044.
 157. Wong KT, Puthucheary SD & Vadivelu J (1995) The histopathology of human melioidosis. *Histopathology* **26**: 51-55.
 158. Wongpokhom N, Kheoruenromne I, Suddhiprakarn A & Gilkes RJ (2008) Micromorphological properties of salt affected soils in Northeast Thailand. *Geoderma* **144**: 158-170.
 159. Wongtrakoongate P, Tumapa S & Tungpradabkul S (2012) Regulation of a quorum sensing system by stationary phase sigma factor RpoS and their co-regulation of target genes in *Burkholderia pseudomallei*. *Microbiol Immunol* **56**: 281-294.
 160. Yabuuchi E & Arakawa M (1993) *Burkholderia pseudomallei* and melioidosis: be aware in temperate area. *Microbiol Immunol* **37**: 823-836.
 161. Yang SJ, Rice KC, Brown RJ, Patton TG, Liou LE, Park YH & Bayles KW (2005) A LysR-type regulator, CidR, is required for induction of the *Staphylococcus aureus*

cidABC operon. *J Bacteriol* **187**: 5893-5900.

ERKLÄRUNG

Hiermit erkläre ich, dass diese Arbeit bisher von mir weder an der Mathematisch-Naturwissenschaftlichen Fakultät der Ernst-Moritz-Arndt-Universität Greifswald noch einer anderen wissenschaftlichen Einrichtung zum Zwecke der Promotion eingereicht wurde.

Ferner erkläre ich, dass ich diese Arbeit selbständig verfasst und keine anderen als die darin angegebenen Hilfsmittel und Hilfen benutzt und keine Textabschnitte eines Dritten ohne Kennzeichnung übernommen habe.

Unterschrift des Promovenden:

Duong Tuan Linh

APPENDICES

Appendix I. Equipment

Cell counting chamber from Neubauer	Assistant Germany
Centrifuge type 5415	Enpendorf tube
Centrifuge type 5417	Enpendorf tube
Centrifuge type 5810	Enpendorf tube
Centrifuge type multifuge 1L-R	Heraeus
Chemical weight type SI-114	Denver Instrument
Chemical weight type SI-2002	Denver Instrument
Chemical weight type SI-603	Denver Instrument
CO ₂ - incubator CB 150	BINDER GmbH
Cooler and freezer combination	Liebherr International
Deep refreeze -70°C, HFU 686 Basic	Heraeus instruments
Digital graphic printer	Sony
Fluorescence microscope BZ-9000	Keyence
Frequency shaker Type W17	Biometra
Gel documentation Biodoc Analyze	Biometra
Gel documentation Fusion FX 7	PeqLab
Heat block	PeqLab
Huber minichiller	Serva
Inverse microscope type Axiovert 40 CFL	Carl Zeiss
MagNA Lyser	Roche
Microwave MG-583 MC	LG
Multi pipette	Enpendorf tube
Multi Temp III	Pharmacia Biotech
Multiple channel pipette 50 µl; 200 µl	Brandt
Nitrogen tank, Arpege 70	Air Liquid DCM
pH/mV- Meter UltraBASIC type UB-10	Denver Instruments
Plate incubator	BINDER GmbH
Plate photometer Tecan infinite type M200 Pro	Tecan
Pressure machine, power pack P25T	Biometra
Protein gel chamber minigel-Twin	Biometra
Semidry blotter	PeqLab
Shaking incubator type KS15 with cover type TH15	Edmund Bühler labor techniques
Sorvall® Ultra centrifuge Pro 80	Thermo Scientific
Spectro photometer Nanodrop	PeqLab
Speedvac, Univapo	Fröbel labor instruments

Speedvac, Concentrator plus	Eppendorf
Sterile airflow box Hera Safe type HS12/2	Heraeus Instruments
Sterile airflow box Hera Safe type KS15	Heraeus Instruments
Stirrer	VWR
Thermo cycler T3000	Biometra
Thermol Haake K20	Conquer scientific
Thermomixer model Hotplate/Stirrer Alu	VWR
Thermomixer Model RCT Basic IKA®	IKA
UV-lamp 312	Bachhofer labor instruments
UV/Vis-Spectrophotometer type Genesys10	Thermo Scientific
Variable micro liter pipettes volume 0.5-10 µl; 10-100 µl; 100-1,000 µl	Brand
Vortex	VWR

Appendix II. Consumption materials

Cell culture flask Cellstar®	Greiner bio-one
Cell culture plate 24 well Cellstar®	Greiner bio-one
Cell culture plate 48 well Cellstar®	Greiner bio-one
Cell culture plate 6 well Cellstar®	Greiner bio-one
Cell culture plate 96 well Cellstar®	Greiner bio-one
Cell scraper 30 Cm	TPP
Cellulose acetate membrane 0.45 µm pore size; Ø 13mm	Sartorius
Centrifuge tube 15 ml Falcons	Sarstedt
Centrifuge tube 50 ml Falcons	BD Falcon
Chamber Slide™ 8 well	Nagle Nunc International
Cotton swabs sterile	Nonmedical
Cover glass 20 mm x 26 mm x 0.4 mm	Haemacytometer
Cover glass, Ø 13mm No1	VWR
Cuvette, PS	Halbmicro 2.5ml; Roth
Cuvette, PS	Halbmicro 1.5ml; Roth
Feather disposal scalpel	Dahlhausen
Filter paper 11µm	Whatman
Filterpur, sterile, Cellulose acetate membrane 0.2 µm pore size	VWR
Filterpur, sterile, Cellulose acetate membrane 0.45 µm pore size	VWR
Gloves	Peha-soft; Hartmann
Injection needle 27Gx¾" 0.4 mm x 19 mm	BD Microlance™ 3
Micro screw tube 2 ml	Nagle Nunc International

Nitrile gloves Nitra-Tex ®	Ansell
Nitrocellulose membrane Protran	Schleicher and Schüll
Object cover 17 mm x 26 mm 3x1 inch, Mattrand	R. Langenbrink
Petri plate 92 mm x 16 mm	Sarstedt
Pipette tips 1 ml	Sarstedt
Pipette tips 200 µl	Sarstedt
Pipette tips 5 ml	Brandt
Pipette tips crystal short and long	Roth
Reaction container 0.2 ml PP	Sarstedt
Reagent container 0.5 ml PP	Sarstedt
Reagent container 1.5 ml PP	Sarstedt
Reagent container 2.0 ml PP safe-seal	Sarstedt
Round bottle tube 14 ml PP	Greiner Bio-one
Round bottle tube 5 ml Polystyrene	BD Falcon
Serological pipette 5 ml	Sarstedt
Serological pipette 10 ml	Sarstedt
Serological pipette 25 ml	Sarstedt
Syringe	Nagle Nunc International

Appendix III. Chemicals

1-Bromo-3-Chloropropan	Sigma-Aldrich
Acetic acid	J. T. Baker
Acrylamide (30% w/v) with bis-acrylamide (0.8% w/v)	Roth
Acrylamide (40% w/v)	AppliChem
Agarose MS	Sigma-Aldrich
Ammonium persulfate (APS)	Roth
Bis-acrylamide (2% w/v)	AppliChem
Crystal violet	AppliChem
Deoxyadenosine triphosphate (dATP)	Roche
Deoxycytidine triphosphate (dCTP)	Roche
Desoxyguanosine triphosphate (dGTP)	Roche
Desoxythymidine triphosphate (dTTP)	Roche
Diaminopimelic acid	Sigma-Aldrich
Di-Potassium hydrogen phosphate	Merck
Di-sodium hydrogen phosphate	Merck
Ethanol 99%	ChemSolute; J. T. Baker
Ethylenediaminetetraacetic acid (EDTA)	Sigma-Aldrich
Glycerol 85%	Merck

Glycine	Merck
Guanidine hydrochloride	AppliChem
Hydrochloric acid	Merck
Hydrogen peroxide	Merck
Isopropanol	ChemSolute
Magnesium sulfate	Sigma-Aldrich
Methanol	J. T. Baker
Neutral red	AppliChem
o-Phenylenediamine dihydrochloride	Sigma-Aldrich
Paraformaldehyde	Serva
Phosphoric acid	Fluka
Ponceau S	Sigma
Potassium acetate	Fluka
Potassium-D-gluconate	Merck
Saccharose	Merck
Saponin	Sigma-Aldrich
Sodium ammonium hydrogen phosphate	Merck
Sodium azid	Merck
Sodium chloride	Roth
Sodium dodecyl sulfate (SDS)	Merck
Sodium hydroxide	Merck
Sodium acetate	Merck
Tergitol TMN3	Fluka®
Tetramethylethylenediamine (TEMED)	Serva
Thiourea	Merck
Trichloroacetic acid	Roth
Tris (-hydroxymethyl)-aminomethane (Tris)	Roth
Triton X-100	Sigma-Aldrich
Urea	Merck
X-Gal (5-bromo-4-chloro-3-indolyl- β -D-galactopyranoside)	Fermentas
X-Gluc (5-Bromo-4-chloro-1H-indol-3-yl β -D-glucopyranosiduronic)	Fermentas
ϵ -Aminocaproic acid	AppliChem

Appendix IV. Solutions, enzyme and kits

Alkaline Phosphatase	Roche
Alkaline Phosphatase FastAP®	Fermentas
Ampli Taq® DNA-Polymerase	Roche Applied Biosystems
Complete™ Mini Protease inhibitor cocktail	Roche
DNase I	Fermentas

Fluorepre	Biomérieux
GenElute™ HP Plasmid Maxiprep Kit	Sigma
GeneRuler™, DNA Ladder Mix	Fermentas
HotStar Taq Plus DNA Polymerase	QIAGEN
Ketamin	Gräub
KOD Xtreme™ Hot Start DNA Polymerase	Novagen
LightCycler® 480 SYBR Green I Master	Roche
LumiGLO™ Reagent (20x) and Peroxide (20x)	Cell Signaling
M-MLV-Reverse Transcriptase	Promega
Maxima® SYBR Green qPCR Master Mix (2x)	Fermentas
Page Ruler, pre-stained Protein marker	Fermentas
Phenol:Chloroform:Isoamyl alcohol (25:24:1)	Applichem
QIAquick Gel Extraction Kit	QIAGEN
QIAquick PCR Purification Kit	QIAGEN
Restriction endonucleases	New England Biolabs
Restriction endonucleases FastDigest®	Fermentas
RNaseA	Fermentas
RNasin®	Promega
Rompun 2%	Bayer
Roti®-Block (10x)	Roth
SYBR® safe	Invitrogen
T4-DNA-Ligase	New England Biolabs
Topo TA Cloning® Kit	Invitrogen
Trizol Reagent™	Invitrogen
Trypsin-EDTA (1x)	PAA
Tryptan Blue (0.4%)	Sigma-Aldrich
Tween®20	Sigma-Aldrich

Appendix V: List of used primers

Primers for semi quantitative expression analysis of bap genes		Product size
BapA-Fw4:	5' – CGCTTCGTGCCGTTGGCGAT – 3'	177 bp
BapA-Rev4:	5' – ATGCGGGTGATGCGGGTGAT – 3'	
BapB-Fw3:	5' – ACGTCGGCCACCGTTGCGAC – 3'	161 bp
BapB-Rev3:	5' – AAGACGCTGCTGGCCGGCAT – 3'	
BapC-Fw3:	5' – CGCGCATAGCGCTCGCTCAA – 3'	298 bp
BapC-Rev3:	5' – TACGGCGTCAATGCCGATCTGC – 3'	

23S rRNA-F	5'- TTTCCCGCTTAGATGCTTT -3'	334 bp
23S rRNA-R	5'- AAAGGTACTCTGGGGATAA -3'	
16S rRNA1	5'- GGCTAGTCTAACCGCAAGGA -3'	82 bp
16S rRNA2	5'- TCCGATACGGCTACCTTGTT -3'	
Primers for bapA gene mutagenesis		
BapASmal-Fw1:	5' – at <u>CCCGGG</u> AACTTCGTCCATCAACAGCA – 3'	619 bp
BapAEcoRI-Rev1:	5' – at <u>GAATTC</u> GCTTGCGGTAACCCTTGTTG – 3'	
BapAEcoRI-Fw3:	5' – at <u>GAATT</u> CACGAAGCCTCGCCAGTGG – 3'	1005 bp
BapASmal-Rev3:	5' – at <u>CCCGGG</u> CCGTTGGCGATCGAATCGTT – 3'	
Primers for bapA gene complementation		
BapAPstI-Com-Fw:	5' – at <u>CTGCAG</u> ATGCCGCCGTCCATTACCG – 3'	
BapASacI-Com-Rev:	5' – at <u>GAGCTC</u> TTCATCGCTTCGTGCCGTTGG – 3'	
BapAEcoRI-comp-Fw	5' – at <u>GAATTC</u> CGATCCGAAGCAACCGACAA – 3'	
BapAXbaI-comp-Rev1:	5' – at <u>TCTAG</u> ATCATCGCTTCGTGCCGTTGG – 3'	
BapAXbaI-comp-Rev2:	5' – at <u>TCTAG</u> ACGCGTATTGGCGTATTGGCG – 3'	
BapAKpnI-comp-Rev2:	5' – at <u>GGTACC</u> GCGTATTGGCGTATTGGCG – 3'	
Fw+Rev1= 2679bp (K9) and 2757bp (1026b) Fw+Rev2= 3692bp (K9) and 3762bp (1026b)		
BapASpeI-comp-Fw:	at <u>ACTAGT</u> GGGCGATGGCGTTTTTATGA – 3'	
BapASpeI-comp-fw + BapAKpnI-comp-Rev2 = 5113bp (K9)		

= 5181 bp (1026b)		
Internal primers for checking BapA orf complementation		
BapAcomp-Fw1:	5' – ACGGGATGGTGAACCGGCA – 3'	757 bp
BapAcomp-Rev1:	5' – GTGGTCCTGACGACCGGATT – 3'	
Primers for BPSL0117 gene complementation		
Bpsl0117-HindIII-compl-fw:	5' – atAAGCTT <u>GACGCTTTTATCGCAACTCTCT</u> <u>ACTGT</u> AGATGAGCGATGGAAGACGG – 3'	1,551 bp
Bpsl0117-KpnI-compl-rev:	5' – atGGTACCCTTGCTTTTGGCGTAGGAGAT – 3'	
Primer to verify of Tn7 – Insertion		
Tn7L:	5' - ATTAGCTTACGACGCTACACCC – 3	
BPGLMS1:	5' - GAGGAGTGGGCGTCGATCAAC – 3'	
BPGLMS2:	5' - ACACGACGCAAGAGCGGAATC – 3'	
BPGLMS3:	5' - CGGACAGGTTTCGCGCCATGC – 3	
Primers for sequencing bapA full length		
PA1-seq:	5' - ACGAACGGGATGGTGAACC- 3'	781 - 799
PA2-seq:	5' - AATCCGGTCGTCAGGACCA – 3'	1558 - 1576
PA3-seq:	5' – ATACGTCGGGCATCGCAC – 3'	2216 - 2234
PA4-seq:	5' - AACTTCGTCCATCAACAGCA – 3'	1521 - 1540
PA5-seq:	5' – AACAAAGGGTTACCGCAAGC – 3'	2122 - 2140
PA6-seq:	5' – ACGTGAACGTGAATCTCGAC – 3'	2579 - 2598
PA7-seq:	5' – AACGAAGCCTCGCCAGTG – 3'	3146 - 3163
PA8-seq:	5' – ATACGTCGGGCATCGCAC – 3'	3680 -3697
PA9-seq:	5' – GAACGATTTCGATCGCCAACG – 3'	4110 - 4129
Under line letters: sequences of restriction enzymes		
Red letters: promoter sequence from <i>Burkholderia thailandensis</i>		

Appendix VI: Bacterial media

YT medium:	10 g/l Yeast extract		
	10 g/l Trypton		
YT/Sucrose agar:	10 g/l Yeast extract		
	10 g/l Trypton		
	15% Sucrose		
	15 g/l Agar		

LB medium (Lennox):	20 g/l LB Lennox (ready-to-use)	Or	10 g/l Trypton
			5 g/l Yeast extract
			5 g/l Sodium chloride
LB medium with NaCl	10 g/l Trypton		
	5 g/l Yeast extract		
	170 mM, 320 mM or 470mM of NaCl		
LB agar:	35g/l LB agar (ready-to-use)	Or	20g/l LB Lennox
			15g/l Agar
LBG agar:	LB agar with 4% Glycerol		
M9 medium:	47.75 mM Na ₂ PO ₄		
	22 mM KH ₂ PO ₄		
	8.56 mM NaCl		
	18.7 mM NH ₄ Cl		
	2 mM MgSO ₄		
	0.1 mM CaCl ₂		
	0.4% glucose		
Vogel-Bonner medium: (Minimal medium)	28 mM NaH ₂ PO ₄		
	37 mM K ₂ HPO ₄		
	3.3 mM Magnesium sulfate		
	10 mM Citric acid		
	0.214 M Potassium-D-Gluconate		
	pH 7		
Ashdown agar:	10g/l Trypton Soya Broth		
	15g/l Agar		
	3.5% Glycerol		
	0.0005% Crystal violet		
	0.005% Neutral red		
	50 µg/ml Gentamycin		
Müller-Hinton agar:	38 g/l Müller-Hinton agar (ready-to-use)		

Columbia agar with 5% sheep blood	Ready-to-use		
--	--------------	--	--

Appendix VII. Buffers and solutions

Lysis buffer for isolation genomic DNA:	50 mM Tris/HCl pH 8
	10 mM Na ₂ EDTA
	0.5% SDS
Electrophoresis buffer (20x):	1.6 M Tris/acetic acid pH 7.9
	50 mM EDTA
DNA ladder buffer (6x):	0.4 g/ml Saccharose
	0.1 mM Na ₂ EDTA
	0.25% Bromphenol blue
Buffer 1 for plasmid preparation:	50 mM Tris/HCl pH8
	10 mM Na ₂ EDTA
	100 µg/ml Rnase A
	(Store at 4°C)
Buffer 2 for plasmid preparation:	200 mM NaOH
	1% SDS
Buffer 3 for plasmid preparation:	3 M Potassium acetate/acetic acid pH 5.5
0.3 M Guanidinium-HCl	Resolved in 96% Ethanol
Washing and lysis buffer	10 mM Tris-HCl pH 8
Bradford reagent:	0.121 mM Coomassie Brilliant blue G-250
	5% Ethanol
	8.5% Phosphoric acid
	Store in dark bottle at RT
Resuspension solution	8M Urea
	2M Thiourea
	in H ₂ O
Stacking gel buffer:	0.5M Tris/HCl pH 6.8

Separating gel buffer:	1.5M Tris/HCl pH 8.8
Running buffer:	25 mM Tris/HCl pH 8.3
	0.2 M Glycin
	0.1% SDS
Coomassie stain solution:	0.1% (w/v) coomassie brilliant G250
	10% (v/v) acetic acid
	40% (v/v) methanol
	In H ₂ O
Protein loading buffer (4x):	2 ml stacking gel buffer
	1.8 ml Glycerol
	3.6 ml 10% SDS
	770 µl of 1 M DTT
	1 spool tip Bromphenol blue
Anode buffer I:	0.3M Tris; pH 10.4
	20% Methanol
Anode buffer II:	25mM Tris; pH 10.4
	20% Methanol
Cathode buffer:	40 mM ε-Aminocapron acid
	20% Methanol
10 x TBS:	0.2 M Tris/HCl; pH 7.6
	1.4 M NaCl
TBST:	1xTBS
	0.1% Tween 20
TBST-BSA:	TBST with 5% BSA
Ponceau S – staining solution:	2.8 mM Ponceau S
	0.2 M Trichloacetic acid
10x PBS:	2 M NaCl
	25 mM KCl
	80 mM Na ₂ PO ₄

	15 mM KH ₂ PO ₄
Immuno fluorescene buffer:	0.2% BSA
	0.05% Saponin
	0.1% Sodium azid
	in PBS pH 7.4 (with HCl adjusted)
Saponin/BSA:	1% Saponin
	0.5% BSA
	in PBS
Tergitol/BSA:	1% Tergitol
	0.5% BSA
	in PBS

Appendix VIII. Cell and bacterial media, antibiotics and antibodies used in this study

DMEM+GlutaMAX™-I (4.5 g/l Glucose)	GIBCO® Invitrogen
DPBS (Dulbecco's Phosphate Buffered Saline)	GIBCO® Invitrogen
F-12K Nutrient Mixture	GIBCO® Invitrogen
Fetus calf serum (FCS)	PANTMBiothech GmbH
PANEXIN® BMM	PANTM Biotech GmbH
rmGM-CSF	PANTM Biotech GmbH
RPMI 1640	GIBCO® Invitrogen
β-Mercaptoethanol (50mM)	GIBCO® Invitrogen
2.6-Diaminopimelin acid (DAP)	Sigma-Aldrich
Bacteriological Agar	OXOID
Columbia agar-Platte with 5% Sheep blood	BD Bioscience
LB Broth Base (Lennox) LB agar	AppliChem
Müller-Hinton agar	Invitrogen
Trypton soja broth	OXOID
Yeast extract	OXOID
Ampicillin	Sigma-Aldrich
Ampicillin MIC strip	BioMérieux
Ceftazidime	BioMérieux
Imipenem	BioMérieux
Gentamycin (50mg/ml)	Sigma-Aldrich
Kanamycin sulfate	Sigma-Aldrich
Polymyxin B- Sulfaphate	Sigma-Aldrich
Zeocin (100mg/ml)	Invitrogen
<i>B. pseudomallei</i> BipD, rabbit monoclonal Ab-Serum	M. P. Stevens, University of Edinburgh, Scotland, UK.
<i>B. pseudomallei</i> BopE, rabbit monoclonal Ab-Serum	
<i>B. pseudomallei</i> Hcp1. mouse monoclonal Ab-Serum	D. DeShazer, U.S. Army Medical Research Institute of Infectious Diseases, Fort Detrick, USA
<i>B. pseudomallei</i> EPS, clone 3015 mouse monoclonal IgGy2b	

<i>B. pseudomallei</i> LPS, clone 3016 mouse monoclonal IgGy1b	
Beta-actin (13E5) rabbit mAb	Cell Signaling Technology
Goat anti-mouse IgGy1b antibody	Cell Signaling Technology
Anti-rabbit- IgG, HRP-conjugated TM	Cell Signaling Technology
Anti-mouse-IgG, HRP-conjugate	Cell Signaling Technology
Goat anti-mouse IgGy2b antibodies-linked Biotin	Sigma

Appendix IX. Relative alteration of content of proteins in the cytoplasmic fraction at logarithmic and early stationary phases of *B. pseudomallei* Δ BPSL0117 compared with E8 WT. The results were considered significantly different if at least two of three reproducible samples are changed and a threshold of at least a 2.0-fold increase or 0.5-fold decrease. One sample of out of ranking value must be ≤ 0.9 or ≥ 1.1 if samples are decreased or increased, respectively.

			Logarithmic phase SILAC-Intensity-Normalized					Stationary phase SILAC-Intensity-Normalized						
			Mutant vs WT at logarithmic phase					Mutant vs WT OD stationary phase						
BPS_E8 loci	K96243 Loci	Protein name	I	II	III	MEAN	CHANGE	I	II	III	MEAN	CHANGE	Main Role	Sub-Role
BPS_00018	BPSL0707	FAD/FMN-containing dehydrogenases	1.9	3.8	1.9	2.5		0.0	0.0	0.0	0.0	DOWN	Energy metabolism	Detoxification
BPS_00025	BPSL0700	Uncharacterized conserved protein	23.9	0.1	38.1	20.7		0.2	0.0	0.3	0.2	DOWN	#NV	#NV
BPS_00214	BPSL0486	Diaminopimelate decarboxylase	0.0	0.0	0.0	0.0	DOWN	0.0	0.1	0.0	0.0	DOWN	Amino acid biosynthesis	#NV
BPS_00217	BPSL0483	Acyl-CoA dehydrogenases	0.0	0.1	0.0	0.0	DOWN	0.5	0.5	0.0	0.3	DOWN	Unknown function	Heme, porphyrin, and cobalamin
BPS_00325	BPSL0373	Isocitrate dehydrogenase kinase/phosphatase	0.1	0.8	0.1	0.3	DOWN	0.0	0.3	0.5	0.3	DOWN	#NV	#NV
BPS_01517	BPSL2703	hypothetical protein	0.6	0.4	0.3	0.4	DOWN	0.1	0.5	0.4	0.3	DOWN	Hypothetical proteins	Conserved
BPS_00094	BPSL0632	7-cyano-7-deazaguanine reductase	0.2	0.5	0.7	0.5		0.4	0.3	0.5	0.4	DOWN	Amino acid biosynthesis	#NV
BPS_00129	BPSL0597	TOMM system kinase/cyclase fusion protein	0.2	0.6	1.8	0.9		0.7	0.3	0.3	0.4	DOWN	Purines, pyrimidines, nucleosides, and nucleotides	Transposon functions
BPS_01598	BPSL2624	diaminohydroxyphosphoribosylaminopyrimidine deaminase (EC 3.5.4.26)	0.1	0.2	0.7	0.3	DOWN	0.7	0.3	0.0	0.3	DOWN	Biosynthesis of cofactors, prosthetic groups, and carriers	#NV
BPS_02110	BPSL2188	isocitrate lyase (EC 4.1.3.1)	0.1	0.1	0.0	0.0	DOWN	0.3	0.3	0.5	0.4	DOWN	Energy metabolism	Detoxification
BPS_02115	BPSL2183	uracil-DNA glycosylase, family 4	0.1	0.2	0.4	0.2	DOWN	0.3	0.4	0.1	0.3	DOWN	DNA metabolism	Detoxification
BPS_02156	BPSS0218	N-acyl-D-glucosamine 2-epimerase	0.1	0.1	0.2	0.1	DOWN	0.2	0.3	0.1	0.2	DOWN	#NV	#NV
BPS_02232	BPSS0144	Glucosylase and related glycosyl hydrolases	0.1	0.1	0.1	0.1	DOWN	0.4	0.2	0.4	0.3	DOWN	Energy metabolism	Detoxification

BPS_02575	BPSS2172	hypothetical protein	0.0	0.1	0.0	0.0	DOWN	0.5	0.0	0.0	0.2	DOWN	Regulatory functions	Transposon functions
BPS_02786	BPSS1352	Predicted hydrolases or acyltransferases (alpha/beta hydrolase superfamily)	0.0	0.1	0.1	0.1	DOWN	0.1	0.0	0.2	0.1	DOWN	Cell envelope	Surface structures
BPS_02814	BPSS0564	Zinc metalloprotease (elastase)	0.1	0.4	0.4	0.3	DOWN	0.1	0.2	0.4	0.2	DOWN	Protein fate	Transposon functions
BPS_02976	BPSS0725	Dehydrogenases with different specificities (related to short-chain alcohol dehydrogenases)	0.0	0.6	0.0	0.2	DOWN	0.0	0.2	0.0	0.1	DOWN	Central intermediary metabolism	Other
BPS_03117	BPSS0852	Inosine-uridine nucleoside N-ribohydrolase	0.3	0.4	0.3	0.3	DOWN	0.4	0.6	0.4	0.5	DOWN	Purines, pyrimidines, nucleosides, and nucleotides	Transposon functions
BPS_03140	BPSS0877	NADH:flavin oxidoreductases, Old Yellow Enzyme family	0.1	0.1	0.2	0.1	DOWN	0.0	0.0	0.1	0.1	DOWN	Unclassified	Heme, porphyrin, and cobalamin
BPS_03142	BPSS0879	Outer membrane protein (porin)	0.0	0.1	0.1	0.1	DOWN	0.1	0.1	0.1	0.1	DOWN	Cell envelope	Surface structures
BPS_00369	BPSS0035	gluconolactonase (EC 3.1.1.17)	12.7	0.7	22.6	12.0		0.0	0.0	0.2	0.1	DOWN	Energy metabolism	Detoxification
BPS_00370	BPSS0034	NAD-dependent aldehyde dehydrogenases	1.2	1.0	1.0	1.0		0.3	0.4	0.4	0.4	DOWN	Energy metabolism	Detoxification
BPS_00503	BPSL0265	tRNA nucleotidyltransferase/poly(A) polymerase	1.4	2.0	1.7	1.7		0.0	0.0	0.0	0.0	DOWN	Transcription	Transposon functions
BPS_03344	BPSL2112	Cytosine deaminase and related metal-dependent hydrolases	0.0	0.1	0.1	0.1	DOWN	0.0	0.0	0.3	0.1	DOWN	Unknown function	Heme, porphyrin, and cobalamin
BPS_00509	BPSL0259	sensor histidine kinase inhibitor, Kipl family	30.8	0.8	3.1	11.6		0.2	0.0	0.5	0.3	DOWN	#NV	#NV
BPS_03354	BPSL2102	L-threonine ammonia-lyase (EC 4.3.1.19)	0.0	0.7	0.4	0.4	DOWN	0.0	0.1	0.3	0.1	DOWN	#NV	#NV
BPS_03409	BPSL1422	Uncharacterized conserved protein	0.3	0.1	0.3	0.2	DOWN	0.1	0.1	0.0	0.1	DOWN	Hypothetical proteins	Conserved
BPS_03426	BPSL1439	hydrolase, TatD family	0.0	0.0	0.6	0.2	DOWN	0.0	0.0	0.0	0.0	DOWN	Unknown function	Heme, porphyrin, and cobalamin
BPS_00674	BPSL0063	3-hydroxyacyl-CoA dehydrogenase	25.2	0.6	11.9	12.6		0.0	0.4	0.0	0.2	DOWN	Cellular processes	Adaptations to

														atypical conditions
BPS_03513	BPSL1525	Predicted phosphoribosyltransferases	0.4	0.3	0.3	0.3	DOWN	0.3	0.3	0.2	0.3	DOWN	Purines, pyrimidines, nucleosides, and nucleotides	Transposon functions
BPS_03763	BPSS1106	Thymidylate synthase	0.0	0.2	0.2	0.1	DOWN	0.1	0.3	0.0	0.1	DOWN	#NV	#NV
BPS_00745	BPSL3422	Adenylate cyclase, class 2 (thermophilic)	1.7	0.9	0.8	1.1		0.2	0.2	0.2	0.2	DOWN	Regulatory functions	Transposon functions
BPS_00751	BPSL3416	amino acid/amide ABC transporter substrate-binding protein, HAAT family (TC 3.A.1.4.-)	0.3	2.0	1.7	1.3		0.1	0.2	0.2	0.1	DOWN	Transport and binding proteins	Amino acids, peptides and amines
BPS_03843	BPSL1212	NADH dehydrogenase subunit B (EC 1.6.5.3)	0.2	0.2	0.3	0.2	DOWN	0.1	0.2	0.0	0.1	DOWN	Energy metabolism	Detoxification
BPS_03844	BPSL1213	NADH dehydrogenase subunit C (EC 1.6.5.3)	0.7	0.3	0.2	0.4	DOWN	0.1	0.9	0.0	0.3	DOWN	Energy metabolism	Detoxification
BPS_03919	BPSL1163	coproporphyrinogen oxidase (EC 1.3.3.3)	0.1	0.6	0.4	0.3	DOWN	0.2	0.6	0.3	0.4	DOWN	Biosynthesis of cofactors, prosthetic groups, and carriers	#NV
BPS_04390	BPSS1777	AMP nucleosidase	0.7	0.4	0.4	0.5	DOWN	0.2	0.3	0.2	0.3	DOWN	Central intermediary metabolism	Other
BPS_00807	BPSL3363	Alginate lyase	7.3	51.3	0.0	19.5		0.4	0.0	0.0	0.1	DOWN	#NV	#NV
BPS_04396	BPSS1770	DNA polymerase I (EC 2.7.7.7)	0.0	0.0	0.0	0.0	DOWN	0.3	0.1	0.3	0.2	DOWN	DNA metabolism	Detoxification
BPS_04541	BPSS1634	amino acid adenylation domain	0.1	0.2	0.1	0.1	DOWN	0.2	0.1	0.1	0.1	DOWN	#NV	#NV
BPS_04742	BPSS0495	Nitroreductase	0.5	0.3	0.6	0.5	DOWN	0.3	0.2	0.3	0.2	DOWN	Central intermediary metabolism	Other
BPS_04847	BPSL1329	malonate decarboxylase, alpha subunit	0.4	0.4	0.6	0.5	DOWN	0.1	0.0	0.4	0.2	DOWN	Biosynthesis of cofactors, prosthetic groups, and carriers	#NV
BPS_04849	BPSL1331	malonate decarboxylase, beta subunit	0.2	0.4	0.7	0.4	DOWN	0.0	0.0	0.0	0.0	DOWN	Biosynthesis of cofactors, prosthetic groups, and carriers	#NV
BPS_05077	BPSS1190	luciferase family oxidoreductase, group 1	0.1	0.2	0.1	0.1	DOWN	0.0	0.1	0.0	0.0	DOWN	Unknown function	Heme, porphyrin, and cobalamin

BPS_05082	BPSS1443	Protein of unknown function (DUF2827)	0.3	0.4	0.6	0.4	DOWN	0.3	0.5	0.4	0.4	DOWN	#NV	#NV
BPS_05096	BPSS1459	Acetyltransferases, including N-acetylases of ribosomal proteins	0.4	0.1	0.1	0.2	DOWN	0.0	0.4	0.0	0.2	DOWN	Unknown function	Heme, porphyrin, and cobalamin
BPS_00902	BPSL3253	3-hydroxyisobutyrate dehydrogenase and related beta-hydroxyacid dehydrogenases	2.2	0.7	5.2	2.7		0.3	0.1	0.3	0.3	DOWN	Central intermediary metabolism	Other
BPS_05138	BPSS1497	type VI secretion protein, EvpB/VC_A0108 family	0.0	0.0	0.0	0.0	DOWN	0.0	0.1	0.0	0.0	DOWN	#NV	#NV
BPS_05139	BPSS1498	type VI secretion system effector, Hcp1 family	0.7	0.3	0.2	0.4	DOWN	0.3	0.3	0.8	0.4	DOWN	#NV	#NV
BPS_05325	BPSS1249	hypothetical protein	0.2	0.5	0.2	0.3	DOWN	0.1	0.3	0.1	0.2	DOWN	Cell envelope	Surface structures
BPS_00947	BPSL3214	SSU ribosomal protein S10P	6.0	1.9	1.1	3.0		0.2	0.4	0.8	0.5	DOWN	Protein synthesis	Transposon functions
BPS_05374	BPSL1969	FAD/FMN-containing dehydrogenases	0.5	0.3	0.5	0.4	DOWN	0.2	0.0	0.6	0.3	DOWN	Energy metabolism	Detoxification
BPS_05525	BPSL1827	Uncharacterized conserved protein	0.4	0.4	0.6	0.5	DOWN	0.4	0.5	0.3	0.4	DOWN	Unknown function	Heme, porphyrin, and cobalamin
BPS_05752	BPSS0243	Putative heme degradation protein	0.4	0.4	0.6	0.5	DOWN	0.1	0.1	0.3	0.2	DOWN	Energy metabolism	Detoxification
BPS_00359	BPSS0045	3-carboxy-cis,cis-muconate cycloisomerase (EC 5.5.1.2)	1.3	12.9	29.9	14.7	UP	0.0	0.6	0.0	0.2	DOWN	Energy metabolism	Detoxification
BPS_00522	BPSL0246	Predicted dehydrogenase	8.5	2.2	15.8	8.8	UP	0.4	0.6	0.3	0.4	DOWN	Energy metabolism	Detoxification
BPS_00572	BPSL0198	Transcriptional regulator	4.1	135.1	1.2	46.8	UP	0.3	0.2	0.3	0.3	DOWN	Regulatory functions	Transposon functions
BPS_01759	BPSL2459	Lactate dehydrogenase and related dehydrogenases	19.8	3.6	7.2	10.2	UP	0.5	0.2	0.1	0.3	DOWN	Central intermediary metabolism	Other
BPS_02186	BPSS0190	O-acetylhomoserine sulphydrylase (EC 2.5.1.49)	1.1	5.3	46.5	17.6	UP	0.0	0.4	0.0	0.1	DOWN	Amino acid biosynthesis	#NV
BPS_02487	BPSS2259	ABC-type transport system involved in Fe-S cluster assembly, permease and ATPase components	2.0	46.1	281.8	110.0	UP	0.8	0.4	0.0	0.4	DOWN	Transport and binding proteins	Amino acids, peptides and amines
BPS_02866	BPSS0618	Acyl-coenzyme A synthetases/AMP-(fatty) acid ligases	1.4	16.6	8.1	8.7	UP	0.0	0.0	0.2	0.1	DOWN	Energy metabolism	Detoxification

BPS_01111	BPSL3070	Xaa-Pro aminopeptidase	21.0	0.5	0.2	7.2		0.0	0.0	0.6	0.2	DOWN	Protein fate	Transposon functions
BPS_03069	BPSS0810	Acetyltransferases, including N-acetylases of ribosomal proteins	76.0	80.0	2.1	52.7	UP	0.0	0.2	0.0	0.1	DOWN	Central intermediary metabolism	Other
BPS_03446	BPSL1458	SSU ribosomal protein S6P	5.2	2.4	2.6	3.4	UP	0.2	0.7	0.2	0.3	DOWN	Protein synthesis	Transposon functions
BPS_03567	BPSL1578	transcriptional regulator, LacI family	2.5	2.3	1.4	2.1	UP	0.3	0.3	0.6	0.4	DOWN	Regulatory functions	Transposon functions
BPS_04454	BPSS1717	succinate dehydrogenase subunit B (EC 1.3.5.1)	4.1	73.2	12.0	29.8	UP	0.1	0.0	0.0	0.0	DOWN	Energy metabolism	Detoxification
BPS_04469	BPSS1704	aspartate semialdehyde dehydrogenase (EC 1.2.1.11)	2.6	2.9	2.9	2.8	UP	0.7	0.3	0.4	0.5	DOWN	Amino acid biosynthesis	#NV
BPS_04636	BPSS0386	hypothetical protein	29.4	237.3	42.0	102.9	UP	0.3	0.1	0.4	0.3	DOWN	Mobile and extrachromosomal element functions	Transposon functions
BPS_05452	BPSL1894	Flp pilus assembly protein, ATPase CpaE	17.2	5.9	2.1	8.4	UP	0.6	0.1	0.0	0.2	DOWN	Cell envelope	Surface structures
BPS_05484	BPSL1863	ADP-ribose pyrophosphatase	6.2	1.3	71.5	26.3	UP	0.7	0.5	0.3	0.5	DOWN	DNA metabolism	Detoxification
BPS_01210	BPSL2980	hypothetical protein	8.9	2.0	1.7	4.2		0.0	0.0	0.0	0.0	DOWN	Hypothetical proteins	Conserved
BPS_06025	BPSS1010	FAD binding domain	1.5	5.5	45.4	17.5	UP	0.0	0.0	0.5	0.2	DOWN	Central intermediary metabolism	Other
BPS_01230	BPSL2960	thiamine-phosphate kinase	0.5	0.8	1.9	1.1		0.7	0.3	0.3	0.4	DOWN	Biosynthesis of cofactors, prosthetic groups, and carriers	#NV
BPS_01252	BPSL2935	glutamate-5-semialdehyde dehydrogenase (EC 1.2.1.41)	0.9	0.6	0.8	0.8		0.4	0.2	0.9	0.5	DOWN	Amino acid biosynthesis	#NV
BPS_01283	BPSL2907	Glutathione S-transferase	38.4	0.1	0.7	13.1		0.4	0.1	0.8	0.4	DOWN	Central intermediary metabolism	Other
BPS_01298	BPSL2892	aminopeptidase P (EC:3.4.11.9). Metallo peptidase. MEROPS family M24B	0.6	0.8	2.4	1.3		0.2	0.5	0.5	0.4	DOWN	Protein fate	Transposon functions
BPS_01325	BPSL2869	tRNA-guanine transglycosylase (EC 2.4.2.29)	0.7	0.8	0.0	0.5		0.5	0.0	0.0	0.2	DOWN	Protein synthesis	Transposon functions
BPS_01356	BPSL2839	3-deoxy-D-arabinoheptulosonate-7-phosphate synthase (EC 2.5.1.54)	6.1	1.0	34.8	14.0		0.0	0.0	0.9	0.3	DOWN	Amino acid biosynthesis	#NV

BPS_01362	BPSL2833	Predicted sugar kinase	1.2	0.8	1.2	1.1		0.3	0.3	0.2	0.3	DOWN	Biosynthesis of cofactors, prosthetic groups, and carriers	#NV
BPS_01501	BPSL2719	2-hydroxychromene-2-carboxylate isomerase	0.1	1.9	0.8	0.9		0.0	0.3	0.0	0.1	DOWN	DNA metabolism	Detoxification
BPS_01514	BPSL2706	Protein of unknown function (DUF2957)	0.5	0.5	0.9	0.6		0.3	0.5	0.2	0.4	DOWN	#NV	#NV
BPS_01515	BPSL2705	Protein of unknown function (DUF2957)	0.6	1.2	1.1	1.0		0.4	0.6	0.3	0.4	DOWN	Cell envelope	Surface structures
BPS_01706	BPSL2505	Deacetylases, including yeast histone deacetylase and acetoin utilization protein	0.4	0.8	0.4	0.5		0.5	0.3	0.5	0.4	DOWN	Central intermediary metabolism	Other
BPS_01735	BPSL2476	dihydrofolate reductase (EC 1.5.1.3)	0.2	2.0	1.7	1.3		0.0	0.0	0.0	0.0	DOWN	Biosynthesis of cofactors, prosthetic groups, and carriers	#NV
BPS_01745	BPSL2470	Acyl-CoA hydrolase	1.1	1.3	0.2	0.9		0.0	0.2	0.5	0.2	DOWN	Cellular processes	Adaptations to atypical conditions
BPS_02034	BPSL2250	Archaeal fructose-1,6-bisphosphatase and related enzymes of inositol monophosphatase family	1.3	0.7	2.2	1.4		0.4	0.1	0.4	0.3	DOWN	Fatty acid and phospholipid metabolism	Degradation
BPS_02035	BPSL2249	RNA methyltransferase, TrmH family, group 1	0.7	0.3	0.5	0.5		0.4	0.2	0.8	0.4	DOWN	Protein synthesis	Transposon functions
BPS_02142	BPSS0230	Lactoylglutathione lyase and related lyases	1.4	0.4	0.5	0.8		0.2	0.3	0.4	0.3	DOWN	Protein fate	Transposon functions
BPS_02161	BPSS0213	Domain of unknown function (DUF1842)/Domain of unknown function (DUF1843)	1.9	1.0	0.8	1.2		0.1	0.1	0.3	0.1	DOWN	Hypothetical proteins	Conserved
BPS_02162	BPSS0212	Domain of unknown function (DUF1842)/Domain of unknown function (DUF1843)	1.5	1.4	1.4	1.4		0.1	0.1	0.2	0.1	DOWN	Hypothetical proteins	Conserved
BPS_02164	BPSS0210	uncharacterized domain 1	0.3	2.0	1.7	1.3		0.2	0.0	0.5	0.3	DOWN	Central intermediary metabolism	Other
BPS_02171	BPSS0203	hypothetical protein	0.3	2.0	1.7	1.3		0.0	0.4	0.1	0.2	DOWN	Cell envelope	Surface structures
BPS_02173	BPSS0201	prolyl aminopeptidase (EC:3.4.11.5). Serine peptidase. MEROPS family S33	0.4	1.2	0.3	0.6		0.3	0.3	0.2	0.3	DOWN	Protein fate	Transposon functions

BPS_02320	BPSS0063	Response regulator containing CheY-like receiver, AAA-type ATPase, and DNA-binding domains	0.3	2.0	1.7	1.3		0.0	0.0	0.0	0.0	DOWN	Regulatory functions	Transposon functions
BPS_02403	BPSS2340	farnesyl-diphosphate farnesyltransferase (EC 2.5.1.21)	0.1	2.1	2.0	1.4		0.1	0.3	0.0	0.2	DOWN	#NV	#NV
BPS_02432	BPSS2312	Predicted Zn-dependent proteases and their inactivated homologs	0.3	1.0	0.9	0.7		0.2	0.3	0.3	0.3	DOWN	#NV	#NV
BPS_02439	BPSS2305	Thioredoxin-like	0.3	2.0	1.7	1.3		0.0	0.0	0.1	0.0	DOWN	#NV	#NV
BPS_02459	BPSS2287	Nitroreductase	0.3	2.0	1.7	1.3		0.0	0.0	0.0	0.0	DOWN	#NV	#NV
BPS_02482	BPSS2264	3-hydroxyisobutyrate dehydrogenase and related beta-hydroxyacid dehydrogenases	0.0	2.0	0.2	0.7		0.1	0.3	0.0	0.1	DOWN	Energy metabolism	Detoxification
BPS_02576	BPSS2171	Glutamate-1-semialdehyde aminotransferase	0.8	8.2	2.1	3.7		0.1	0.3	0.0	0.1	DOWN	Biosynthesis of cofactors, prosthetic groups, and carriers	#NV
BPS_02691	BPSS2042	Acyl-CoA synthetases (AMP-forming)/AMP-acid ligases II	0.3	2.0	1.7	1.3		0.1	0.0	0.0	0.0	DOWN	#NV	#NV
BPS_02694	BPSS2039	Cyclopropane fatty acid synthase and related methyltransferases	2.5	1.9	1.7	2.0		0.1	0.1	0.1	0.1	DOWN	Cell envelope	Surface structures
BPS_02695	BPSS2038	Acyl carrier protein	0.3	2.0	1.7	1.3		0.0	0.2	0.0	0.1	DOWN	Unknown function	Heme, porphyrin, and cobalamin
BPS_02708	BPSS2025	Glutamate decarboxylase and related PLP-dependent proteins	0.7	2.3	2.0	1.6		0.0	0.1	0.2	0.1	DOWN	#NV	#NV
BPS_02712	BPSS2021	Glutamate decarboxylase and related PLP-dependent proteins	0.3	2.0	1.7	1.3		0.0	0.1	0.0	0.0	DOWN	#NV	#NV
BPS_02776	BPSS1960	thymidine phosphorylase (EC 2.4.2.4)	0.8	1.0	1.3	1.1		0.0	0.0	0.0	0.0	DOWN	Purines, pyrimidines, nucleosides, and nucleotides	Transposon functions
BPS_02780	BPSS1956	acetate kinase	0.3	2.0	1.7	1.3		0.0	0.0	0.0	0.0	DOWN	Central intermediary metabolism	Other
BPS_02781	BPSS1955	phosphate butyryltransferase (EC 2.3.1.19)	0.3	2.0	1.7	1.3		0.0	0.0	0.0	0.0	DOWN	#NV	#NV
BPS_02787	BPSS0537	Glycosyl transferases, related to UDP-glucuronosyltransferase	0.1	0.4	16.4	5.6		0.0	0.0	0.0	0.0	DOWN	Cell envelope	Surface structures
BPS_02868	BPSS0620	3-hydroxyisobutyrate dehydrogenase (EC 1.1.1.31)	0.3	2.0	1.7	1.3		0.0	0.0	0.0	0.0	DOWN	Energy metabolism	Detoxification

BPS_02884	BPSS0635	Glycogen debranching enzyme	0.1	1.1	4.0	1.7		0.1	0.4	0.1	0.2	DOWN	#NV	#NV
BPS_02955	BPSS0707	Uncharacterized Fe-S protein	0.3	187.5	1.7	63.2		0.4	0.0	0.6	0.4	DOWN	Cell envelope	Surface structures
BPS_02964	BPSS0715	Protein of unknown function (DUF3455)	10.2	0.7	3.9	4.9		0.3	0.1	0.6	0.3	DOWN	Hypothetical proteins	Conserved
BPS_02972	BPSS0721	Enoyl	1.4	0.4	7.6	3.1		0.0	0.0	0.0	0.0	DOWN	Energy metabolism	Detoxification
BPS_03001	BPSS0748	Uncharacterized protein conserved in bacteria	0.3	2.0	1.7	1.3		0.3	0.0	0.9	0.4	DOWN	Cell envelope	Surface structures
BPS_03067	BPSS0808	aromatic amino acid amidotransferase apoenzyme (EC 2.6.1.57)	0.3	1.0	0.6	0.6		0.3	0.2	0.2	0.2	DOWN	Amino acid biosynthesis	#NV
BPS_03100	BPSS0837	Universal stress protein UspA and related nucleotide-binding proteins	0.9	17.6	1.3	6.6		0.0	0.0	0.0	0.0	DOWN	Cellular processes	Adaptations to atypical conditions
BPS_03102	BPSS0839	Universal stress protein UspA and related nucleotide-binding proteins	45.3	1.0	0.1	15.5		0.0	0.0	0.1	0.1	DOWN	Cellular processes	Adaptations to atypical conditions
BPS_03118	BPSS0853	ribokinase	0.8	1.3	0.4	0.8		0.0	0.2	0.6	0.3	DOWN	Energy metabolism	Detoxification
BPS_03128	BPSS0864	Predicted oxidoreductases (related to aryl-alcohol dehydrogenases)	0.9	0.5	0.2	0.5		0.4	0.3	0.6	0.4	DOWN	Central intermediary metabolism	Other
BPS_03144	BPSS0881	Domain of unknown function (DUF4148)	0.0	2.0	1.7	1.2		0.0	0.0	0.0	0.0	DOWN	#NV	#NV
BPS_03145	BPSS0882	Predicted signal-transduction protein containing cAMP-binding and CBS domains	4.8	2.0	1.9	2.9		0.3	0.2	0.9	0.5	DOWN	#NV	#NV
BPS_03176	BPSS0913	Cystathionine beta-lyases/cystathionine gamma-synthases	1.1	0.9	1.1	1.0		0.2	0.3	0.0	0.2	DOWN	#NV	#NV
BPS_03249	BPSS0984	UDP-N-acetylglucosamine 1-carboxyvinyltransferase (EC 2.5.1.7)	0.6	0.4	0.7	0.5		0.0	0.3	0.1	0.1	DOWN	#NV	#NV
BPS_03251	BPSS0985	Uncharacterized conserved protein	1.1	0.8	0.6	0.9		0.3	0.4	0.0	0.2	DOWN	Unknown function	Heme, porphyrin, and cobalamin
BPS_03253	BPSS0987	hypothetical protein	57.8	2.0	1.7	20.5		0.0	0.0	0.0	0.0	DOWN	#NV	#NV

BPS_03290	BPSL2153	1-deoxy-D-xylulose 5-phosphate reductoisomerase (EC 1.1.1.267)	0.9	0.7	0.4	0.6		0.5	0.0	0.0	0.2	DOWN	Biosynthesis of cofactors, prosthetic groups, and carriers	#NV
BPS_03357	BPSL2100	transcription-repair coupling factor	4.1	12.0	0.4	5.5		0.0	0.2	0.0	0.1	DOWN	DNA metabolism	Detoxification
BPS_03400	BPSL1413	glucose-6-phosphate isomerase (EC 5.3.1.9)	1.4	0.5	0.5	0.8		0.3	0.4	0.8	0.5	DOWN	Energy metabolism	Detoxification
BPS_03401	BPSL1414	yjeF C-terminal region, hydroxyethylthiazole kinase-related/yjeF N-terminal region	0.2	0.8	0.8	0.6		0.3	0.2	0.7	0.4	DOWN	Cell envelope	Surface structures
BPS_03410	BPSL1423	Acyl-CoA synthetases (AMP-forming)/AMP-acid ligases II	1.6	0.2	0.6	0.8		0.0	0.8	0.2	0.3	DOWN	Protein synthesis	Transposon functions
BPS_03420	BPSL1433	Uncharacterized conserved protein	1.2	0.9	0.3	0.8		0.2	0.1	0.1	0.1	DOWN	#NV	#NV
BPS_03421	BPSL1434	folate-binding protein YgfZ	2.1	0.5	0.8	1.1		0.3	0.1	0.5	0.3	DOWN	#NV	#NV
BPS_03435	BPSL1448	L-asparaginase, type II	0.8	1.7	1.0	1.2		0.3	0.6	0.4	0.5	DOWN	Amino acid biosynthesis	#NV
BPS_03450	BPSL1462	primary replicative DNA helicase (EC 3.6.1.-)	1.5	1.2	13.2	5.3		0.4	0.2	0.9	0.5	DOWN	DNA metabolism	Detoxification
BPS_03494	BPSL1505	RNA polymerase, sigma 38 subunit, RpoS	0.7	1.1	2.1	1.3		0.0	0.0	0.7	0.2	DOWN	Cellular processes	Adaptations to atypical conditions
BPS_03496	BPSL1507	Metal-dependent hydrolase	0.3	2.0	1.7	1.3		0.0	0.0	0.0	0.0	DOWN	#NV	#NV
BPS_03517	BPSL1527	Transcriptional accessory protein	0.8	1.5	0.6	0.9		0.6	0.0	0.2	0.3	DOWN	Cell envelope	Surface structures
BPS_03519	BPSL1529	Protein of unknown function (DUF465)	3.0	0.4	0.0	1.1		0.2	0.1	0.3	0.2	DOWN	#NV	#NV
BPS_03573	BPSL1586	amino acid adenylation domain/thioester reductase domain	0.0	0.0	1.7	0.6		0.1	0.0	0.1	0.1	DOWN	#NV	#NV
BPS_03578	BPSL1592	Predicted kinase	8.2	0.4	6.3	5.0		0.0	0.2	0.3	0.2	DOWN	Amino acid biosynthesis	#NV
BPS_03599	BPSL1613	homodimeric dihydroxyacetone kinase (EC 2.7.1.29)	0.4	0.7	58.1	19.7		0.4	0.3	0.3	0.3	DOWN	#NV	#NV
BPS_03706	BPSL1734	Acyl-CoA synthetases (AMP-forming)/AMP-acid ligases II	0.9	0.4	0.9	0.7		0.3	0.2	0.0	0.2	DOWN	#NV	#NV
BPS_03743	BPSS1045	Uncharacterized conserved protein	0.3	2.0	1.7	1.3		0.0	0.0	0.0	0.0	DOWN	Cell envelope	Surface structures
BPS_03754	BPSS1098	hypothetical protein	0.3	2.0	1.7	1.3		0.0	0.0	0.2	0.1	DOWN	Hypothetical proteins	Conserved
BPS_03758	BPSS1101	hypothetical protein	3.6	33.1	0.1	12.3		0.3	0.4	0.2	0.3	DOWN	Cell envelope	Surface

														structures
BPS_03766	BPSS1109	Methyltransferase domain	1.4	1.6	4.7	2.6		0.0	0.0	0.1	0.1	DOWN	Fatty acid and phospholipid metabolism	Degradation
BPS_03775	BPSL1278	ABC-type Fe3+ transport system, periplasmic component	6.1	1.0	0.8	2.6		0.3	0.3	0.3	0.3	DOWN	Transport and binding proteins	Amino acids, peptides and amines
BPS_03784	BPSL1250	Phosphoglycerate dehydrogenase and related dehydrogenases	0.5	0.5	0.6	0.5		0.4	0.4	0.5	0.4	DOWN	Amino acid biosynthesis	#NV
BPS_03847	BPSL1216	NADH dehydrogenase subunit F (EC 1.6.5.3)	17.1	0.3	0.2	5.8		0.0	0.3	0.4	0.3	DOWN	Energy metabolism	Detoxification
BPS_03867	BPSL1236	Fructose-2,6-bisphosphatase	0.9	0.6	1.4	1.0		0.0	0.3	0.0	0.1	DOWN	Energy metabolism	Detoxification
BPS_03868	BPSL1237	short chain enoyl-CoA hydratase (EC 4.2.1.17)/Enoyl-CoA hydratase (EC 4.2.1.17)	1.3	0.9	5.9	2.7		0.6	0.2	0.5	0.4	DOWN	Fatty acid and phospholipid metabolism	Degradation
BPS_03924	BPSL1111	formate-dependent phosphoribosylglycinamide formyltransferase (EC 6.3.4.-)	0.6	0.5	1.0	0.7		0.6	0.0	0.0	0.2	DOWN	Purines, pyrimidines, nucleosides, and nucleotides	Transposon functions
BPS_03927	BPSL1105	transcriptional regulator, TetR family	2.0	1.0	0.5	1.2		0.5	0.3	0.7	0.5	DOWN	Regulatory functions	Transposon functions
BPS_03947	BPSL1098	MoxR-like ATPases	3.0	1.8	1.5	2.1		0.7	0.3	0.4	0.5	DOWN	Unknown function	Heme, porphyrin, and cobalamin
BPS_03958	BPSL1020	NAD-dependent aldehyde dehydrogenases	0.0	1.5	1.1	0.9		0.0	0.0	0.0	0.0	DOWN	Energy metabolism	Detoxification
BPS_03963	BPSL1026	NAD+ synthetase	3.0	0.5	0.3	1.3		0.2	0.2	0.7	0.4	DOWN	Biosynthesis of cofactors, prosthetic groups, and carriers	#NV
BPS_04017	BPSL0979	nicotinate-nucleotide-dimethylbenzimidazole phosphoribosyltransferase (EC 2.4.2.21)	0.6	1.1	0.8	0.8		0.5	0.1	0.8	0.4	DOWN	Biosynthesis of cofactors, prosthetic groups, and carriers	#NV
BPS_04044	BPSL1006	argininosuccinate lyase (EC 4.3.2.1)	0.3	0.7	0.7	0.6		0.5	0.5	0.4	0.4	DOWN	Amino acid biosynthesis	#NV
BPS_04130	BPSL0874	Dehydrogenases with different specificities (related to short-chain alcohol dehydrogenases)	9.0	0.8	0.8	3.5		0.5	0.2	0.4	0.3	DOWN	Fatty acid and phospholipid metabolism	Degradation
BPS_04139	BPSL0883	cAMP-binding proteins - catabolite gene activator and regulatory subunit of cAMP-dependent protein kinases	0.4	2.6	1.7	1.6		0.1	0.4	0.0	0.2	DOWN	Unknown function	Heme, porphyrin, and

														cobalamin
BPS_04166	BPSL0908	formyltetrahydrofolate-dependent phosphoribosylglycinamide formyltransferase (EC 2.1.2.2)	1.7	0.4	0.4	0.8		0.2	0.5	0.2	0.3	DOWN	Purines, pyrimidines, nucleosides, and nucleotides	Transposon functions
BPS_04246	BPSS1915	Predicted exonuclease of the beta-lactamase fold involved in RNA processing	0.3	2.0	1.7	1.3		0.0	0.0	0.0	0.0	DOWN	Cellular processes	Adaptations to atypical conditions
BPS_04251	BPSS1909	Amidases related to nicotinamidase	0.7	0.8	0.5	0.7		0.8	0.5	0.4	0.5	DOWN	Unknown function	Heme, porphyrin, and cobalamin
BPS_04292	BPSS1869	2-haloalkanoic acid dehalogenase, type II	2.6	0.6	1.0	1.4		0.4	0.2	0.7	0.4	DOWN	Central intermediary metabolism	Other
BPS_04311	BPSS1852	Putative NADP-dependent oxidoreductases	0.3	2.0	1.7	1.3		0.2	0.0	0.0	0.1	DOWN	Unknown function	Heme, porphyrin, and cobalamin
BPS_04446	BPSS1725	2-methylcitrate dehydratase (EC 4.2.1.79)	0.3	2.0	1.7	1.3		0.0	0.0	0.0	0.0	DOWN	#NV	#NV
BPS_04458	BPSS1713	Lactoylglutathione lyase and related lyases	0.3	2.0	1.7	1.3		0.0	0.0	0.2	0.1	DOWN	Hypothetical proteins	Conserved
BPS_04472	BPSS1700	phosphoribosylanthranilate isomerase (EC 5.3.1.24)	0.9	2.4	1.6	1.6		0.2	0.1	0.0	0.1	DOWN	Amino acid biosynthesis	#NV
BPS_04480	BPSS1692	amidophosphoribosyltransferase (EC 2.4.2.14)	0.9	0.6	1.3	1.0		0.2	0.7	0.4	0.4	DOWN	Purines, pyrimidines, nucleosides, and nucleotides	Transposon functions
BPS_04483	BPSS1689	Nucleoside-diphosphate-sugar epimerases	0.9	2.6	1.8	1.8		0.0	0.0	0.0	0.0	DOWN	Energy metabolism	Detoxification
BPS_04486	BPSS1686	hypothetical protein	0.2	87.0	3.1	30.1		0.0	0.0	0.0	0.0	DOWN	Hypothetical proteins	Conserved
BPS_04514	BPSS1663	L-seryl-tRNA(Sec) selenium transferase (EC 2.9.1.1)	0.3	2.0	1.7	1.3		0.0	0.1	0.0	0.0	DOWN	Protein synthesis	Transposon functions
BPS_04524	BPSS1652	Patatin	1.1	0.9	0.4	0.8		0.8	0.1	0.4	0.4	DOWN	#NV	#NV
BPS_04537	BPSS1638	Acyl dehydratase	0.3	2.0	1.7	1.3		0.0	0.0	0.0	0.0	DOWN	#NV	#NV
BPS_04539	BPSS1636	pyruvate dehydrogenase (quinone) (EC 1.2.5.1)	0.3	2.0	1.7	1.3		0.0	0.2	0.0	0.1	DOWN	Energy metabolism	Detoxification
BPS_04613	BPSS0363	Domain of unknown function (DUF1857)	0.8	1.1	0.5	0.8		0.1	0.1	0.2	0.1	DOWN	Hypothetical proteins	Conserved
BPS_04625	BPSS0375	acetyl-coenzyme A synthetase (EC 6.2.1.1)	0.7	1.4	1.4	1.2		0.3	0.5	0.5	0.4	DOWN	#NV	#NV

BPS_04655	BPSS0410	hypothetical protein	0.3	1.7	19.5	7.1		0.3	0.3	0.1	0.2	DOWN	#NV	#NV
BPS_04668	BPSS0421	Predicted pyridoxal phosphate-dependent enzyme apparently involved in regulation of cell wall biogenesis	0.4	1.8	0.8	1.0		0.4	0.3	0.2	0.3	DOWN	#NV	#NV
BPS_04688	BPSS0439	Amidases related to nicotinamidase	113.3	0.3	1.1	38.2		0.0	0.0	0.0	0.0	DOWN	Unknown function	Heme, porphyrin, and cobalamin
BPS_04690	BPSS0441	Predicted metal-dependent hydrolase with the TIM-barrel fold	0.7	2.5	0.6	1.3		0.1	0.5	0.2	0.3	DOWN	#NV	#NV
BPS_04691	BPSS0442	hypothetical protein	0.3	2.0	1.7	1.3		0.0	0.0	0.0	0.0	DOWN	Hypothetical proteins	Conserved
BPS_04693	BPSS0444	Predicted hydrolases or acyltransferases (alpha/beta hydrolase superfamily)	0.9	2.0	49.5	17.5		0.0	0.2	0.0	0.1	DOWN	Cellular processes	Adaptations to atypical conditions
BPS_04697	BPSS0448	hypothetical protein	0.6	0.4	0.5	0.5		0.4	0.3	0.6	0.4	DOWN	#NV	#NV
BPS_04727	BPSS0479	ribonucleoside-diphosphate reductase class II (EC 1.17.4.-)	0.1	0.5	17.4	6.0		0.0	0.0	0.1	0.0	DOWN	Purines, pyrimidines, nucleosides, and nucleotides	Transposon functions
BPS_04794	BPSSL1282	Exonuclease V gamma subunit	0.2	2.6	5.5	2.8		0.3	0.6	0.1	0.3	DOWN	DNA metabolism	Detoxification
BPS_04795	BPSSL1283	DNA helicase/exodeoxyribonuclease V, beta subunit (EC 3.1.11.5)	0.6	1.4	3.0	1.7		0.2	0.5	0.1	0.3	DOWN	DNA metabolism	Detoxification
BPS_04843	BPSSL1325	3-hydroxyacyl-CoA dehydrogenase	1.1	7.2	4.0	4.1		0.2	0.6	0.4	0.4	DOWN	Fatty acid and phospholipid metabolism	Degradation
BPS_04930	BPSSL2065	Response regulators consisting of a CheY-like receiver domain and a winged-helix DNA-binding domain	0.3	200.0	0.0	66.8		0.0	0.0	0.0	0.0	DOWN	Regulatory functions	Transposon functions
BPS_05076	BPSS1187	Acyl-CoA synthetases (AMP-forming)/AMP-acid ligases II	0.6	4.5	3.6	2.9		0.0	0.5	0.0	0.2	DOWN	Hypothetical proteins	Conserved
BPS_05078	BPSS1191	1-aminocyclopropane-1-carboxylate deaminase	0.6	3.2	3.2	2.3		0.1	0.2	0.1	0.1	DOWN	Unknown function	Heme, porphyrin, and cobalamin
BPS_05079	BPSS1192	hypothetical protein	0.3	0.7	0.5	0.5		0.0	0.0	0.0	0.0	DOWN	#NV	#NV
BPS_05086	BPSS1446	Enoyl-CoA hydratase/carnithine racemase	0.3	2.0	0.1	0.8		0.0	0.0	0.0	0.0	DOWN	Fatty acid and phospholipid metabolism	Degradation

BPS_05087	BPSS1447	Acetyl-CoA carboxylase, carboxyltransferase component (subunits alpha and beta)	0.3	49.8	21.5	23.9		0.0	0.0	0.0	0.0	DOWN	Fatty acid and phospholipid metabolism	Degradation
BPS_05092	BPSS1453	carboxynorspermidine decarboxylase (EC 4.1.1.-)	1.7	0.2	9.1	3.7		0.1	0.1	0.0	0.1	DOWN	Energy metabolism	Detoxification
BPS_05093	BPSS1454	Protein of unknown function (DUF3326)	0.2	0.4	0.9	0.5		0.0	0.0	0.0	0.0	DOWN	#NV	#NV
BPS_05103	BPSS1466	NAD-dependent aldehyde dehydrogenases	0.6	1.0	0.9	0.8		0.3	0.4	0.4	0.4	DOWN	Energy metabolism	Detoxification
BPS_05215	BPSS1346	Serine proteases of the peptidase family S9A	0.3	1.7	0.7	0.9		0.2	0.5	0.5	0.4	DOWN	Protein fate	Transposon functions
BPS_05250	BPSS1312	Phospholipase C	4.6	2.0	1.7	2.8		0.0	0.0	0.1	0.0	DOWN	#NV	#NV
BPS_05252	BPSS1311	Beta-lactamase class C and other penicillin binding proteins	0.4	0.7	1.1	0.7		0.1	0.2	0.2	0.2	DOWN	Cellular processes	Adaptations to atypical conditions
BPS_05379	BPSL1964	FOG: CBS domain	2.0	0.6	0.9	1.2		0.2	0.2	0.7	0.4	DOWN	Cell envelope	Surface structures
BPS_05526	BPSL1826	Uncharacterized conserved protein	3.5	0.1	0.4	1.3		0.2	0.1	0.3	0.2	DOWN	#NV	#NV
BPS_05562	BPSS1412	Uncharacterized conserved protein, contains double-stranded beta-helix domain	1.1	0.0	1.7	0.9		0.0	0.7	0.4	0.4	DOWN	Hypothetical proteins	Conserved
BPS_05682	BPSS0303	diaminopimelate decarboxylase (EC 4.1.1.20)	0.3	2.2	1.6	1.4		0.4	0.4	0.0	0.3	DOWN	Amino acid biosynthesis	#NV
BPS_05683	BPSS0302	Acyl-CoA synthetases (AMP-forming)/AMP-acid ligases II	0.2	1.0	0.8	0.7		0.1	0.3	0.2	0.2	DOWN	#NV	#NV
BPS_05772	BPSL0790	SnoAL-like domain	1.4	0.4	0.4	0.7		0.0	0.6	0.3	0.3	DOWN	Hypothetical proteins	Conserved
BPS_05814	BPSS1198	hypothetical protein	0.7	0.7	0.9	0.8		0.1	0.3	0.2	0.2	DOWN	#NV	#NV
BPS_05815	BPSS1199	hypothetical protein	15.3	2.3	0.9	6.2		0.2	0.2	0.6	0.4	DOWN	#NV	#NV
BPS_05820	BPSS1203	aspartate carbamoyltransferase (EC 2.1.3.2)	0.9	0.9	0.7	0.8		0.2	0.6	0.4	0.4	DOWN	Purines, pyrimidines, nucleosides, and nucleotides	Transposon functions
BPS_05966	BPSS1019	2-keto-4-pentenoate hydratase/2-oxohepta-3-ene-1,7-dioic acid hydratase (catechol pathway)	0.3	2.0	0.0	0.8		0.0	0.0	0.0	0.0	DOWN	Energy metabolism	Detoxification
BPS_00053	BPSL0673	Phosphate starvation-inducible protein PhoH, predicted ATPase	3.3	2.0	1.0	2.1		572.4	218.4	1.3	264.0	UP	#NV	#NV
BPS_00063	BPSL0663	lactoylglutathione lyase	0.0	0.0	1.7	0.6		256.0	1.9	546.6	268.2	UP	Energy metabolism	Detoxification

BPS_00096	BPSL0630	N-acyl-D-aspartate/D-glutamate deacylase	0.6	55.4	6.0	20.7		7.1	3.8	7.1	6.0	UP	Central intermediary metabolism	Other
BPS_00113	BPSL0613	hypothetical protein	0.5	0.5	15.7	5.6		2.3	1.9	2.1	2.1	UP	Protein synthesis	Transposon functions
BPS_00125	BPSL0601	Ribulose-5-phosphate 4-epimerase and related epimerases and aldolases	0.3	1.9	1.7	1.3		307.8	309.2	9.3	208.8	UP	#NV	#NV
BPS_00126	BPSL0600	bacteriocin biosynthesis cyclodehydratase domain	0.6	2.7	3.8	2.4		19.0	5.5	1.2	8.5	UP	Unknown function	Heme, porphyrin, and cobalamin
BPS_00127	BPSL0599	ribosomal natural product, two-chain TOMM family	2.6	1.3	0.8	1.5		2.3	2.8	1.9	2.3	UP	#NV	#NV
BPS_00128	BPSL0598	ribosomal natural product, two-chain TOMM family	5.1	1.2	0.8	2.4		2.7	2.9	2.2	2.6	UP	#NV	#NV
BPS_00130	BPSL0596	FHA domain protein	0.3	1.0	1.4	0.9		281.7	6.7	1.5	96.6	UP	#NV	#NV
BPS_00132	BPSL0594	hypothetical protein	0.8	0.4	2.5	1.3		2.5	7.0	4.2	4.6	UP	#NV	#NV
BPS_00134	BPSL0592	hypothetical protein	0.3	2.0	1.7	1.3		17.8	15.7	14.7	16.1	UP	#NV	#NV
BPS_00142	BPSL0585	hypothetical protein	0.3	11.1	1.7	4.4		2.3	1.9	2.1	2.1	UP	#NV	#NV
BPS_00143	BPSL0584	hypothetical protein	0.3	2.0	1.7	1.3		1973.5	9.4	16.1	666.3	UP	#NV	#NV
BPS_00159	BPSL0538	KpsF/GutQ family protein	0.3	2.0	1.7	1.3		3.8	1.9	1647.9	551.2	UP	Cell envelope	Surface structures
BPS_00204	BPSL0496	N-acetylglucosamine 6-phosphate deacetylase (EC 3.5.1.25)	5.0	1.4	1.1	2.5		8.1	23.3	2.5	11.3	UP	Central intermediary metabolism	Other
BPS_00222	BPSL0478	ABC-type multidrug transport system, permease component	0.3	74.0	0.1	24.8		2.3	95.2	8.7	35.4	UP	Transport and binding proteins	Amino acids, peptides and amines
BPS_00248	BPSL0453	cytochrome c oxidase, subunit II	0.3	2.0	1.7	1.3		64.2	208.9	591.3	288.1	UP	Energy metabolism	Detoxification
BPS_00261	BPSL0440	phosphoenolpyruvate--protein phosphotransferase (EC 2.7.3.9)	38.2	0.3	13.1	17.2		16.3	4.0	2.9	7.7	UP	Transport and binding proteins	Amino acids, peptides and amines
BPS_00265	BPSL0436	glutamate--cysteine ligase, T. ferrooxidans family	3.7	6.4	0.2	3.4		2.5	1.7	2.7	2.3	UP	Biosynthesis of cofactors,	#NV

													prosthetic groups, and carriers	
BPS_00271	BPSL0430	Predicted thioesterase involved in non-ribosomal peptide biosynthesis	3.9	2.0	0.2	2.0		2.3	1.9	2.1	2.1	UP	Fatty acid and phospholipid metabolism	Degradation
BPS_00352	BPSS0051	Domain of Unknown Function (DUF1259)	0.3	2.0	1.7	1.3		463.2	1.9	1746.1	737.1	UP	#NV	#NV
BPS_00397	BPSS1057	Protein of unknown function (DUF3396)	15.5	4.3	1.0	6.9		14.0	1.8	4.3	6.7	UP	Transcription	Transposon functions
BPS_00418	BPSL0346	dihydropyridine synthase	0.9	0.6	0.9	0.8		654.0	1.8	6.0	220.6	UP	Amino acid biosynthesis	#NV
BPS_00429	BPSL0335	Predicted dioxygenase of extradiol dioxygenase family	0.3	2.0	0.0	0.8		2.3	1.9	2.1	2.1	UP	Energy metabolism	Detoxification
BPS_00436	BPSL0329	Predicted hydrolases or acyltransferases (alpha/beta hydrolase superfamily)	0.3	2.0	1.7	1.3		2.3	1.9	2.1	2.1	UP	Energy metabolism	Detoxification
BPS_00443	BPSL0321	N-acyl-D-glucosamine 2-epimerase	0.3	2.0	1.7	1.3		410.5	50.6	147.1	202.7	UP	#NV	#NV
BPS_00508	BPSL0260	Predicted transcription regulator, contains HTH domain (MarR family)	11.1	2.0	1.7	4.9		226.9	64.6	1.3	97.6	UP	Hypothetical proteins	Conserved
BPS_00546	BPSL0222	NAD-dependent aldehyde dehydrogenases	0.3	2.0	1.7	1.3		2.3	1.9	2.1	2.1	UP	Central intermediary metabolism	Other
BPS_00565	BPSL0204	HslV component of HslUV peptidase. Threonine peptidase. MEROPS family T01B	3.5	0.9	0.7	1.7		6.0	3.0	2.4	3.8	UP	Protein fate	Transposon functions
BPS_00566	BPSL0203	ATP-dependent protease HslVU, ATPase subunit	2.8	1.2	1.0	1.7		2.8	6.1	5.2	4.7	UP	Protein fate	Transposon functions
BPS_00570	BPSL0200	N-acetylglutamate kinase (EC 2.7.2.8)	0.3	2.2	1.7	1.4		2.3	1.9	763.8	256.0	UP	#NV	#NV
BPS_00576	BPSL0194	Peptidase family M48	4.3	56.6	0.6	20.5		1.6	3.0	2.0	2.2	UP	Energy metabolism	Detoxification
BPS_00577	BPSL0193	transcriptional regulator, AraC family	0.3	2.0	1.7	1.3		28.9	24.1	134.3	62.4	UP	Regulatory functions	Transposon functions
BPS_00579	BPSL0191	exodeoxyribonuclease III	26.0	2.0	1.7	9.9		2.3	1.9	8.4	4.2	UP	DNA metabolism	Detoxification
BPS_00600	BPSL0124	Heat shock protein. Metallo peptidase. MEROPS family M48B	13.9	2.0	1.7	5.9		2.3	1.9	607.8	204.0	UP	Protein fate	Transposon functions
BPS_00603	BPSL0121	peptide deformylase (EC 3.5.1.88)	3.1	0.3	1.2	1.5		9.8	3.0	16.5	9.8	UP	Protein fate	Transposon functions

BPS_00617	BPSL0110	N-carbamoylputrescine amidase	0.3	2.0	1.7	1.3		2.3	1.9	2.1	2.1	UP	#NV	#NV
BPS_00626	BPSL0100	transcriptional regulator, AraC family	0.3	2.0	1.7	1.3		685.7	379.9	122.2	395.9	UP	DNA metabolism	Detoxification
BPS_00630	BPSL0097	hypothetical protein	0.3	204.3	0.0	68.2		2.3	1.9	1072.0	358.7	UP	#NV	#NV
BPS_00642	BPSL0089	Uncharacterized protein conserved in bacteria	0.2	0.7	0.6	0.5		18.2	5.5	19.6	14.4	UP	Hypothetical proteins	Conserved
BPS_00654	BPSL0080	tRNA modification GTPase trmE	0.3	0.6	62.8	21.2		1.9	360.4	635.0	332.4	UP	Protein synthesis	Transposon functions
BPS_00655	BPSL0079	hypothetical protein	0.3	0.8	1.7	1.0		3.4	1.3	30.0	11.6	UP	#NV	#NV
BPS_00670	BPSL0067	hypothetical protein	17.0	2.0	0.0	6.3		2.3	1.9	2.1	2.1	UP	Hypothetical proteins	Conserved
BPS_00672	BPSL0065	hypothetical protein	0.3	2.0	1.7	1.3		305.7	1.9	274.3	193.9	UP	Cell envelope	Surface structures
BPS_00735	BPSL3431	transcriptional regulator, MarR family	0.3	2.0	1.7	1.3		2739.4	278.8	6235.7	3084.6	UP	Regulatory functions	Transposon functions
BPS_00740	BPSL3426	Response regulators consisting of a CheY-like receiver domain and a winged-helix DNA-binding domain	2.1	1.3	1.0	1.4		9.3	2.8	2.6	4.9	UP	Regulatory functions	Transposon functions
BPS_00744	BPSL3423	transcriptional regulator, AsnC family	0.3	2.0	1.7	1.3		263.7	1.9	317.3	194.3	UP	Regulatory functions	Transposon functions
BPS_00760	BPSL3407	16S rRNA m(7)G-527 methyltransferase (EC 2.1.1.170)	0.3	2.0	1.7	1.3		831.2	1.9	1583.3	805.4	UP	Unknown function	Heme, porphyrin, and cobalamin
BPS_00762	BPSL3405	chromosome segregation DNA-binding protein	3.3	2.0	1.0	2.1		3616.0	2.9	5.1	1208.0	UP	Cellular processes	Adaptations to atypical conditions
BPS_00772	BPSL3395	ATP synthase F1 subcomplex epsilon subunit	2.1	0.8	0.9	1.3		1.3	4.1	3.3	2.9	UP	Energy metabolism	Detoxification
BPS_00781	BPSL3387	Acyl-CoA synthetases (AMP-forming)/AMP-acid ligases II	0.3	2.0	1.7	1.3		2.3	9.4	2.1	4.6	UP	#NV	#NV
BPS_00794	BPSL3376	Conserved TM helix	0.6	0.2	28.7	9.8		150.4	46.0	1.2	65.9	UP	Cell envelope	Surface structures
BPS_00801	BPSL3369	NAD-dependent aldehyde dehydrogenases	3.6	1.2	0.3	1.7		2.3	1.9	2.1	2.1	UP	Energy metabolism	Detoxification
BPS_00809	BPSL3361	glycine cleavage system H protein	6.7	1.7	0.9	3.1		1.2	2.3	2.7	2.0	UP	Energy metabolism	Detoxification

BPS_00810	BPSL3360	glycine cleavage system T protein	1.3	0.6	0.3	0.7		2.4	2.1	3.3	2.6	UP	Energy metabolism	Detoxification
BPS_00837	BPSL3332	Methyltransferase domain	0.0	2.0	1.7	1.2		2.3	1.9	2.1	2.1	UP	#NV	#NV
BPS_00848	BPSL3317	DNA-3-methyladenine glycosylase I (EC 3.2.2.20)	0.3	2.0	1.7	1.3		231.9	36.4	2.1	90.1	UP	DNA metabolism	Detoxification
BPS_00864	BPSL3301	Chemotaxis response regulator containing a CheY-like receiver domain and a methylesterase domain	1.1	0.5	0.5	0.7		2.3	1.9	680.2	228.1	UP	Cellular processes	Adaptations to atypical conditions
BPS_00865	BPSL3300	Response regulator containing CheY-like receiver, AAA-type ATPase, and DNA-binding domains	4.3	0.9	0.7	2.0		2.6	1.2	2939.9	981.2	UP	Cellular processes	Adaptations to atypical conditions
BPS_00884	BPSL3282	Putative heme iron utilization protein	0.3	2.0	1.7	1.3		2.3	1.9	411.3	138.5	UP	Biosynthesis of cofactors, prosthetic groups, and carriers	#NV
BPS_00894	BPSL3272	Predicted periplasmic or secreted lipoprotein	6.3	2.0	1.7	3.3		2.3	57.7	173.7	77.9	UP	#NV	#NV
BPS_00981	BPSL3181	Cytochrome c553	0.3	2.0	1.7	1.3		2.3	1.9	2.1	2.1	UP	#NV	#NV
BPS_00986	BPSL3176	diaminopimelate decarboxylase (EC 4.1.1.20)	9.1	0.9	1.3	3.8		3.4	4.7	8.7	5.6	UP	Amino acid biosynthesis	#NV
BPS_00994	BPSL3169	shikimate kinase (EC 2.7.1.71)	0.3	2.0	1.7	1.3		332.2	1.9	724.9	353.0	UP	Amino acid biosynthesis	#NV
BPS_01001	BPSL3162	Glycerophosphoryl diester phosphodiesterase	3.7	0.8	3.5	2.7		2.8	2.8	4.1	3.2	UP	Fatty acid and phospholipid metabolism	Degradation
BPS_01003	BPSL3160	Transposase and inactivated derivatives	4.7	1.9	1.7	2.8		2.3	2.5	3.4	2.7	UP	Unknown function	Heme, porphyrin, and cobalamin
BPS_01018	BPSL3146	ABC-type transport system involved in resistance to organic solvents, auxiliary component	1.4	0.7	1.0	1.0		3.9	2.0	2.6	2.8	UP	DNA metabolism	Detoxification
BPS_01033	BPSL3131	phosphoribosyl-ATP pyrophosphatase (EC 3.6.1.31)	0.3	96.6	1.7	32.9		4.4	6.6	7641.4	2550.8	UP	Amino acid biosynthesis	#NV
BPS_01034	BPSL3130	Predicted membrane protein	0.3	2.0	1.7	1.3		2.3	1.9	2.1	2.1	UP	Cell envelope	Surface structures
BPS_01035	BPSL3129	Diadenosine tetraphosphate (Ap4A) hydrolase and other HIT family hydrolases	6.5	0.4	0.5	2.5		2.4	2.1	2.9	2.4	UP	Unknown function	Heme, porphyrin, and cobalamin

BPS_01069	BPSS1077	Putative transcription activator	0.3	2.0	1.7	1.3		2770.0	2.0	2469.8	1747.3	UP	DNA metabolism	Detoxification
BPS_01075	BPSL3107	type VI secretion protein, VC_A0107 family	2.7	1.8	1.0	1.8		1.9	5.7	2.6	3.4	UP	Cellular processes	Adaptations to atypical conditions
BPS_01076	BPSL3106	type VI secretion protein, EvpB/VC_A0108 family	1.7	1.4	1.0	1.4		4.8	3.8	3.7	4.1	UP	Central intermediary metabolism	Other
BPS_01077	BPSL3105	type VI secretion system effector, Hcp1 family	2.7	1.2	1.5	1.8		4.1	6.2	5.7	5.3	UP	#NV	#NV
BPS_01103	BPSL3077	Uncharacterized conserved protein	0.3	2.0	1.7	1.3		1579.0	68.8	1269.6	972.5	UP	Amino acid biosynthesis	#NV
BPS_01107	BPSL3073	bacterial peptide chain release factor 1 (bRF-1)	0.0	2.0	0.4	0.8		2.3	1.9	30.4	11.5	UP	Protein synthesis	Transposon functions
BPS_01113	BPSL3068	haloacid dehalogenase superfamily, subfamily IA, variant 3 with third motif having DD or ED	3.5	2.0	0.0	1.8		2.3	1.9	2.1	2.1	UP	Central intermediary metabolism	Other
BPS_01144	BPSL3041	phenylacetic acid degradation protein paaN	4.5	2.0	1.7	2.7		1342.9	166.3	23.1	510.8	UP	Central intermediary metabolism	Other
BPS_01150	BPSL3037	Acyl-CoA synthetases (AMP-forming)/AMP-acid ligases II	2.6	2.0	0.3	1.6		1515.5	627.5	220.5	787.8	UP	Fatty acid and phospholipid metabolism	Degradation
BPS_01154	BPSL3033	16S rRNA (cytosine(1402)-N(4))-methyltransferase	2.1	171.8	0.0	58.0		#####	11.7	11.7	4281.2	UP	Unknown function	Heme, porphyrin, and cobalamin
BPS_01158	BPSL3029	UDP-N-acetylmuramoyl-tripeptide--D-alanyl-D-alanine ligase (EC 6.3.2.10)	1.2	1.3	1.8	1.4		10.1	8.2	8.5	8.9	UP	Cell envelope	Surface structures
BPS_01160	BPSL3027	UDP-N-acetylmuramoylalanine--D-glutamate ligase (EC 6.3.2.9)	4.0	1.0	5.5	3.5		4.5	5.5	7.8	5.9	UP	Cell envelope	Surface structures
BPS_01162	BPSL3025	UDP-N-acetylglucosamine-N-acetylmuramylpentapeptide N-acetylglucosamine transferase	0.3	2.0	1.7	1.3		2.3	3.7	9.6	5.2	UP	Cell envelope	Surface structures
BPS_01163	BPSL3024	UDP-N-acetylmuramate--L-alanine ligase (EC 6.3.2.8)	7.2	3.2	0.8	3.7		15.2	9.0	10.5	11.6	UP	Cell envelope	Surface structures
BPS_01164	BPSL3023	D-alanine--D-alanine ligase (EC 6.3.2.4)	1.5	2.1	2.0	1.8		8.8	9.5	16.1	11.5	UP	#NV	#NV
BPS_01174	BPSL3013	ADP-ribose pyrophosphatase	0.7	2.0	1.7	1.5		2.3	34.5	2.1	13.0	UP	DNA metabolism	Detoxification

BPS_01192	BPSL2996	Hypoxanthine-guanine phosphoribosyltransferase	0.0	2.0	14.1	5.4		356.6	1.9	2.1	120.2	UP	Purines, pyrimidines, nucleosides, and nucleotides	Transposon functions
BPS_01200	BPSL2990	Histone H1-like nucleoprotein HC2	5.9	2.0	0.8	2.9		2.9	1.5	6.7	3.7	UP	#NV	#NV
BPS_01205	BPSL2985	prmA; ribosomal protein L11 methyltransferase (EC:2.1.1.-); K02687 ribosomal protein L11 methyltransferase [EC:2.1.1.-]	1.7	1.1	3.6	2.1		39.0	2.3	9.5	16.9	UP	Protein synthesis	Transposon functions
BPS_01206	BPSL2984	acetyl-CoA carboxylase, biotin carboxylase subunit	1.3	0.5	1.6	1.1		2.2	1.9	2.8	2.3	UP	Fatty acid and phospholipid metabolism	Degradation
BPS_01207	BPSL2983	biotin carboxyl carrier protein	0.9	2.0	1.9	1.6		2.4	1.8	3.0	2.4	UP	Fatty acid and phospholipid metabolism	Degradation
BPS_01208	BPSL2982	3-dehydroquinate dehydratase (EC 4.2.1.10)	0.2	0.8	0.5	0.5		3.5	3.8	6.4	4.5	UP	Amino acid biosynthesis	#NV
BPS_01214	BPSL2976	shikimate dehydrogenase (EC 1.1.1.25)	7.7	0.0	0.5	2.7		28.4	191.9	199.4	139.9	UP	Amino acid biosynthesis	#NV
BPS_01216	BPSL2974	Carboxypeptidase C (cathepsin A)	0.2	2.4	0.3	1.0		31.0	168.1	46.1	81.7	UP	Cell envelope	Surface structures
BPS_01217	BPSL2973	hypothetical protein	0.3	2.2	10.1	4.2		22.7	38.2	1804.0	621.7	UP	#NV	#NV
BPS_01220	BPSL2970	2-keto-3-deoxy-phosphogalactonate aldolase (EC 4.1.2.21)	23.4	2.0	1.7	9.0		2.3	1.9	2.1	2.1	UP	Energy metabolism	Detoxification
BPS_01243	BPSL2947	transcriptional regulator, GntR family	1.4	36.5	1.7	13.2		2.0	2.2	4.5	2.9	UP	Regulatory functions	Transposon functions
BPS_00054	BPSL0672	probable rRNA maturation factor YbeY	0.2	0.4	0.5	0.4	DOWN	29.7	226.5	2.9	86.4	UP	Hypothetical proteins	Conserved
BPS_01267	BPSL2920	hypothetical protein	16.5	1.0	1.7	6.4		672.9	1.9	739.6	471.5	UP	#NV	#NV
BPS_01270	BPSL2918	Molecular chaperone (small heat shock protein)	0.3	1.7	0.0	0.7		703.8	1.9	4.4	236.7	UP	Protein fate	Transposon functions
BPS_01291	BPSL2899	Holliday junction DNA helicase subunit RuvB	10.7	0.0	1.7	4.2		2.3	1.9	2.1	2.1	UP	DNA metabolism	Detoxification
BPS_01299	BPSL2891	Glutathione S-transferase	0.3	2.0	1.7	1.3		980.7	2.1	2873.0	1285.3	UP	Central intermediary metabolism	Other
BPS_01307	BPSL2885	NAD/NADP transhydrogenase beta subunit	0.3	2.0	1.7	1.3		136.1	1.9	111.1	83.0	UP	Central intermediary metabolism	Other

BPS_01310	BPSL2883	Predicted enzyme related to lactoylglutathione lyase	0.0	0.2	1.7	0.6		2.3	1.9	2.1	2.1	UP	#NV	#NV
BPS_01324	BPSL2870	protein translocase subunit yajC	0.3	2.0	1.7	1.3		2.3	1.9	2.1	2.1	UP	Protein fate	Transposon functions
BPS_01328	BPSL2866	Transcriptional regulator	10.2	2.0	1.7	4.6		1048.4	5.1	1674.9	909.5	UP	Regulatory functions	Transposon functions
BPS_01330	BPSL2865	catalase/peroxidase HPI	1.3	2.3	1.7	1.8		2.7	4.8	5.9	4.5	UP	Cellular processes	Adaptations to atypical conditions
BPS_00215	BPSL0485	acyl-CoA ligase (AMP-forming), exosortase A-associated	0.0	0.0	0.1	0.0	DOWN	2.3	1.9	2.1	2.1	UP	Protein synthesis	Transposon functions
BPS_00219	BPSL0481	Methylase involved in ubiquinone/menaquinone biosynthesis	0.3	0.0	0.0	0.1	DOWN	2.3	1.9	2.1	2.1	UP	Amino acid biosynthesis	#NV
BPS_01355	BPSL2840	Hemoglobin-like flavoprotein	0.3	175.3	111.6	95.8		2.3	1.9	2.1	2.1	UP	Cellular processes	Adaptations to atypical conditions
BPS_00224	BPSL0476	diaminobutyrate-2-oxoglutarate transaminase [EC:2.6.1.76]	0.0	0.0	0.0	0.0	DOWN	2.3	1.9	2.1	2.1	UP	#NV	#NV
BPS_01368	BPSL2827	chaperone protein DnaK	2.0	1.0	0.8	1.3		1.6	2.6	3.4	2.5	UP	Protein fate	Transposon functions
BPS_01369	BPSL2826	chaperone protein DnaJ	0.9	0.7	0.6	0.7		13.3	2.1	1.6	5.6	UP	Protein fate	Transposon functions
BPS_01370	BPSL2825	Anthranilate/para-aminobenzoate synthases component I	0.3	2.0	1.7	1.3		2.3	18.2	6.4	8.9	UP	Biosynthesis of cofactors, prosthetic groups, and carriers	#NV
BPS_01382	BPSL2812	Small-conductance mechanosensitive channel	3.0	0.6	0.5	1.4		21.6	24.5	1089.4	378.5	UP	#NV	#NV
BPS_01392	BPSL2802	Sulfotransferase family	4.7	34.7	0.2	13.2		60.8	60.8	2.1	41.2	UP	#NV	#NV
BPS_01396	BPSL2798	dTDP-4-dehydrohamnose reductase (EC 1.1.1.133)	0.7	1.6	1.1	1.1		3.7	3.2	1.8	2.9	UP	#NV	#NV
BPS_01400	BPSL2794	Nucleoside-diphosphate-sugar pyrophosphorylase involved in lipopolysaccharide biosynthesis/translation initiation factor 2B, gamma/epsilon subunits (eIF-	4.5	2.0	1.7	2.7		2.3	1.9	2.1	2.1	UP	#NV	#NV

		2Bgamma/elf-2Bepsilon)												
BPS_01452	BPSL2766	tol-pal system protein YbgF	4.6	1.3	0.7	2.2		2.5	2.0	2.6	2.4	UP	Unknown function	Heme, porphyrin, and cobalamin
BPS_01454	BPSL2764	tol-pal system beta propeller repeat protein TolB	2.0	1.3	1.4	1.6		2.8	2.4	3.3	2.8	UP	Transport and binding proteins	Amino acids, peptides and amines
BPS_01462	BPSL2757	transcriptional regulator NrdR	13.0	2.0	1.7	5.6		111.2	1.9	1107.7	406.9	UP	Hypothetical proteins	Conserved
BPS_01470	BPSL2749	Uncharacterized conserved protein	1.5	1.6	0.8	1.3		1.7	6.7	2.8	3.7	UP	Hypothetical proteins	Conserved
BPS_00367	BPSS0037	Uncharacterized conserved protein	0.0	0.0	0.0	0.0	DOWN	2.3	1.9	2.1	2.1	UP	#NV	#NV
BPS_00467	BPSL0297	NADPH-glutathione reductase (EC 1.8.1.7)	0.4	0.2	0.0	0.2	DOWN	449.8	6.1	6.6	154.2	UP	Energy metabolism	Detoxification
BPS_00474	BPSL0294	porin, OprB family (TC 1.B.19)	0.0	0.2	0.5	0.2	DOWN	4838.4	21.1	6.5	1622.0	UP	#NV	#NV
BPS_01486	BPSL2733	transcriptional regulator, LysR family	0.9	1.0	0.9	0.9		3.9	5.0	3.6	4.2	UP	Regulatory functions	Transposon functions
BPS_00834	BPSL3333	acid phosphatase (EC 3.1.3.2)	0.0	0.2	0.2	0.1	DOWN	2.3	1.9	2.1	2.1	UP	Central intermediary metabolism	Other
BPS_01505	BPSL2715	Carboxypeptidase C (cathepsin A)	1.0	238.0	1.9	80.3		948.9	118.0	1240.2	769.0	UP	Cell envelope	Surface structures
BPS_01507	BPSL2713	drug resistance transporter, EmrB/QacA subfamily	0.3	2.0	1.7	1.3		2.3	1.9	956.2	320.1	UP	Cell envelope	Surface structures
BPS_00836	BPSL3332	Amio acid efflux protein	0.0	0.3	0.1	0.1	DOWN	2.3	1.9	2.1	2.1	UP	#NV	#NV
BPS_00846	BPSL3319	Flagellin and related hook-associated proteins	0.4	0.4	0.4	0.4	DOWN	3462.6	2.4	9.7	1158.2	UP	Cellular processes	Adaptations to atypical conditions
BPS_00868	BPSL3297	Protein of unknown function (DUF3443)	0.3	0.1	0.1	0.2	DOWN	2.3	41.8	177.0	73.7	UP	#NV	#NV
BPS_00893	BPSL3273	Phosphoheptose isomerase	0.0	0.3	0.6	0.3	DOWN	11.1	1.8	4.1	5.7	UP	Cell envelope	Surface structures
BPS_01604	BPSL2618	D-cysteine desulhydrase (EC 4.4.1.15)	8.8	2.0	0.2	3.6		2.3	1.9	2.1	2.1	UP	#NV	#NV

BPS_01613	BPSL2609	carbohydrate ABC transporter membrane protein 2, CUT1 family (TC 3.A.1.1.-)	1.0	2.0	0.1	1.0		2.3	1.9	2.1	2.1	UP	Transport and binding proteins	Amino acids, peptides and amines
BPS_01082	BPSL3100	type VI secretion-associated protein, ImpA family	0.3	0.0	0.0	0.1	DOWN	2.3	1.9	2.1	2.1	UP	DNA metabolism	Detoxification
BPS_01652	BPSL2557	cold-shock DNA-binding protein family	4.2	3.9	0.6	2.9		2.3	1.8	3.7	2.6	UP	Regulatory functions	Transposon functions
BPS_01687	BPSL2524	2-phosphoglycolate phosphatase, prokaryotic	25.9	2.7	0.4	9.7		2.3	1.9	464.8	156.3	UP	Energy metabolism	Detoxification
BPS_01593	BPSL2629	Aspartate/tyrosine/aromatic aminotransferase	0.2	0.1	0.0	0.1	DOWN	2.3	1.9	2.1	2.1	UP	Unknown function	Heme, porphyrin, and cobalamin
BPS_01697	BPSL2514	integration host factor, beta subunit	0.3	2.0	1.7	1.3		2.8	232.7	1167.3	467.6	UP	DNA metabolism	Detoxification
BPS_01721	BPSL2490	tRNA (Guanine37-N(1)-) methyltransferase (EC 2.1.1.31)	0.3	2.0	1.7	1.3		30.9	1.9	263.5	98.7	UP	Protein synthesis	Transposon functions
BPS_01790	BPSL2428	GTP-binding protein Era	0.3	69.6	49.7	39.9		6.7	5.7	2.9	5.1	UP	Cellular processes	Adaptations to atypical conditions
BPS_01819	BPSL2402	pyridoxal kinase	0.3	2.0	1.7	1.3		181.5	55.0	2.1	79.5	UP	Biosynthesis of cofactors, prosthetic groups, and carriers	#NV
BPS_01833	BPSL2388	arginine N-succinyltransferase	0.3	1.4	1.7	1.2		2.3	1.9	5.2	3.1	UP	Energy metabolism	Detoxification
BPS_01835	BPSL2386	succinylarginine dihydrolase (EC 3.5.3.23)	0.3	0.4	2.3	1.0		2.3	1.9	2.2	2.1	UP	Energy metabolism	Detoxification
BPS_01881	BPSL2339	formimidoylglutamate deiminase (EC 3.5.3.13)	0.3	2.0	1.7	1.3		2.3	1.9	2.1	2.1	UP	Energy metabolism	Detoxification
BPS_01933	BPSL2288	FeS assembly scaffold apoprotein IscU	0.3	0.0	0.0	0.1	DOWN	5.1	10.8	8942.1	2986.0	UP	Biosynthesis of cofactors, prosthetic groups, and carriers	#NV
BPS_02821	BPSS0571	Domain of unknown function (DUF4148)	0.0	0.0	0.0	0.0	DOWN	2.3	1.9	2.1	2.1	UP	#NV	#NV
BPS_01887	BPSL2334	hypothetical protein	0.3	2.0	1.7	1.3		2.3	1.9	547.1	183.7	UP	Hypothetical proteins	Conserved
BPS_02936	BPSS0688	Response regulators consisting of a CheY-like receiver domain and a winged-helix DNA-binding domain	0.1	0.0	0.1	0.1	DOWN	2.3	1.9	2.1	2.1	UP	Regulatory functions	Transposon functions
BPS_03089	BPSS0827	Peptidase family M9 N-terminal/Collagenase	0.8	0.1	0.0	0.3	DOWN	2.3	1.9	2.1	2.1	UP	Protein fate	Transposon

														functions
BPS_01924	BPSL2298	phasin family protein	7.1	1.3	0.9	3.1		1.5	2.7	5.6	3.3	UP	#NV	#NV
BPS_01931	BPSL2290	transcriptional regulator, BadM/Rrf2 family	2.1	0.2	0.0	0.8		3051.5	#####	3.7	1419.4	UP	#NV	#NV
BPS_01932	BPSL2289	cysteine desulfurase IscS	1.2	1.0	2.4	1.6		7.2	10.5	3.8	7.2	UP	Biosynthesis of cofactors, prosthetic groups, and carriers	#NV
BPS_03297	BPSL2146	lipid-A-disaccharide synthase (EC 2.4.1.182)	0.3	0.0	0.0	0.1	DOWN	2.3	1.9	2.1	2.1	UP	Cell envelope	Surface structures
BPS_01934	BPSL2287	Iron-binding apoprotein IscA	0.3	2.0	14.4	5.6		2.3	119.0	464.0	195.1	UP	Biosynthesis of cofactors, prosthetic groups, and carriers	#NV
BPS_01935	BPSL2286	Co-chaperone protein HscB	36.1	0.7	378.7	138.5		2.7	2.2	6.3	3.7	UP	Protein fate	Transposon functions
BPS_01936	BPSL2285	Chaperone protein HscA	0.6	0.9	2.6	1.4		5.0	4.9	8.3	6.1	UP	Cell envelope	Surface structures
BPS_01938	BPSL2283	FeS assembly protein IscX	0.3	2.0	1.7	1.3		1155.0	195.0	845.2	731.7	UP	Unknown function	Heme, porphyrin, and cobalamin
BPS_03687	BPSL1716	Cysteine synthase	0.2	0.4	0.1	0.2	DOWN	2.3	1.9	2.1	2.1	UP	Amino acid biosynthesis	#NV
BPS_01957	BPSL2264	Lysophospholipase	0.3	2.0	1.7	1.3		132.6	178.0	2.1	104.2	UP	Central intermediary metabolism	Other
BPS_01967	BPSL2254	FKBP-type peptidyl-prolyl cis-trans isomerases 2	0.3	2.0	1.7	1.3		3.3	171.5	1729.9	634.9	UP	Protein fate	Transposon functions
BPS_02070	BPSL2217	sulfate adenylyltransferase subunit 2 (EC 2.7.7.4)	0.4	1.1	1.0	0.8		3.4	2.4	4.8	3.5	UP	Biosynthesis of cofactors, prosthetic groups, and carriers	#NV
BPS_02076	BPSL0965	aminopeptidase A. Metallo peptidase. MEROPS family M17	3.5	0.2	0.7	1.5		7.6	1.3	3.7	4.2	UP	Protein fate	Transposon functions
BPS_02082	BPSL2212	methionine aminopeptidase, type I (EC 3.4.11.18)	0.3	2.0	1.7	1.3		4.0	133.5	1.3	46.3	UP	Protein fate	Transposon functions
BPS_03780	BPSL1247	Xaa-Pro aminopeptidase	0.3	0.0	0.1	0.1	DOWN	2079.8	566.8	3484.1	2043.6	UP	Protein fate	Transposon functions

BPS_02112	BPSL2186	Acyl-CoA-binding protein	0.3	2.0	1.7	1.3		2.3	1.9	2.1	2.1	UP	Transport and binding proteins	Amino acids, peptides and amines
BPS_02113	BPSL2185	tRNA threonylcarbamoyl adenosine modification protein YeaZ	5.4	2.0	1.7	3.0		2.3	1.9	2.1	2.1	UP	Protein fate	Transposon functions
BPS_04284	BPSS1878	NAD-dependent aldehyde dehydrogenases	0.0	0.0	0.0	0.0	DOWN	2.3	1.9	2.1	2.1	UP	Central intermediary metabolism	Other
BPS_02146	BPSS0227	Uncharacterized protein involved in outer membrane biogenesis	0.1	2.1	10.7	4.3		2.3	1.9	2.1	2.1	UP	Cell envelope	Surface structures
BPS_04330	BPSS1833	UDP-glucose dehydrogenase	0.0	0.3	0.0	0.1	DOWN	244.5	1.9	560.0	268.8	UP	Cell envelope	Surface structures
BPS_04588	BPSS1588	hypothetical protein	0.2	0.1	0.1	0.1	DOWN	2.3	1.9	2.1	2.1	UP	#NV	#NV
BPS_02203	BPSS0173	type VI secretion protein, VC_A0107 family	0.8	0.8	1.7	1.1		1661.0	84.3	3068.0	1604.4	UP	Unknown function	Heme, porphyrin, and cobalamin
BPS_02204	BPSS0172	type VI secretion protein, EvpB/VC_A0108 family	0.9	224.3	1.7	75.6		184.2	1.9	745.6	310.5	UP	#NV	#NV
BPS_04774	BPSS0517	type VI secretion protein, EvpB/VC_A0108 family	0.3	0.5	0.1	0.3	DOWN	2.3	1.9	2.1	2.1	UP	#NV	#NV
BPS_02247	BPSS0131	Nucleoside-diphosphate-sugar epimerases	0.5	68.5	0.6	23.2		2.3	1.9	2.1	2.1	UP	Energy metabolism	Detoxification
BPS_02248	BPSS0130	Acyl-CoA synthetases (AMP-forming)/AMP-acid ligases II	0.3	6.6	1.7	2.9		2.3	7.2	26.9	12.1	UP	#NV	#NV
BPS_04860	BPSL1344	hydroxyacylglutathione hydrolase	0.4	0.0	0.1	0.2	DOWN	2.3	1.9	2.1	2.1	UP	Energy metabolism	Detoxification
BPS_05137	BPSS1496	type VI secretion protein, VC_A0107 family	0.3	0.0	0.0	0.1	DOWN	2.3	1.9	2.1	2.1	UP	#NV	#NV
BPS_02369	BPSS0021	Siderophore-interacting protein	3.4	1.3	0.5	1.7		2.3	1.9	449.4	151.2	UP	Transport and binding proteins	Amino acids, peptides and amines
BPS_02389	BPSS0001	Plasmid replication region DNA-binding N-term	3.0	0.7	0.4	1.4		85.1	1.3	2.1	29.5	UP	#NV	#NV
BPS_02390	BPSS2351	Initiator Replication protein	11.8	2.0	1.7	5.1		2252.3	425.5	3829.0	2168.9	UP	DNA metabolism	Detoxification
BPS_02392	BPSS2349	plasmid segregation oscillating ATPase ParF	0.3	2.0	1.7	1.3		120.3	39.5	704.0	287.9	UP	#NV	#NV
BPS_05160	BPSS1523	Tir chaperone protein (CesT) family (BicP chaperon)	0.1	0.0	0.0	0.0	DOWN	4.0	1.9	2.1	2.6	UP	#NV	#NV

BPS_05179	BPSS1545	Type II secretory pathway, component PulD	0.0	0.0	0.2	0.1	DOWN	2.3	1.9	2.1	2.1	UP	Cellular processes	Adaptations to atypical conditions
BPS_02577	BPSS2170	Aromatic ring-cleaving dioxygenase	0.3	2.0	1.7	1.3		2.3	1.9	2.1	2.1	UP	#NV	#NV
BPS_02597	BPSS2142	transcriptional regulator, XRE family with cupin sensor	1.9	0.2	0.5	0.8		3.9	2.3	1.6	2.6	UP	Regulatory functions	Transposon functions
BPS_02608	BPSS2131	DNA-binding protein H-NS	9.9	1.8	1.1	4.3		6.3	3.3	3.6	4.4	UP	#NV	#NV
BPS_02610	BPSS2130	Acyl-CoA synthetase (NDP forming)	0.3	2.0	1.7	1.3		40.3	20.3	24.6	28.4	UP	Central intermediary metabolism	Other
BPS_02618	BPSS2121	Cysteine sulfinate desulfinase/cysteine desulfurase and related enzymes	0.3	2.0	1.7	1.3		2.3	31.6	1380.0	471.3	UP	#NV	#NV
BPS_02643	BPSS2099	type VI secretion protein, EvpB/VC_A0108 family	0.3	2.0	1.7	1.3		2.3	1.9	635.2	213.1	UP	#NV	#NV
BPS_02672	BPSS2080	hypothetical protein	0.2	1.0	0.7	0.6		2.3	1.9	2.1	2.1	UP	Hypothetical proteins	Conserved
BPS_02743	BPSS1992	dipeptidyl-peptidase IV (EC 3.4.14.11). Serine peptidase. MEROPS family S15	0.3	2.0	1.7	1.3		118.7	1.9	609.9	243.5	UP	Central intermediary metabolism	Other
BPS_05386	BPSL1959	acyl-CoA thioester hydrolase [EC:3.1.2.-]	0.4	0.5	0.2	0.3	DOWN	10.2	4.9	2.4	5.9	UP	Unknown function	Heme, porphyrin, and cobalamin
BPS_00038	BPSL0687	glycerol kinase (EC 2.7.1.30)	140.9	529.6	6.0	225.5	UP	3.7	6.2	7.5	5.8	UP	Energy metabolism	Detoxification
BPS_00075	BPSL0651	Enoyl-CoA hydratase (EC 4.2.1.17)	10.2	2.0	24.7	12.3	UP	2.3	1.9	2.1	2.1	UP	#NV	#NV
BPS_00088	BPSL0638	Uncharacterized protein conserved in bacteria	6.1	4.2	2.4	4.3	UP	22.6	125.4	16.1	54.7	UP	Cell envelope	Surface structures
BPS_02894	BPSS0644	transcriptional regulator, RpiR family	0.3	0.1	1.7	0.7		15.2	43.2	2.1	20.2	UP	#NV	#NV
BPS_02906	BPSS0656	hypothetical protein	0.3	2.0	1.7	1.3		403.0	1.9	1743.2	716.0	UP	#NV	#NV
BPS_02913	BPSS0665	Probable taurine catabolism dioxygenase	0.3	2.0	1.7	1.3		285.1	178.9	378.9	281.0	UP	Energy metabolism	Detoxification
BPS_00091	BPSL0635	Diadenosine tetraphosphate (Ap4A) hydrolase and other HIT family hydrolases	4.3	1.9	2.6	2.9	UP	2.3	1.3	4.2	2.6	UP	Unknown function	Heme, porphyrin, and cobalamin

BPS_02961	BPSS0712	Uncharacterized protein conserved in bacteria	3.2	1.1	1.5	1.9		1.5	2.1	2.6	2.1	UP	Unknown function	Heme, porphyrin, and cobalamin
BPS_02970	BPSS0720	NADH:flavin oxidoreductases, Old Yellow Enzyme family	0.5	2.0	0.1	0.8		2.3	1.9	2.1	2.1	UP	#NV	#NV
BPS_03008	BPSS0755	transcriptional regulator, LysR family	0.3	51.6	1.7	17.9		2.3	1.9	2.1	2.1	UP	Regulatory functions	Transposon functions
BPS_03017	BPSS0764	Dehydrogenases with different specificities (related to short-chain alcohol dehydrogenases)	0.3	2.0	1.7	1.3		2.3	1.9	2.1	2.1	UP	Central intermediary metabolism	Other
BPS_03021	BPSS0767	Cytochrome c peroxidase	0.3	2.0	1.7	1.3		2.3	1.9	401.8	135.3	UP	#NV	#NV
BPS_00131	BPSL0595	hypothetical protein	3.6	6.3	1.8	3.9	UP	22.4	14.9	9.9	15.7	UP	#NV	#NV
BPS_00160	BPSL0537	3-deoxy-D-manno-octulosonate 8-phosphate phosphatase, Yrbl family	35.0	4.6	37.0	25.5	UP	2.2	4.0	12.4	6.2	UP	Cell envelope	Surface structures
BPS_03198	BPSS0935	Response regulators consisting of a CheY-like receiver domain and a winged-helix DNA-binding domain	0.3	2.0	1.7	1.3		2.3	1.9	2.1	2.1	UP	Hypothetical proteins	Conserved
BPS_03244	BPSS0979	Outer membrane protein (porin)	0.3	2.0	1.7	1.3		2.3	1.9	2.1	2.1	UP	Cell envelope	Surface structures
BPS_03260	BPSS0993	Catalase	0.3	54.6	1.7	18.9		139.1	21.7	678.0	279.6	UP	#NV	#NV
BPS_03279	BPSL2164	DNA ligase, NAD-dependent	0.3	2.0	1.7	1.3		2.3	1.9	123.4	42.5	UP	DNA metabolism	Detoxification
BPS_03311	BPSL2133	Glutamine cyclotransferase	0.3	2.0	1.7	1.3		2.3	1.9	313.5	105.9	UP	Hypothetical proteins	Conserved
BPS_03314	BPSL2129	inosine-5-monophosphate dehydrogenase (EC 1.1.1.205)	6.0	1.0	0.6	2.5		1.5	4.2	5.5	3.8	UP	Purines, pyrimidines, nucleosides, and nucleotides	Transposon functions
BPS_03334	BPSL2121	transcriptional regulator, GntR family	0.3	2.0	1.7	1.3		2.3	27.2	313.7	114.4	UP	Regulatory functions	Transposon functions
BPS_00360	BPSS0044	3-oxoadipate CoA-transferase beta subunit	6.7	164.3	13.5	61.5	UP	2.3	1.9	2.1	2.1	UP	Energy metabolism	Detoxification
BPS_03361	BPSL2096	Peroxiredoxin	3.0	1.4	0.9	1.8		2.0	3.3	2.3	2.5	UP	Cellular processes	Adaptations to atypical conditions
BPS_00437	BPSL0328	Dioxygenases related to 2-nitropropane dioxygenase	5.5	2.0	14.3	7.3	UP	2.3	4.4	1479.3	495.3	UP	Cellular processes	Adaptations to

														atypical conditions
BPS_00555	BPSL0213	Protein involved in biosynthesis of mitomycin antibiotics/polyketide fumonisins	52.8	5.5	186.8	81.7	UP	2.9	1.1	2.4	2.1	UP	#NV	#NV
BPS_03373	BPSL1390	hypothetical protein	0.0	3.7	0.1	1.3		13.0	7.3	5.9	8.7	UP	#NV	#NV
BPS_00578	BPSL0192	Zn-dependent alcohol dehydrogenases	3.0	168.2	2.8	58.0	UP	4.2	2.5	4.7	3.8	UP	Central intermediary metabolism	Other
BPS_00629	BPSL0098	Uncharacterized protein conserved in bacteria	5.1	2.0	34.1	13.7	UP	2.3	68.8	484.9	185.3	UP	#NV	#NV
BPS_00631	BPSL0096	Acetyltransferases, including N-acetylases of ribosomal proteins	2.0	3.1	2.6	2.6	UP	26.3	17.3	11.1	18.2	UP	Central intermediary metabolism	Other
BPS_00675	BPSL0062	acetyl-CoA acetyltransferases	57.9	117.6	2.0	59.2	UP	2.3	1.9	2.1	2.1	UP	Fatty acid and phospholipid metabolism	Degradation
BPS_00676	BPSL0061	Acyl-CoA dehydrogenases	130.5	343.4	148.9	207.6	UP	2.3	1.9	60.4	21.5	UP	Fatty acid and phospholipid metabolism	Degradation
BPS_03454	BPSL1466	Predicted ATPase related to phosphate starvation-inducible protein PhoH	60.9	1.7	0.7	21.1		1.4	3.4	2.5	2.4	UP	Unknown function	Heme, porphyrin, and cobalamin
BPS_00730	BPSL0004	Bacterial nucleoid DNA-binding protein	10.4	3.4	2.2	5.3	UP	1.3	2.0	36.7	13.3	UP	DNA metabolism	Detoxification
BPS_03471	BPSL1483	transcriptional regulator, BadM/Rrf2 family	0.3	2.0	1.7	1.3		183.7	1.9	2.1	62.6	UP	#NV	#NV
BPS_03484	BPSL1497	thioredoxin	3.3	1.5	1.4	2.1		2.8	2.4	4.4	3.2	UP	Energy metabolism	Detoxification
BPS_03493	BPSL1504	Membrane proteins related to metalloendopeptidases	0.3	37.5	1.7	13.2		475.7	1.9	191.8	223.1	UP	Protein fate	Transposon functions
BPS_03498	BPSL1509	Integral membrane protein, interacts with FtsH	0.3	2.0	31.1	11.1		2.3	1.9	2.1	2.1	UP	Cell envelope	Surface structures
BPS_00761	BPSL3406	chromosome segregation ATPase	9.7	10.1	34.1	17.9	UP	1.4	2.4	4.1	2.6	UP	Unknown function	Heme, porphyrin, and cobalamin
BPS_03516	BPSL1526	K+ transporter	0.3	12.9	1.7	5.0		249.9	1.9	178.8	143.5	UP	Transport and binding proteins	Amino acids, peptides and

														amines
BPS_03537	BPSL1547	Uncharacterized protein involved in outer membrane biogenesis	0.3	2.0	1.7	1.3		865.2	1.9	2.1	289.7	UP	Cell envelope	Surface structures
BPS_03577	BPSL1591	Saccharopine dehydrogenase and related proteins	0.3	2.0	1.7	1.3		2.3	1.9	2.1	2.1	UP	Hypothetical proteins	Conserved
BPS_03612	BPSL1627	P pilus assembly protein, chaperone PapD	1.5	0.0	1.7	1.1		3.0	2.0	7606.2	2537.0	UP	Cell envelope	Surface structures
BPS_03622	BPSL1633	two component transcriptional regulator, LuxR family	0.3	2.0	1.7	1.3		732.3	12.8	830.1	525.1	UP	#NV	#NV
BPS_03627	BPSL1637	Lipase (class 3)	4.3	0.6	0.0	1.7		139.1	43.1	48.4	76.9	UP	#NV	#NV
BPS_03639	BPSL1650	ABC-type spermidine/putrescine transport system, permease component I	0.3	77.7	85.7	54.6		1260.3	1.9	397.8	553.3	UP	Transport and binding proteins	Amino acids, peptides and amines
BPS_03681	BPSL1711	Predicted carbamoyl transferase, NodU family	1.8	13.2	1.8	5.6		2.3	1.9	2.1	2.1	UP	Unknown function	Heme, porphyrin, and cobalamin
BPS_03682	BPSL1712	amino acid adenylation domain	0.1	0.4	0.9	0.5		2.2	1.4	10.7	4.7	UP	Protein synthesis	Transposon functions
BPS_03685	BPSL1714	L-threonine aldolase (EC 4.1.2.5)	0.3	2.0	1.7	1.3		2.3	1.9	2.1	2.1	UP	#NV	#NV
BPS_03688	BPSL1717	hypothetical protein	0.3	2.0	1.7	1.3		2.3	1.9	2.1	2.1	UP	#NV	#NV
BPS_00767	BPSL3400	ATP synthase F0 subcomplex B subunit	24.7	472.5	6.7	167.9	UP	8.3	2.8	2.6	4.5	UP	Energy metabolism	Detoxification
BPS_00852	BPSL3313	DNA-binding protein H-NS	57.6	179.3	1.7	79.5	UP	28.9	2.0	#####	#####	UP	#NV	#NV
BPS_03698	BPSL1727	Thioesterase domains of type I polyketide synthases or non-ribosomal peptide synthetases	0.2	0.9	0.8	0.6		351.9	1.9	2.1	118.6	UP	#NV	#NV
BPS_03726	BPSL1754	Uncharacterized protein conserved in bacteria	0.9	1.5	0.6	1.0		2.3	1.9	2.1	2.1	UP	#NV	#NV
BPS_03767	BPSS1110	Probable taurine catabolism dioxygenase	0.3	2.0	1.7	1.3		373.8	11.2	13.5	132.8	UP	#NV	#NV
BPS_03806	BPSL1273	Putative NADH-flavin reductase	7.3	1.9	1.2	3.4		2.0	1.5	4.4	2.7	UP	Hypothetical proteins	Conserved
BPS_03808	BPSL1275	transcriptional regulator, AsnC family	0.3	2.0	1.7	1.3		2.1	1.4	2117.5	707.0	UP	Regulatory functions	Transposon functions
BPS_03810	BPSL1180	Truncated hemoglobins	0.3	2.0	0.0	0.8		2.3	1.9	2.1	2.1	UP	#NV	#NV

BPS_03861	BPSL1230	Acyl dehydratase	0.3	2.0	1.7	1.3		577.8	1.9	1302.4	627.4	UP	#NV	#NV
BPS_03881	BPSL1172	K+-transporting ATPase, B subunit	0.3	2.0	1.7	1.3		2.3	111.9	92.8	69.0	UP	Transport and binding proteins	Amino acids, peptides and amines
BPS_03915	BPSL1159	MAF protein	0.3	0.2	1.7	0.7		2.3	1.9	2.1	2.1	UP	Cellular processes	Adaptations to atypical conditions
BPS_03917	BPSL1161	iojap-like ribosome-associated protein	0.3	1.1	1.7	1.1		445.0	57.3	2.0	168.1	UP	Unknown function	Heme, porphyrin, and cobalamin
BPS_00885	BPSL3281	DNA-binding protein H-NS	22.0	6.3	3.2	10.5	UP	1.9	2.5	3.9	2.7	UP	#NV	#NV
BPS_01030	BPSL3134	1-(5-phosphoribosyl)-5	4.9	2.5	2.8	3.4	UP	2.1	1.8	5.6	3.2	UP	Amino acid biosynthesis	#NV
BPS_03937	BPSL1087	Molecular chaperone, HSP90 family	2.6	0.9	0.9	1.5		1.6	2.6	2.9	2.4	UP	Protein fate	Transposon functions
BPS_01059	BPSL3119	hypothetical protein	13.1	3.5	1.1	5.9	UP	1.5	2.2	5.8	3.2	UP	Cellular processes	Adaptations to atypical conditions
BPS_01128	BPSL3056	Acyl carrier protein phosphodiesterase	80.2	98.0	92.0	90.1	UP	8.9	2.1	24.7	11.9	UP	Fatty acid and phospholipid metabolism	Degradation
BPS_03974	BPSL1038	hypothetical protein	32.5	2.0	1.7	12.1		506.1	1.9	2.1	170.0	UP	#NV	#NV
BPS_03980	BPSL1044	trehalose 6-phosphate synthase (EC 2.4.1.15)	0.3	2.0	1.7	1.3		170.4	148.9	1219.3	512.8	UP	Cellular processes	Adaptations to atypical conditions
BPS_01151	BPSL3036	Outer membrane protein (porin)	3.7	16.1	23.9	14.6	UP	22.9	11.7	14.9	16.5	UP	Cell envelope	Surface structures
BPS_01153	BPSL3034	mraZ protein	19.0	54.6	1.7	25.1	UP	16.7	8.1	23.1	16.0	UP	Unknown function	Heme, porphyrin, and cobalamin
BPS_01157	BPSL3030	UDP-N-acetylmuramoylalanyl-D-glutamate--2,6-	5.7	29.5	6.3	13.8	UP	5.5	11.2	12.4	9.7	UP	Cell envelope	Surface

		diaminopimelate ligase (EC 6.3.2.13)												structures
BPS_04056	BPSL0970	Transcriptional regulator	0.3	2.0	1.7	1.3		2.3	1.9	156.3	53.5	UP	#NV	#NV
BPS_04085	BPSL0931	Uncharacterized protein, homolog of Cu resistance protein CopC	0.3	2.0	1.7	1.3		2.3	1.9	856.2	286.8	UP	Cellular processes	Adaptations to atypical conditions
BPS_01166	BPSL3021	cell division protein FtsA	3.4	1.3	2.2	2.3	UP	12.3	3.2	4.8	6.8	UP	Cellular processes	Adaptations to atypical conditions
BPS_04094	BPSL0955	Transcriptional regulator	0.3	2.0	1.7	1.3		212.9	1.9	486.3	233.7	UP	Regulatory functions	Transposon functions
BPS_04103	BPSL0847	Kynureninase (EC 3.7.1.3)	0.3	2.0	1.7	1.3		314.7	2.3	110.1	142.4	UP	Energy metabolism	Detoxification
BPS_04107	BPSL0851	methionine-S-sulfoxide reductase	0.8	0.6	1.0	0.8		2.7	3.7	1.5	2.6	UP	Cellular processes	Adaptations to atypical conditions
BPS_04136	BPSL0880	Superoxide dismutase	1.5	0.9	1.3	1.3		3.2	1.9	2.8	2.6	UP	Cellular processes	Adaptations to atypical conditions
BPS_01167	BPSL3020	cell division protein FtsZ	9.0	3.8	#####	848.8	UP	75.6	8.7	171.2	85.2	UP	Cellular processes	Adaptations to atypical conditions
BPS_01197	BPSL2992	ribonucleoside-diphosphate reductase, alpha subunit	3.1	3.1	4.9	3.7	UP	29.6	18.1	30.2	26.0	UP	Purines, pyrimidines, nucleosides, and nucleotides	Transposon functions
BPS_01198	BPSL2991	Ribonucleotide reductase, beta subunit	35.0	21.0	30.1	28.7	UP	14.2	45.9	2.8	20.9	UP	Purines, pyrimidines, nucleosides, and nucleotides	Transposon functions
BPS_04187	BPSL0824	ABC-type metal ion transport system, periplasmic component/surface adhesin	0.3	2.0	1.7	1.3		2.3	63.9	2.1	22.8	UP	Transport and binding proteins	Amino acids, peptides and amines
BPS_04197	BPSL0815	The (Largely Gram-negative Bacterial) Hydrophobe/Amphiphile Efflux-1 (HAE1) Family	0.3	2.0	1.7	1.3		326.0	89.5	590.9	335.5	UP	Cell envelope	Surface structures

BPS_04206	BPSS1118	RND family efflux transporter, MFP subunit	0.3	2.0	1.7	1.3		230.7	63.3	2.1	98.7	UP	Cell envelope	Surface structures
BPS_01480	BPSL2739	homogentisate 1,2-dioxygenase (EC 1.13.11.5)	5.8	8.6	10.1	8.2	UP	5.4	4.8	6.1	5.5	UP	Energy metabolism	Detoxification
BPS_01481	BPSL2738	fumarylacetoacetate hydrolase (EC 3.7.1.2)	21.5	9.6	22.7	17.9	UP	7.2	5.0	12.3	8.2	UP	Energy metabolism	Detoxification
BPS_04317	BPSS1846	Uncharacterized conserved protein	10.5	1.7	1.5	4.6		2.2	4.8	2.6	3.2	UP	Cell envelope	Surface structures
BPS_01749	BPSL2466	hypothetical protein	18.4	106.3	1.7	42.1	UP	3.6	2.3	2.7	2.9	UP	#NV	#NV
BPS_04323	BPSS1840	Negative regulator of beta-lactamase expression	0.4	0.9	0.9	0.7		2.9	3.1	2.1	2.7	UP	Cell envelope	Surface structures
BPS_01885	BPSL2336	Glutamine synthetase	7.4	2.0	18.7	9.4	UP	2.3	1.9	2.1	2.1	UP	Protein synthesis	Transposon functions
BPS_04349	BPSS1815	amino acid adenylation domain	2.4	15.0	0.1	5.8		4368.9	#####	1509.1	2295.6	UP	Unknown function	Heme, porphyrin, and cobalamin
BPS_04353	BPSS1811	Demethylmenaquinone methyltransferase	46.6	2.0	0.1	16.2		2.3	1.9	2.1	2.1	UP	Unknown function	Heme, porphyrin, and cobalamin
BPS_01886	BPSL2335	Adenosylmethionine-8-amino-7-oxononanoate amiransferase	69.5	7.5	449.5	175.5	UP	1.2	2.9	3725.7	1243.3	UP	Central intermediary metabolism	Other
BPS_02016	BPSL2089	hypothetical protein	2.0	1.2	4.8	2.7	UP	2.3	1.9	2.1	2.1	UP	#NV	#NV
BPS_02018	BPSL2089	hypothetical protein	7.9	3.1	2.4	4.5	UP	2.5	1.8	4.5	2.9	UP	#NV	#NV
BPS_04402	BPSS1764	Exodeoxyribonuclease VII small subunit (EC 3.1.11.6)	0.3	2.0	1.7	1.3		495.3	1.9	2.1	166.4	UP	DNA metabolism	Detoxification
BPS_02019	BPSL1386	hypothetical protein	3.8	2.6	2.3	2.9	UP	4.4	3.7	1.6	3.2	UP	#NV	#NV
BPS_04415	BPSS1753	Methyltransferase domain	12.9	2.0	1.7	5.5		2.3	1.9	2.1	2.1	UP	#NV	#NV
BPS_04484	BPSS1688	GDP-mannose 4,6-dehydratase	0.3	0.6	1.2	0.7		2.3	1.9	2.1	2.1	UP	Cell envelope	Surface structures
BPS_04496	BPSS1678	Predicted membrane protein	0.3	19.1	1.7	7.1		2.3	1.9	2.1	2.1	UP	#NV	#NV
BPS_04500	BPSS1674	amino acid ABC transporter substrate-binding protein,	0.0	2.0	146.4	49.5		2.3	1.9	2.1	2.1	UP	Cell envelope	Surface

		PAAT family (TC 3.A.1.3.-)												structures
BPS_04536	BPSS1639	Citrate lyase beta subunit	0.3	1.0	1.7	1.0		2.3	1.9	2.1	2.1	UP	#NV	#NV
BPS_02020	BPSL1387	hypothetical protein	12.0	1.5	2.4	5.3	UP	2.7	3.3	2.0	2.7	UP	Hypothetical proteins	Conserved
BPS_04616	BPSS0366	outer membrane transport energization protein ExbD (TC 2.C.1.1.1)	0.3	2.0	1.7	1.3		328.0	3.4	150.6	160.6	UP	Transport and binding proteins	Amino acids, peptides and amines
BPS_04617	BPSS0367	outer membrane transport energization protein ExbB (TC 2.C.1.1.1)	3.7	0.3	0.5	1.5		10.2	8.1	3.5	7.3	UP	Transport and binding proteins	Amino acids, peptides and amines
BPS_04622	BPSS0372	fumarase, class I, homodimeric (EC 4.2.1.2)	31.3	0.0	0.0	10.4		2256.0	79.7	2.1	779.3	UP	Energy metabolism	Detoxification
BPS_04729	BPSS0482	3-oxoacyl	6.4	2.0	1.7	3.4		2.3	1.9	2.1	2.1	UP	#NV	#NV
BPS_04733	BPSS0486	Acyl-CoA synthetases (AMP-forming)/AMP-acid ligases II	0.1	1.1	2.2	1.1		2.3	1.9	2.1	2.1	UP	Fatty acid and phospholipid metabolism	Degradation
BPS_02198	BPSS0178	type VI secretion protein, VC_A0110 family	2.4	6.7	1.7	3.6	UP	2.3	1.9	2.1	2.1	UP	#NV	#NV
BPS_04779	BPSS0522	type VI secretion ATPase, ClpV1 family	8.6	0.0	1.7	3.5		2.3	1.9	2.1	2.1	UP	Transport and binding proteins	Amino acids, peptides and amines
BPS_04780	BPSS0523	Rhs element Vgr protein	0.7	2.0	0.1	0.9		2.3	1.9	2.1	2.1	UP	Mobile and extrachromosomal element functions	Transposon functions
BPS_04787	BPSS0530	type VI secretion protein, VC_A0114 family	0.6	1.2	2.5	1.5		2.4	1.4	18.8	7.6	UP	#NV	#NV
BPS_04802	BPSL1290	hydroxymethylpyrimidine synthase	2.2	0.3	0.5	1.0		3.6	3.4	1.6	2.9	UP	Biosynthesis of cofactors, prosthetic groups, and carriers	#NV
BPS_04820	BPSL1306	diguanylate cyclase (GGDEF) domain	0.3	0.0	1.7	0.7		17.0	32.0	9.8	19.6	UP	#NV	#NV
BPS_02205	BPSS0171	type VI secretion system effector, Hcp1 family	50.2	6.8	2.7	19.9	UP	9.5	18.8	58.2	28.8	UP	#NV	#NV
BPS_04840	BPSL1323	Molecular chaperone (small heat shock protein)	3.7	2.3	1.0	2.3		4.4	3.1	2.7	3.4	UP	#NV	#NV
BPS_02312	BPSS0075	Acetyltransferases	5.4	3.3	1.2	3.3	UP	8.2	5.3	3.2	5.6	UP	Transport and binding proteins	Amino acids, peptides and amines

BPS_04881	BPSL1364	phosphate regulon transcriptional regulatory protein PhoB	0.3	53.4	15.4	23.0		2.3	1.9	2.1	2.1	UP	Regulatory functions	Transposon functions
BPS_02323	BPSS0060B	DNA-binding protein H-NS	8.7	8.3	5.2	7.4	UP	2.3	1.5	2.3	2.1	UP	#NV	#NV
BPS_02963	BPSS0714	dimethylhistidine N-methyltransferase	6.4	4.9	1.7	4.4	UP	2.3	1.9	2.1	2.1	UP	Hypothetical proteins	Conserved
BPS_04906	BPSL1387	hypothetical protein	0.0	118.2	143.9	87.4		2.3	1.9	2.1	2.1	UP	Hypothetical proteins	Conserved
BPS_04920	BPSL2074	Glycosidases	0.3	2.0	1.7	1.3		1.5	4.7	2.1	2.8	UP	Energy metabolism	Detoxification
BPS_04922	BPSL2073	esterase, PHB depolymerase family	2.8	2.0	1.7	2.2		2.3	1.9	2.1	2.1	UP	#NV	#NV
BPS_03285	BPSL2158	translation elongation factor Ts (EF-Ts)	3.7	4.0	2.2	3.3	UP	1.4	2.6	34.3	12.8	UP	Protein synthesis	Transposon functions
BPS_05062	BPSS0490	Transposase and inactivated derivatives	0.3	0.6	1.7	0.9		2.3	1.9	451.8	152.0	UP	#NV	#NV
BPS_03333	BPSL2122	murein tetrapeptidase LD-carboxypeptidase (EC:3.4.17.13). Serine peptidase. MEROPS family S66	1.4	2.1	2.9	2.1	UP	3.8	3.6	1.5	3.0	UP	#NV	#NV
BPS_05130	BPSS1490	Negative regulator of beta-lactamase expression	0.9	0.3	0.6	0.6		32.1	60.5	56.4	49.7	UP	Cell envelope	Surface structures
BPS_03603	BPSL1617	Dehydrogenases (flavoproteins)	12.3	105.9	22.5	46.9	UP	24.6	390.6	21.1	145.4	UP	#NV	#NV
BPS_03604	BPSL1618	hypothetical protein	18.2	35.0	11.1	21.4	UP	17.2	32.1	56.4	35.2	UP	#NV	#NV
BPS_03695	BPSL1724	Histidinol-phosphate/aromatic amidotransferase and cobayric acid decarboxylase	3.9	4.6	1.7	3.4	UP	2.3	1.9	2.1	2.1	UP	#NV	#NV
BPS_03696	BPSL1725	Cupin-like domain	10.5	1.7	4.0	5.4	UP	2.3	1.9	2.1	2.1	UP	#NV	#NV
BPS_03833	BPSL1203	Carbonic anhydrase	51.4	58.8	18.5	42.9	UP	1037.8	289.0	1483.3	936.7	UP	#NV	#NV
BPS_05238	BPSS1324	1-aminocyclopropane-1-carboxylate deaminase	0.8	2.0	1.7	1.5		2.3	1.9	2.1	2.1	UP	Central intermediary metabolism	Other
BPS_05257	BPSS1306	ABC-type dipeptide transport system, periplasmic component	0.3	2.0	1.7	1.3		10.5	41.5	#####	9682.7	UP	#NV	#NV
BPS_05313	BPSS1260	Peptidase M66	0.0	1.3	0.2	0.5		2.3	1.9	2.1	2.1	UP	#NV	#NV
BPS_05332	BPSS1244	Nitrate/nitrite transporter	0.0	2.0	1.7	1.2		2.3	1.9	2.1	2.1	UP	Transport and binding proteins	Amino acids, peptides and

														amines
BPS_05371	BPSL1971	Transcriptional regulator	0.3	2.0	1.7	1.3		2.3	97.0	716.0	271.8	UP	Regulatory functions	Transposon functions
BPS_03992	BPSL1057	Inhibitor of vertebrate lysozyme (Ivy)	4.2	1.8	2.3	2.8	UP	2.6	3.3	2.6	2.8	UP	Hypothetical proteins	Conserved
BPS_05387	BPSL1958	hypothetical protein	0.9	5.4	1.6	2.6		5.8	2.0	3.7	3.8	UP	#NV	#NV
BPS_04090	BPSL0936	Dihydrodipicolinate synthase/N-acetylneuraminate lyase	2.5	3.3	6.7	4.1	UP	32.0	105.2	86.5	74.6	UP	#NV	#NV
BPS_04091	BPSL0937	Ribulose-5-phosphate 4-epimerase and related epimerases and aldolases	4.9	175.7	134.5	105.0	UP	32.4	#####	5609.8	2407.8	UP	Unknown function	Heme, porphyrin, and cobalamin
BPS_04095	BPSL0956	sulfite reductase (NADPH) beta subunit (EC 1.8.1.2)	24.1	2.3	3.2	9.9	UP	2.3	1.9	2.1	2.1	UP	Central intermediary metabolism	Other
BPS_04096	BPSL0957	Uncharacterized protein conserved in bacteria	1.2	37.5	9.4	16.0	UP	2.3	176.7	2.1	60.3	UP	Central intermediary metabolism	Other
BPS_04157	BPSL0899	ATP-dependent Clp protease ATP-binding subunit ClpA (EC 3.4.21.92)	15.1	1.3	162.8	59.7	UP	688.8	74.4	628.8	464.0	UP	Transport and binding proteins	Amino acids, peptides and amines
BPS_05429	BPSL1917	ribosome-binding factor A	42.0	1.3	1.7	15.0		1187.6	570.7	3842.4	1866.9	UP	Transcription	Transposon functions
BPS_05434	BPSL1912	transcriptional regulator, MarR family	0.3	2.0	1.7	1.3		671.0	269.7	764.7	568.5	UP	Regulatory functions	Transposon functions
BPS_04316	BPSS1847	Uncharacterized conserved protein	46.8	4.9	43.7	31.8	UP	2.8	3.0	2.9	2.9	UP	Cell envelope	Surface structures
BPS_05454	BPSL1892	Flp pilus assembly protein TadB	0.3	185.9	48.5	78.3		2.3	1.9	2.1	2.1	UP	Cell envelope	Surface structures
BPS_04351	BPSS1813	chlorinating enzyme	9.1	5.5	2.0	5.5	UP	1.2	167.1	6.4	58.3	UP	Unclassified	Heme, porphyrin, and cobalamin
BPS_04384	BPSS1782	peroxiredoxin, Ohr subfamily	35.6	76.4	72.6	61.5	UP	2.5	5.1	#####	5056.9	UP	Cellular processes	Adaptations to atypical

														conditions
BPS_04403	BPSS1763	farnesyl-diphosphate synthase (EC 2.5.1.10)	18.0	52.4	36.6	35.7	UP	2.3	8.3	2.1	4.2	UP	Biosynthesis of cofactors, prosthetic groups, and carriers	#NV
BPS_05624	BPSS1354	betaine aldehyde dehydrogenase (EC 1.2.1.8)	0.7	0.5	1.6	0.9		1.3	466.6	4.2	157.3	UP	Cellular processes	Adaptations to atypical conditions
BPS_04455	BPSS1716	Uncharacterized conserved protein	6.3	2.0	65.8	24.7	UP	277.4	1.9	2.1	93.8	UP	Unknown function	Heme, porphyrin, and cobalamin
BPS_05754	BPSL0808	periplasmic serine protease, Do/DeqQ family	6.7	0.0	73.7	26.8		2.3	1.9	2.1	2.1	UP	Protein fate	Transposon functions
BPS_05764	BPSL0798	fructose-bisphosphate aldolase (EC 4.1.2.13)	2.3	1.7	1.1	1.7		2.3	1.3	3.5	2.4	UP	Energy metabolism	Detoxification
BPS_04493	BPSS1680	Bacterial DNA-binding protein	11.7	3.2	1.7	5.5	UP	6.4	2.4	11.3	6.7	UP	DNA metabolism	Detoxification
BPS_05908	BPSL1797	ABC-type bacteriocin/lantibiotic exporters, contain an N-terminal double-glycine peptidase domain	11.8	2.0	1.7	5.1		862.7	8.7	9.4	293.6	UP	Transport and binding proteins	Amino acids, peptides and amines
BPS_05909	BPSL1797	hypothetical protein	0.8	1.3	117.2	39.7		4130.4	#####	1.5	1778.5	UP	Transport and binding proteins	Amino acids, peptides and amines
BPS_05911	BPSL1795	Transglutaminase-like superfamily	0.4	0.7	0.8	0.6		19.9	3.7	2.1	8.6	UP	Hypothetical proteins	Conserved
BPS_04839	BPSL1322	Molecular chaperone (small heat shock protein)	77.5	182.3	1.4	87.1	UP	4.5	6.5	4.6	5.2	UP	Protein fate	Transposon functions
BPS_05982	BPSS0343	2-aminoethylphosphonate--pyruvate transaminase (EC 2.6.1.37)	0.3	2.0	1.7	1.3		2.3	1.9	2.1	2.1	UP	Central intermediary metabolism	Other
BPS_06003	BPSL1763	chitinase family 18 (EC:3.2.1.14)	81.0	0.0	0.1	27.0		2.3	1.9	2.1	2.1	UP	Energy metabolism	Detoxification
BPS_05516	BPSL1835	Transcriptional regulator	3.8	1.8	3.3	3.0	UP	4.8	18.8	2.5	8.7	UP	Regulatory functions	Transposon functions
BPS_05788	BPSL0776	protein RecA	7.3	3.8	2.6	4.5	UP	18.3	10.4	18.6	15.8	UP	DNA metabolism	Detoxification
BPS_06046	BPSS1528	hypothetical protein	0.0	2.0	0.0	0.7		2.3	1.9	2.1	2.1	UP	#NV	#NV

BPS_05895	BPSL1809	amino acid ABC transporter substrate-binding protein, PAAT family (TC 3.A.1.3.-)	3.2	120.9	1.7	41.9	UP	2.3	2.2	298.4	100.9	UP	Transport and binding proteins	Amino acids, peptides and amines
BPS_06072	BPSL1779	ABC-type siderophore export system, fused ATPase and permease components	0.8	0.5	0.4	0.5		20.6	3.4	2.5	8.8	UP	#NV	#NV
BPS_06014	BPSS1196	Probable taurine catabolism dioxygenase	2.2	9.5	7.6	6.4	UP	2.3	108.6	294.4	135.1	UP	#NV	#NV

ACKNOWLEDGEMENTS

In 2006, during the spring course of the Joint Graduate Education Program (JGEP) at Hanoi University of Science, I had the great opportunity to hear many scientific research topics presented by active professors from the Ernst Moritz Arndt University of Greifswald. Of those interesting topics, I was most impressed on melioidosis as a human infectious disease and research topic that I wished to pursue for a PhD position. Now, I am very happy to thank everyone who has helped me throughout my studies. Without your care and consideration, my dream could never have become true.

Firstly, I would like to express my deepest gratitude to Prof. Dr. med. Steinmetz, my research supervisor, for giving me an excellent opportunity to work at his laboratory. You are the first one who introduced me the basic concepts of melioidosis, and inspired me with enthusiasm to discover the forgotten subject in the field of infectious disease in my country.

My special thanks also go to:

Dr. med. Breitbach for her throughout and patient guidance, enthusiastic encouragement and useful critiques of this research work.

Dr. rer. nat. Kohler for performing proteomics project, analysing biological data, reading and discussing my dissertation.

Prof. Dr. rer. nat. Riedel, Dr. rer. nat. Hochgräfe and Dr. rer. nat. Mostertz and her group for performing proteomics project and discussing invaluable.

Dr. rer. nat. Göhler, Dr. rer. nat. Hopf and doctoral candidate Bartel for sharing not only the life in Germany but also lab and office works.

All laboratory members for experiment assistance, and guiding my life in Germany.

I deeply appreciate financial assistance from the Vietnam government, Deutscher Akademischer Austausch Dienst (DAAD), and the Faculty of Medicine, University of Greifswald. I would also thank the people organizing the JGEP program, Vietnam Ministry of Education and Training, especially Dr. Le Tran Binh, Dr. Le Thi Lai, and Dr. Kasbobm, for giving us a great chance to study in Germany.

My greatest gratitude goes to my beloved family, especially to my grandparents, my father and all family members for their regards, help, encouragement, and patience.